MARCH, 1952

Journal of METALS

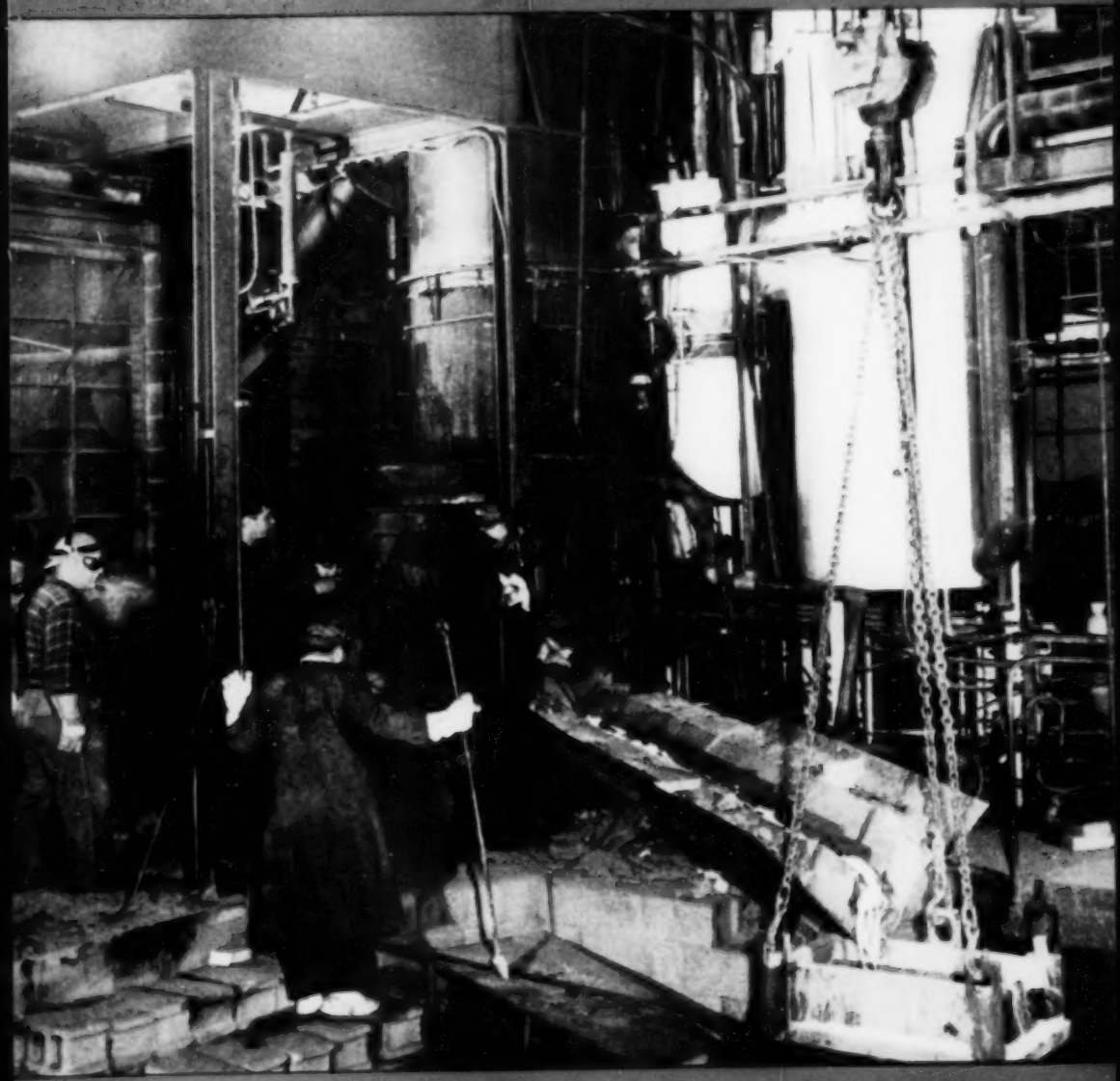

March JOURNAL OF METALS Highlights:

"Magnesium-Rare Earth Casting Alloys" - p. 242
"Hydrogen Reduction of Iron Ore" - p. 250
"Properties of Mg-Th and Mg-Th-Ce Alloys" - p. 287

In producing Aristoloy Steels, Copperweld Steel Company employs up-to-date methods, including an advanced refractory practice. After every heat, BRI Guns are used to restore furnace linings with a light application of Gundol.

BRI Guns + Gundol = 550 heats per lining at Copperweld

THE record is convincing. In 1951, Copperweld's seven electric furnaces at Warren, Ohio, tapped over 13,000 heats, averaging above 40 tons. Two furnaces set new lining life records—each averaging better than 550 heats. Shop average was 397.5 heats.

In addition to this increase in over-all lining life, operations at Copperweld cite two further benefits from the use of BRI Guns and Gundol: Balanced lining life, with brick patching during campaigns practically eliminated, and maximum furnace availability. To meet critical mill schedules, furnaces have been held two or three days beyond normal relines.

Copperweld Steel Company is one of many electric steel producers now using BRI Gun refractories. If you operate electric furnaces, large or small, you, too, will be interested in the economies possible with the BRI Gun and Gundol or Gunmix.

Basic Refractories Incorporated 845 HANNA BUILDING, CLEVELAND 15, OHIO

Exclusive Agents in Canada: REFRACTORIES ENGINEERING AND SUPPLIES, LTD., Hamilton and Montreal

Journal of **METALS**

Published to provide a continuing, authoritative, and up-to-date record of technological, engineering, and economic progress in all branches of the metals industry by the Metals Branch American Institute of Mining and Metallurgical Engineers, Inc. 29 West 39th Street, New York 18

JOHN V. BEALL
Manager of Publications

A. S. COHAN — Associate Editor
D. G. GARRETT — MARGARET BAGG
Assistant Editors
GRACE PUGSLEY — Production Manager
W. J. SEWING — Asst. Prod. Mgr

METALS BRANCH COUNCIL
C. C. Long — Chairman
E. O. Kirkendall — Secretary
R. M. Brick — IMD Chairman
T. L. Joseph — ISD Chairman
O. C. Ralston — EMD Chairman
M. Gensamer — D. S. Eppelsheimer
H. K. Work — Evan Just

TECHNICAL PUBLICATIONS COMMITTEE
J. I. Laudermilk — Chairman
E. J. Kennedy, Jr. — Secretary

AUXILIARY PUBLICATIONS COMMITTEE CHAIRMEN
M. Gensamer — Institute of Metals Div.
A. G. Forrest — Iron & Steel Div.
J. Glasser — Extract. Metal Div.

JAMES A. STANGARONE
Advertising Manager
B. C. SNELL
Regional Manager, Pittsburgh
1110 McDonald Place, Sewickley, Pa.

The AIME Publishes:
Journal of Metals
Mining Engineering
Journal of Petroleum Technology

COVER

The photograph shows spiegel being cast into a large metal mold during pilot plant tests to recover manganese from open hearth slags conducted by the U. S. Bureau of Mines, Pittsburgh. The single tuyere blast furnace has a capacity of three tons per day. One of the pebble stoves used to heat the hot blast can be seen immediately to the right of the furnace.

NEWS

Journal of Metals Reporter	241	New Products	231
Employment Service	224	AIME News	317
Meet the Authors	223	Coming Events	320
"Drift of Things"	239	Personals	321
Industrial Notes	236	Books for Engineers	234

Blast Furnace, Coke Oven and Raw Materials Conference Program 318
National Open Hearth Steel Conference Program 317
IMD New England Regional Meeting Program 318

TECHNICAL FEATURES

Magnesium—Rare Earth Casting Alloys	J. C. McDonald	242
Titanium Alloys in Stainless Steel Production	F. St. Vincent, R. W. Rebholz	245
Properties of Some Bottom Ramming Materials	M. P. Fedick	247
Hydrogen Reduction of Iron Ore	C. A. Schorschu	250
India's Iron & Steel Industry		252

TRANSACTIONS

Equilibrium Between Blast-Furnace Metal and Slag as Determined by Remelting	E. W. Filer, L. S. Darken	253
Isothermal Martensite Formation in an Iron-Chromium-Nickel Alloy	S. A. Kulin, G. R. Speich	258
Time-Temperature-Transformation Characteristics of Titanium-Molybdenum Alloys	D. J. DeLisanti, M. Hansen, R. E. Riley, W. Rostoker	265
Solubility of Carbon and Oxygen in Molybdenum	W. E. Few, G. K. Manning	271
Influence of Carbon on the Lattice Parameter of Molybdenum	R. Spenser, J. W. Szretter, W. E. Few, R. M. Parke	275
Preferred Orientation of Arc-Cast Molybdenum Sheet	M. Semchyshen, G. A. Timmins	279
Properties of Magnesium-Thorium and Magnesium-Thorium-Cerium Alloys	T. E. Leontis	287
Plastic Deformation of Magnesium Single Crystals	E. C. Burke, W. R. Hibbard, Jr.	295
Zirconium-Chromium Phase Diagram	E. T. Hayes, A. H. Roberson, M. H. Davies	304
On the Mechanism of Precipitation in Copper-Beryllium Alloys	A. H. Geisler, J. H. Mallery, F. E. Steigert	307

TECHNICAL NOTES

Origin of Recrystallization Textures	J. E. Burke	263
Extent of Strain of Primary Glide Planes in Extended Single Crystalline Alpha Brass	P. Maddin	270
Relation Between the Volume of Martensite and the Number of Martensite Plates per Unit Volume	E. S. Machlin	277

Published the first day of each month by the American Institute of Mining and Metallurgical Engineers, Inc., 29 West 39th Street, New York 18, N. Y. Telephone: PEnnsylvania 6-9220. Subscription $8 per year for non-AIME members in United States and North, South and Central America; $9, foreign; $6 for AIME members, or $4 additional in combination with a subscription to "Mining Engineering" or "Journal of Petroleum Technology". Single copies, 75 cents; special issues, $1.50. . . The AIME is not responsible for any statement made or opinion expressed in its publications. . . . Copyright 1952 by the American Institute of Mining and Metallurgical Engineers, Inc. . . . Registered cable address: AIME New York. . . . Indexed in Engineering Index, Industrial Arts Index and Chemical Abstracts. . . . Entered as second-class matter Sept. 21, 1949, at the post office at New York, N. Y., under the Act of March 3, 1879. Additional entry established at Manchester, N. H.

Are you taking full advantage of the constantly growing range of forgings? Typical is this aluminum alloy forging with a projected area of more than 1,000 square inches used in the wing structure of a modern military bomber. Such forgings are today made possible by the use of the largest die forging press in America (18,000 tons). For hammer or press die forgings of aluminum, magnesium or steel, Wyman-Gordon engineers are ready to serve you—there is no substitute for Wyman-Gordon experience.

Standard of the Industry for More Than Sixty Years

WYMAN-GORDON

FORGINGS OF ALUMINUM • MAGNESIUM • STEEL

WORCESTER, MASSACHUSETTS

HARVEY, ILLINOIS DETROIT, MICHIGAN

MEET THE AUTHORS

R. E. RILEY

A. H. ROBERSON

D. J. DELAZARO

E. C. BURKE

J. H. MALLERY

G. K. MANNING

R. E. Riley (p. 265) was born in Chambersburg, Pa., and received his B.S. in metallurgy from Missouri School of Mines. Since graduation, he has been associated with Armour Research Foundation and is now assistant metallurgist. His hobbies are rather diversified—hunting, bowling, and mineralogy.

A. H. Roberson (p. 304), chief, technical services branch, Bureau of Mines, Albany, Ore. was born in Carson, Iowa. He received his B.S. and M.S. from the University of Arizona. From 1924 to 1928 he was assistant chief chemist for the Magma Copper Co., Superior, Ariz.; held the same position with United Verde Copper Co., Jerome, Ariz., and became associated with the Bureau in 1935. He was engaged in titanium alloy research at Salt Lake City and is presently working on zirconium alloys. He has authored several AIME Transactions papers, is a member of ASM, and enjoys gun collecting and fishing in his spare time.

E. T. Hayes (p. 304) graduated from Idaho College (B.S. and M.S.Met.) and Maryland (Ph.D.Chem.Eng.). He has been with the Bureau of Mines since 1936. Now located in Albany, Ore., he spent two years at College Park, Md.; eight, at Salt Lake City; and has been in Albany since 1948. A member of ASM, Electrochemical Society, Sigma Xi, he is area governor of Toastmasters International, and also bowls.

G. A. Timmons (p. 279) metallurgical engineer with Climax Molybdenum Co., Detroit, was born in New York. Graduating from Wayne University (B.S. Chem. Eng.) and University of Michigan (M.S. Met. Eng.), he joined the American Sheet & Tin Plate Co. in 1935. He was employed by the Ford Motor Co. as a metallurgist, and in 1936 joined Climax as a metallurgical engineer. Camping and canoeing are his hobbies, in addition to being a member of AIME, ASM, American Foundry Society, American Welding Society, and Engineering Society of Detroit.

D. J. DeLazaro (p. 265) research assistant in the metals research dept., Armour Research Foundation, studied at the Illinois Institute of Technology (B.S.Met.). Following graduation, he joined Armour as assistant metallurgist. Residing in Chicago, his hobbies are baseball and fishing.

Edmund C. Burke (p. 295), born in Bridgeport, Conn., attended Missouri School of Mines (B.S. 1943); Case Institute of Technology (M.S. 1948); and Yale (Ph.D. in metallurgy 1951). A Junior Member of AIME, Mr. Burke was employed as a metallographer in the Cleveland research labs of Aluminum Co. of America from 1943 to 1948 and is presently in the laboratory development labs of Dow Chemical Co.'s magnesium div. Fishing is terrific in northern Michigan—and he likes to fish.

Rudolph Speiser (p. 275) was born in New York City. He received his B.S. and M.A. from Ohio State University, and his Ph.D. from Polytechnic Institute of Brooklyn. From 1942 to 1946 he was a physical chemist with the Eastern Regional Research Labs at Philadelphia. He is now associate professor in the dept. of metallurgy at Ohio State University. Handball, golf, and tennis are his hobbies.

R. M. Parke (p. 275) was born in the Bluegrass state, and earned his B.S. and M.S. at University of Michigan. From 1933 to 1946 he was director of research for Climax Molybdenum Co.; from 1946 to 1948 was division engineer for Kellex Corp. and Johns Hopkins University's applied physics laboratory; and since 1948 has been technical adviser at Battelle Memorial Institute. In 1946 he wrote AIME Transaction paper: "Melting of Molybdenum in the Vacuum Arc."

W. E. Few (p. 275) was born at Niagara Falls, N. Y., and attended Ohio State University (B.S. Met. Engr.). A Junior Member of AIME, he has worked for Carbide & Carbon Chemical Corp., at Oak Ridge, Tenn. Presently he is associated with Battelle Memorial Institute.

G. R. Speich (p. 258) was born in Chicago and studied at Illinois Institute of Technology (B.S.) and University of Wisconsin (M.S.) He is presently employed in the Westinghouse Electric Corp.'s atomic power div.

J. W. Spretnak (p. 275) is from North Industry, Ohio. He attended Ohio State University, Case Institute of Technology, Carnegie Institute of Technology, and the University of Pittsburgh. His degrees include B.Sc., M.Sc., and Ph.D. From 1940 to 1943 he was research metallurgist at National Malleable & Steel Casting Co.; from 1943 to 1948 he was a member of the staff of the metals research laboratory of Carnegie Institute of Technology; and since 1948 he has been associate professor of metallurgy at Ohio State University.

Joyce H. Mallery (p. 307) was born in Yonkers, N. Y., and attended (B.S.) New Jersey College for Women at Rutgers University. She is presently employed in the chemical metallurgy section of the metallurgy research dept., General Electric Research Laboratory. Skiing, hiking, and canoeing, after her wifely chores, are her hobbies.

G. K. Manning (p. 271), a Hoosier from Anderson, went to Franklin College (B.S.) and University of Michigan (M.S.E.). From 1939 to 1943 he was employed by Republic Steel Corp. in Chicago, and since 1943 has been with Battelle Memorial Institute. He is supervisor in Battelle's metallurgical engineering group. He has authored two previous AIME Transactions papers.

S. A. Kulin (p. 258) hails from Webster, Mass. He attended Worcester Polytechnical Institute and Massachusetts Institute of Technology (B.S. and Sc.D.) His employment record shows that he was associated with Crompton & Knowles Loom Works in 1941 and 1942; was chief metallurgist at Raytheon Mfg. Co.'s power tube div. from 1942 to 1946; research assistant at MIT from 1947 to 1951; and since that time has been research metallurgist in the atomic power div., of Westinghouse Electric Corp. in Pittsburgh. He wrote AIME Transaction paper: "On the Martensitic Transformation at Temperatures Approaching Absolute Zero." He likes sailing and music.

Marion Semchyshen (p. 279) was born in Detroit. He received his B.S. from Wayne University and his M.S. from University of Michigan. Since 1942 he has been metallurgist and project engineer for Climax Molybdenum Co. in Detroit.

Personnel Service

New York 18 Detroit
San Francisco
Chicago 7

POSITIONS OPEN

Engineers. (a) Plant superintendent experienced in handling overall operation of a plant comprising quarrying and processing of limestone, and operation of rotary and gas fired upright kilns. (b) Mechanical engineer with broad experience in maintenance and repairing of equipment in heavy industry, such as cement, lime, refractory, stone mining, processing, etc. Some traveling between several plants located in the middle Atlantic States, east of Chicago. Headquarters, West Virginia. Y6633.

Metallurgist, recent graduate preferred, who is interested in gaining experience in the manufacture of steel, wire and wire products. Location, northern New Jersey. Y6628.

Production Manager, 35 to 45, with considerable experience on direct line production for metal forming, plant layout, scheduling and costs. Salary, $10,000 to $12,000 a year. Location, southern New Jersey. Y6618.

Junior Sales Engineer, 26 to 35, with chemical engineering, metallurgy or mechanical engineering training, and some experience in industrial sales, and/or chemical plant operating experience, to sell corrosion service valves to chemical, petroleum, etc. industrial and engineering companies. Will receive factory and field training and probably be assigned to New York district office. Some traveling and willing to relocate if necessary. Salary, $3600 to $4800 a year plus bonus. Company furnishes car, and pays all traveling expenses. Location, New York. Y6613.

Assistant Editor, young, mining or metallurgical engineering graduate, with at least two years' experience in ore dressing, extractive metallurgy and allied fields, to prepare and edit articles covering mining, metallurgy. Salary, $4000 to $5400 a year. Location, New York. Y6577.

Engineers. (a) Mill metallurgist, preferably with previous plant experience, as well as experience in testing laboratories. Should be capable of carrying out ore beneficiation tests and research work, and making reports on results obtained. Work will be in the nature of laboratory testing, gravity concentration, flotation concentration and cyanidation and some roasting tests. Salary, $4200 to $4300 a year depending upon qualifications. Room and board and transportation, if single; and if married, furnished house, plus $75 a month board allowance after three months single status. (b) Junior mill metallurgist with some laboratory experience, with knowledge of the technique to carry out assigned tasks with supervision. Salary, $3000 to $3300 a year, plus board allowance, etc. Location, Central America. Y6573.

Metallurgical Engineer, technical graduate, with metallurgical background or experience, for electrolytic copper refinery. Opportunity for supervisory work in operating departments. Salary open. Location, Texas. Y6565.

Chemist-Metallurgist, 25 to 35, for work in nonferrous metal plant. Location, Brooklyn, N. Y. Y6535.

Junior Metallurgist, metallurgical engineer, electro-chemist or chemical engineer, to conduct research on metallurgical problems assigned, apply basic principles such as chemistry, physics, and mathematics to the work performed; develop reports and perform other work functionally required. Salary, $3900 to $4900 a year. Location, New Jersey. Y6524.

Mining or Metallurgical Engineer, graduate, with degree in mineral dressing engineering, not over 28, preferably with one or two years' experience in the milling of metals for sales contact work. Prefer single men. Salary, $4800 to $5400 a year. Location, New York. Y6494.

Metallurgists, with an interest and some experience in research work, preferably in the general field of nonferrous physical metallurgy. Work will involve analysis of metallurgical problems and will not entail laboratory research. Salaries, $5900 to $9600 a year. Location, Washington, D. C. Y6490.

Control Metallurgist with some experience in induction melting of stainless and high temperature alloys, to be responsible for incoming and outgoing materials, inspection and pouring. Location, Ohio. Y6463.

Assistant Process Metallurgist, metallurgical degree, with background in nonferrous metallurgy, with some welding and brazing experience. Must be interested in solving the metallurgical problems which arise in casting, in drawing of rod and tube, and in rolling of nonferrous metals. Will advise production supervisors, and take charge of new processes, etc., from a metallurgical standpoint. Salary, $4316 to $5200 a year. Location, Connecticut. Y6460(a).

Physical Metallurgist, with three or four years' experience handling heat treatment of steels, hardening, etc. Salary open. Location, Brooklyn, N. Y. Y6347.

Research Fellowship in metallurgy at eastern university. Post graduate work for Ph.D. degree. Selection of research problem in variety of fields, including welding, induction heating, powder metallurgy, electrometal-

FOR SALE

Zeiss Neophot Metallograph (horizontal), modified.

Kennametal Inc.
Latrobe, Pa.

Attention: A. D. Stevens, Metallurgist

METALLURGIST. Recent graduate age 21-26 to be engaged in investigation of processing problems and maintenance of quality in Mid-Western plant producing copper and brass mill products. Excellent opportunity to obtain knowledge of and experience in nonferrous metal processing. Please include details such as education, age, draft status, etc.

Reply to Box B-4
JOURNAL OF METALS

PHYSICAL METALLURGIST

Experienced Ph.D. or equivalent, interested in wide variety petroleum metallurgical problems. Leading Midwest research organization.

BOX C-6, JOURNAL OF METALS

SUPERVISOR
EXTRACTION METALLURGY
RESEARCH

Excellent opportunity for experienced metallurgical or chemical engineer to organize and direct an important program in extractive metallurgy. Graduate study to this level or the equivalent and practical experience desired, coupled with knowledge of modern research methods required. Permanent position in outstanding research laboratory offers unusual opportunity for personal and professional advancement. Salary commensurate with qualifications.

BOX C-7, JOURNAL OF METALS

Metallurgical or Mechanical Engineer. Large Eastern metal producing company has excellent opening for technical service and development work in fuel and steel fabrication of nonferrous alloys. Knowledge of design desirable. State age, education and experience.

Box C-8, JOURNAL OF METALS

lurgy and magnetic materials. Location, Pennsylvania. Y6330.

Junior Engineer. 26 to 30. B.S. degree in metallurgical or mining engineering, with mining and milling equipment experience, or junior executive background with business school education, to assist in office engineering covering correspondence, purchasing, specifications, expediting, etc. Occasional trips. Salary, $4200 to $4500 a year. Location, New York. Y6325.

Metallurgist with B.S. or engineering degree in metallurgy or chemistry, and two years or more ferrous products experience, to do physical or chemical testing, check heat treatment, analyze production difficulties in steel products manufacturing plant. Salary, $4200 to $4800 a year. Location, Elizabeth, N. J. Area. Y6323(a).

Engineers. (a) Metallurgical engineers, with two to five years' experience in powder metallurgy, precision casting, finishing, etc., and/or general metalworking industries, with some mechanical aptitude. (b) Research and development engineers with two to five years' experience on existing and new products with some knowledge of coal heading operations and/or design aptitude on new models on small arms. Salaries to $6600 a year. Location, central New York. Y6301.

Metallurgists, project leader with M.S. degree and several assistants, graduates, for fatigue studies. Work will involve studies of grain size effect on high temperature fatigue, notch effects, fatigue gage for metals and related work. Salary, $4680 to $6240 a year. Location, western New York State. Y6297.

Assistant Professor, recent graduate, with Doctor's degree, capable of working out courses in advanced physical metallurgy or metallurgical thermodynamics. For first two years will not be expected to teach more than one course a term. The rest of time will be devoted to helping carry out and supervise some of the research work. Excellent opportunity. Salary, $5400 a year depending on experience. Location, New Jersey. Y6295.

Metallographer with good understanding of the principles of physical metallurgy, to investigate and work on a new family of alloys; technically interesting work in a growing industry. Salary open. Location, Pennsylvania. Y6291.

Instructor in basic welding and heat treating laboratories, graduate metallurgical or mechanical engineer, possibly with some related industrial experience. Salary, $3000 for 8½ months with opportunity for graduate

(Continued on page 226)

Why not find out whether we can help reduce costs beyond what you have worked out for yourself, or that somebody else has worked out with you?

In plant after plant, our Field Engineers have achieved splendidly. Given the opportunity, they'd probably add solution of your problems to their impressive lists of successes.

With their analyses of your objectives in hand, our laboratory technicians can produce *specific purpose* grinding wheels that will assure you an efficiency that will result in a wholly new degree of economy for you.

May we, at our risk, undertake to prove it?

Electro Refractories & Abrasives Corporation
344 Delaware Avenue, Buffalo 2, N. Y.
Regional Warehouse: Los Angeles 58, California
Plants: Buffalo, N. Y. and Cap-de-la Madeleine, P. Q., Canada

Electro SINCE 1919

SPECIFIC PURPOSE
GRINDING WHEELS
for
CUTTING OFF
•
PRECISION GRINDING
•
SNAGGING
•
MANUAL 645 AND SPEED CALCULATOR FREE ON REQUEST

Electro
SPECIFIC PURPOSE GRINDING WHEELS

work toward advanced degree; free of tuition. Location, Indiana. Y6289.

Instructor or Assistant Professor, physical and/or process metallurgist, with Master's or preferably Doctor's degree, to teach elements of metallurgy, electrometallurgy, ferrous metallurgy, metallurgical calculations, principles of physical metallurgy, metallography and the direction of advanced students in individual projects and research. Must be citizen of the U. S. Location, West. Y6270.

Materials and Process Engineer for work involving selection and testing of materials for precision engineered products. Five years' experience in work involving evaluation of the application of a wide range of ferrous and nonferrous metals for precision equipment manufacture required. Mechanical, metallurgical or chemical degree. Salary, $6000 to $9000 a year. Location, Brooklyn, N. Y. Y6258(a).

Metallurgist, graduate, 30 to 45, with practical experience in Martempering and Austempering. State salary expected. Location, Pennsylvania. Y6231.

Staff Aluminum Engineer, 35 to 45, with extrusion and forging experience. Should have a metallurgical or mechanical degree and considerable experience in aluminum production. Location, Michigan. Y6227D.

Engineers. (a) Executive, 30 to 50, with experience and record of accomplishment in administration of large mining and metallurgical operations. Salary, $15,000 a year. (b) Executive with minimum of ten years' experience in operation of heavy chemical plants. Salary, $15,000 a year. Location, New Mexico. Y6226.

Metallurgist with engineering or physics and four years experience in light metals and familiarity with Government specifications related to heat treating, plating, finishing, magnafluxing, etc. Salary, $5200 to $6500 a year. Location, Michigan. Y6176(cv).

Metallurgist with at least three years' experience covering ferrous and nonferrous materials for test work, preparation of material specifications, heat treatment, welding, annealing at heavy industry manufacturing plant. Salary, $4800 to $5400 a year. Location, central Pennsylvania. Y6111.

Engineers, for company making cutting tools and dies by powder metallurgy methods. Will work with present personnel in surveying and evaluating present production processes; adapting research results to production and conducting production scale research and development. (a) Materials engineer, metallurgical degree, to analyze material failures and specify materials for development and production applications. (d) Observers, recent graduates. Salary, $3000 to $3840 per year. Location, Pennsylvania. Y6044.

Chemists, Chemical Engineers and Metallurgists, B.S., M.S., Ph.D., for process design, development and pilot plant, analytical laboratory and plant technical service. Position offers opportunity to become familiar with latest developments in ore processing, metal refining and fabrication. Salary open. Location, southern Ohio. Y6042(J).

Recent Chemical or Metallurgical Engineering Graduates for work in connection with metallurgical testing and evaluation work in connection with a prospecting program. Excellent opportunity for advancement. Location, Florida. Y6013.

Concentrator Metallurgist, 30 to 35, graduate in ore dressing with practical experience, to take charge of laboratory testing for large mining company. Spanish helpful. Three-year contract, transportation, living quarters. Location, South America. Y6010.

Junior Engineer, metallurgical or chemical graduate, to do analysis, make physical tests, covering materials, heat treatment, coatings, etc. Salary, $3900 to $4420 a year. Location, Connecticut. Y5997.

Recent Graduate Metallurgical Engineer, to do testing on nonferrous materials. Salary, $3600 to $3900 a year. Location, New England. Y5879(b).

Metallurgical Product Engineer, recent graduate, B.S. in metallurgy, for product engineering work on rod and wire. Excellent living conditions, housing available. Reply giving training, experience, age, salary desired, etc. Location, northern Pennsylvania. Y5852.

Instructor, B.S. or M.S. in metallurgical engineering, to teach physical metallurgical courses and do research work. Location, South. Y5827.

Engineers. (a) Metal processing engineer, familiar with metal processing equipment for melting, forging and rolling. Liaison between research laboratory and production personnel. Emphasis is on the equipment aspects of processing, but an appreciation of the metallurgical factors involved important. (b) Junior research physical metallurgist, recent graduate, to work in research lab assisting experienced metallurgists in the physical metallurgy research of a series of new alloys. Liking and aptitude for laboratory work essential, and experimental resourcefulness desirable. (c) Senior research physical metallurgist, to conduct alloy research on a new series of materials. Advanced degree in physical metallurgy or its equivalent in metallurgical research necessary. Location, midwest area. Y5826.

Engineers. (a) Chemical engineer or metallurgist to take charge of process control of nonferrous metal, and in addition, do limited amount of research for company engaged in the manufacture of lime and magnesium. (c) Plant superintendent with experience in lime, cement or gypsum for production and maintenance. Location, Connecticut. Y5733.

Instructor and Assistant Professor, Ph.D. in metallurgy, with good physical metallurgy background with emphasis on engineering mechanics and mechanical metallurgy, to teach undergraduate class in physical metallurgy, graduate class in mechanical metallurgy and also conduct fundamental research on mechanical properties of metals. $3600 to $4200 instructor, $5000 assistant professor. Location, Pennsylvania. Y5708.

Assistant Refinery Superintendent, metallurgical engineering graduate, with electrolytic refinery and copper casting experience, to be responsible for shift operations. Salary open. Location, South Central Africa. Also require metallurgical assistant with experience for staff position in consultant's office. Same location. Y5138.

Metallurgist, graduate, with six or eight years' experience in laboratory investigations covering beneficiation and reduction of nonferrous ores, including flotation, testing, roasting, smelting, hydrometallurgy, gas measurement and analyses. Actual plant experience or pilot plant work desirable. Salary open. Location, Texas. Y4886.

Research and Graduate Assistants. (a) Metallurgist with advanced training and chemistry background for projects concerned with the chemical metallurgy and processes for the production of highly purified metals. (b) Metallurgists acquainted with the mechanics of metallurgy and the testing of metals for project concerned with the mechanical properties and the effect of composition on mechanical properties of steels. Salaries: Research assistants, $2400 to $3300 a year, six credits of graduate work per semester permissible. Graduate assistants $1344 a year half-time, ten credits per semester permissible. Location, East. Y4688.

MEN AVAILABLE

Metallurgical Manager, E.Met., registered professional Engineer (N.Y.). Fifteen years' experience operation, supervision, development and design of nonferrous and precious metals beneficiation. Now employed in consulting organization. Desires position operating group with opportunity for executive advancement. M-670.

Advertisement

ELECTROMET *Data Sheet*

A Digest of the Production, Properties, and Uses of Steels and Other Metals

Published by Electro Metallurgical Company, a Division of Union Carbide and Carbon Corporation, 30 East 42nd Street, New York 17, N. Y. • In Canada: Electro Metallurgical Company of Canada, Limited, Welland, Ontario.

How NITROGEN Refines Grain Size...

Produces Harder, Stronger, Tougher Chromium Steels

When nitrogen is added to high-chromium steel, it greatly refines the grain size of the metal and materially increases its strength, toughness, hardness, and wear resistance without sacrificing ductility or reducing corrosion resistance. For these reasons nitrogen-bearing chromium steels are well suited for cutlery, turbine blades, and various machinery parts that are subject to extreme wear.

Added to Steel In Ferrochrome

Nitrogen is usually added to chromium steels in the form of nitrogen-bearing ferrochrome containing 0.75 per cent and up of nitrogen, 70 per cent chromium, and a maximum of 0.10 per cent carbon. Depending upon the chromium content of the steel, which can range between 12 and 30 per cent, the nitrogen content may vary between 0.06 and 0.20 per cent. The amount of nitrogen added to high-chromium steels should be 1 part of nitrogen to between 100 and 200 parts of chromium, depending upon the chromium content of the steel.

Nitrogen-bearing ferrochrome is added to the furnace in the same manner as ordinary ferrochrome. Nitrogen recovery will average about 90 per cent.

Improves Cutlery Steel

Cutlery steels and other martensitic stainless steels, such as the 12 to 14 per cent chromium low-carbon steels that are used for turbine blades, are hardenable by heat treatment. Hardenability and strength increase with the carbon content. And, since nitrogen is a more powerful austenite former than carbon, it is sometimes used as a substitute for part of the carbon, or as a supplement to the carbon, to increase the strength and hardenability of these steels.

Nitrogen has distinct advantages over carbon for this purpose because ductility, toughness, and corrosion resistance are retained when nitrogen is added to steel. It increases the hardness of cutlery steels without detrimentally affecting toughness or corrosion resistance. The effect of small additions of nitrogen in increasing the hardness of cutlery steels is shown in the table below.

Reduces Grain Growth During Hot-Working

The ferritic high-chromium stainless steels to which nitrogen is added have a finer grain size than ferritic steels without nitrogen, which are comparatively coarse-grained. These include the 16 to 18 per cent chromium wrought steels, high-chromium steels containing small percentages of nickel, and both the cast and wrought 20 to 30 per cent chromium steels. The function of nitrogen when added to the ferritic high-chromium steels is to preserve a fine grain size.

The nitrogen-bearing, high-chromium wrought steels are more readily rolled and forged than comparable steels containing no nitrogen, because grain growth is inhibited during hot-working operations. Greater yields are therefore obtained in rolling and fabricating. Also, strength and toughness are increased as a result of the grain refinement caused by the nitrogen addition.

Effect of Nitrogen on the Hardness of Cutlery Steels*

% Cr	% C	% Si	% Mn	% Mo	% N	Rockwell C Hardness	Brinell Hardness Numbers (by conversion)
13.15	0.12	0.30	0.38	...	0.03	41	387
13.25	0.13	0.29	0.42	...	0.10	48	460
13.36	0.23	0.28	0.40	...	0.03	46	437
13.27	0.21	0.34	0.32	...	0.08	51	496
12.70	0.32	0.30	0.37	...	0.04	50	484
13.41	0.35	0.31	0.41	...	0.11	56	560
17.37	0.41	0.32	0.41	0.75	0.036	41	382
17.25	0.44	0.30	0.42	0.75	0.09	53	522
17.30	0.66	0.29	0.38	...	0.03	51	496
17.08	0.60	0.31	0.40	...	0.11	55	547
17.26	0.80	0.28	0.39	0.76	0.032	52	509
17.25	0.80	0.27	0.45	0.74	0.09	57	573

*Steels oil-quenched from 950°C. Held 5 hr. at 200°C. and air-cooled.

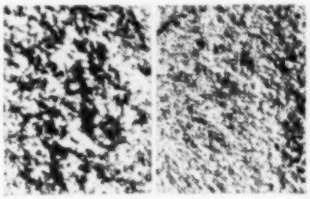

Note the extent to which nitrogen refines the grain size of these specimens containing about 27 per cent chromium and 0.35 per cent carbon. The specimen at the left contains 0.05 per cent nitrogen; the one at the right, 0.10 per cent nitrogen.

Greater Strength for Austenitic Steels

Small percentages of nitrogen will increase the yield point and tensile strength of the austenitic chromium-nickel steels. These include the well-known 18 per cent chromium, 8 per cent nickel steels, and also the 25 per cent chromium, 12 per cent nickel steels. The improvement in strength is gained at practically no sacrifice of workability. Furthermore, nitrogen promotes the formation of austenite.

Metallurgical Service Available

ELECTROMET nitrogen-bearing ferrochrome is furnished in the following standard analysis:

Chromium	67 to 71 %
Carbon	0.10 % max.
Silicon	0.30 to 1.00 %
Nitrogen	0.75 % approx., or higher if desired.

It is produced in lump sizes of 25 lb. by 8 mesh, or 15 lb. by 8 mesh; also, in a crushed size of 2 in. by down.

If you would like additional information about the production of nitrogen-bearing steels, ask to have one of our metallurgists call, or ask for the booklet, "Nitrogen In Chromium Alloy Steels." Write to the address given above or to the ELECTROMET office nearest to you. Offices are in Birmingham, Chicago, Cleveland, Detroit, Los Angeles, New York and San Francisco. In Canada: Welland, Ontario.

The term "Electromet" is a registered trademark of Union Carbide and Carbon Corporation.

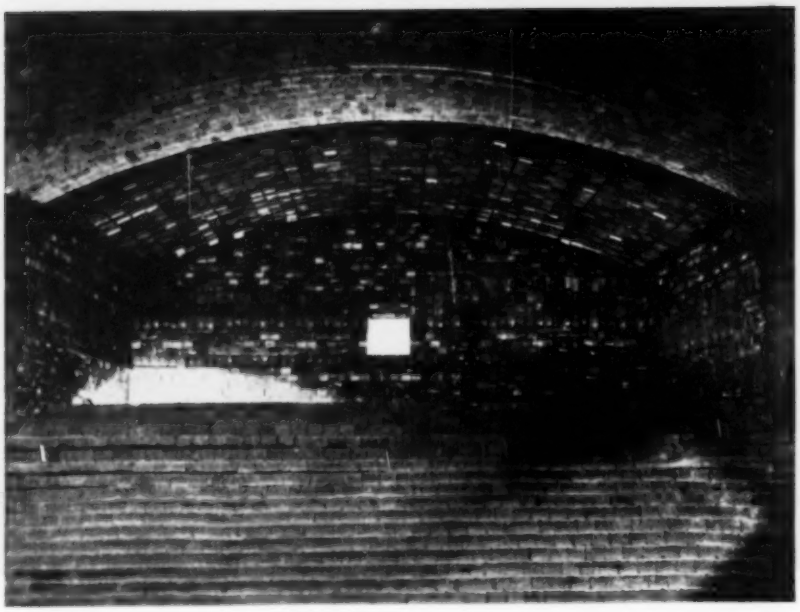

Photograph Courtesy of Weirton Steel Company, Division of National Steel Corporation

• • • • This is a suspended basic end in the world's largest open-hearth furnace. Such construction was pioneered by Grefco with its STEELKLAD basic brick. In the picture you'll find STEELKLAD in the end wall, the sidewalls and the port roof.

STEELKLAD is a patented, unburned basic brick, permanently jacketed in a steel shell, with the metal an integral part of the brick. A STEELKLAD wall rapidly becomes a tight, monolithic structure in service. It will deliver the longest possible life under the most severe conditions.

Nothing Could Be More Basic!

GENERAL REFRACTORIES

GENERAL REFRACTORIES COMPANY
PHILADELPHIA

Grefco's STEELKLAD is resistant to spalling, has low thermal conductivity, high hot strength and great accuracy to specified dimensions.

With products like these, General Refractories is playing an important part in providing the steel industry with a complete refractories service. 43 mines, 29 plants, 18 sales offices, 200 distributing agencies and the world's most modern research laboratories—are helping to meet industry's ever-growing demand for steel!

A Complete Refractories Service

●

The Heart of a Steel Plant

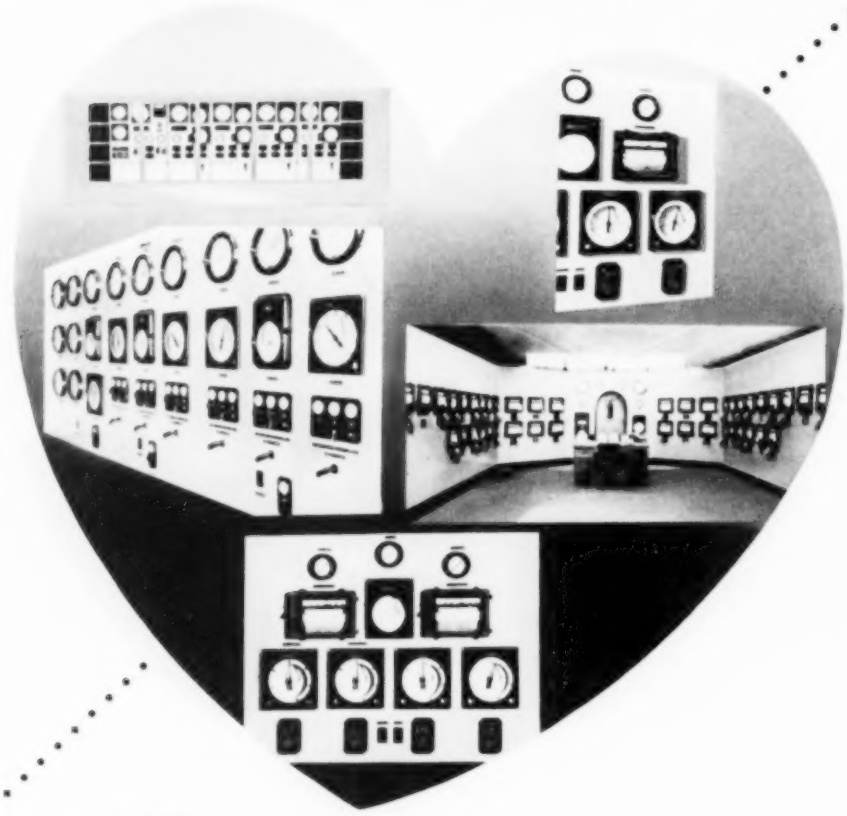

Nearly 2000 Brown Recording and Controlling Instruments In One Large Steel Producing Plant

Just *one plant* of this very large producer uses nearly 2,000 Brown instruments . . . *Electronik* Potentiometers, Pressure Gauges, Flow Meters with pneumatic or electric control. They're found in every important operation . . . Coke Oven, Blast Furnace, Open Hearth, Soaking Pit, Re-Heating Furnace . . . Pickling, Annealing, Normalizing, Tinning, Galvanizing.

These Brown instruments work together as a great team . . . coordinating operations and processes . . . providing precision control and flexibility for this industrial giant.

MINNEAPOLIS-HONEYWELL REGULATOR CO., *Industrial Division*, 4573 Wayne Ave., Philadelphia 44, Pa.

MINNEAPOLIS
Honeywell
BROWN INSTRUMENTS
First in Controls

New Products

New Products | New Literature | New Services

For Further Information or Literature on any Product, Fill in the Coupon and Send to JOURNAL OF METALS
Students are Requested to Apply Directly to Manufacturers for Bulletins and Information

1—ELECTRIC TRACTOR: Medium duty class tractor is available from *Mercury Mfg. Co.* for use in automotive, aviation, and metalworking

industries. The two-wheel drive tractor is rated at 400 lb normal and 2000 lb maximum drawbar pull.

2—MICAMAT: A new special process produced by *General Electric Co.* by which minute mica flakes are treated so a force is generated that holds the tiny particles. Capable of being impregnated with resins and bonded to paper, glass and cloth for greater strength and improved electrical properties, G-E micamat tapes and sheets can be used in heating devices, molded into shapes for motors and generators, or machine-wrapped on bars and cable.

3—WATER REPELLENT: A new silicone base water repellent has been developed by the *Rauetite Mfg. Co., Inc.* It is easy to apply either by spraying or brushing, can be applied at temperatures as low as freezing, and may be painted over.

4—FLOOR PLATE: Designed to fit 1-ft increments of floor area, there is no need for cutting to fit plates around posts, machinery, and corners. They are $11\frac{3}{4}$ in. sq plates of 0.068 in. hot-rolled steel. Each plate contains 100 small rectangular holes approximately $12x\frac{3}{4}$ in. and 100 barbed prongs $\frac{3}{4}$ in. long. *Acme Steel Co.*

5—VACUUM PRINTING FRAME: Announced by the *Miller-Trojan Co.* this vacuum printing frame is used for producing templates by the photographic method. Side and bottom reflectors have high reflective quality and there is an even illumination. The overall printing area is 68x144 in.

6—TOOL HOLDER: An eight-position tool holder designed for use on vertical boring and turning mills has been announced by the Davis Boring Tool Div., *Giddings & Lewis Machine Tool Co.* It will enable an operator to turn, undercut, bore, and chamfer in one setup.

7—SELF-SETTING CLAMPS: These clamps are constructed on a design based on the use of three interrelated curved contact surfaces. Distributed by the *Alpha Tool & Supply Co.*, they are available in sizes ranging from 3 in. long with $1\frac{1}{8}$ in. height capacity, to 8 in. long with $3\frac{3}{4}$ in. height capacity.

8—VINYL PRIMER: Specifically developed for use on rusted steel surfaces a new vinyl primer has been announced by *U. S. Stoneware Co.* It is easily applied by brushing, spraying, or dipping and no previous preparation is necessary.

9—REFRACTORY BRICK: A new slag resistant, clay-graphite refractory brick has been developed by the *North American Refractories Co.* It is a prefired product and has the ability of shedding slag, preventing rapid deterioration of the refractory. These bricks are available in 9 in. straights and most standard 9 in. series brick. Special shapes can be produced.

10—CONICAL BLENDER: Recently completed by *Patterson Foundry & Machine Co.* this conical dry blender has a 13 ft diam and a total capacity of 1000 cu ft and a working capacity in excess of 700 cu ft. The blender is essentially a mixer of dry, free-flowing materials.

11—DISPLACEMENT PUMP: Magnamite pump is now in production at *Milwaukee Hydropower, Inc.* It has a capacity of $1\frac{1}{2}$ gpm down to $\frac{1}{4}$ gpm, and is suitable for handling

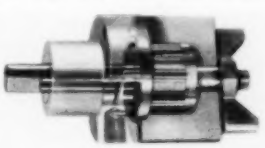

fuel oil, gasoline, hydraulic fluid, lubricating oils and other light viscosity fluids. The action of the rollers against the inner periphery of the pressure chamber induces the formation of an oil wedge between the contacting surfaces to insure proper lubrication at this point.

12—JOINT COMPOUND: A noncorrosive, nonshrinking, and nontoxic joint compound is offered by *Phoenix Asbestos Mfg. Co.* It is air and heat hardening, satisfactory for permanently tight joints. Available in $1\frac{1}{2}$, 6, and 25 lb cans. It is applicable for various industries, among them being: Oil refineries, power plants, industrial plants, chemical processing plants, building services, sugar refineries, and public utility plants.

13—LOCATING DEVICE: Machining accessory announced by *Queen City Machine Tool Co.* permits quick and accurate location of parts for drilling, boring, or milling. The base of

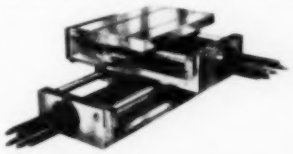

the unit has ample space for mounting screw holes to fit any machine tool. The working surfaces are provided with two standard $\frac{5}{8}$ in. T-slots.

14—GERMANIUM RECTIFIERS: Development of a new line of industrial rectifiers which can operate at current densities up to 1000 times greater than existing copper oxide or selenium stacks has been announced by the *General Electric Co.* Models being produced include those in single-phase, half wave ratings of 12 v/0.4 amps; 21 v/0.4 amps; 27 v/0.4 amps; and 6 v/6 amps.

15—HAND PAD: Leather hand pad for handling brick, tile, metal sheets, stamping, and sharp edged castings is available from *General Scientific Equipment Co.* They are adjusted to any size.

16—WAX LUBRICANT: A blend of special solid waxes put up in stock form in order to facilitate use in certain types of metalworking operations is now being marketed by *S. C. Johnson & Son.* It is said to provide a durable, clean lubrication for metal standing, metal sawing, pipe cutting and threading. Burrs are eliminated when metal is cut or drilled and a smoother finish is achieved when grinding or sanding metal surfaces.

17—TILTING MELTING FURNACE: A 25,000 lb hydraulic tilting type melting pot furnace has been designed and manufactured by *Bellevue Industrial Furnace Co.* Furnace and pot are tilted by means of hy-

drauli- cylinders which are completely piped with flow control valves installed in oil lines, allowing adjustment of flow control to give desired tilting speed. The internal lining of the furnace is made from first quality fire brick, backed up with sufficient insulation to minimize heat losses, reducing fuels for each heat. The pot size is 76 in. diam by 37 in. depth.

18—LAMP STARTER: A new automatic reset fluorescent lamp starter, has been announced by *Sylvania Electric Products, Inc.* The robot cop starter protects ballasts from overheating and also eliminates manual for restarting. The new unit for use with 40 watt lamps, cuts flickering lamps out of the circuit and lowers the current through the ballast to a safe value.

Free Literature

20—METALLURGICAL GRINDING: This bulletin describes the equipment available for fine grinding of specimens with emery papers or wet type silicon carbide papers or cloths. Available from *Buehler Ltd.*, it covers both hand and motor powered grinders.

21—MACHINING CU ALLOYS: A 32 page booklet suggesting cutting speeds, feeds, tool rakes and clearances to be used on more than 40 different copper alloys is offered by the *American Brass Co.* Tables show compositions, weights and conversion factors.

22—DIE SECTIONS: Booklet containing complete data on 35 standard die sections is available from *Allegheny Ludlum Steel Corp.* Full information on special die sections is also included.

23—POWER TRANSMISSION: Speed reducers, clutches, pulleys, and rolling bearings are several of the items mentioned in bulletin A604 issued by the *Dodge Mfg. Corp.*

24—CORE BLOWERS: Completely automatic core blowing cycle control is described in catalog obtainable from *Beardsley & Piper.* Blo-Matic offers a quick selection of three forms of control: Automatic, semiautomatic, and manual.

25—MILL MOTOR BRUSHES: A new catalog section listing complete line of *National Carbon Co.* brushes is available. These brushes are built to conform to AISE standard specifications. The catalog lists AISE standard and code numbers, corresponding National brush numbers, brush sizes, grades and cost.

26—ASBESTOS PACKING: A brochure published by *Phoenix Asbestos Mfg. Co.* describes the conventional types of packing produced for all conditions and services. Excelpax style 320 is a multi-purpose plastic asbestos packing designed for all services met in commercial practice up to 1500°F. It is for water, steam, gases, petroleum and industrial oils, salt solutions, fuels, and acids. Packaged 1/8 and 5/16 in. round, 1 and 5 lb spools, 3/8 in. sq. and up spirals, 22 ft.

27—TEMPERATURE CONTROLS: Catalog describes design, operating characteristics and installation of 10 variations on basic *Fenwal Inc.* thermostatic device. Illustrated with drawings, graphs, tables, and photos, a section covers selection and application of the thermoswitch.

28—STACKER: Folder providing information on new Universal power booster and stacker may be obtained from *Industrial Engineering & Mfg. Co., Inc.* Cutaway diagram includes specifications.

29—PRESSURE CONTROLLER: A new non-indicating pressure controller is fully described in bulletin 16-1 issued by *Minneapolis-Honeywell Regulator Co.* Principle of operation, design features, mounting dimensions, and other pertinent information are contained.

30—X-RAY DIFFRACTION: Booklet entitled *What is X-Ray Diffraction* is available from *North American Philips Co., Inc.* It points out how this nondestructive analysis method identifies raw materials or components to assure uniformity.

31—TUBING FAILURES: Factors affecting tube life in high pressure, high temperature applications are presented in 40-page booklet published by the tubular products div., *Babcock & Wilcox Co.* The booklet presents results of investigations of failures of carbon steel, Cr-Mo alloy steel and stainless steel tubing, to mention a few.

32—POWER TRANSMISSION: Speed reducers, pillow blocks, sheaves, clutches, couplings, hangers, collars, conveyor pulleys, takeups, and bearings used in power transmission machinery are described in bulletins A-600 and A-604 published by *Dodge Mfg. Corp.*

33—METAL ARMORPLY: A brochure entitled *Rigidized Metal Armorply* has been published by *U. S. Plywood Corp.* This metal is an extremely rugged structural panel made by bonding a sheet of roll-embossed aluminum, stainless steel or other metal to exterior grade Weldwood plywood. The metal-clad plywood panels are used for elevator cars, railroad car interiors, and truck panels.

34—V-S DRIVE: Pointing up the efficiency-improving advantages that packaged, all-electric, adjustable speed drives bring to a wide range of production machines and processing equipment, a new 8-page booklet has been issued by the *Reliance Electric & Engineering Co.* The booklet presents a simplified explanation of the drive. It is available in drives of five types ranging in ratings from ¾ up to and including 200-hp.

35—POLISHING MATERIALS: A 20-page booklet describes and includes sample of emery, aluminum oxide and silicon carbide papers and also 12 polishing cloths. Trade names, particle sizes, etc. are given for many abrasives. *Buehler Ltd.*

Journal of Metals
29 West 39th St.
New York 18, N. Y.

March

Please send me ☐ More Information ☐ Free Literature ☐ Free Data ☐ on items indicated.

1	2	3	4	5	6	7	8	9	10
11	12	13	14	15	16	17	18	19	20
21	22	23	24	25	26	27	28	29	30
31	32	33	34	35	36	37	38	39	40

Name _____ Title _____

Company _____

Street _____

City and Zone _____ State _____

U·S·S CARILLOY BORON STEELS PROVE EFFECTIVE IN CONSERVING "CRITICAL" ALLOYS

● Today American industry is faced with the unpleasant fact that, after military needs are met, there is not nearly enough nickel and molybdenum available to produce steels containing these alloys. Actually the alloy shortage is worse now than in World War II.

However, insofar as heat treating steels are concerned, the picture is not as grim as it might be. For in the last war, the potentialities of the element boron for increasing the hardenability of steel became widely recognized and thousands of tons of boron steels were produced by United States Steel and used in military equipment, such as armor, projectiles, torsion springs for tanks, etc.

These and post-war applications of boron steels in large diesel locomotive crankshafts, heavy-duty tractor axles, in wrenches and hand tools, have thoroughly demonstrated boron's ability to replace several hundred times its own weight of other hardening alloys such as nickel, chromium, molybdenum and manganese. Not only have boron steels helped to conserve these critical alloying elements, where they are necessary only for adequate hardenability, but they have effected considerable savings both in the cost of steel and in fabricating costs as well.

U·S·S SuperKore—a pioneer boron steel

More than six years ago, United States Steel Company developed U·S·S SuperKore A, which is essentially a 4312, plus boron and 0.03-0.07% vanadium. Used by a leading aircraft engine builder, this steel (designated as TS 43BV12) has successfully replaced 3310, in heavy-duty gears, shafts and pinions for large air-cooled reciprocating engines and is approved for aircraft use under AMS Spec. 6266. Not only does SuperKore A save one-half the nickel and two-thirds the chromium formerly required but the manufacturer reports improved carburizing characteristics—with less retained austenite and fewer undissolved carbides on direct quenching.

Similarly, U·S·S SuperKore AA—a 4315 plus boron—shows improved hardness near the surface and large tonnages have been used by a leading heavy-duty truck builder who reports that transmission countershafts made from it have been in service for five years with excellent results. Used to replace 4800 types, this steel now designated as TS 43BV14 reduces nickel and molybdenum requirements by one-half.

Another U·S·S SuperKore Steel—SuperKore B—which is a 4615 plus boron, designated TS 46B12, has been successfully used for more than three years to replace 4812, in making a famous line of rock bit cutters, and saves one-half the nickel formerly required.

U·S·S SuperKore C—a 8615 plus boron—originally developed to replace 4300 carburizing grade, and which reduces nickel by one-half and molybdenum by one-fifth has shown good results.

Our work on these alloy-saving carburizing steels has shown that lower alloy steels containing boron will have the same core properties as the higher alloy steels they match in hardenability. In addition to conserving critical alloys they (1) improve hot and cold working, (2) require a shorter annealing cycle, and (3) have improved machinability. All these factors result in fabricating economies.

Because in some cases boron steels require more care in their selection and treatment than do the conventional alloy steels, we offer you the assistance of our metallurgists who have pioneered their development and whose practical cooperation will be of material benefit in applying boron steels to your equipment. Simply write United States Steel, 525 William Penn Place, Pittsburgh 30, Pa., Room 2801H.

There are other approaches to the alloy problem

Although the substitution of boron steels for standard alloy grades has enabled many customers to meet their requirements, such substitution is only one of the ways our metallurgists and research specialists are able to solve today's alloy problems.

For example, in some cases, emergency alloys, without boron, have proved entirely satisfactory. In others, improved heat treating procedures have provided adequate hardness and other physical properties in lean standard alloy steels.

In addition to the use of U·S·S SuperKore A in this engine, SuperKore steels are being used in other aircraft power plants.

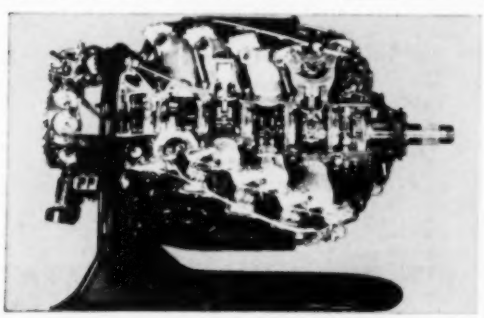

Heavy-duty truck transmission gears and rear differential gears and pinions such as these are made of U·S·S SuperKore AA.

COLUMBIA-GENEVA STEEL . . . . TENNESSEE COAL & IRON . . . . UNITED STATES STEEL SUPPLY, WAREHOUSE DISTRIBUTORS

Division of **UNITED STATES STEEL COMPANY, PITTSBURGH**

UNITED STATES STEEL EXPORT COMPANY, NEW YORK

U·S·S Carilloy Steels

Electric Furnace or Open Hearth · Complete Facilities in Chicago and Pittsburgh

2-415

UNITED STATES STEEL

Books for Engineers

Foundry Work, prepared in cooperation with the Textbook Committee, Educational Div., American Foundrymen's Society. *John Wiley & Sons.* $1.75. 108 pp.—This text is intended to teach the principles of foundry practice by referring to the several phases of the industry in a general way, and by arranging a series of molding problems that will show practical applications. A glossary and a list of foundry job classifications are included.

Plastics Molding, by John Delmonte. *John Wiley & Sons.* $9.00. 493 pp.—The book, approaching the subject from an engineering viewpoint, offers a carefully planned analysis of the plastics molding industry and its equipment. The application of scientific principles to molding processes is shown.

Analysis of Electroplating and Related Solutions, by K. E. Langford. *Electroplating and Metal Finishing.* $8.00. 357 pp.—A practical book for all concerned with the operation of electroplating, anodizing and related solutions. Over 300 methods for determining principal constituents and impurities are indexed and cross referenced, and chapters on sampling, cleaners, etches are included.

The Engineer's Illustrated Thesaurus, by Herbert Herkimer. *Chemical Publishing Co.* $6.00. 572 pp.—This book contains over 3000 illustrations of machine elements for the engineer, designer, draftsman and manufacturer, and where necessary an explanation of the function of the part is given. Typical subjects covered are fasteners, combustion, industrial processes, transmission of liquids and gases.

Corrosion—Causes and Prevention, by Frank N. Speller. *McGraw-Hill Book Co.* $10.00. 606 pp.—This revised edition endeavors to give a comprehensive view of the subject. Technical detail has been restricted to that necessary for a sound understanding of the many factors involved in corrosion and the principles of corrosion prevention, mainly in relation to ferrous metals.

Inventions and Their Management, by Alf K. Berle, L. Sprague de Camp. *International Textbook Co.* $7.50. 472 pp.—This comprehensive work presents the principles and practices governing the technical, legal, and business procedures of invention. Numerous illustrative cases from actual experience are given.

Chemical Trade Names and Commercial Synonyms, by Williams Haynes. *D. Van Nostrand Co., Inc.* $5.50. 279 pp.—More than 20,000 special names are listed for chemicals and chemical specialties sold in the industrial field. Commercial synonyms are distinguished from trade names. In the case of trade names the manufacturer is indicated, and for all listings the compositions are given, as far as is known, and uses are indicated.

ORDER YOUR BOOKS THROUGH AIME—Address Irene K. Sharp, Book Department. Ten per cent discount given whenever possible. Order Government publications direct from the agency concerned.

Manufacturing Processes, by Myron L. Begeman. *John Wiley & Sons.* $6.00. 605 pp.—This volume presents technical fundamentals of the important manufacturing processes, discusses engineering materials, and describes the machine tools necessary for processing these materials. New material in this third edition includes continuous casting of metals, hydrodynamic forming, plastic molds, special welding techniques, jigs and fixtures, and automatic and semi-automatic production machines.

Materials Handling, by Harry E. Stocker. *Prentice-Hall, Inc.* $5.00. 330 pp.—The fundamental principles involved in the economical handling of those materials not handled in bulk, and the equipment and methods used, are described and explained. A large amount of information about trucks, tractors, conveyors, cranes, and other equipment is provided.

Thermodynamics, by Alfred W. Porter. (Methuen's Monographs on Physical Subjects). *John Wiley & Sons.* $1.50. 124 pp.—The opening chapter of this small book gives a historical account of the laws and other basic aspects of thermodynamics. The remaining four chapters present the text material under the following headings: Reversible changes; miscellaneous applications; irreversible operations; equilibrium.

Modern Pyrometry, by Charles H. Campbell. *Chemical Publishing Co.* $4.00. 150 pp.—This book deals with the relatively common as well as the new techniques in pyrometric practice and equipment. It describes in detail the construction and operation of selected types of apparatus including indicating, recording, and controlling devices, and also covers the care and maintenance of pyrometers.

Company Procedural Manual on Equipment Analysis. *William Kelly & Co.* $5.00. 45 pp.—This manual provides basic instructions on a procedure for determining the economic advantages of new equipment, replacement, and plant expansion, based on researches of the Machinery & Allied Products Institute.

PROFESSIONAL SERVICES

Limited to AIME members, or to companies that have at least one AIME member on their staffs. Rates $40 per year per inch.

ST & CO. INC.
ENGINEERS
CONSULTANTS
METALLURGISTS
Small Jobs Welcomed
SAM TOUR & CO., INC.
Laboratories and offices
44 Trinity Place, New York 6, N. Y.
Testing—Certifying
American Standards
Testing Bureau, Inc.

LEWIS B. LINDEMUTH
Consulting Engineer
140 CEDAR STREET NEW YORK 6, N. Y.
STEEL PRODUCTION
DESIGN · OPERATION · CONSTRUCTION · METALLURGY

R. S. DEAN LABORATORIES, INC.
Consulting Research Development
Chemistry, Electrochemistry & Metallurgy. Laboratory Research on a Contract Basis
5810—47TH AVENUE AP. 2821
RIVERDALE, MD.

MAX STERN
Consulting Engineer
150 Broadway New York 7, N. Y.

T. STARLING WINTERS
Consulting Engineer
100 East Palisade Ave. Englewood, N. J.

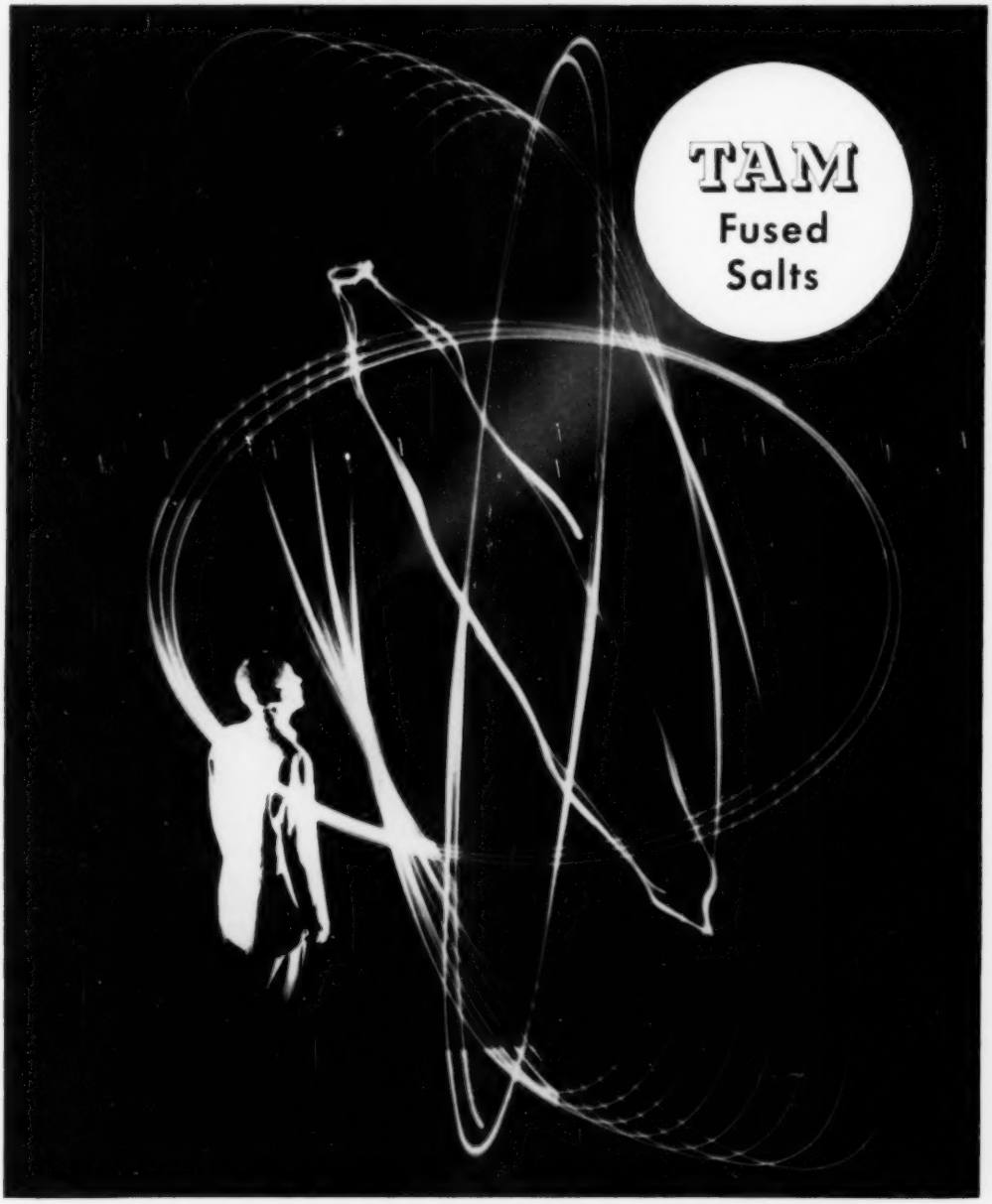

HAVE YOU INVESTIGATED THE ADVANTAGES OF TAM FUSED SALTS RECENTLY?

These TAM products are finding increasingly successful use as a source of zirconium for magnesium alloys. By refining grain size, they help improve strength in castings and eliminate problems in extruding bars. Ask our field engineers for details or write us at New York.

*TAM is a registered trademark.

TAM PRODUCTS

Registered U. S. Pat. Off.

TITANIUM ALLOY MFG. DIVISION
NATIONAL LEAD COMPANY

Executive and Sales Offices: 111 BROADWAY, NEW YORK CITY
General Offices, Works and Research Laboratories: NIAGARA FALLS, N. Y.

Techniques improved with alloy powders

TITANIUM ZIRCONIUM

BASES --→ of many MH alloy powders

Vastly improved techniques in development of alloys are made possible by the use of alloy powders incorporating titanium and zirconium. From these base powders many true alloy powders are available in varying percentages. Among these are chromium, nickel, cobalt etc. Each particle or grain is a true alloy obviating the need of diffusion during the sintering process.

Write today — without obligation — for further technical information.

METAL HYDRIDES INC.

12-24 CONGRESS STREET • BEVERLY • MASS.

Industrial Notes . . .

• The Johnson Bronze Co., New Castle, Pa., opened its No. 2 plant designed for a new method of cladding bearings with aluminum, which is in the experimental stage. The plant has two electric and two gas furnaces, and will also be used to produce universal bronze bars by both the chill and centrifugal casting process.

• *Eleven companies in the metals field were among the 298 firms in the United States and Canada that were awarded Certificates of Management Excellence for 1951 by the American Institute of Management. Cited were New Jersey Zinc Co., St. Joseph Lead Co., Aluminum Co. of America, the American Metal Co., Ltd., International Nickel Co. of Canada, Ltd., Kennecott Copper Corp., National Lead Co., Phelps Dodge Corp., Union Carbide & Carbon Corp., the Consolidated Mining & Smelting Co. of Canada, Ltd., and U. S. Smelting, Refining & Mining Co.*

• As part of the $140 million expansion program at its Indiana Harbor plant, Youngstown Sheet & Tube Co. awarded a contract to United Engineering & Foundry Co. for a 56-in. tandem cold rolling mill and two skin-pass mills.

• American Metallurgical Products Co. will move its manufacturing facilities for the production of metallurgical silicon carbides from Hays, Pa. to a new and larger plant in Newcastle, Pa. General offices of the company, which also supplies rare earth metals for steelmaking, will remain in Pittsburgh.

• **Allegheny Ludlum Steel Corp. has changed the name of its carbide production and sales units from Carbide Alloys Div. to Carmet Div. Carmet Div. is a principal producer of tungsten and other sintered carbides.**

• Shenango Alloy Tube Co. of Sharon, Pa. will build a large plant addition to make precision alloy tubing for the defense program. A loan has been granted by the RFC for this project.

• *The new 66-in. high lift blooming slabbing mill at Pittsburgh Steel Co. has been completed. Other projects expected to be completed this year are an increase in blast furnace capacity of 100,000 tons annually, a ½ million ton annual increase in open hearth capacity, installation of a 66-in. continuous hot-rolled strip mill, and installation of a 66-in. four-stand tandem cold rolled strip mill.*

• Eriez Mfg. Co., producers of magnetic separation and magnetic steel handling equipment have purchased the Erie, Pa. plant of Northern

• • • •

Equipment Co., a division of Continental Foundry & Machine Co. Northern will transfer to the former Talon, Inc. plant in Erie.

• Reynolds Metals Co. will build a new aluminum reduction plant at Gum Springs, Ark., that will have an annual capacity of 110 million lb of metal. The plant will have potrooms more than ¼ mile long, and will utilize the Soderburg process. A carbon electrode plant and a laboratory will also be built. Aluminum bus bars will be used for power transmission to the aluminum cells in the pot lines. Alumina will come from the company's alumina plant at Hurricane Creek, Ark. In addition, new facilities to be installed at the company's plant in Longview, Wash., will increase primary aluminum capacity there from 63 million to 100 million lb. Reynolds expects to produce 829 million lb of aluminum by 1953.

• Sharples Chemicals Inc. has combined with Pennsylvania Salt Mfg. Co., but will continue to operate as a separate unit of Pennsalt.

• *Basic Refractories, Inc., and its wholly owned subsidiary, Defense Project, Inc., will construct a processing plant at Narlo, Ohio. The plant will have an annual capacity of 320,000 tons of refractory dolomite and will be built under an agreement with the Defense Materials Procurement Administration.*

• P. R. Mallory & Co., Inc., Indianapolis, announced a $2½ million expansion program to provide new facilities for its capacitor, and metal and ceramic units.

• *Jet engines for the Navy will be produced in a $50 million plant to be built at Romulus, Mich., by Ford Motor Co. Fabrication and sub-assembly of engine parts will be done by Lincoln-Mercury Div. at its Wayne, Mich. plant, now under construction. Lincoln-Mercury will build and operate the Romulus plant, which will be owned by the Navy.*

• Koppers Co., Inc. is building a pilot plant to make gasoline from coal by hydrogenation. The process uses powdered coal in a slurry, with reactions taking place under high pressure. New laboratories for the company are nearing completion at Verona, Pa.

• Research and Development Board, Dept. of Defense, predicts that research and development expenditures in the U. S. during 1952 will reach $2.93 billion, of which $1.64 billion will come from the government. Of these funds, $1.82 billion will be used by industry, $280 million by universities, and $830 million by the government.

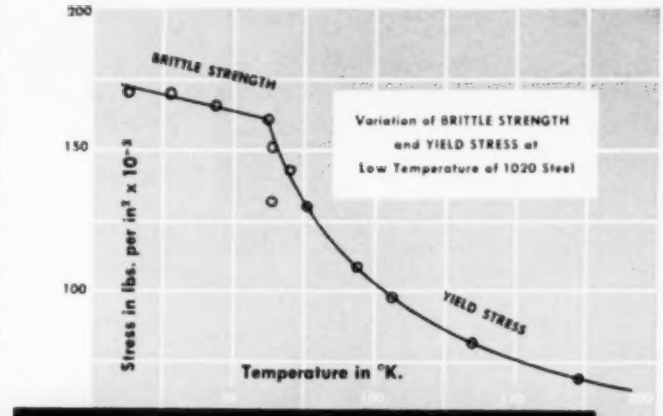

1020 Steel at 61.5°K.

A need for measurements of brittle strength as a function of temperature prompted the results shown in the curve above. Several samples of hot-rolled 1020 steel were tested at various temperatures in the interval 12°K. to 61.5°K. All exhibited brittle fracture with no reduction in area. At 75°K., however, a definite yield point was observed and the increase in length before rupture was unexpectedly large. Several additional specimens were broken at temperatures lying between 61.5° and 75°K. The results indicate a sharp transition near 61.5°K., below which no reduction of area occurs and above which the reduction of area increases rapidly as the temperature at which the sample is broken rises above 61.5°.

The ADL Collins Liquid Helium Cryostat, by providing test chamber temperatures from ambient to —271°C., makes many research projects like this possible. Superconductivity, resistance minima in metals at low temperature, and thermal conductivity are a few of the studies utilizing the ADL Collins Cryostat, the basic tool of a new research frontier.

For further information request Bulletin JM-1
including details of the Collins Helium Cryostat and a reprint of "Fracture and Yield Stress of 1020 Steel at Low Temperatures" by A. S. Eldin and S. C. Collins.

ADL Mechanical Division

ARTHUR D. LITTLE, Inc.
Mechanical Division
30 MEMORIAL DRIVE • CAMBRIDGE, MASS.

How to make MORE steel with LESS FUEL

IT'S been proved many times that the Morgan-Isley equipped regenerative furnace will outperform the conventional natural draft furnace in many ways. The Morgan-Isley produces more because it speeds up the furnace. The Morgan-Isley reduces fuel consumption because it provides a constant, measured flow of high temperature combustion air.

The Morgan-Isley System has decreased fuel consumption more than 15% and increased production more than 12% as compared to ordinary natural draft furnaces in the same shop.

Let's get together and talk Morgan-Isley in relation to your problem.

MORGAN-ISLEY
Regenerative Furnace Control

CCC-29

MORGAN CONSTRUCTION COMPANY WORCESTER, MASS.

ROLLING MILLS • MORGOIL BEARINGS • REGENERATIVE FURNACE CONTROLS • EJECTORS • PRODUCER GAS MACHINES

PITTSBURGH, PA., 2815 Koppers Bldg. *English Rep.*, International Construction Co., 56 Kingsway, London W. C. 2, England

THE DRIFT OF THINGS

by Edward H. Robie

THOUGH the final figures are not available as this is written, it seems certain that the Institute accounts will show $7000 to $8000 surplus for the year 1951. This is the first time this has happened since 1941. No money had to be taken from any of the Funds to bring about this happy condition. Furthermore, the amounts allowed for depreciation, bad debts, and inventory adjustment were more liberal than in the past.

Income increased some $29,000 over 1950. Dues received from old members increased moderately, but dues from new members dropped off $2000 and from initiation fees quite severely—from $17,000 to $11,000. The number of new members did not come up to expectations and a change in procedure caused a delay in getting some of them on the rolls. A large number of the new members paid an installment of $5 on their initiation instead of the full $20. Junior Members, of course, pay no initiation fee.

Brightest spot in the income picture was the increase in advertising income—from $103,000 in 1950 to $143,000 in 1951. All three of the journals shared in this, Mining being up $18,000; Metals, $9000; and Petroleum $13,000. Nonmember sales of the journals dropped off slightly, and sales of Transactions volumes more so—from $35,000 in 1950 to $27,000 in 1951, with a further drop of $5000 accounted for by a change in accounting procedure. On the other hand, sales of other publications increased by $10,000.

Expenditures in 1951 increased by only about $6000 over 1950, an exceptionally good showing in view of the decrease in the value of the 1935-39 dollar from 58¢ at the end of 1950 to 53¢ at the end of 1951. This decrease means higher prices for the things the Institute has to buy; especially, higher salaries have to be paid for the office help who do the work at Institute headquarters and in its branch offices.

A marked saving in publishing costs was made because no Directory of members was published in 1951. This cost $19,000 in 1950 but the officer and committee list issued last year cost only $2000.

Expenses chargeable to technical Divisions and Branches increased from $39,000 in 1950 to $54,000 in 1951, the increase being chiefly in the Mining Branch. One reason was that the expense of the Salt Lake City office was all met out of operating income in 1951, whereas its cost was taken out of income in the Barron Fund in 1950.

Expense for the three journals dropped $11,000. This is quite surprising considering the high quality that was maintained. It shows particular care on the part of the editorial and publishing staffs in condensation and editing of articles, and avoidance of luxurious printing practices. Costs of both the Mining and Metals journals decreased, but improvement in the Petroleum journal increased its cost about $7000.

Compared with 1950, general and administrative salaries, and accounting and membership department expenses increased from $93,000 to $95,000, a most modest increase in view of the higher salaries that had to be paid. A saving of $8000 was made in the pension account because of staff changes. Miscellaneous expenses increased $5000; the allowance for depreciation of equipment, furniture, and fixtures, including adjustment for prior years, accounted for $12,500 added expense; and a reserve was set up of $3000 for bad debts, an accumulation of some years.

Branchwise, the Petroleum Branch again, as in 1950, operated on practically a balanced budget as between income and expense. The Mining Branch had a surplus of $35,000 compared with $24,000 in 1950; and the Metals Branch decreased its deficit from $42,000 in 1950 to $27,000 in 1951.

Emphasis in 1952 must be made on increasing income in two main directions: Increasing the advertising, and getting more new members. The latter not only adds dues and initiation income, but adds to the circulation of the journals thus making them better advertising media. In 1950, 21 pct of the AIME income came from advertising and 63 pct from dues and initiation; in 1951 the respective figures were 28 pct and 59 pct. Contrast these figures with those of a sister society, such as the American Society of Mechanical Engineers for instance, which last year received 41 pct of its income from advertising and only 40 pct from dues and initiation fees, even though it has 37,500 members and its dues, for the Member grade, are $25.

By getting more new members and more advertising the expected continued increase in costs due to inflation may be met. Other avenues of income also will be studied. Publication of a Directory in 1952 will add a substantial item to costs. On the whole, it would seem that a surplus should be shown again in 1952 but it will probably be only a modest one, as it was last year.

It would appear that there is little hope, before 1953, of doing much in the way of rebuilding the Institute's funds available for meeting deficits. They almost reached the vanishing point in 1950.

AIME Fall Meeting in Chicago

Plans have been concluded for the dates and location of the AIME Fall Meeting in Chicago next September. This will be in connection with the Centennial of Engineering celebration, which is to cover the first two weeks of the month. A total of 51 engineering organizations will hold meetings during that fortnight.

AIME technical sessions will be held in the Palmer House on Friday and Saturday, September 5 and 6, with a dinner-dance Saturday night. One or more Divisions, that contemplate an extensive program with field trips, may add Thursday, the 4th, to their meeting dates. Already, the Industrial Minerals Div. and the Minerals Beneficiation Div. are definitely planning to participate; the Mining, Geology, and Geophysics Div. is almost a certainty; and several other Divisions planned to make their decision at the Annual Meeting.

The dates selected will enable those who attend to have Sunday for visiting the Museum of Science and Industry, where many special engineering exhibits will be installed. On Monday and Tuesday following, there will be special convocations on the metals industries, with leading speakers, arranged by the Centennial committee. On Wednesday night there will be a banquet for the entire engineering group, which should attract several thousand people.

It looks as though Chicago should be included in the vacation plans of all engineers in 1952.

NICKEL-CHROMIUM MOLYBDENUM STEEL VALVE CASTING

Retains Stamina after 50,000 Hours at 900° F!

After exposure to steam at 900° F. for more than 6 years, a Lunkenheimer gate valve cast in nickel-chromium-molybdenum steel was made available for study through cooperation of The Detroit Edison Company.

Despite its long continuous service, examination of specimens taken at random, including sections of welds, revealed the following characteristics:

NO LOSS OF STRENGTH
NO EMBRITTLEMENT
NO OCCURRENCE OF GRAPHITE

This confirms extensive laboratory tests and provides convincing evidence that valves and fittings cast in nickel-chromium-molybdenum steel, conforming to requirements of grade WC-4, ASTM Specifications A-217, will adequately meet the severe conditions imposed by steam at high pressures and temperatures up to 900° F.

At present time, the bulk of the nickel produced is being diverted to defense. Through application to appropriate authorities, nickel is obtainable for the production of engineering alloy steels for many end uses in defense and defense supporting industries.

MANUFACTURED BY THE LUNKENHEIMER COMPANY, Cincinnati 14, Ohio, the valve selected for test was identical to the 4-in. gate valve shown above. Before removal for study, it served continuously for 53,810 hrs. at a nominal temperature of 900° F. and at an average pressure of 841 p.s.i.

INCO

THE INTERNATIONAL NICKEL COMPANY, INC. 67 WALL STREET NEW YORK 5, N. Y.

The first hot extrusion plant designed specifically to produce seamless stainless steel tubing by the "Ugine-Sejournet" extrusion process is in operation by Tubular Products Div., Babcock & Wilcox Co., Beaver Falls, Pa. Outstanding feature of this method is the use of glass as a lubricant for the hot worked metal and as an insulator to protect the die system. The plant is licensed by Comptoir Industriel d'Etirage & Profilage de Metaux, Paris, developers of the process.

Proposals for basic research projects to be contracted with the Office of Ordnance Research, established by the Army Ordnance Corps, are being solicited from staff members of educational and other research institutions. Information concerning preparation of proposals or details of the program can be obtained from Office of Ordnance Research, 2127 Myrtle Drive, Duke Station, Durham, N. C.

Iron ore shipments from U. S. Steel's Cerro Bolivar in Venezuela are expected to begin in 1954. Orinoco Mining Co., U. S. Steel's subsidiary operating the property, has awarded contracts for the construction of mine facilities to Constructora Bechtel, S. A.

Anaconda Copper Mining Co. will supply uranium to the AEC from an ore processing plant to be built at Grants, N. Mex. A market will be provided at the plant site for uranium ore produced by other operators in the area. American Smelting & Refining Co. will operate the purchasing station for uranium-bearing ores established by the AEC at Shiprock, N. Mex.

A new record in blast furnace production of pig iron and ferroalloys was set in 1951 with 71,232,761 net tons. This is an increase of 5,700,000 tons over the previous record set in 1950.

Aluminium Ltd. will expand bauxite-alumina production in Jamaica by 150 pct, from 200 to 500 short tons per day. Alcan's new aluminum smelter at Kitimat, B. C., which will have an initial capacity of 90,000 short tons of aluminum, will receive the bulk of the Jamaica shipments.

Production of slab zinc by U. S. smelters was 931,833 tons in 1951, 2 pct above the previous year. Domestic requirements of zinc concentrates for 1952 are estimated at 1,100,000 tons of recoverable zinc.

Ohio Manganese, Inc. will build a $2¼ million plant to recover manganese from open hearth slags.

The first detinning plant to be owned and operated by a steel company was put in operation by Weirton Steel Co., Div. of National Steel Corp. Capacity of the plant will be 300,000 lb of tin and 30,000 tons of high quality scrap per year, utilizing steel scrap from Weirton's tin mills.

Curtiss-Wright Corp. has asked the Air Force to install a 12,000 ton extrusion press at its Buffalo plant. The company proposes to press out 12-ft propeller blades for turbo-prop power plants for transonic and supersonic planes.

The creep resistance of magnesium-thorium alloys in the range of 500° to 600°F is the highest observed in any magnesium alloy.

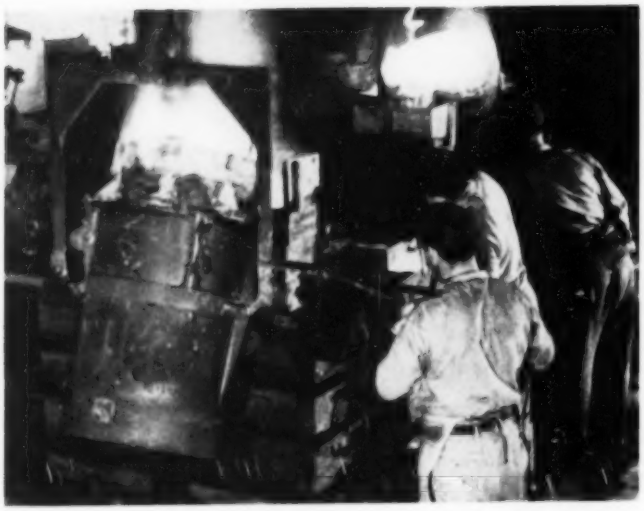

Two crucibles are used to pour this 950-lb magnesium casting, which will be part of a large pump

Lighter Designs Possible With

Magnesium-Rare Earth Casting Alloys

by J. C. McDonald

RARE earth metal alloy additions have particular merit in magnesium casting alloys for service at elevated temperatures. The Mg-Al-Zn type casting alloys that have been made for many years can be used efficiently at elevated temperatures, depending on the magnitude of the stresses imposed. However, somewhere between 200° and 400°F, a lighter design usually can be accomplished if a magnesium-rare earth metal alloy can be used. This will be true particularly when the operative stresses are high enough so that wall thicknesses greater than the minimum that can be cast are necessary.

Consideration of mechanical properties, as well as service experience, indicates that creep must be taken into account in designs that are to operate at elevated temperature. Loads are applied to castings, as used on jet engines for example, that persist over the several hundred hours, during which the engine is expected to give satisfactory service. These stresses can arise from the weight of the engine and from the maneuvers of the airplane, as well as from differential thermal expansion. Over a long period of time the material will deform gradually until satisfactory functioning is lost. It is not correct to speak of the range of service of an alloy in terms of temperature alone. The stresses and the times of operation should be known for both peak and normal conditions to determine what material will be required.

Again, from laboratory data as well as service experience, problems of fatigue strength probably are much less important at elevated temperature than they are at lower temperatures. At lower temperatures the vibrating component of service loads may eventually cause fracture by the fatigue process, but in the hot engines of today it is more likely for the gradual deformation attributed to creep to cause eventual scrapping of the part. Although much data from fatigue tests in the laboratory have been gathered, the application of these data to actual ser-

J. C. McDONALD is Assistant Technical Director, Magnesium Dept., The Dow Chemical Co., Midland, Mich. This paper was presented at the Magnesium Assn. Meeting in New York, Nov. 15, 1951.

For additional information on the use of the rare earth metals as alloying agents read the following articles that appeared in JOURNAL OF METALS: *"The Properties of Sand Cast Magnesium-Rare Earth Alloys," December 1949, June 1951; "Extrusion of Powdered Magnesium Alloys," February 1950; "Effect of Rare Earth Metals on Properties of Extruded Magnesium," November 1951; and "Hot Workability of Stainless Steel Improved by Adding Cerium and Lanthanum," November 1951.*

vice is somewhat uncertain. At this time it is felt that laboratory creep data can be related more directly to service performance than can fatigue data.

The material must have strength to withstand steadily applied loads that may act for short periods of time only, but which may be considerably higher than the loads that produce gradual creep over long periods of time. Rational design is possible only when the magnitude of the stresses generated by these loads, as well as the temperature, can be stated. These stresses can be compared to the yield strength, determined by static test at temperature.

Other properties that are measured routinely in static testing at elevated temperature are tensile strength and elongation. It is not apparent that these properties have any close or direct relation to the service of parts at elevated temperatures. Elongation is usually considerably higher than it is at room temperature and the tensile strength is higher than the yield strength.

In the interest of maximum quality and minimum cost, casting alloys should be as easy as possible for the foundry to handle. Many factors are involved: The amount of protection which the magnesium alloy requires during melting and pouring; the complexity of the rigging required to insure good internal soundness as well as external surface quality; and the fluidity of the alloy.

If it is possible to use the alloy without any further heat treatment, an additional advantage cost-wise may be gained. As is well known, the more highly alloyed engineering materials are hardly ever sold without some kind of heat treatment.

Finally, the cost and availability of the ingredients from which the alloy can be made will determine the cost of the alloy and the ease of its procurement in times of national emergency. Again, some of the most desirable improvements in alloys can be brought about only through more expensive constituents.

Magnesium-rare earth metal alloys were investigated many years ago in Germany. A review of what was known at the time is contained in Beck's *Technology of Magnesium*, published in 1939. Research in this country and abroad has resulted in a number of technical publications. In the last few years cast alloys have become commercially available. They all use Zr as a second essential alloying element. This element refines the grain of the casting, thus preventing cracking during freezing, and also improves the properties.

The main cast alloys now being produced commercially contain about 3 pct rare earth metal as *mischmetal* as shown in Table I. At its current price of $4.50 per lb, it is evident that alloys containing mischmetal will cost more than those using Al or Zn, everything else being equal. While the price of Zr in compounds is not high, the actual cost of Zr in the casting is a function of the efficiency of alloying obtained in each foundry. From the foundry standpoint, 0.25 pct Zr is adequate for grain refining.

Table I. Composition and Heat Treatment

Designation	Alloy, Pct Zr	Alloy, Pct Other	Heat Treatment: Solution	Heat Treatment: Precipitation
EK30A-T5	0.25	3M	—	400°F, 16 Hr
EK30A-T6	0.25	3M	1050°F, 16 Hr	400°F, 16 Hr
EK31A-T5	0.55	3M	—	400°F, 16 Hr
EK31A-T6	0.55	3M	1050°F, 16 Hr	400°F, 16 Hr
EZ33A-T5	0.7	3M, 3Zn	—	350°F, 12 Hr
EK31D-T6	0.55	2Di[2]	1000°F, 16 Hr	400°F, 16 Hr
JK31A-T6	0.7	3Th	1050°F, 2 Hr	400°F, 16 Hr

[1] M — Mischmetal: Ce, La, Nd, Pr.
[2] Di — Didymium: Mischmetal minus Ce and La.

With respect to mechanical properties, Table I lists several of the alloys and heat treatments that are in current use. Table II compares properties of separately cast test bars of these materials as well as some other alloys and conditions of heat treatment. Table III compares the properties of bars cut from castings of three of the present alloys.

As can be seen from these tables, there are several alternative ways of achieving creep strengths at elevated temperature that are much higher than can be obtained in the Mg-Al-Zn type of alloy (a comparable value at 400°F would be 1500 psi for example, compared to about 8000 psi for the rare earth metal alloys). Either low or high Zr may be used. A solution heat treatment may or may not be used, but a precipitation heat treatment is used in all cases. One alternative composition also contains 3 pct Zn. In general, the T6 heat treatment will cost more than the T5, in the same alloy, because of the extra solution heat treatment. Likewise, the higher Zr will cost more than the lower Zr. EK31A and EZ33A have been recommended by some for use in the T5 temper. EK30A and EK31A have been recommended by others for use in the T6 condition.

Referring to the laboratory data in Table II, it is evident that the creep strengths of the mischmetal containing alloys are quite comparable; and it is concluded that they should all function equally satisfactorily at elevated temperature. There is some difference in respect to tensile properties which might lead some designers to choose one or the other of these compositions on the basis of small differences shown. In actual practice, EK30A-T5 has not come into commercial use. On the basis of bars cut from castings, Table III, the comparison is

Table II. Properties of Separately Cast Test Bars

Alloy	Tensile Strength, 1000 Psi: Temperature, °F 70°	400°	600°	Yield Strength, 1000 Psi: Temperature, °F 70°	400°	600°	Elongation, Pct: Temperature, °F 70°	400°	600°	Stress for 0.2 Pct Total Extension in 100 Hr, 1000 Psi: Temperature, °F 400°	600°
EK30A-T5	29	20	10	15	12	7	0.5	16	56	7.4	1.6
EK30A-T6	27	20	12	16	14	7	3	18	56	7.2	1.5
EK31A-T5	22	20	12	17	13	7	2	20	60	7.7	1.3
EK31A-T6	23	21	13	19	16	9	4	19	78	8.0	1.5
EZ33A-T5	22	21	12	16	10	8	3	21	50	7.5	1.4
EK31D-T6	32	21	12	16	10	8	2	21	50	7.5	1.4
JK31A-T6	38	27	15	21	20	15	7	16	51	9.0	1.3
	29	24	19	18	14	13	4	21	10	11.2	3.1

Table III. Properties of Bars Cut from Castings

	EK30A-T6		EK31A-T6		EZ33A-T5	
	Min	Avg	Min	Avg	Min	Avg
70° F						
Tensile Strength, 1000 Psi	14	18	18	22	16	20
Yield Strength, 1000 Psi	12	14	14	15	12	14
Elongation, Pct	0.5	1.0	1.0	3.5	1.0	2.5
400° F						
Tensile Strength, 1000 Psi	14	16	15	17	16	18
Yield Strength, 1000 Psi	9	11	10	12	9	10
Elongation, Pct	2	6	4	12	7	14
Stress for 0.2 Pct Ex.						
Stress, 100 Hr, 1000 Psi	9.0	8.9	8.8	9.8	5.8	9.0
400° F						
Tensile Strength, 1000 Psi	10	11	10	11	11	11
Yield Strength, 1000 Psi	5	7	5	7	6	7
Elongation, Pct	15	39	30	51	25	44
Stress for 0.2 Pct Ex.						
Stress, 100 Hr, 1000 Psi	1.1	1.8	1.2	1.8	0.8	1.6

very close. The range of creep strength reported is based on the scatter observed in over 40 tests.

Experience has shown that these alloys behave similarly in the foundry. While offering more difficulties in respect to control of composition, and oxidation, than the older alloys, these factors can be and are controlled. The alloys are much easier to produce free from internal shrinkage than the older alloys. The factor for shrinkage from pattern dimensions is higher for these alloys than for the Mg-Al-Zn alloy. This makes it difficult to use existing patterns on large castings. Service experience with corrosion has been satisfactory to date on all these alloys. Laboratory tests on corrosion resistance in salt water appear to rate them in order of increasing resistance: EZ33A, EK30A, EK31A.

Published work by Leontis in respect to didymium, and by Sauerwald, as well as Leontis, in respect to Th, has indicated certain merits of these materials for magnesium base alloys intended for use at high temperature. In Table II the last two lines compare laboratory data on selected compositions containing these metals, as well as Zr. While use of didymium does produce superior tensile properties up to 400° F it is noteworthy that the alloy with Th not only has equal or superior tensile properties compared to the rare earth metal alloys at all temperatures up to 600° F, but in addition possesses a much higher creep strength at 600° F. The primary need for future development is an improvement in the creep strength at temperatures above 400° F. For this reason research and development should be concerned with bringing the Th containing alloys into production. Work on this subject is proceeding and looks promising.

Alloying Methods

Mischmetal usually is added to these alloys as a metallic substance which can be bought on the open market. The literature contains references to other methods of adding rare earth elements. Zr, on the other hand, while alloyable in metallic form, is usually alloyed from Zr containing salts.

Sauerwald and Zeppelin in Germany used $ZrCl_4$ added to Mg as a source of Zr. The Mg reduces the $ZrCl_4$, liberating Zr and $MgCl_2$. In work on these alloys in this country it was recognized early that, because of the favorable economics of the $ZrCl_4$ reduction in terms of raw materials and substantial reduction efficiency, the problem of possible inclusions caused by the saline reaction products had to be eliminated.

The best evidence that this problem has been effectively solved and that high Zr can be added is that for more than five years Mg-6Zn-0.7Zr alloys have been produced and sold in extruded form, and satisfactory service was obtained in a number of aircraft parts with no corrosion troubles. A smaller amount of Mg-mischmetal-Zr alloy castings has been made by this process and sold with satisfactory service results.

The process used for making the bulk of this material depended on the use of one of a mixture of salts (about 50-50 $ZrCl_4$ and KCl or KCl + NaCl) in which $ZrCl_4$ is reduced by Mg at an average direct (single use) efficiency of about 30 pct.

With the advent of commercial usage of cast Mg-rare earth metal-Zr alloys some modifications were required in the foundry because of the nature of the melting processes. The first approach was the offering of metal hardener alloys of Mg-high rare earth metal. Special fluxes containing no $MgCl_2$ (to prevent loss of rare earth metal), and inspissating agents such as CaF_2, were used to refine the metal and eliminate inclusions by controlling the composition and consistency of the flux phase.

A further improvement consists in using a hardener which again depends on $ZrCl_4$ in the salt mixture as the Zr source. A hardener alloy of Zr and Mg is produced separately by direct reaction of an excess of Mg with the $ZrCl_4$. This hardener mixture is then added, either liquid as made or after cooling and storing, to the Mg alloy to produce or maintain the Zr content desired. This material alloys readily and with reasonably good efficiency. It eliminates to a large extent the reaction product salts in the production foundry premelters or crucibles. Although, obviously the Zr cost is proportional to the amount of Zr in the alloy, this process permits a free choice of Zr content and can be handled through conventional tilters and crucibles with relatively low loss of either Zr or rare earth metal content. Based on rather extensive investigation and testing of alternate methods it is considered that this process is the most economical of these currently known.

With respect to the patented fluoride processes, tests based on following the patent teachings would indicate that good alloys and Zr contents can be achieved. It remains to be proved by experience whether these methods can compete on a cost basis in this country with the $ZrCl_4$ processes.

The Mg-mischmetal-Zr, Mg-mischmetal-Zn-Zr, and Mg-Th-Zr compositions discussed (as well as Mg-Zn-Zr alloys) are not patented in the United States. Certain patent applications which might have covered these alloys were seized by the Alien Property Custodian early in the last war and transferred to the U. S. Office of Alien Property. This office subsequently abandoned prosecution of the applications and published them for use by anyone interested. There are U. S. patents on other rare earth metal and Th alloys.

No such clear cut statement about patents can be made regarding the preferred method of alloying Zr by the $ZrCl_4$ reduction. It is a very active field and it is possible that new patent coverage will appear from time to time. There is considerable patent literature dating back to the late 1930's suggesting the alloying of Zr by means of $ZrCl_4$. It includes two patents issued to Zeppelin (2,214,211; 2,235,508) now owned by the U. S. Office of Alien Property, and two to Stroup and Sager of Alcoa (2,373,515; 2,373,516) which are pertinent to present practices.

Efficient Utilization Of

Titanium Alloys In Stainless Steel Production

by F. St. Vincent and R. W. Rebholz

INCREASED production of titanium-stabilized stainless steels has focused attention on the efficient utilization of ferrotitanium alloys. The ability of titanium to form stable oxides and nitrides has necessitated the adoption of modified furnace practices for obtaining reasonable recoveries.

The titanium alloys available for the production of stainless steel ingots are listed in Table I in the order of increasing titanium content. Alloy No. 3 has a higher titanium to aluminum ratio (12.5 to 1) than the other ferrotitanium alloys. This grade also is produced with a minimum titanium to aluminum ratio of 20 to 1 for applications where very low aluminum alloys are desirable. Within the range shown in Table I the melting point increases with increasing titanium content. The iron-titanium diagram shown in Fig. 1 is not a true representation of the commercial ferroalloy; however, experience indicates that the relationship between the solidus and liquidus temperatures of the various commercial alloys is approximately as indicated by the diagram. The melting point of pure titanium, which should be a good approximation of the melting point of alloy No. 5, is reported to be 3050°F.

Producers of titanium-stabilized steels have recognized the necessity for precautions in adding ferrotitanium, and have devised various melting procedures for obtaining reasonable recoveries. All practices involve normal working of the heat up to and including removal of the oxidizing slag. In general, the procedure beyond this point is to employ a lime-alumina slag prior to the ferrotitanium addition. In some instances, it is formed immediately after removal of the oxidizing slag, and is removed and replaced by a fresh lime-alumina slag just prior to the ferrotitanium addition. In others a lime-silica slag is used until the regular alloys have been adjusted; after which it is removed and replaced by a lime-alumina slag or, as in one practice, by a slag covering formed with the addition of cryolite.

The metal usually is deoxidized prior to the ferrotitanium addition by adding sufficient silicon to bring it within specification and/or by plunging aluminum into the bath. There are some cases, however, where bath deoxidation consists only of adding the final silicon required with the ferrotitanium addition.

F. ST. VINCENT is Service Engineer and R. W. REBHOLZ is Metallurgical Engineer for Vanadium Corp. of America, Pittsburgh.
This paper was presented at the Electric Furnace Steel Conference, Pittsburgh, Dec. 7, 1951.

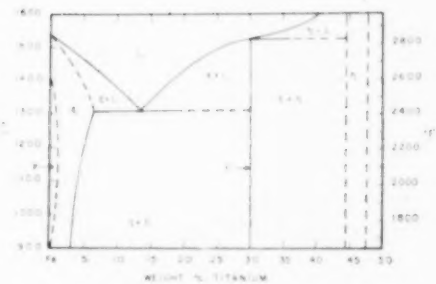

Fig. 1—Iron-titanium constitution diagram by Comstock & Southard.

In general, the difficulties experienced in obtaining reasonable recoveries probably are caused by the formation of titanium oxides. There is the possibility that a part of the titanium carbo-nitrides, formed at the time of the titanium addition, are taken into the slag. However, any appreciable loss incurred in this manner would be evidenced in a reduction of the carbon and nitrogen contents of the steel. No such evidence has appeared. The possibility of titanium losses through vaporization have been considered. In the production of ferrotitanium, however, no ten-

Table I. Titanium Alloys Available for Production of Stainless Steel Ingots

Alloy	Ti, Pct Max	Al, Pct Max	Si, Pct Max	C, Pct Max
1	20 to 25	3.5	4.0	0.10
2	26 to 29	7.0	3.5	0.10
3	27 to 32	0.08 x Ti	0.16 x Ti	0.10
4	38 to 43	8.0	4.0	0.10
5	99.5	Commercially pure titanium		

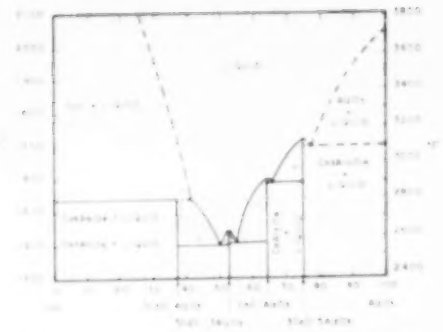

Fig. 2—Constitution diagram for the CaO-Al_2O_3 system by Rankin & Wright

dency on the part of titanium to vaporize has been detected and therefore it has been assumed that it is unlikely to occur in steelmaking. The principal problem, then, would appear to be that of controlling the oxygen in the slag-metal system. With the exception of the oxides of calcium, magnesium and aluminum, titanium will reduce any of the oxides ordinarily present in the stainless steel slag-metal system. It should be emphasized that silica is not an exception and can be reduced by titanium.

A large portion of the oxides present in the system during the oxidizing portion of the heat are removed through the first slagoff. The completeness with which this slag is removed would seem to be very important. In cases where removal is not complete, the oxides remaining must eventually be converted to oxides more stable than TiO, if titanium oxidation in the slag is to be prevented. In instances where the slag may be removed from the furnace completely, the character of the second slag (which is used until just prior to the ferrotitanium addition) would not seem critical. Where complete removal of the slag is not practical, the principal objective from the standpoint of titanium recovery is to convert the remaining reducible oxides to alumina. For this reason, it may be advantageous to form a lime-alumina slag following removal of the oxidizing slag. In most cases such a slag is formed from the addition of lime and aluminum, the aluminum serving to reduce the oxides remaining from the oxidizing slag. When aluminum is the principal source of alumina for the slag, it is necessary to add amounts in excess of that needed for reduction of oxides in order to form sufficient slag to cover the bath. The excess aluminum is assumed to oxidize in the furnace atmosphere. Under these conditions there would appear to be a definite possibility of introducing aluminum into the bath. In applications where this would be detrimental, it would perhaps be logical to form the slag from lime and a sintered bauxite low in impurities, and limit the amount of aluminum to that necessary for reduction of oxides.

The constitution diagram for the CaO-Al_2O_3 system shown in Fig. 2 indicates the necessity for close control of the slag composition to produce a low melting fluid slag. The system does not represent the slag composition, but it is a good indication of the behavior of well deoxidized CaO-Al_2O_3 slags.

Deoxidation of the bath also must be considered. The level of oxygen will not be excessively high in a bath containing the normal amount of chromium after removal of the oxidizing slag. The addition of titanium at this level of oxygen, however, would result in some deoxidation and a loss of titanium. The effectiveness of silicon as a deoxidizer under these conditions is difficult to conclude on a theoretical basis, but since it appears to be desirable to prevent the formation of silica, it seems logical to deoxidize the bath with aluminum prior to the silicon addition.

Titanium will oxidize in the furnace atmosphere and some consideration should be given to preventing such an occurrence. The melting point and fluidity of the slag seem to be important considerations in this aspect of the problem. The fluid slag will allow penetration of the ferrotitanium and protect it against atmospheric oxidation. There will be localized chilling of the slag layer when the alloy is added and a low melting point slag would be an advantage. Because the density of the alloy is lower than that of the bath, it may be assumed that it goes into solution near the slag-metal interface to produce a layer of metal relatively high in titanium. If this condition is not corrected before the heat is tapped, there is the increased possibility of titanium oxidation as the richer alloy is poured from the furnace.

The problem of titanium recoveries has been considered from the viewpoint of preventing its oxidation insofar as is possible. This approach seems necessary because of the difficulties associated with reducing titanium from its oxides. For example, in the production of ferrotitanium, the TiO_2 remaining in the slag at the end of the operation, and in presence of a substantial amount of aluminum in the metal, is considerably higher than would be found in stainless slags. A relatively high aluminum content in the ferroalloy may serve a useful purpose in steelmaking; that is, in minimizing the oxidation of titanium as the alloy goes into solution under circumstances where oxygen is available for combination with titanium. An appreciable aluminum content in the bath probably would reduce titanium losses during tapping and pouring; however, the amount necessary may be excessive from other considerations. Experience in making small induction furnace heats of titanium-bearing steels indicates that a high silicon content in the bath at the time of the titanium addition improves titanium recoveries. For example, silicon levels of 1 pct or more are associated with higher titanium recoveries than silicon levels of 0.25 or 0.30 pct. Confirmation of this finding in large arc furnaces would be interesting.

Since the high chromium content of stainless steels increases the solubility of nitrogen in the bath, some consideration should be given to controlling nitrogen. Considering the fact that titanium nitride is present in the solid steel, the extent to which its formation influences titanium recoveries is questionable. The purpose of the titanium addition, however, is to form titanium carbide, and the fact that the nitride formation takes precedence over the formation of the carbide is ample reason for controlling nitrogen.

Another aspect of titanium recovery that may warrant some consideration is the sampling of the heat for titanium analysis. The segregation of carbo-nitrides in ingots is extreme in some cases. If similar conditions are present in the cast tests taken for chemical analysis, the true titanium content can be determined only by a careful sampling of the heat. Presumably a spectroscopic pin test would be more uniform, and it would be interesting to compare the results obtained by the two sampling techniques.

Properties of Some

Bottom Ramming Materials

by M. P. Fedock

ELECTRIC furnace bottoms have been discussed frequently, and various methods and individual operators' preferences for methods and materials have been presented in detail. For example, H. C. Bigge in his paper *Bottom Building and Maintenance*, presented at the Eighth Annual Electric Furnace Steel Conference, AIME, reviewed the various methods of bottom building and the materials used as well as the change in chemistry of the bottom material after service. The discussion that followed the paper reflected the interest in electric furnace bottoms and the appreciation that their installation requires much care and supervision. In all papers and discussions on this subject, however, installation methods have been emphasized to the exclusion of any mention of the properties of the materials, except for occasional reference to chemistry, particle size or rammed density. Little data has been presented on the physical properties of the materials and their behavior on firing.

It is known that after a relatively short time of service on a newly installed bottom, its working surface becomes so changed that it bears little resemblance chemically or physically to the original installation. After a campaign, it is not unusual to find only 20 to 30 pct MgO contained in the bottom that contained 65 to 85 pct MgO when the bottom was installed. The bottom material to a considerable depth at such time is essentially burned dolomite grains cemented with furnace slag and often with a network of metal. From these observations it can be concluded that steel is made on the expendable burned dolomite dressing applied to the banks and bottom after each heat. Because of the difficulties in assessing the desirable quality and properties of burned dolomite, effectiveness of its usage, and the varied and severe conditions imposed on an electric furnace bottom, it is not surprising that bottom performance is difficult to evaluate. Therefore, the selection of method and materials for a bottom installation becomes one which enables an operator to bring his furnace back into production with a minimum of effort and time. Rammed bottoms that can be installed rapidly have, therefore, replaced burned in bottoms and are generally accepted as standard practice for electric furnaces. In addition, it is becoming common practice to periodically clean out and resurface a bottom to keep bottom difficulties at a minimum. With the present interest and acceptance of rammed bottoms and since the rammed portion of the bottom becomes the second line of defense against bottom troubles, it seems appropriate to examine and compare the properties of some proprietary ramming materials.

M. P. FEDOCK is Ceramic Engineer for Republic Steel Corp., Central Alloy District, Canton, Ohio. This paper was presented at the Electric Furnace Steel Conference, Pittsburgh, Dec. 7, 1951.

At present, studies on electric furnace bottom life, behavior, and properties are by no means complete; therefore, only a selected group of data is presented. It includes test data on six of the more popular bottom ramming materials that were selected to emphasize the wide variation in properties of the different materials.

All materials for study were taken from melt shop stock and mixed with water according to the manufacturers' instructions in preparation for ramming test briquettes. The briquettes were rammed in an AFA rammer and the number of blows of the rammer to obtain maximum density was tabulated as an indication of rammability. The least number of blows required to obtain the maximum density for the material was considered an indication of good rammability. From this procedure it immediately was apparent that a close range in water content need be maintained for maximum rammability and density for all materials. The water content accordingly was adjusted to produce briquettes of maximum density for each material and enough briquettes were made to allow duplicate testing.

Table I. Properties of Some Bottom Ramming Materials

Material	A	B	C	D	E	F
Chemistry						
MgO	94.70	83.60	84.00	83.00	82.42	70.30
CaO	0.20	—	3.40	2.80	0.90	10.00
SiO_2	2.40	—	6.80	10.88	12.76	12.00
FeO	0.17	—	0.26	0.30	0.13	0.25
Fe_2O_3	0.80	—	4.96	3.04	3.04	3.35
Cr_2O_3	0.96	—	0.00	0.00	0.00	3.49
Bulk Density, Lb per Cu Ft						
Original	152.0	171.0	154.5	165.0	140.0	147.0	153.0
4 hr at 1650°F	151.0	167.0	150.0	165.0	147.0	145.0	147.0
4 hr at 2050°F	150.0	167.0	149.0	158.0	148.0	146.0	146.0
4 hr at 2250°F	148.5	171.5	152.0	159.5	149.0	146.0	145.5
4 hr at 2500°F	152.0	173.0	158.0	165.0	168.0	158.0	148.5
2 hr at 2925°F	154.0	175.0	160.0	178.0	186.5	191.0	173.0
Apparent Porosity, Pct						
Original	13.8	9.2	24.9	15.1	24.2	26.8	21.1
4 hr at 1650°F	27.4	16.7	26.2	18.2	25.3	27.6	25.6
4 hr at 2050°F	31.9	16.7	27.5	21.2	25.2	27.0	27.4
4 hr at 2250°F	29.9	16.2	26.5	20.6	24.8	28.8	27.8
4 hr at 2500°F	28.2	16.0	18.6	19.9	18.3	22.5	26.1
2 hr at 2925°F	27.3	15.3	22.8	17.9	8.1	2.8	14.9
Cold Crushing Strength, Psi							
Original	1895	2495	530	1770	975	340	1745
4 hr at 1650°F	120	245	1235	3750	1690	1665	1205
4 hr at 2050°F	1130	1640	1780	3485	2055	3040	1575
4 hr at 2250°F	1455	1725	2140	4035	2705	2005	2665
4 hr at 2500°F	2005	2565	2910	4260	4775	3815	2155
2 hr at 2925°	2145	4080	5265	7475	14,300	14,835	7280
Shrinkage after Firing at 2925°F for 2 Hr, In. per Ft	1/8	1/8	7/16	1 11/16	1 5/16	1/8
Rammability, number of blows with sand rammer to obtain max density:	41	35	35	37	38	41

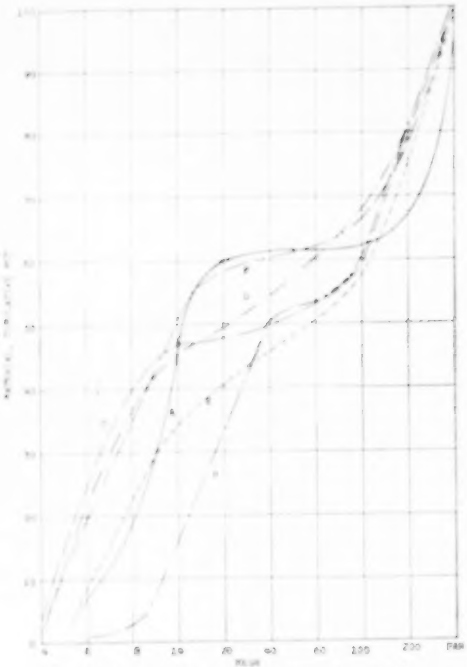

Fig. 1—Sieve analysis of various ramming materials.

The original materials were analyzed chemically and sized. Values for apparent porosity, bulk density, and cold crushing strength were obtained for the as rammed samples as well as after firing for 4 hr at 1650°, 2050°, 2250°, and 2500°F and for 2 hr at 2925°F. Shrinkage at these temperatures was determined but was nil for all materials fired below 2500°F. The firing temperatures were selected partly from past experiences with cold setting and unburned refractories and also to determine the properties of the materials at the different temperature levels that exist in a rammed bottom when it is burned in and in service. A gas fired reheat furnace with an oxidizing furnace atmosphere maintained at all temperatures was used for the test.

The results of the testing are summarized in Table I. Screen analyses for these materials are plotted in Fig. 1. Reference to the table reveals considerable differences for the various materials. Particular attention, however, is drawn to the similar properties of materials D and E. These materials have a smooth gradation in particle sizing. It is believed that the low rammed densities are caused by the particle sizing and that the manufacturers of these materials made little attempt toward sizing of the material to obtain maximum rammed density.

An increase in porosity on firing in the range 1650° to 2250°F and a subsequent decrease on firing to higher temperatures is characteristic of all materials. This trend is, of course, reflected by a reverse behavior for bulk density. That is, bulk density decreases from the original value on firing to some 2250°F and increases on firing to higher temperatures.

Material A which has the lowest porosity as-rammed shows a remarkable increase in porosity when fired to 1650° and 2050°F. This was accompanied by a marked drop in cold crushing strength. For this material, because of its high refractoriness, little shrinkage was observed even when fired to 2925°F for 2 hr. Two sets of data for this material are included to demonstrate the difference in behavior between a dense and a poorly rammed sample. It is believed the pronounced increase in porosity on firing at the lower temperatures explains the strong tendency toward heaving that bottoms rammed with this material show when being burned in. These bottoms require a slow heating rate for drying and burning.

The high densities and low porosities for several of the materials when fired to 2925°F result from a considerable amount of fusion and shrinkage. For example, material E with 191 lb per cu ft and 2.8 pct apparent porosity after firing to 2925°F for 2 hr showed a shrinkage of 1 5/16 in. per ft. In sharp contrast the relatively low porosity and slight changes in porosity of material C as well as its progressive increase in strength when fired to the various temperatures should be noted.

A rough indication of the development of liquids or pyro-plasticity in the materials at different temperatures can be gained from study of the cold crushing strength. A more pronounced impression of this behavior is the appearance of sag bars after firing at the same time under the same furnace conditions to a temperature of 2900°F in 5 hr then furnace cooling. The appearance of five of the six materials studied is shown in Fig. 2. The low refractoriness of materials D and E (80+ pct MgO) is in sharp contrast with the higher refractoriness of material C (80+ pct MgO) and the still higher refractoriness of material A (95 pct MgO). Although not included in Fig. 2, material B (80+ pct MgO) behaved exactly like material C in this test. The test pointedly illustrates that magnesia content alone is no measure of refractoriness for bottom materials and that such expressions as pct MgO or *lb* of MgO per cu ft convey little information as regards the quality or behavior of a bottom material.

To observe the behavior of the various materials under simulated laboratory testing, a furnace was constructed so that a 4½ in. thickness of material 9 in. diam could be rammed and fired from one side

Fig. 2—Sag bars of bottom ramming materials A, C, F, D, E, as they appeared after firing slowly to 2900°F and furnace cooling.

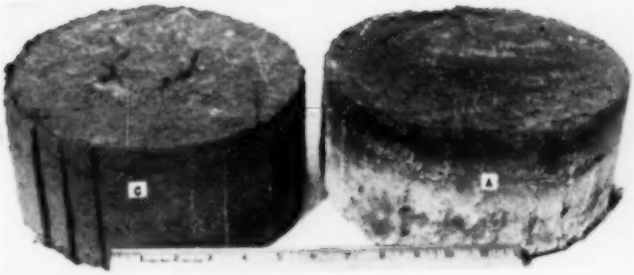

Fig. 3—Appearance of rammed test plugs of materials C and A. The top face was fired at 2950°F for 4 hr.

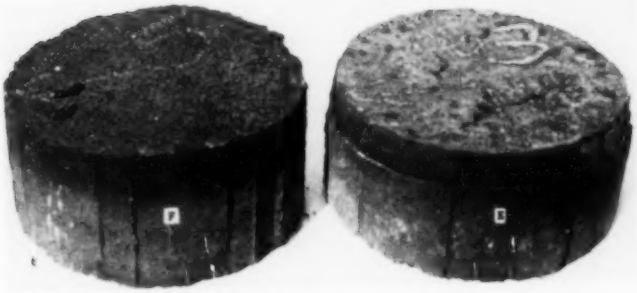

Fig. 4—Appearance of rammed test plugs of materials F and E. The top face was fired at 2950°F for 4 hr.

as is the situation when burning in a rammed bottom. The test bottom consisted of a $4\frac{1}{2}$ in. course of 2400°F insulating brick, a 3 in. course of burned magnesite and the $4\frac{1}{2}$ in. thickness of the rammed bottom plug. A roof which was esentially an enlarged burner block was placed over this bottom and the furnace fired with natural gas. The burner was so positioned that the flame travelled circumferentially around the inner portion of the roof with no direct impingement on the test plug and it was heated essentially by radiation. Many different materials were tested. The appearance of a few after firing for 4 hr at 2950°F is shown in Figs. 3 and 4. Cross-sections of materials E and F are shown in Fig. 5. The fusion and shrinkage and the resulting cracks for the individual materials as well as changes in strength are well illustrated in these test bottom plugs. In essence these test plugs completely summarize the quantitative information gained from the previously described tests and give a good impression of the behavior of a bottom on burning in.

The relatively good volume stability of material A is evident from Fig. 3. However, the material only burned in to a depth of about 1 in. and the colder portions of this plug were weak and crumbly. Material F burned in to a depth of about 2 in. and had only a narrow zone of friable material separating the burned face from the cooler bottom. The other materials were burned in throughout the $4\frac{1}{2}$ in. thickness, but the fired face and to a depth of from $\frac{1}{2}$ to $1\frac{1}{2}$ in. contained rather large cracks.

Temperatures also were taken at the bottom of the test section and a temperature drop of from 800° to 1350°F across the $4\frac{1}{2}$ in. thickness of the materials was observed after the hot face was maintained at a temperature of 2950°F for 4 hr. This phase of the studies is incomplete. It is evident, however, that sharp temperature gradients exist for basic bottom materials.

There has been no opportunity to study in detail the service behavior of these various ramming materials. In view of the differences found for the various materials, however, it seems unusual that furnace men and operators have no definite impressions on the serviceability of the different ramming materials.

Fig. 5—Cut sections of test plugs F and E are shown here.

Hydrogen Reduction Of Iron Ore

By C. A. Scharschu

SCARCITY of melting scrap and poor quality of a large part of the available scrap has created renewed interest in processes that might yield this scarce commodity. Much work has been done on the direct reduction of ore to iron and many methods and types of equipment have been tried, but no processes have passed to the commercial stage in this country.

Hydrogen reduction of iron ores has been carried out in rotary kilns, vertical shafts, pressure retorts, and mechanical rabbling furnaces. The temperatures used vary from 1100 F to the point of sticking, roughly about 1830 F. The hydrogen used ranges from a gas of 95 pct purity to a gas containing some 15 or 20 pct hydrogen. Ores of many different types have been tried. Size of ore has varied from 100 mesh up to pieces of approximately 2 in.

The reduction of ore by hydrogen is endothermic—heat must be supplied. This heat has been supplied by 1—heating the gas to the desired temperature; 2—heating the initial charge to the reaction temperature by means of carbon and air, and 3—maintaining the reaction temperature by heated reducing gases, or by heating externally or internally by means of gas as is the case with the rotary kiln. The reduction also has been carried out at atmospheric pressure and at pressures up to 2 or 3 atm.

Equilibrium is reached between hydrogen, water, and iron oxide at quite high concentrations of hydrogen. Therefore, to obtain rapid reduction and economical use of hydrogen, it is necessary to remove the reaction products from the gas and recirculate the gas. When relatively pure hydrogen is used, the product of reaction is water, which is easily removed.

Although Allegheny Ludlum was familiar with the various direct processes used for the reduction of iron ore, particular interest was evidenced in the use of fairly pure hydrogen for the reduction, and some two or three years ago small pilot tests in vertical shafts were carried on. Conclusions and appraisal of the use of hydrogen for the direct reduction of ores were necessarily tempered by this experience.

Work was carried out on a rather small scale. The largest unit employed was an alloy steel tube about 1 ft diam and 4½ ft long, heated externally by electrical means. The ore was fed by gravity, with the hydrogen passing in the opposite direction to the downward movement of the ore. With this furnace some 1200 lb of ore could be treated in a 24-hr period. The reduced ore was drawn off from the bottom through a water seal. The work covered laboratory investigation of the effect of various factors such as hydrogen concentration, which was varied from 40 to about 90 pct, and ore sizes used were from ¼ in. mesh up to 2 in. Several different types of ores were used, including magnetites and hematites, and the effect of small amounts of coke in the charge was investigated.

This work and work performed by others showed there is nothing wrong technically with the hydrogen reduction of iron ores. No impurities, such as sulphur from coke, are introduced into the iron, and it appears that some sulphur may be eliminated from high sulphur ores. Since hydrogen reduces nothing but the iron, the gangue materials in the ore are concentrated to the extent by which oxygen is removed. Where fine ores are used, the resulting product is pyrophoric and must be protected from oxygen. With hydrogen reduction it does not appear difficult to obtain a product in which metallic iron is at least 90 pct of the total iron.

From the data obtained, further work was carried on by engineers who had experience along these lines to design a pilot plant of 500 tons per day using 75 pct hydrogen as the reducing agent. Coke oven gas, natural gas, and propane were considered as a source of hydrogen. Two different processes of obtaining the hydrogen were considered.

It is difficult to come up with anything but an estimate of the cost unless the location of the plant is known, together with the type of ore and the kind of raw materials that will be used. To reduce 1 ton of iron from Fe_2O_3 requires theoretically approximately 18,000 cu ft of hydrogen, so it is apparent that the cost of hydrogen will be important. The amount of gas consumed, however, will be far in excess of the amount required to reduce the ore, as additional gas is required to manufacture the hydrogen and to heat the ore.

Based upon a study in 1949, it was estimated that, with coke oven gas at 15¢ or natural gas at 37¢ per M cu ft, the cost of making 75 pct hydrogen was about the same, or approximately 30¢ per M cu ft. Using propane, the estimated cost of 75 pct hydrogen was approximately 70¢ per M cu ft and using coke oven gas at 35¢ per M cu ft, the estimated cost of hydrogen was approximately 45¢ per M cu ft. Using the cost of natural gas at 37¢ per M cu ft, coke oven gas at 15¢ per M cu ft, and ore at $15.00 per short ton of contained iron, an estimated cost of about $38.00 per ton of iron was obtained. These estimated costs apply to the Pittsburgh district. To this cost must be added transportation charges of the scrap to the plant in question. This is the cost of the operation, including the cost of raw materials, and should not be confused with selling price.

In these cost estimates, the amount of gas required, it is believed, was estimated on the high side. Therefore, it is possible that some reduction in the cost would result as a more economical use of gas was achieved. These costs were based upon the process in which Allegheny Ludlum was interested. It is felt, however, that costs using other processes would be of the same order of magnitude

C. A. SCHARSCHU is Chief Metallurgist and Assistant Technical Director, Allegheny Ludlum Steel Corp., Brackenridge, Pa. This paper was presented at the Electric Furnace Steel Conference, Pittsburgh, Dec. 6, 1951.

when based upon the same locality and operating conditions.

The physical appearance of the reduced product will vary, depending upon the method of production. When ore of fairly large size, say from $^1/_4$ to 1-in. diam or larger, is reduced at temperatures below the softening point of the iron, the physical appearance of the reduced ore will not differ materially from that of the original product. Its apparent specific gravity, however, will be lower. Where fine ores are used and where it is necessary to protect them from oxidation in the air, briquetting of some kind probably would have to be considered. In connection with fine ores, agglomerating or producing nodules has been studied; and this type of product could be made in a rotary kiln operation.

Some quantities of hydrogen reduced iron have been melted in electric furnaces. Where the reduced ore was a fairly large size, it has been charged into the furnace without any protection, and the results obtained indicated that there was no undue amount of oxidation. This probably would be true with finer ores that have been briquetted or nodulized. Ores that have been ground to a small size before hydrogen reduction oxidize quite readily in air. As pointed out, the reduction product will contain, in addition to the reduced iron, all of the gangue material in the ore. With ores containing 8 or 9 pct gangue, there would be a considerable amount of gangue material in the reduced iron. Such a product might be used in electric furnace practice, particularly as a part of the charge, but except at times of emergencies this product undoubtedly would meet with objections. Therefore, it means that unless a subsequent operation is used to remove the gangue material from the ore, which is not too practical, consideration will have to be given to the amount of gangue material in the ore used, and it has been stated that the gangue material in the ore should not exceed 2 or 3 pct when hydrogen reduction is used.

Many details of the process have been worked out on a small scale involving pilot plants where production has been comparatively small. During World War II, Republic Steel Corp. carried out hydrogen reduction at their Warren, Ohio plant. This plant utilized a Herreshoff furnace and a gas composed of both hydrogen and carbon monoxide, and was designed to treat 100 tons of ore per day. The plant might have operated under some disadvantage as it was stipulated that the plant be constructed using readily available equipment, and it was eventually discontinued, presumably because of production costs.

The Madaras Process has been operating on a pilot plant basis for a number of years, and the Bureau of Mines leased the plant for testing and development work. The reducing chamber in this plant was capable of making 8 to 10 tons of metallic iron in one charge and 100 to 150 tons of iron in one day. It was reported that the difficulties experienced were largely mechanical and could be avoided by suitable engineering and design. The tests were carried on with a gas relatively low in hydrogen and high in nitrogen. Since that time, it was announced that development of this process has been carried to the point where it is ready for industrial utilization. A number of people have investigated this process; but it is believed there is no contemplation of its utilization for industrial use. It recently has been rumored that basic changes have been made in this process and that further work is contemplated.

Although pilot plant work has shown that satisfactory results could be obtained by hydrogen reduction of ore, there remains, however, further information to be obtained from large scale operation before this process can be fully evaluated. Removal of the reduced ore from the furnace and protection of finely divided reduced ore from oxidation are still problems. In vertical shaft furnaces, for example, the question of channeling gases and only partial reduction of the charge is an important factor. Considering the amount of gas necessary to reduce a ton of ore, consideration must be given to the location of the plant. Natural gas seems a logical source for the production of hydrogen, although coke oven gas can be used equally as well. Hydrogen also can be produced from hydrocarbons such as propane. By using propane entirely as a source of hydrogen, costs of the reduced iron would be considerably higher. Coal also might be used. It is felt that the use of any of these materials as a source of heat and hydrogen for the process would bring the cost close to the market price of scrap at the present time or probably above the market price of scrap in normal times. The cost of producing the hydrogen reduced ore has been the biggest factor against investigation of the process on a large scale.

At present, there is probably no equipment in existence by which hydrogen reduced iron could be made available in quantity in the immediate future. Various estimates have been made on the costs of plants necessary to produce this product. For example, the cost of the plant for producing sufficient hydrogen for 500 tons of iron per day would vary from $5 million to $12 million, depending upon the process and whether coke oven gas or natural gas was used. Estimates of the cost of a plant to produce 3000 tons of iron per day by hydrogen reduction vary from $15 million to $20 million. Judging from the cost involved, it is evident that considerable time would be necessary for the construction of such plants, and such plants probably would have to be supported by the Government as an emergency measure.

A review of the work done on reduction of iron ore with hydrogen to produce a product suitable for electric furnace melting would indicate that this process well might be considered *in the case of an emergency*. There are still some details to be worked out in connection with large scale operation, but it is felt that the difficulties encountered might be overcome. A product could be made from selected ores that would be far superior to much of the electric furnace charge scrap now available and at a cost comparable to current (1951) scrap prices.

It is not to be concluded that the hydrogen reduction of ores in the case of an emergency should be the only process to consider. Other direct reduction processes have been used, and some of these have been operated commercially in Europe under special conditions for long periods of time.

The direct reduction processes, however, might not be the immediate answer in cases of an emergency. Present steelmaking facilities might be used to greater advantage in obtaining more iron from ore, by the utilization of larger quantities of ore in the open hearth. Others who have studied the direct reduction of ores feel that the field of these processes is not to produce scrap except in times of emergency.

India's Iron & Steel Industry

The present status and expected future developments of India's iron and steel industry are summarized here. The details were presented in an address by Phiroz Kutar, President of the Indian Institute of Metals.

INDIA, with rich and large deposits of iron ore, large reserves of coal and other raw materials required for the steel industry, has made no noticeable progress in the production of iron and steel. If full advantage were taken of these natural resources, the economic strength and national security of the country would be increased many fold.

Only about a million tons of finished steel is produced annually, against a current demand of 2½ million tons. The per capita consumption of steel, which is a good index of the economic progress of a country, is 7 lb for India, well below the 600 lb in the United Kingdom and over 1100 lb in the United States. An expansion program was under consideration in 1945 by the Indian Government and the private steel companies. However, because of financial limitations and the difficulties of obtaining capital equipment and technical personnel, these programs had to be modified. Present expansion programs call for an increased annual output of 400,000 tons of finished steel in 6 or 7 years, still far short of requirements. Pig iron available to the foundries was considered sufficient until recently; projected expansion of steel capacity will cause a shortage of foundry grade pig iron in 2 to 3 years.

Two privately owned and operated companies account for the major production of iron and steel. Tata Iron & Steel Co. has a fully integrated plant with an annual capacity of 750,000 tons of finished steel. An expansion and modernization program is in the planning stage that will increase output to 950,000 tons a year. Projects under consideration are a new steel melting shop with 540,000 tons of ingot capacity per year, a skelp mill, a Fretz-Moon tube plant that will be worked jointly with Stewarts & Lloyds to produce welded tubes, and a plant for the manufacture of refractories.

The Steel Corp. of Bengal in conjunction with the Indian Iron & Steel Co. produce 250,000 tons of steel yearly. The state owned and financed Mysore Iron & Steel Co. produces 40,000 tons, and Government Ordnance factories have a capacity of 56,000 tons. Steel Corp. of Bengal will increase capacity by 200,000 tons to reach 450,000 tons of finished steel per year. Melting capacity will be increased, auxiliary facilities provided, and new rolling mills for finishing structural and merchant material will be added. Mysore Iron & Steel Works will add two 100-ton electric blast furnaces. To utilize the increased pig iron tonnage, a Bessemer converter-electric furnace duplex plant will be installed. A new billet mill and light structural mills will also be added.

New industries that are proposed include the automotive, locomotive, aircraft, machine tool, electrical machinery, industrial and scientific equipment, and telephone and telegraph industries. These industries create a demand for alloy and tool steels, yet there is no properly equipped plant to produce these steels in India. Tata Iron & Steel Co. did supply a wide range of steel, from the straight carbon tool steels to aircraft quality steels during World War II. However, these were produced on an improvised emergency basis, which cannot be expected to be successful in normal times.

A need also has developed for flat products—plates, sheet and strip, both hot and cold rolled. This is essential to the development of the automotive, canning, and food packing industries. To this end, a continuous strip mill is needed. A modern strip mill will permit more efficient production of electrical steel sheet, stainless sheet, etc. It also will serve as a basis for a tinplate industry.

An aluminum industry has been established, and the production of aluminized steel may be investigated. This is necessary because the zinc shortage will require curtailment of galvanized sheet production. The utilization of lead-zinc deposits of the Zawar mines in Rajputana is under consideration, but the supply would be limited.

India's iron resources, estimated at 10 billion tons of high grade ore, are located in three zones: 1—Eastern zone comprising deposits in Orissa and at Singhbhum in Bihar; 2—Central zone with deposits in the districts of Raipur, Drug, Chanda and Bastar in Madhya Pradesh; and 3—Southern zone with deposits in Mysore, Sandur and Salem. The only exports to date have been small quantities of ore from the Eastern zone. It would be desirable to sell ore to the United States and Japan where capital and consumer goods can be bought. To do this, however, would require tapping unworked deposits and providing transportation and dock facilities.

India is one of the chief sources of manganese ore, exporting close to a million tons a year. However, only the easily mined ore and grades over 38 pct Mn have been exploited. No attention has been paid to the beneficiation of low grade ores, which account for almost 70 pct of the total output. Methods of mining manganese ore are primitive, and mechanization is necessary for increasing efficiency. India would be able to earn higher amounts of foreign exchange by exporting more profitable ferromanganese, rather than manganese ore. The possibility of manufacturing ferromanganese in the electric furnace will have to be considered, as it is difficult to make ferromanganese in the blast furnace that will meet American requirements. Specifications call for 78 to 82 pct Mn and a maximum phosphorus content of 0.30 pct. Although high grade ores could be used to meet the manganese demand, available coals contain high phosphorus and it would be impossible to produce ferromanganese in the blast furnace with less than 0.5 pct phosphorus. Against 2.25 tons of coke per ton of ferromanganese used in the blast furnace, only 0.8 tons of coke would be needed in the electric furnace. In addition, the electric furnace could utilize 70 pct of the total fuel charge as coke breeze, which is obtained as a waste product in the manufacture of metallurgical coke.

Equilibrium Between Blast-Furnace Metal and Slag

As Determined by Remelting

by E. W. Filer and L. S. Darken

ONE of the primary purposes of this investigation was to determine how far blast-furnace metal and slag depart from equilibrium, particularly with respect to sulphur distribution. In studying the equilibrium between blast-furnace metal and slag, there are two approaches that can be used. One method is to use synthetic slags, as was done by Hatch and Chipman;[1] the other is to equilibrate the metal and slag from the blast furnace by remelting in the laboratory. In the set of experiments here reported, metal and slag tapped simultaneously from the same blast furnace were used for all the runs. The experiments were divided into two groups: 1—a time series at each of three different temperatures to determine the time required for metal and slag to equilibrate in various respects under the experimental conditions of remelting, and 2—an addition series to determine the effect of additions to the slag on the equilibrium between the metal and slag. An atmosphere of carbon monoxide was used to simulate blast-furnace conditions.

The furnace used for this investigation was a vertically mounted tubular Globar type with two concentric porcelain tubes inside the heating element. The control couple was located between the two porcelain tubes. The carbon monoxide atmosphere was introduced through a mercury seal at the bottom of the inner tube. On top, a glass head (with ground joint) provided access for samples and a long outlet tube prevented air from sucking back into the furnace. The charge used was iron 6 g, slag 5 g for the time series, or iron 9 g, slag 7½ g for the addition series. This slag-to-metal ratio of 0.83 approximates the average for blast-furnace practice, which commonly ranges from about 0.6 to 1.1. A crucible of AUC graphite containing the above charge was suspended by a molybdenum wire in the head and, after flush, was lowered to the center of the furnace as shown in Fig. 1. The cylindrical crucible was 2 in. long x ¾ in. OD. The furnace was held within ±3°C of the desired temperature for all the runs. The temperature was checked after the end of each run by flushing the inner tube with air and placing a platinum-platinum-10 pct rhodium thermocouple in the position previously occupied by the crucible; the temperature of the majority of the runs was much closer than the deviation specified above. The couple was checked against a standard couple which had been calibrated at the gold and palladium points, and against a Bureau of Standards couple.

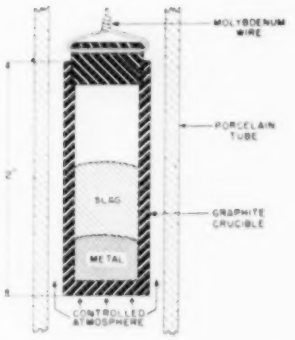

Fig. 1—Experimental arrangement for remelting blast-furnace metal and slag inside tubular Globar furnace.

The carbon monoxide atmosphere was prepared by passing CO_2 over granular graphite at about 1200°C. It was purified by bubbling through a 30 pct aqueous solution of potassium hydroxide and passing through ascarite and phosphorus pentoxide. The train and connections were all glass except for a few butt joints where rubber tubing was used for flexibility. The rate of gas flow was 25 to 40 cc per min. As atmospheric pressure prevailed in the furnace, the pressure of carbon monoxide was only slightly higher than the partial pressure thereof in the bosh and hearth zones of a blast furnace—by virtue of the elevated total pressure therein.

Simultaneous samples of blast-furnace metal and slag were taken for these remelting experiments. The composition of each is given in the first line of Table I. There is considerable uncertainty as to the significant temperature in a blast furnace at which to compare experimental results. This uncertainty arises not only from lack of temperature measurements in the furnace, but also from lack of knowledge of the zone where the slag-metal reactions occur. (Do they occur principally at the slag-metal interface in the crucible, or as the metal is descending through the slag, or even higher as slag and metal are splashing over the coke?) The known temperatures are those of the metal at cast, which averages about 2600°F, and of the cast or flush slag, which is usually about 100°F hotter. To bridge this uncertainty, remelting temperatures were chosen as 1400°, 1500° (2732°F), and 1600°C. For the time series the duration of remelt was 1, 2, 4, 8, 17, or 66 hr; crucible and contents were quenched in brine. The addition series were quenched by rapidly transferring the crucible and contents from the furnace to a close-fitting copper "mold." Of incidental interest here is the fact that the slag wet the crucible

E. W. FILER and L. S. DARKEN, Member AIME, are associated with the Research Laboratory, U. S. Steel Co., Kearny, N. J.

Discussion on this paper, TP 3233C, may be sent, 2 copies, to AIME by April 1, 1952. Manuscript, Sept. 13, 1951. St. Louis Meeting, February 1951.

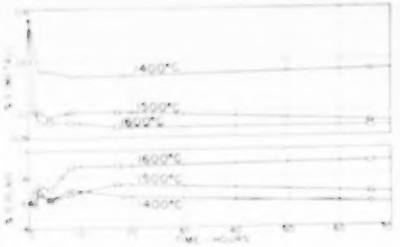

Fig. 2 (above)—Remelted blast furnace metal and slag. Change of sulphur as a function of time at temperature. Top: Pct S in metal. Bottom: Pct S in slag.

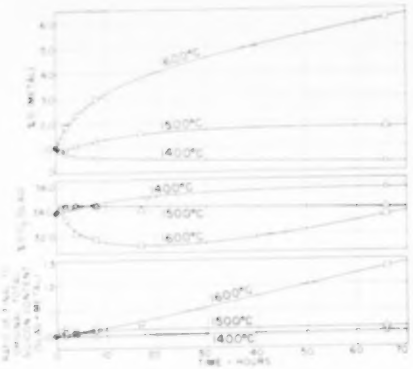

Fig. 3 (right)—Remelted blast furnace metal and slag. Change of silicon as a function of time at temperature. Top: Pct Si in metal. Center: Pct Si in slag. Bottom: Ratio of final to initial total Si (slag + metal).

(that is, climbed the wall) at 1600°C in all the runs, while at 1400° and 1500°C it did not. All slags were glassy after quench and exhibited no evidence of incomplete melting. Complete results of all the analyses are given in Table I.

The sulphur analyses for the time series shown in Fig. 2 indicate that the metal and slag in the blast furnace were not at equilibrium in regards to sulphur. Between 1 and 2 hr were required for the sulphur in the metal to attain a steady value on remelting at each temperature. Fig. 2 also shows that the sulphur in the slag showed a slight increase as the temperature was increased. Most of this increase was due to evaporation loss of the slag at the higher temperatures. The ratio of the percentage of sulphur in the slag to that in the metal (initially 54) increased markedly as equilibrium was approached, particularly at the higher temperature. This ratio at 1400°C was 89, increasing at 1500°C to 154, while at 1600°C it was 205. The approach to sulphur equilibrium was considerably more rapid than expected from consideration of the work by Hatch and Chipman,[1] who report times up to 7 hr required for equilibration in spite of rather vigorous stirring. Only once do they report a time of 2 hr as sufficient for equilibrium; this for a highly basic slag at 1500°C.

Fig. 3 shows the effect of time at temperature on the silicon content of the metal and slag. There was an increase in the silicon content of the metal at 1500° and 1600°C, while at 1400°C there was a

Table I. Composition of Remelted Blast Furnace Metal and Slag

Temperature, °C	Time, Hr	Addition	Metal, Pct				Slag, Pct					
			S	Si	Mn	S	SiO_2	MnO	FeO	Al_2O_3	CaO	MgO
Time Series												
Orig.*			0.028	1.01	2.04	1.50	33.71	1.11	0.21**	12.79	42.81	6.87
1400	2		0.018	0.71	2.04	1.53	34.25	1.11	0.18			
1400	4		0.018	0.67	2.06	1.51	34.72	1.12	0.20			
1400	8		0.017	0.60	2.05	1.55	34.62	1.16	0.29			
1400	8		0.017	0.54	2.09	1.52	34.95	0.87	0.15			
1400	16½		0.017	0.38	2.09	1.49	35.85	0.83	0.39	13.04	42.60	6.70
1400	66		0.018	0.38	1.90	1.49	35.85	0.83	0.39			
1500	1		0.030	0.86	2.22	1.55	34.40	0.72	0.13			
1500	2		0.019	0.97	2.33	1.54	34.30	0.61	0.14			
1500	4		0.019	1.06	2.32	1.51	34.30	0.55	0.15			
1500	8		0.016	1.25	2.30	1.53	34.25	0.40	0.10			
1500	8		0.016	1.39	2.19	1.57	33.87	0.40	0.12			
1500	17		0.016	1.59	2.19	1.53	34.10	0.31	0.23	13.40	44.84	6.30
1500	66		0.060	1.78	1.73	1.53						
1600	1		0.011	1.30	2.30	1.49	33.90	0.46	0.13			
1600	2		0.009	1.86	2.38	1.57	33.25	0.34	0.13			
1600	4		0.009	2.32	2.24	1.55	32.15	0.20	0.15			
1600	8		0.008	2.06	2.22	1.64	31.65	0.21	0.11			
1600	17		0.007	3.72	1.92	1.64	31.20	0.17	0.17	14.00	46.97	5.27
1600	66		0.009	6.36	0.96	1.54	33.20	0.11	0.15	14.88	48.70	1.63
1600	66		0.007	6.19	1.38	1.65	33.50	0.17	0.17	13.77	47.17	2.86
Addition Series												
1400	17	5 pct CaO	0.014	0.43	2.02	1.49	33.78	0.70	0.12	12.37	45.60	6.56
1400	17	5 pct MgO	0.014	0.39	2.13	1.51	32.52	0.70	0.14	12.41	41.08	11.45
1400	17	5 pct Al_2O_3	0.021	0.69	1.96	1.49	32.96	1.01	0.14	16.99	41.08	6.59
1400	17	5 pct SiO_2	0.025	0.77	1.93	1.49	37.72	1.16	0.14	12.35	40.75	6.09
1500	4	5 pct CaO	0.011	0.84	2.47		33.58	0.33	0.06	12.61	46.38	6.75
1500	4	5 pct MgO	0.011	1.01	2.48		33.28	0.30	0.14	12.39	41.54	11.58
1500	4	5 pct Al_2O_3	0.016	1.02	2.35		32.90	0.34	0.16	17.30	41.50	6.61
1500	4	5 pct SiO_2	0.018	1.25	2.19		37.30	0.74	0.11	12.52	41.79	6.45
1500	4	1 pct Si	0.011	1.74	2.41	1.57	35.18	0.47	0.14	12.95	43.40	7.02
1500	4	2 pct Si	0.011	2.46	2.43	1.60	35.46	0.44	0.17	12.91	43.49	6.96
1600	2	5 pct CaO	0.013	1.32	2.39	1.52	32.76	0.19	0.13	12.44	46.06	6.57
1600	2	5 pct MgO	0.011	1.56	2.40	1.53	32.26	0.17	0.18	12.39	42.33	11.58
1600	2	5 pct Al_2O_3	0.013	1.68	2.32	1.51	32.12	0.13	0.18	18.28	42.57	6.73
1600	2	5 pct SiO_2	0.017	2.17	2.24	1.51	36.03	0.43	0.16	12.80	42.97	6.89

* Initial phosphorus in metal, 0.288 pct.

** As charged; 0.13 pct after magnetic extraction.

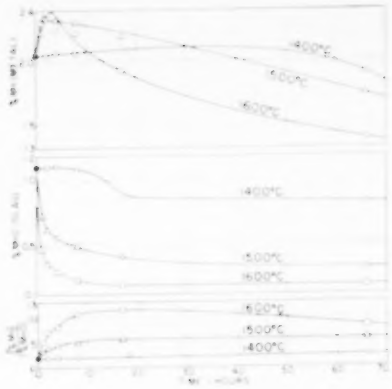

Fig. 4 (left)—Remelted blast-furnace metal and slag. Change of manganese as a function of time at temperature. Top: Pct Mn in metal. Center: Pct MnO in slag. Bottom: Pct Mn distribution coefficient.

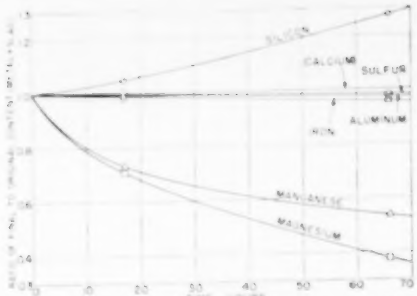

Fig. 5 (above)—Remelted blast-furnace metal and slag. Evaporation loss (or gain) of components at 1600°C (based on assumption of no gain or loss of CaO).

decrease. This indicates that the silicon equilibrium temperature for this blast-furnace metal and slag is between 1400° and 1500°C. Fig. 3 also shows that the SiO_2 in the slag increases at lower temperature, but decreases at higher temperature. The fact that the curve for 1600°C rises, after dropping steadily until 17 hr, is apparently due to evaporation from the porcelain tube to the slag and metal over the long period of time. This can be seen more clearly from the bottom curves of Fig. 3, which indicate that the total silicon content of the system (slag + metal) increases with time notably at 1600°C but insignificantly at 1400°C.

There was considerable loss of manganese (by evaporation) from the metal-slag system, as shown in Fig. 4. It is worth noting that at 1500° and 1600°C the manganese in the metal increased considerably in 2 hr and then started to decrease; the MnO in the slag decreased at all times. The well-known tendency of increased temperature to favor increased manganese recovery in the metal is masked by evaporation in these small scale experiments. The behavior of manganese is shown more clearly at the bottom of Fig. 4 in terms of the ratio of manganese in the metal to MnO in the slag. The pronounced effect of temperature is quite evident here. In each series the ratio levels off, indicating approach to equilibrium, in about 10 hr. The later drop at 1600°C is undoubtedly due to vaporization (increased acidity of the slag). Although the rather marked increase of this ratio with temperature is in accord with general physicochemical knowledge and experience, a quantitative comparison with fundamental data is difficult.

In a number of the runs the material was weighed before and after the run; from this information and the analyses of the metal and slag, it was possible to calculate the loss or gain of components at the different temperatures. Table II shows these losses for CaO, Al_2O_3, and S and also the percentage of mechanical loss of the slag based on the average loss of CaO and Al_2O_3. Since the actual mechanical loss is believed to be small, these figures indicate that the materials balance may best be based on CaO. On the assumption that there is no loss or gain of CaO, the evaporation loss or gain of a number of the components of the system at 1600°C are shown in Fig. 5. The graph shows that there is considerable pickup of silicon, as was previously discussed. There is very little loss of the sulphur, aluminum, and iron of the system, while there is considerable loss of manganese and magnesium at 1600°C. The maximum loss of manganese in metal + slag is about 46 pct of the original and that of magnesium is about 62 pct (presumably by the reaction $C + MgO = CO + Mg$). These changes by volatilization were much less at the lower temperature.

In order to investigate the effect of moderate change in slag composition on the sulphur equilibrium, a 5 pct addition of either CaO, MgO, Al_2O_3, or SiO_2 was made to the charge. In this series of experiments the time of holding at 1400°, 1500°, or 1600°C was at 17, 4, or 2 hr respectively. The times were chosen to allow adequate time for sulphur equilibration, as indicated by the time series, Fig. 2, and to minimize evaporation losses. As shown in Fig. 6, the sulphur content of the metal is lowered in all cases during remelt. It is found, as anticipated, that in general the sulphur content of the metal decreases with increasing basicity. The largest effect is seen at 1400°C where the sulphur content ranges from 0.025 pct for the 5 pct SiO_2 addition to 0.014 pct for 5 pct CaO or MgO addition. In view of the definite effect of the acid additions SiO_2 and Al_2O_3, the apparently negligible effect of the MgO and CaO additions at 1500° and 1600°C may be due in part to analytical error; possibly a longer equilibration time should have been allowed in these cases.

Table II. Loss (or Gain) of CaO, Al_2O_3, and S as Determined from Analyses and Total Weights of Sample Before and After Melting (Percentages are Based on Initial Weight of Slag)

	1400°C 17 Hr	1500°C 4 Hr	1600°C 2 Hr	1600°C 66 Hr
Pct CaO lost (Initial pct CaO 42.81)	1.4, 0.3	0.1, 0.7, (0.4)* 0.2, (0.1)*		0.9
	0.7, 0.8	0.4, 0.7, 0	0.3, 0.4	0.9
Pct Al_2O_3 lost (Initial pct Al_2O_3 12.79)	0.3, 0.1	0.1, 0.1, (0.3)* 0.2, (0.2)*		0.7
	0.7, 0.3	0.2, 0.3, 0.3	0.5, 0.2	0.6
Pct S lost	(0.04)*, (0.01)* (0.02)*, 0	0, (0.04)*	(0.03)*, 0.02 (0.01)*, 0	0.06
Pct Mechanical loss of slag based on:				
1. Average loss of CaO	1.8	0.5	0.4	2.2
2. Average loss of Al_2O_3	2.7	1.1	1.5	4.9

* Indicates gain instead of loss.

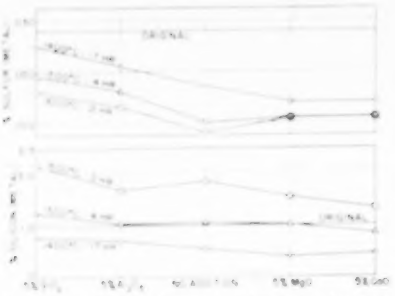

Fig. 6—Remelted blast furnace metal and slag. Effect of indicated additions on sulphur and silicon content of metal.

In Fig. 6 the effect of the additions to the slag on the silicon content of metal is also shown. Change of slag composition in this range seems to have relatively small effect on the silicon content of the metal. Although the time (particularly at 1600 C) was probably insufficient for silicon equilibration, if a large compositional change was required, the negligible change in the center of the 1500 C curve indicates close approach to silicon equilibrium in these cases. Two runs were made at 1500 C for 4 hr to determine the effect of 1 and 2 pct additions of metallic silicon to the metal, thus approaching this equilibrium from the other side. Table III summarizes these results. This indicates that the equilibrium silicon at 1500 C is slightly over 1 pct, about 1.1 pct. However, as noted previously, longer time runs (no additions) give 1.39 pct Si at 17 hr, 1.78 pct Si at 66 hr; this discrepancy is probably due to the evaporation gains and losses over the longer time periods.

The effects of the additions of SiO_2, Al_2O_3, MgO, and CaO on the behavior of manganese are shown in Fig. 7. Here again, although insufficient time was allowed for equilibration at higher temperature, the expected effect of increased temperature or basicity in improving manganese recovery is apparent. MgO and CaO are seen to have substantially identical effect as in the case of the sulphur equilibrium, Fig. 6. The apparent disparity of the 1600 C curve for the manganese content of the metal is due to evaporation loss, correction for which leads to the dashed curve. The effect of temperature and composition on the behavior of manganese is brought out more clearly by the distribution coefficient [pct Mn]/(pct MnO) shown in the bottom of Fig. 7. This coefficient is higher than that for the original blast-furnace products except for the 1400 C series with the acid

Fig. 7—Remelted blast furnace metal and slag. Effect of indicated additions on the behavior of manganese. Top: Pct Mn in metal. Center: Pct MnO in slag. Bottom: Mn distribution coefficient.

additions SiO_2 and Al_2O_3, where the coefficient is substantially the same as the original.

Since the crucible was held quietly in the furnace for an extended period of time and was cooled without any serious agitation, it was expected that substantially all the metallic iron in the slag would settle out and that the iron left in the cooled slag would be principally ferrous. This proved not to be the case. The slag was ground to pass a 60 mesh sieve in preparation for analysis. It was then placed in a brass pan with ether (which facilitated extraction) and extracted with a point electromagnet. Extraction was continued in a standardized manner well after no further iron was removed; this point was determined not only visually but by a preliminary set of analyses of samples extracted for various periods of time. Relatively large quantities of metallic iron were removed by this process and the residual "FeO content" of the slag as thus determined and tabulated (Table I) seems to vary in no orderly manner.

Calcium Sulphide Precipitation

A series of runs were made at 1500 C in a CO atmosphere with holding times of 17 and 41 hr in which additions of FeS were made to the slag varying the sulphur content by 1 pct intervals from 1.5 to 5.5 pct. The slags containing 4.5 and 5.5 pct S, on fracture, exhibited yellow crystals. These were easily visible to the naked eye. Despite the absence of color in Fig. 8, these crystals (right) are easily distinguished by their contrast with the smooth conchoidal fracture (left) characteristic of the glassy quenched slags. These crystals were much larger than could reasonably be expected to form on cooling; moreover they were at or near the slag-metal interface indicating they had ample time to settle. The runs with 3.5 pct S for 17 and 41 hr did not exhibit any such crystals. X-ray examination of extracted crystals indicated that they are of the cubic NaCl type. The lattice parameter of the crystals shown in Fig. 8 is 5.70A as compared to 5.69A, given by the ASTM table for calcium sulphide. Similar crystals extracted from other melts were found to have a parameter of 5.56 and 5.60A. As the only other sulphide likely to appear under these circumstances is MnS, some of this (which is green) was prepared and its parameter determined as 5.21A, in agreement with the accepted value of 5.213A. Hence it was concluded that the observed precipitate was CaS containing in some cases relatively small amounts of another sulphide in solid solution. Its solubility in this particular blast-furnace slag corresponds to less than 4.5 pct S and (except for the unlikely event of supersaturation) to more than 3.5 pct S at 1500 C. This solubility is considerably lower than that (10 pct S) calculated by Rosenqvist[1] or than the estimate (8 to 11 pct) of McCaffery and Oesterle.[2]

Comparison of Remelts with Blast-Furnace Product

From the above data it is possible to estimate the composition of the metal after equilibration with a slag of the original composition at each temperature, if there had been no evaporation loss or gain. Table

Table III. Results of Additions of Metallic Silicon to Metal

Silicon Addition, Pct	Silicon, Pct	
	Initial	After Remelt
None	1.01	1.06
1	2.01	1.74
2	4.01	2.46

IV gives these results. In this tabulation the results for sulphur at all temperatures and for silicon and manganese at 1400°C are taken directly from the experimental data, Figs. 2, 3, and 4. The equilibrium of the percentage of silicon at 1500°C was discussed previously. The equilibrium of the percentage of manganese at 1400° or 1500°C is calculated from the observed level or maximum [Mn]/(MnO) ratio of Fig. 4.

Under the conditions of remelting the sulphur seems to equilibrate fairly rapidly; nevertheless the distribution coefficient is substantially greater than is common in blast-furnace practice though lower than has been reported for some synthetic slags. Silicon and manganese reactions seemed more sluggish than that of sulphur. At 1600°C the silicon rose to values which were very high in comparison with actual blast-furnace practice. The manganese equilibrium seemed to be approached within the time limit of the experiment, and the distribution between metal and slag at 1500° and 1600°C was more favorable than the original blast-furnace product.

In view of the uncertainties as to blast-furnace temperature and reaction zone it is difficult to compare fruitfully the original and the equilibrium compositions of Table IV to determine the departure of the blast-furnace metal and slag from equilibrium. However, in the case of each element it is relatively easy to determine from this table the temperature of its reaction zone, if equilibrium were attained in the blast furnace. Thus the original sulphur content corresponds to an equilibrium temperature of about 1300°C, the original manganese to 1400°C, and the original silicon to slightly less than 1500°C. The rather wide disparity here indicates that a state of complete equilibrium is not approached in the blast furnace. Silicon reduction must have occurred at temperatures approaching 1500°C or higher—a temperature which seems quite reasonable for the hearth of the blast furnace. It is slightly puzzling that more manganese was not reduced at this temperature level if silicon was; the abundance of silica as compared to manganese oxide in the slag may account for this. It is more difficult to reconcile the relatively great departure from sulphur equilibrium in the blast furnace with the relatively rapid sulphur equilibration attained in the remelts. A possible interpretation here is that the sulphur transfer is probably accompanied by evolution of carbon monoxide ($CaO + C + \underline{S} = CaS + CO$), a reaction which does not readily occur except where a gas phase is already present; hence a small melt surrounded by gas (or porous graphite) would react more readily than the much larger quantities in the crucible of the blast furnace where contact with the gas phase is limited. Under such circumstances sulphur transfer may well be controlled by the reducing action of manganese or of silicon rather than of carbon, as in the above reaction. This is suggested by the findings of Grant, Kalling, and Chipman[7] and of Grant, Troili, and Chipman,[8] who showed that the addition of MnO

Table IV. Estimated Composition of Metal in Equilibrium with Slag (On Assumption of No Evaporation Loss or Gain)

	Original	1300°C	1500°C	1600°C
Pct S	0.028	0.017	0.010	0.008
Pct Si	1.01	0.5	1.4	(4)
Pct Mn	2.04	2.1	2.4	2.6
(Pct Si)/(Pct S)	54	88	154	205

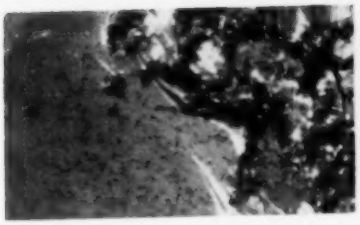

Fig. 8—Crystals of calcium sulphide (right) in fracture of otherwise glassy slag (left) containing 5.5 pct S.

leads to temporary sulphur reversion and that increased silicon content accelerates sulphur transfer from metal to slag.

In fact some evidence of the coupling of the manganese and sulphur distributions in the blast furnace may be deduced from the present experiments. This combined reaction may be written $\underline{Mn} + \underline{S} = Mn^{++} + S^{=}$ where the ionic designation of the slag constituents is not essential to the argument but simplifies the equation. The mass law "constant" (MnO)(S)/[Mn][S] is found from our data for this particular slag to be 36, 29, and 20 at 1400°, 1500°, and 1600°C, respectively. The corresponding quotient for the initial blast-furnace metal and slag is 29, in good agreement with the equilibrium value for 1500°C. Hence, if this temperature is accepted as reasonable for the blast-furnace reaction zone, it is tempting to consider the possibility that this coupled reaction of manganese and sulphur approaches equilibrium although, as shown previously, neither the manganese nor the sulphur distribution approaches individually the equilibrium value for this temperature. A conclusion as to whether or not this is generally so for the blast furnace must await further data.

Conclusions

Remelting of blast-furnace metal and slag in a small graphite crucible yields relatively rapid equilibration of sulphur; the sulphur content of the equilibrated metal is substantially lower than that of the initial blast-furnace product. Equilibration of manganese or silicon requires a longer time. Increased temperature or basicity favors high sulphur distribution ratio and high manganese recovery. Low silicon is favored by low temperature or high basicity. Comparison of the equilibrium compositions with the initial indicates that complete equilibrium is by no means achieved in the blast furnace. If means could be found for the blast furnace to approach more closely to equilibrium, desulphurization and manganese recovery would both be improved. Of the equilibria considered, silicon reduction and the reaction of manganese with sulphur seem the only ones which were possibly approached in the blast furnace. Saturation of the slag with calcium sulphide was reached at about 4 pct S.

References

[1] G. G. Hatch and J. Chipman: *Trans.* AIME (1949) **185**, p. 274; JOURNAL OF METALS (April 1949).

[2] T. Rosenqvist: *Trans.* AIME (1951) **191**, p. 535; JOURNAL OF METALS (July 1951).

[3] R. S. McCaffery and J. F. Oesterle: *Trans.* AIME (1923) **69**, p. 606.

[4] N. J. Grant, U. Kalling, and J. Chipman: *Trans.* AIME (1951) **191**, p. 666; JOURNAL OF METALS (August 1951).

[5] N. J. Grant, O. Troili, and J. Chipman: *Trans.* AIME (1951) **191**, p. 672; JOURNAL OF METALS (August 1951).

Isothermal Martensite Formation

In an Iron-Chromium-Nickel Alloy

by S. A. Kulin and G. R. Speich

The isothermal formation of martensite at subzero temperatures has been studied in an austenitic stainless steel. The amount of martensite formed isothermally in a given time was found to follow a C-curve behavior with decreasing temperature. Since isothermal martensitic transformation occurs at temperatures above the true M_s temperature of the alloy, the observed M_s temperature is dependent on the cooling rate. It is believed that a general martensite theory must include the basic concepts of the strain embryo theory, and also the important role of thermal fluctuations.

UNTIL recently the isothermal component of the martensitic transformation had been considered as a trivial effect in theoretical considerations of this type of transformation. One of the postulates used in defining a martensitic transformation was that the reaction was temperature dependent but not time dependent. Cohen and his associates [1] were the first to report the isothermal formation of martensite. They observed the time dependency of the martensite reaction at room temperature in plain carbon steels and certain tool steels. They found that a small amount of additional transformation occurred after the specimen reached the quenching temperature and that the rate of this isothermal transformation decreased rapidly with time. These authors considered this phenomenon to be a "tailing-off" of the main athermal reaction.

Kurdjumov and Maksimova[2] studied the isothermal formation of martensite at subatmospheric temperatures in steels containing 0.6 pct C-6 pct Mn, 1.6 pct C, and in an iron-base alloy containing 23 pct Ni and 3.4 pct Mn. In each case it was found that both the initial rate and the total amount of isothermal transformation exhibited sharp maxima with decreasing temperature. They stated that it was possible to completely suppress the martensitic transformation in the 0.6 pct C-6 pct Mn steel by drastic quenching in liquid nitrogen. They interpreted their results in terms of a thermally activated process. The maximum in the rate of nucleation vs. temperature curve was assumed to be a result of the temperature dependence of the rate of growth of the martensite plates. It has been demonstrated,[3] however, that martensite plates can form with great rapidity even at temperatures approaching absolute zero. In addition,[4] attempts to confirm the reported suppression of the martensitic transformation by rapid cooling of a 0.6 pct C-6 pct Mn steel have proved unsuccessful. On this basis, and on other theoretical grounds, the validity of some of Kurdjumov's results and conclusions is open to serious question.

Cohen, Machlin, and Paranjpe[5] have proposed a theory of martensite formation based on the nucleation of strain embryos and a growth mechanism involving cooperative atomic displacements. According to this theory thermal fluctuations can make a strain embryo supercritical and thereby produce martensite isothermally.

Das Gupta and Lement[6] have investigated the isothermal formation of martensite in a 17 pct Cr-0.7 pct C steel at temperatures below the ambient. They found that partial suppression of the martensitic reaction occurred on quenching into liquid nitrogen. That part of the reaction which can be suppressed is taken to correspond to the isothermal rather than the athermal part of the martensitic transformation. The initial rate of isothermal transformation for this steel was found to go through a maximum with decreasing temperature. This is in conformity with the findings of Kurdjumov and Maksimova for the steels used in their investigation. Das Gupta and Lement conclude that isothermal martensite formation occurs by the nucleation of new plates and is always preceded by some athermal transformation.

An iron-base alloy containing 14 pct Cr-9 pct Ni was used in this investigation to study further the kinetics of the austenite to martensite transforma-

S. A. KULIN, Student Associate AIME, and G. R. SPEICH are associated with Westinghouse Research Laboratories, East Pittsburgh, Pa.

Discussion on this paper, TP 3255E, may be sent, 2 copies, to AIME by May 1, 1952. Manuscript, Sept. 17, 1951. New York Meeting, February 1952.

tion at subatmospheric temperatures and to ascertain the generality of the previously reported phenomena. Such studies on a wide variety of materials should demonstrate the validity, or deficiencies, of the present martensite theories.

Experimental Procedure

Material and Heat Treatment: The chemical composition (wt pct) of the alloy used in this investigation is as follows: Cr, 14.38; Ni, 9.06; C, 0.008; N, 0.034; Mn, 1.21; and Si, 0.36. A 2½ in. square ingot was rolled and then swaged to wire of 0.100 in. diam. All specimens were austenitized at 1095°C for 20 min in a tube furnace having a dry hydrogen atmosphere and then were oil-quenched to room temperature. This treatment resulted in a completely austenitic specimen with an A.S.T.M. grain size of 5.

Electrical Resistance Measurements: The extent of transformation was determined by precise measurement of the electrical resistance using a Kelvin double-bridge circuit. The ends of each specimen were formed into loops prior to heat treatment in order to facilitate making the current connections. A clamp device, attached to the specimen, enabled the resistance measurement to be made between two hardened steel knife edges which were about 2 in. apart. These knife edges also served as potential leads. To prevent specimen heating, momentary current flow was obtained by use of a key in the circuit. Bridge balance was determined by use of a Leeds and Northrup type 2430C galvanometer.

Low Temperature Baths: Specimens were either cooled or quenched in a liquid bath held in a Dewar flask. The baths were vigorously agitated by a motor-driven stirrer. Powdered solid CO_2 additions were made to an acetone bath for cooling or maintaining a constant temperature down to about −78°C. Additions of liquid nitrogen were made from a pipette to a bath consisting of 75 pct petroleum ether and 25 pct methylcyclohexane for obtaining temperatures down to −150°C. A liquid nitrogen bath was used to obtain a temperature of −196°C. A calibrated copper-constantan thermocouple was used for temperature measurement. During the isothermal transformation experiments, the bath temperature was generally maintained to within 0.2°C of the reported temperature.

Calibration of Electrical Resistance Measurements: The martensitic phase in this alloy was found to have a considerably higher electrical resistivity than that of the austenite. It was assumed that the electrical resistance at a constant temperature is a linear function of the volume percentage of transformation. This was found to be in good agreement with later experimental results. It was necessary to determine the extent of transformation in a specimen of known resistance for calibration purposes. The lineal analysis method[7] could not be used because of the difficulty in distinguishing the martensite plates metallographically. The X-ray integrated intensity method[8] was also found to be unsuitable, since the intensities of certain of the austenite lines did not correspond to the theoretical powder reflection intensities. This was a result of the preferred orientation of the austenite grains in the wire specimens.

Since the above methods were not applicable, a density method was used for the calibration. The lattice parameters of both the austenite and martensite were obtained from the X-ray data, and the density of each phase was then calculated. The calculated and measured densities of a completely austenitic specimen were in excellent agreement. It was not possible to obtain a completely martensitic specimen and therefore it was necessary to assume that the calculated density of this phase was correct. Density determinations were made on several specimens of known electrical resistance. The calibration factor for the volume percentage of martensite as a function of electrical resistance and temperature of measurement was then determined by a graphical method.

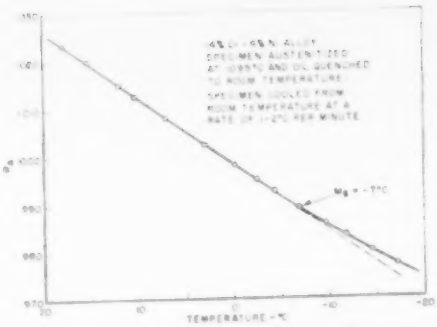

Fig. 1—Determination of M_s temperature.

The Kelvin double-bridge readings (R_r) were made to four significant figures. A change of less than one in the fourth significant figure could easily be detected from the galvanometer deflection. During isothermal transformation experiments, the time readings were taken when the bridge was in perfect balance. This resulted in a sensitivity of about two in the fifth significant figure of the R_r value. These R_r values are related to the electrical resistance of the specimen by a proportionality factor. The calibration of the absolute volume percentage of martensite may be in error by approximately ±2 pct. This error would represent a constant value throughout most of the present work. On the other hand, the relative sensitivity of the measurement of the percentage of transformation is dependent on the temperature and is of the order of 0.04 pct martensite. The conversion factor relating the change in the R_r value (fourth significant figure) per percentage of martensite at various temperatures is as follows:

Temperature, °C	1.5	−18.5	−28.5	−38.5	−78	−122.5	−196
ΔR_r pct martensite	4.8	5.0	5.1	5.3	5.7	6.3	7.2

Experimental Results

Determination of M_s Temperature on Slow Cooling: All specimens used in this investigation were austenitized at 1095°C for 20 min and then oil-quenched to room temperature. Electrical resistance readings taken during cooling (1° to 2°C per min) in an acetone bath showed that the resistance decreased linearly with temperature until some martensite formed. The transformation resulted in a positive deviation from the straight line relationship. This is shown in Fig. 1 where the bridge readings, R_r, are plotted vs. the temperature. The M_s temperature is indicated at −7°C. Identical results were

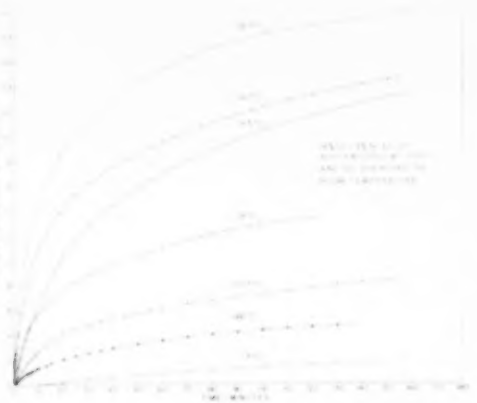

Fig. 2—Percentage of isothermal martensite vs. time.

obtained with another specimen. It is interesting to observe that the burst phenomenon did not occur, although these specimens had a No. 5 A.S.T.M. grain size.

Isothermal Martensite Formation with Variable Initial Martensite Contents. A number of specimens were quenched to various subatmospheric temperatures and allowed to transform isothermally. Electrical resistance readings were taken as a function of time at temperature. The following temperatures were used: −18.5°, −28.5°, −38.5°, −78°, −122.5°, and −196°C. In each case the rate of isothermal transformation was greatest at zero time and decreased with increasing time. In some cases the rate of martensitic transformation was still appreciable even after 2 hr. In every case the rate was measurable after this period of time. The volume percentage of isothermally formed martensite as a function of time is shown in Fig. 2 for the temperatures listed above.

The percentage of martensite formed athermally on quenching to these temperatures was determined by plotting electrical resistance readings vs. time and extrapolating to zero time. These extrapolated values gave the initial martensite content prior to each isothermal run. Fig. 3 gives the amount of athermal and isothermal martensite (after 2 hr) as a function of the temperature. The athermal curve corresponds to the usual martensite range curve. The fact that this athermal curve decreases at the low temperatures indicates that some isothermal martensite had formed during quenching to the higher temperatures. Das Gupta and Lement[7] have designated such transformation as "anisothermal." More martensite can be obtained by quenching and holding at about −30°C than by quenching directly to −196°C.

The position of the M_s temperature is extremely significant. Previous measurements during slow cooling gave an M_s temperature of −7°C, whereas the athermal martensite data yields a value of approximately −20°C. This indicates the possibility of isothermal martensite formation at temperatures above the true M_s. The latter temperature is the limiting value which would be obtained for the start of the martensitic reaction with increasing rates of cooling.

The rate of nucleation of isothermal martensite at zero time was obtained by drawing tangents on expanded plots of the resistance readings vs. time. The rate of nucleation, N, as presented herein is expressed in terms of the percentage of martensite per unit time per unit volume of untransformed phase. The circled points in Fig. 4 represent the values obtained in the previously described isothermal transformation experiments. In order to express N in terms of the number of nuclei per unit time per unit volume of untransformed phase, a value must be determined for the average volume of a martensite plate. The curve of Fig. 4 has the expected form of a rate of nucleation vs. temperature curve and is similar to that obtained for ordinary nucleation and growth transformations. The general characteristics of the temperature dependence of the initial rate of nucleation are in agreement with the findings of Kurdjumov[8] despite the fact that he arbitrarily defined the rate of nucleation as being the number of

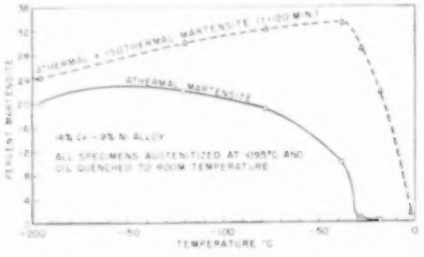

Fig. 3—Percentage of martensite vs. temperature.

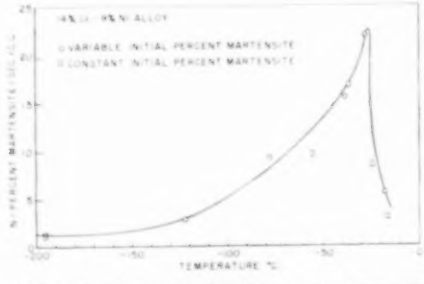

Fig. 4—Rate of nucleation of isothermal martensite vs. temperature.

Fig. 5 (above)—Martensite plates formed by quenching and holding at −30°C. Electropolished and etched with perchloric acid solution. 14 pct Cr, 9 pct Ni iron-base alloy.

Fig. 6 (right)—Percentage of isothermal martensite vs. time.

Fig. 7 (below)—Percentage of martensite vs. temperature.

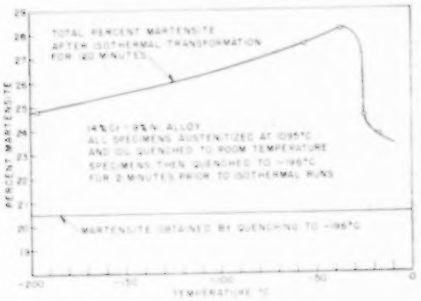
TOTAL PERCENT MARTENSITE AFTER ISOTHERMAL TRANSFORMATION FOR 120 MINUTES
PERCENT MARTENSITE
MARTENSITE OBTAINED BY QUENCHING TO −196°C
TEMPERATURE °C

nuclei formed per unit time per unit volume of that portion of the untransformed phase capable of transformation.

Martensite plates that formed in a specimen which was cooled and held at −30°C are shown in Fig. 5. The specimen was electrolytically polished both before and after this treatment. Some etching was obtained in the final polishing operation. This martensite has the familiar acicular appearance characteristic of martensitic transformation products.

Isothermal Martensite Formation With Constant Initial Martensite Contents: In the preceding experiments the initial martensite content at the start of isothermal transformation varied between 0 and about 23 pct. In order to determine the effects of this variable, a series of isothermal transformation experiments were performed by quenching specimens to −196°C for 2 min prior to up-quenching and holding at the following temperatures: −16.8°, −24.1°, −37.1°, and −55.5°C. Each of these specimens contained 20.5 pct martensite at the beginning of each isothermal run. The results obtained are given in Fig. 6, which shows the amount of isothermal transformation as a function of time at the various temperatures used. The curve for −196°C is the same as in Fig. 2 except that zero time is now taken after 2 min. The maximum amount of martensite formed isothermally in the times employed is about 9 pct, whereas a maximum of about 30 pct formed in the previous experiments. The high initial rates of isothermal transformation decrease rapidly with time until a fairly constant but low rate of transformation is attained. Fig. 7 indicates the total amount of martensite present after 2 hr as a function of the temperature. The temperature at which the maximum amount of martensite is obtained (approximately −35°C) is evidently not affected by a variation from 9 to 21.5 pct in the initial athermal martensite content.

The points which are indicated by squares in Fig. 4 represent the rate of nucleation at zero time for the specimens having a constant initial percentage of martensite. The curve in this figure was drawn to fit the data obtained with variable initial martensite

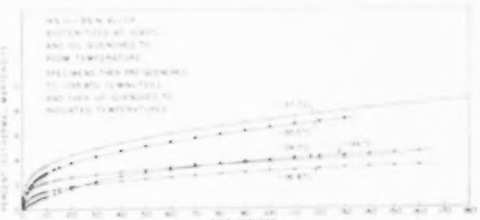

contents. It is evident that, within the limits investigated, the initial rate of nucleation is not significantly affected by variations in the initial amount of martensite. The data, Fig. 4, indicate that if such an effect is present, it would give lower initial rates of transformation for specimens with higher initial martensite contents. The total amount of martensite obtainable in a given time is, however, dependent on the thermal treatment employed.

Isothermal Martensitic Transformation Above M_s: From the preceding data it is evident that the measured M_s temperature for this alloy is dependent on the cooling rate. Slow cooling (1° to 2°C per min) yields a value of −7°C for the M_s, whereas approximately −20°C is obtained on quenching from room temperature. The following critical experiment was performed to demonstrate that isothermal martensitic transformation can take place at temperatures above the true M_s temperatures. A specimen was slowly cooled (1° to 2°C per min) to −5°C. Simultaneous electrical resistance and temperature measurements were made during this treatment. Fig. 8a shows the linear relationship between the electrical resistance and the temperature. As soon as the specimen reached −5°C, it was up-quenched to room temperature and its resistance was again measured. The value obtained is indicated by the triangle in Fig. 8a and demonstrates that no transformation had occurred on cooling to −5°C. The specimen was then quenched to −1.5°C (indicated by the dashed line in the figure) and held at that temperature.

The amount of martensite formed isothermally as a function of time at −1.5°C is shown in Fig. 8b. Although less than 2 pct martensite formed in 140 min, the sensitivity of the measurements was such that the course of the transformation could be easily followed. Since the initial resistance of the specimen did not allow precise bridge balance (using only four significant figures), the initial value is subject to the greatest inaccuracy. Subsequent

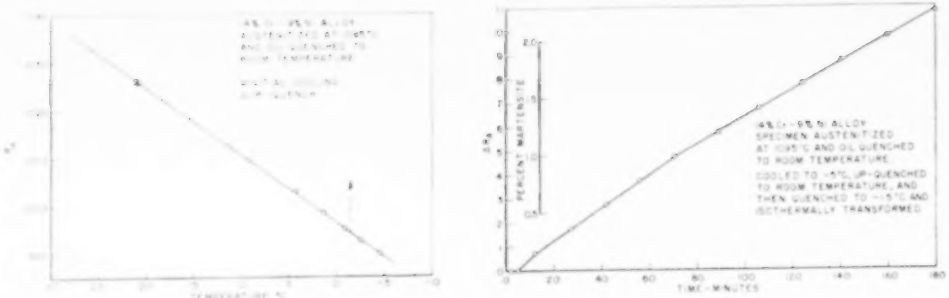

Fig. 8a and b—Isothermal formation of martensite above M_s.

bridge readings, as previously explained, are reliable to about two in the fifth significant figure. Because of the inaccuracy in the first readings, the curve of Fig. 8b could possibly be shifted slightly in the vertical direction. This means that the assumption of an incubation period is not justified. These results clearly demonstrate the phenomenon of isothermal martensitic transformation at temperatures above the M_s temperature.

Discussion of Results

A distinguishing feature of the martensitic transformation in the alloy used in this investigation is the extensive isothermal transformation at low temperatures. The amount of martensite formed isothermally follows a C-curve behavior with decreasing temperature. In the higher temperature range, the amount of isothermal martensite is much larger than the athermal portion of the transformation. It is possible to obtain much more martensite by an isothermal treatment at a high temperature than by quenching to extremely low temperatures. Similar results would be expected in certain other stainless steels of the 18-8 variety.

The M_s temperature for this alloy is dependent on the cooling rate employed in its determination. The strong tendency for isothermal transformation results in higher observed M_s temperatures with slower cooling rates. It has been shown conclusively that isothermal transformation occurs at temperatures above the true M_s temperature. The latter temperature must be defined as the limiting value obtained with increasing cooling rates. Previously the M_s temperature was defined as being independent of the rate of cooling except in cases where stabilization effects supposedly occurred. On the basis of the present work, this formerly accepted characteristic of the martensitic reaction cannot be used as a defining principle.

The shape of the rate of nucleation vs. temperature curve, Fig. 4, is similar to that obtained for ordinary nucleation and growth transformations. This does not mean, however, that the martensitic reaction can be described by the usual nucleation and growth theories. Some of the variables affecting the isothermal nucleation of martensite are the size and distribution of the embryos with respect to the critical size, the possibility of certain thermal fluctuations, stress fields, microstress relief, and the partitioning effect. The leveling off of the athermal martensite range curve, Fig. 3, cannot be explained by the partitioning effect, since greater amounts of transformation take place at higher temperatures. Greater partitioning is obtained at these temperatures even though the chemical driving force is smaller. Evidently, in this case, the stress fields and microstress relief are more important variables. Work has been done elsewhere[7] which showed that a compressive hydrostatic stress component can suppress the nucleation of martensite.

Kurdjumov and Maksimova[2] plotted the logarithm of the initial isothermal nucleation rate vs. the reciprocal of the absolute temperature and obtained essentially two straight lines. They interpreted their results in terms of ordinary nucleation and growth theory using an activation energy for the rate of growth to describe the low temperature behavior. A similar plot of the data obtained in this investigation showed a marked deviation from linearity at low temperatures. This means that the low temperature kinetics of the martensitic reaction cannot be described in terms of a single activation energy. In addition, such a treatment is not valid since, as mentioned previously, it has been found that martensite plates can form with great rapidity at very low temperatures.[7]

It is obvious that thermal fluctuations play a vital role in the kinetics of the martensitic transformation. However, the nature of this type of transformation is such that this variable cannot be treated as in ordinary nucleation and growth transformations, since other controlling variables are present. The strain embryo theory[7] differs from the ordinary nucleation and growth theory both in regard to the nature of the nucleus and its mechanism of growth. On the basis of the present work, it is believed that a general martensite theory must include not only the basic concepts of the strain embryo theory, but also the important role played by thermal fluctuations.

Summary

The results of the present work can be summarized as follows:

1—Extensive isothermal formation of martensite occurs in the 14 pct Cr-9 pct Ni-Fe base alloy studied.

2—The observed M_s temperature of this alloy was found to depend on the cooling rate. The true M_s temperature is defined as the limiting value obtained with increasing cooling rates.

3—Isothermal martensitic transformation takes place at temperatures above the M_s temperature of this alloy.

4—The amount of martensite formed isothermally in a given time follows a C-curve behavior with decreasing temperature.

5—The curve of the initial rate of nucleation of

isothermal martensite as a function of temperature has the same form as that obtained for ordinary nucleation and growth transformations.

6—The transformation at low temperatures cannot be described in terms of the temperature dependence of the rate of growth.

7—The initial martensite content, within the limits investigated, has no significant effect on the initial rate of isothermal nucleation.

8—It is possible to obtain a greater amount of martensite by an isothermal treatment at a high temperature than can be produced by quenching to a very low temperature.

9—A prequench to −196°C, and subsequent isothermal transformation for 2 hr at a temperature lower than −30°C, results in less total transformation than can be obtained by an identical isothermal treatment which is not preceded by the prequench.

10—It is believed that a general martensite theory must include not only the basic concepts of the strain embryo theory, but also the important role of thermal fluctuations.

Acknowledgments

The authors wish to express their appreciation to the Metallurgy Section of the Westinghouse Research Laboratories for making this work possible and especially to George Eichelman who supplied the alloy used in this investigation.

References

[1] B. L. Averbach, M. Cohen, and S. G. Fletcher: The Dimensional Stability of Steel. Part III—Decomposition of Martensite and Austenite At Room Temperatures. *Trans.* A.S.M. (1948) **40**, p. 728.

[2] B. L. Averbach and M. Cohen: The Isothermal Decomposition of Martensite and Retained Austenite. *Trans.* A.S.M. (1949) **41**, p. 1024.

[3] G. V. Kurdjumov and O. P. Maksimova: Kinetics of the Transformation of Austenite to Martensite at Low Temperatures. *Doklady Akad. Nauk, SSSR* (1948) **61**, p. 83.

[4] G. V. Kurdjumov and O. P. Maksimova: On the Energy of Formation of Martensite Nuclei. *Doklady Akad. Nauk, SSSR* (1950) **73**, p. 95.

[5] G. V. Kurdjumov, O. P. Maksimova, and T. V. Tagunova: On the Transformation of Deformed Austenite Into Martensite. *Doklady Akad. Nauk, SSSR* (1950) **73**, p. 307.

[6] S. A. Kulin and M. Cohen: On the Martensitic Transformation At Temperatures Approaching Absolute Zero. *Trans.* AIME (1950) **188**, p. 1139; JOURNAL OF METALS (September 1950).

[7] M. Cohen, E. S. Machlin, and V. G. Paranjpe: Thermodynamics of The Martensitic Transformation. Thermodynamics in Physical Metallurgy. A.S.M., p. 242 (1949).

[8] S. C. Das Gupta and B. S. Lement: Isothermal Formation of Martensite at Subzero Temperatures in a High Chromium Steel. *Trans.* AIME (1951) **191**, p. 727; JOURNAL OF METALS (September 1951).

[9] R. T. Howard and M. Cohen: Quantitative Metallography by Point-Counting and Lineal Analysis. *Trans.* AIME (1947) **172**, p. 413; METALS TECHNOLOGY (August 1947).

[10] M. Cohen and B. L. Averbach: X-ray Determination of Retained Austenite by Integrated Intensities. *Trans.* AIME (1948) **176**, p. 401; METALS TECHNOLOGY (February 1948).

[11] E. S. Machlin and M. Cohen: Burst Phenomenon in the Martensitic Transformation. *Trans.* AIME (1951) **191**, p. 746; JOURNAL OF METALS (September 1951).

[12] S. A. Kulin and M. Cohen: The Effect of Stress on The Martensitic Transformation. Submitted to AIME.

Technical Note

Origin of Recrystallization Textures

by J. E. Burke

THE origin of recrystallization textures continues to be a matter of controversy. One explanation is that a recrystallization texture occurs because only grains having a limited range of orientations ever appear in the deformed matrix—the oriented nucleation* hypothesis. Another explanation is that grains essentially having all orientations are nucleated but that those having certain orientations grow much more rapidly than any others in the deformation texture, and thus only the rapidly growing grains survive when recrystallization is complete.

There has recently appeared a great deal of evidence[1-4] to indicate that recrystallized grains of face-centered cubic metals are frequently related to their parent grains by rotations of 20° to 40° about a common [111] direction. Furthermore, it has been observed that the growth rate of the new grains depends upon their orientations with respect to the matrix,[5-8] and that the most rapidly growing grains lie within the stated range of orientations. In a recent note, Beck[9] has concluded from observations of this type that oriented growth alone is responsible for the appearance of preferred orientations in recrystallized metals. It should be pointed out, however, that many of the available data indicate that oriented nucleation operates in addition to oriented growth. Thus, while oriented growth may permit a selection to be made among nuclei of several orientations, only a limited number of orientations are available in the first place for such selection.

J. E. BURKE, Member AIME, is associated with Knolls Atomic Power Laboratory, General Electric Co., Schenectady.

TN 104E. Manuscript, Aug. 27, 1951.

* The terms "nuclei" and "nucleation" are used only to refer to the new grains that appear and grow during recrystallization, and imply nothing regarding the mechanism of their formation.

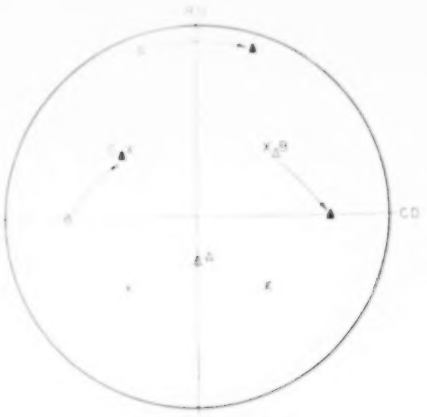

Fig. 1 — Deformation textures of aluminum

The argument is as follows. If recrystallization textures arise from a selection of only a few orientations from an array of randomly oriented nuclei, then all crystallographically equivalent orientations should appear in the recrystallized specimen. For example, if rotations occur about [111], they should also occur about [1$\bar{1}$1], [11$\bar{1}$], and [$\bar{1}$11]. In no case has this full symmetry developed. It is repeatedly observed that only a reproducible few of the numerous equivalent orientations are found, which indicates that there is a reproducible preference in orientations of nuclei from which selection may be made by oriented growth.

Kronberg and Wilson[3] found that the new grains appearing after secondary recrystallization of copper were rotated by 22° or 38° about a [111] direction held in common with the cube texture matrix. If all crystallographically equivalent orientations developed, 16 new orientations should appear, corresponding to rotations in either sense of two possible amounts about four ⟨111⟩ axes. Actually, with one exception in 63 observations, they found 22° rotations either clockwise about northwest and southeast ⟨111⟩ directions, or counterclockwise about northeast and southwest ⟨111⟩ directions. The rolling direction is north, and all 38° rotations are opposed to 22° rotations. Thus, only eight new orientations appear.

There is also evidence to indicate that the new grains may be related to the parent by rotation about only a reproducible few of the possible four ⟨111⟩ directions. Maddin, Mathewson, and Hibbard[4] found that upon recrystallizing deformed single crystals of brass, the new grains were related by rotations about the poles of the octahedral planes upon which slip occurred, and about no others. Similar observations have been made in copper by Becker.[5] The deformation fiber texture of aluminum wire has a [111] axis parallel to the wire axis, and the fiber axis is apparently unchanged by recrystallization.[6] Beck[7] has pointed out that if all new grains are related to their parents by a rotation about an appropriate [111] direction, the new texture would be indistinguishable from the old. The rotation must be about the [111] axis which is parallel to the fiber axis in each grain however, so that only one of the four possible axes are chosen. Had the new grains been related by rotations about more than one of the [111] axes, a much more random texture would have been obtained.

The recrystallization texture of rolled aluminum differs only slightly from the deformation texture. Beck and Hu[8] have explained this also by a rotation about ⟨111⟩ directions. The deformation texture of aluminum consists of two pairs of orientations, one of which is shown by triangles in Fig. 1. One half of the pair is shown as open triangles and the other by closed triangles. The two halves of the pair are related by a rotation of approximately 40° about an octahedral pole, *A*, which they have in common. If the new grains are related to the old by rotations in the correct direction about this pole, the halves of this component of the texture interchange, and the new texture will be indistinguishable from the old. A rotation of about 40° around pole *B* for the open triangles or around pole *C* for the closed triangles, in an appropriate direction, will transpose the deformation texture into the well-known cube texture, as shown by the positions indicated by *X*. Beck and Hu find traces of the cube texture in the recrystallized aluminum and have presented microscopic evidence to show that the first mentioned reorientation (about pole *A*) does in fact occur. Thus again, while the new and apparently identical textures can be explained in terms of a rotation about a single [111] direction, not all such poles are used, nor are rotations of both senses used. Again it seems necessary to assume that while some selection of orientations may have been made by oriented growth, only a limited number of orientations were produced at the time of nucleation.

Beck[7] has considered the problem created by the appearance of only a few of the crystallographically identical orientations in a recrystallization texture and has offered two possible explanations "in terms of the oriented growth hypothesis." One is that nominally equivalent orientations do not have equal growth rates. While this explanation is consistent with the oriented growth hypothesis, there seems to be no evidence to support it. The other suggestion is that nuclei of all orientations do not appear. While this second explanation permits the operation of oriented growth as an assisting factor in producing a well-defined recrystallization texture, it appears to also state that oriented nucleation exists.

References

[1] J. S. Bowles and W. Boas: *Journal* Inst. Metals (1948) **74**, p. 501.

[2] M. L. Kronberg and F. H. Wilson: *Trans.* AIME (1949) **185**, p. 501; JOURNAL OF METALS (August 1949).

[3] R. Maddin, C. H. Mathewson, and W. R. Hibbard, Jr.: *Trans.* AIME (1949) **185**, p. 655; JOURNAL OF METALS (September 1949).

[4] Joseph Becker: *Trans.* AIME (1951) **191**, p. 115; JOURNAL OF METALS (February 1951).

[5] P. A. Beck, P. R. Sperry, and Hsun Hu: *Journal of Applied Physics* (1950) **21**, p. 420.

[6] J. E. Burke: The Migration of Grain Boundaries. A.S.M. Seminar, "Atom Movements," A.S.M. (1951).

[7] Paul A. Beck: *Trans.* AIME (1951) **191**, p. 475; JOURNAL OF METALS (June 1951).

[8] C. S. Barrett: *The Structure of Metals.* (1946) New York. McGraw-Hill Book Co.

[9] P. A. Beck and Hsun Hu: *Trans.* AIME (1949) **185**, p. 627; JOURNAL OF METALS (September 1949).

[10] P. A. Beck and Hsun Hu: JOURNAL OF METALS (October 1950) pp. 1214, 1215.

Time-Temperature-Transformation Characteristics Of Titanium-Molybdenum Alloys

by D. J. DeLazaro, M. Hansen, R. E. Riley, and W. Rostoker

KNOWLEDGE of the isothermal transformation behavior and the TTT chart method of graphically summarizing such information has been of invaluable aid to the ferrous metallurgist in understanding and developing heat treatments intended to provide specific mechanical properties. It is to be expected that similar lines of study directed to titanium-base alloys will be as profitable. This paper summarizes, on conventional TTT charts, the isothermal transformation products and pertinent reaction rate data for binary alloys of titanium containing 1, 3, 5, 7, 9, and 11 pct Mo, respectively. The results so presented were derived from metallographic examination. Some X-ray diffraction work was done to clarify certain points of question.

Ti-Mo System

To the authors' knowledge, TTT charts have only been used to describe the reaction rates of eutectoidal decompositions. It would seem that the kinetics of decomposition of any unstable solid solution might be conveniently described in this manner. The equilibrium diagram of the Ti-Mo system[1] is shown in Fig. 1. The similarity with the Fe-Ni system will be recognized. Additions of molybdenum serve to stabilize the β phase to increasingly lower temperatures. The solubility of molybdenum in the α phase is restricted to less than 1 pct at 600°C. Under normal conditions, a homogeneous β structure quenched to a temperature in the $\alpha + \beta$ field will reject α of invariant composition. The rate at which this occurs depends on the degree of undercooling and the degree of supersaturation of β. The structural character of the rejected phase may also be expected to be related to the undercooling.

Materials and Experimental Methods

A sponge titanium was used which has a nominal impurity content as reported in Table I. The nominal composition of the molybdenum used is also included. The alloys were prepared in 150 g melts by arc melting in an evacuated water-cooled copper crucible of the type reported in an earlier paper.[2] The pancake-type ingots were forged to $\frac{1}{4} \times \frac{1}{4}$ in. bars and homogenized for 24 hr at 1000°C in evacuated Vycor bulbs. Specimens $\frac{1}{4}$ in. thick were cut from these bars for heat treatment. The heat treatment cycles followed an invariant procedure. The specimens were soaked at 1000°C for 20 min under a helium protective atmosphere prior to quenching into a lead bath held at a temperature corresponding to a chosen degree of undercooling. After a prescribed period of time at this temperature, the specimen was removed and water quenched. A series of specimens so treated for progressively longer periods served to establish the times for initiation and completion of the decomposition of the β phase at a particular temperature.

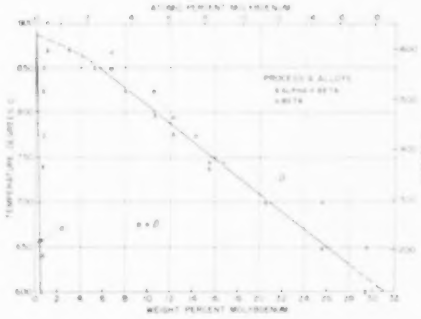

Fig. 1—Ti-Mo equilibrium diagram.

Although heat treatment of unprotected specimens in a lead bath does permit surface contamination by lead diffusion, this method is necessary to insure sufficiently rapid quenching rates. As long as the bath treatments were of less than 1 hr duration, the contaminated surface was not unduly deep and could be removed without excessive grinding. Metallographically, the contaminated zone could be readily distinguished from the pure binary alloy.

Transformation Characteristics of Ti-Mo Alloys

Metallographic examination showed that a supersaturated β phase may decompose by one of two processes. Alloys containing 1 to 9 pct Mo, when quenched in water from the homogeneous β field,

Table I. Nominal Composition of Titanium and Molybdenum

	Ti, Pct		Mo, Pct
Ti	99.71	Mo	99.9+
Fe	0.10	C	0.015 max
C	0.02	Co + Ni	0.02 max
O	0.14	O	0.045 max
N	0.005-0.009		
H	0.006		

D. J. DeLAZARO is Research Assistant, M. HANSEN, Member AIME, is Assistant Chairman, R. E. RILEY is Research Assistant, and W. ROSTOKER is Research Metallurgist, Metals Research Dept., Armour Research Foundation of Illinois Institute of Technology, Chicago.

Discussion on this paper, TP 3256E, may be sent, 2 copies, to AIME by Dec. 1, 1952. Manuscript, Oct. 11, 1951. Philadelphia Meeting, October 1952.

This paper is based on reports to the Flight Research Laboratory under Contract No. AF 33(038)-16347.

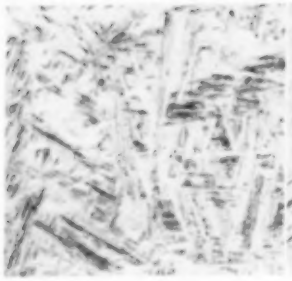

Fig. 2—Ti 1 pct Mo alloy.

Fig. 3—Ti 5 pct Mo alloy.

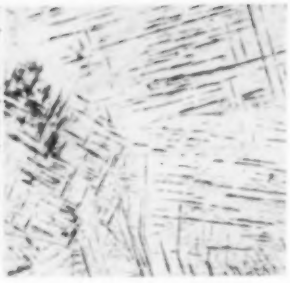

Fig. 4—Ti 9 pct Mo alloy.

Figs. 2-4—Ti-Mo alloys in the as quenched condition. X150. Etchant: 60 pct glycerine, 20 pct HNO_3, 20 pct HF.

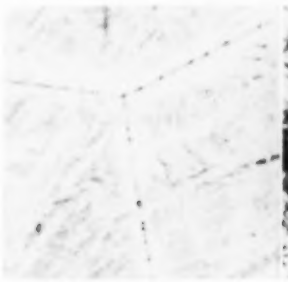

Fig. 5—10 sec.

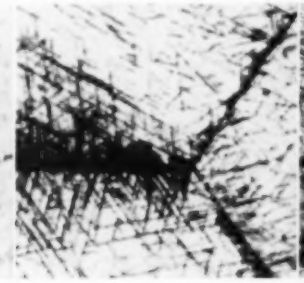

Fig. 6—30 sec.

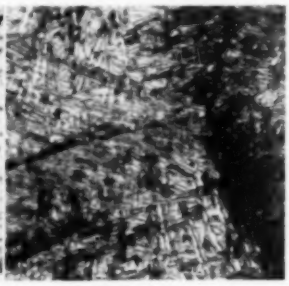

Fig. 7—60 min.

Figs. 5-7—Ti 3 pct Mo alloy held at 700° C for indicated times prior to quenching. X750.
Etchant: 60 pct glycerine, 20 pct HNO_3, 20 pct HF.

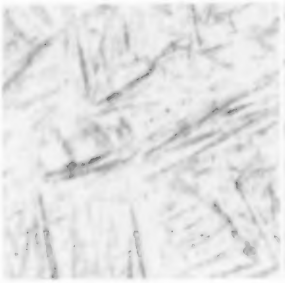

Fig. 8—10 sec.

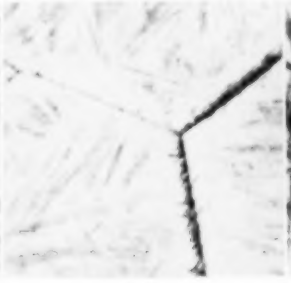

Fig. 9—30 sec.

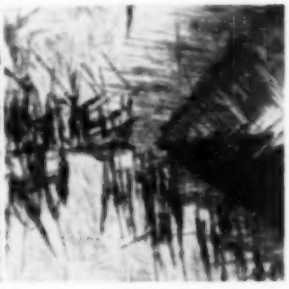

Fig. 10—10 min.

Figs. 8-10—Ti 7 pct Mo alloy held at 700° C for indicated times prior to quenching. X750.
Etchant: 60 pct glycerine, 20 pct HNO_3, 20 pct HF.

Fig. 11—2 min.

Fig. 12—10 min.

Fig. 13—60 min.

Figs. 11-13—Ti 11 pct Mo alloy held at 700° C for indicated times prior to quenching. X750.
Etchant: 60 pct glycerine, 20 pct HNO_3, 20 pct HF.

Fig. 14—TTT chart for Ti 1 pct Mo alloy

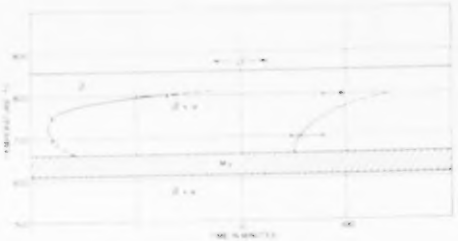

Fig. 15—TTT chart for Ti 3 pct Mo alloy

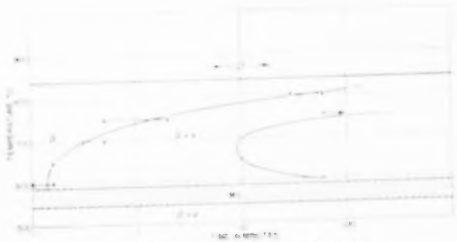

Fig. 16—TTT chart for Ti 5 pct Mo alloy

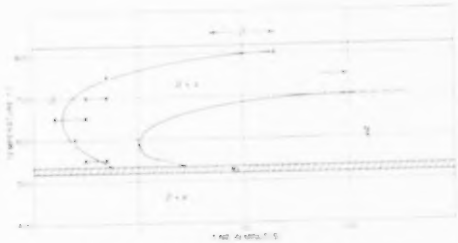

Fig. 17—TTT chart for Ti 7 pct Mo alloy

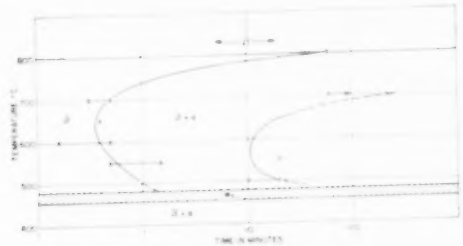

Fig. 18—TTT chart for Ti 9 pct Mo alloy

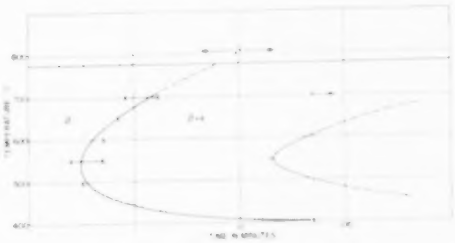

Fig. 19—TTT chart for Ti 11 pct Mo alloy

exhibit a uniform acicular structure. As may be seen from Figs. 2, 3, and 4, the general appearance changes somewhat with increasing molybdenum content. It is generally accepted that an efficient water quench provides a cooling rate which is rapid enough to almost completely suppress the decomposition of an unstable phase, by a nucleation and growth mechanism. From its large volume, it is reasonable to conclude that this acicular structure belongs to the family of metastable phases which form by some diffusionless process and which, in ferrous terminology, are referred to as martensites. In recent years, it has been recognized that this type of transformation is quite common both in ferrous and in nonferrous systems. Nor is the martensite type of reaction confined to suppressed eutectoid transformations but, as in the case of Fe-Ni alloys, may occur in systems with open γ (or β) fields. In line with nomenclature which has been used in this country,* it is proposed to refer to this phase as α', as distinct from the normal equilibrium phase α.

On examination of slow cooled specimens or specimens which have undergone isothermal heat treatments at moderate undercooling temperatures, decomposition appears to proceed by a time dependent nucleation and growth process. The characteristics of this type of reaction are well known, and it will suffice to mention that the rejection of α from β shows no unusual features.

To determine the structure of the α' phase and to obtain some idea of the extent to which β is converted to α', a series of quenched powder samples with from 1 to 11 pct Mo was examined by X-ray diffraction. The lines from the β phase could be readily distinguished, and their sharpness lent support to the assumption that no significant concentration gradients had been established by a diffusion dependent reaction. The lines belonging to the new phase were generally broad and diffuse. They were identified as the pattern for a hexagonal close-packed structure with an axial ratio, as well as could be estimated from broad lines, which was very close to that of the normal equilibrium α phase. It may therefore be reasonably concluded that the acicular structure is a supersaturated α phase having the composition of the original β. Similar conclusions have been drawn regarding the nature of analogous phases in the Fe-Ni[4] and the Fe-Mn[5] systems.

The diffraction patterns further showed that the proportion of β transformed to α' on quenching to room temperature decreased with increasing molybdenum content. An 11 pct Mo alloy showed only a

* In several British papers, the term α_1 has been used.

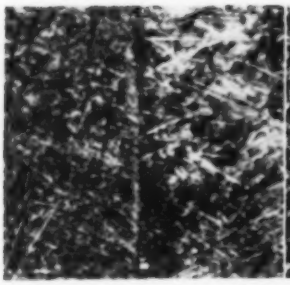

Fig. 20—Ti 3 pct Mo alloy quenched to 610 C, raised to 700 C, and held for 60 min prior to quenching. X750. Etchant: 60 pct glycerine, 20 pct HNO_3, 20 pct HF.

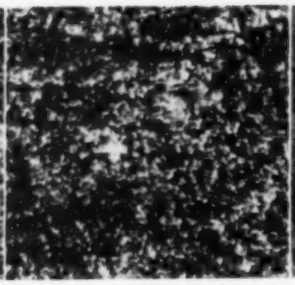

Fig. 21—Ti 3 pct Mo alloy quenched to 660 C, raised to 700 C, and held for 60 min prior to quenching. X750. Etchant: 60 pct glycerine, 20 pct HNO_3, 20 pct HF.

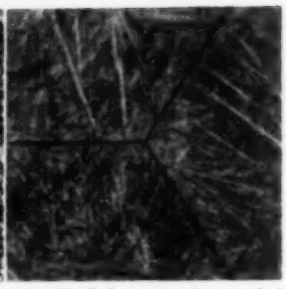

Fig. 22—Ti 9 pct Mo alloy quenched to 454 C, raised to 600 C for 12 min prior to quenching. X750. Etchant: 60 pct glycerine, 20 pct HNO_3, 20 pct HF.

few faint lines which could be interpreted as belonging to the α' pattern.

Isothermal Transformations

Contemporary knowledge regards the isothermal decomposition of a supersaturated phase by a nucleation and growth process as continuous with time. The rate of reaction, however, is often initially exceedingly slow and decomposition products can only be detected after some time has elapsed. The boundary marking the start of precipitation on a TTT chart is therefore based on the times for a detectable amount of new phase to appear.

The rejection of α originates predominantly at the grain boundaries. The effect is often quite striking. By careful examination of the grain boundaries it was relatively easy to detect the first onset of transformation. A time sequence for each of three alloys heat treated isothermally is shown in Figs. 5 to 13.

It is considerably more difficult to decide when the transformation has reached completion. This condition was adjudged to have been reached when the dark etching decomposition structure had apparently consumed the light etching untransformed β. This criterion provides only an approximation, and represents a phase of solid state reaction studies where metallographic techniques are not advantageous.

The TTT charts for alloys containing 1 to 11 pct Mo are presented in Figs. 14 to 19. The manner of plotting is conventional. An upper temperature level is marked, above which β is stable. A lower temperature level marks the M_s temperature, whose determination is discussed in the next section. Between these two levels, two continuous curves delineate the time-temperature conditions for initiation and completion of isothermal rejection of α.

The charts are, in general, of the form normally encountered. Reaction rates seem to be accelerated with molybdenum additions from 1 to 7 pct. From 7 to 11 pct Mo, reaction rates again become progressively more sluggish.

Determination of M_s Temperatures

The metallographic determination of the M_s temperature in steels is usually carried out by the well-known Greninger-Troiano method.[7] This method depends on the rapid tempering characteristics of the martensite and its darkly etched appearance, which stands in sharp contrast to originally retained austenite transformed to martensite or retained on final quenching. Unfortunately, this method as it stands cannot be successfully applied to Ti-Mo alloys. The reason for this is that α', on tempering, does not reject a fine dispersion of a second phase, as carbide in steel, with consequent dark etching properties. In fact, the α' probably "tempers" by growth into adjacent β areas until the original molybdenum content is diluted to the composition of α. It is not possible to distinguish metallographically between α' originally formed and that rejected by some later quench to room temperature. Accordingly, some modification of the Greninger-Troiano method was necessary.

The problem of fixing the condition of β such that it can be readily distinguished from α' is solved by isothermally transforming residual β at a temperature in the region of the "knee" of the TTT curve.

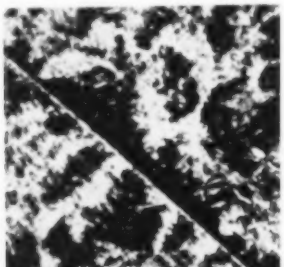

Fig. 23—Ti 9 pct Mo alloy quenched to 478 C, raised to 600 C for 12 min prior to quenching. X750. Etchant: 60 pct glycerine, 20 pct HNO_3, 20 pct HF.

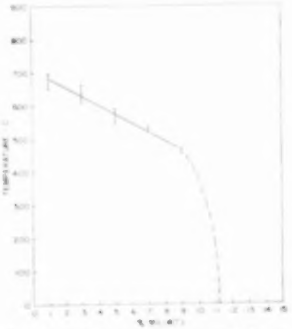

Fig. 24—M_s temperature vs. molybdenum content.

The α' platelets during this stage of heat treatment are relatively unchanged in their light etching characteristics. The isothermally decomposed β is dark etching and may be readily distinguished from α'. Figs. 20 to 23 show micrographs of alloys which have been quenched to temperatures above and below the M_s temperature prior to isothermal decomposition of the retained β. By this method, the M_s temperature could be estimated to an accuracy of about ±20°C.

The dependence of M_s temperature on molybdenum content is illustrated in Fig. 24. It will be seen that between 1 and 9 pct Mo a linear relationship obtains. This linearity is in accordance with the behavior of the plain carbon and alloy steels and Cu-Al alloys.[7] Extrapolation of the line intersects the temperature axis well below the α/β inversion temperature for pure titanium. This is also in general agreement with the behavior of other alloy systems.

While 9 pct Mo exhibits α' in profusion on quenching directly to room temperature, the 11 pct Mo alloy

Fig. 25—Ti-9 pct Mo alloy held at 700°C for 2 sec prior to quenching. X750.
Etchant: 60 pct glycerine, 20 pct HNO_3, 20 pct HF

presents an apparently undisturbed field of residual β. This radical suppression of α' formation seems to derive from some sort of stabilization. As an example of this, a specimen of 9 pct Mo quenched from 1000° to 700°C and held there for just 2 sec prior to water quenching, shows no evidence of α' on examination, see Fig. 25. The structure is apparently completely retained β. On the other hand, the same alloy, when directly quenched into water, exhibits a pronounced α' structure, see Fig. 4. Presumably then, even the extremely short time required to quench an 11 pct Mo alloy to room temperature is sufficient to suppress the formation of α'.

Hardness of Heat Treated Ti-Mo Alloys

Some general observations of hardnesses may be of interest, and are therefore reported. As-quenched hardnesses fall in the general range of 290 to 350 VHN with no particular trend evident. It is difficult to say whether the α' contributes hardness over and above that which the β structure would have at room temperature. The hardness of stabilized β in 7 and 9 pct Mo is higher than that of $\alpha' + \beta$ mixtures. However, this may well be a pre-precipitation phenomenon. The as-quenched 11 pct alloy with completely retained β has a hardness of 300 VHN, while a 9 pct alloy which has a high proportion of α' possesses a hardness of 350 VHN. These observations do not resolve the question, but would seem to indicate that α' does not have as predominating an influence as martensite in steels.

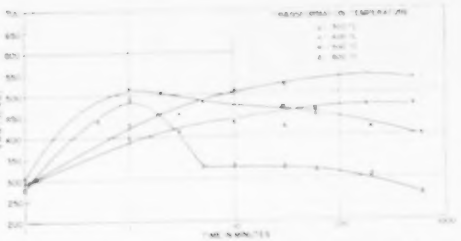

Fig. 26—Hardnesses of an 11 pct Mo alloy isothermally decomposed at various temperatures.

Isothermal decomposition heat treatments generally yield significantly higher hardnesses than quenching. A series of typical hardness vs. time curves for an 11 pct Mo alloy is shown in Fig. 26. The hardness trend is similar to age hardening in that the peak hardness occurs at about the first visible appearance of decomposition. Further, the time for peak hardness and the magnitude of the peak increase with decreasing aging temperature in accordance with normal age hardening behavior.

Reheating of quenched alloys yields results which depend upon the amount of retained β. A 1 pct alloy is unaffected by any combination of time-temperature of reheating. Alloys containing 3, 5, 7, and 9 pct Mo show successively increasing hardness peaks on reheating. From our knowledge of relative proportions of α' and β on quenching to room temperature, it is evident that these hardness increases reflect the isothermal decomposition of retained β. It would appear from these preliminary experiments that direct isothermal heat treatment provides superior control and maximum hardness to any combination of quenching and reheating cycles.

Summary

1—It has been shown that a supersaturated β phase may decompose either by nucleation and growth of α or by a diffusionless transformation to α'.

2—The transformation products and pertinent reaction rate information may be represented on conventional TTT charts.

3—The M_s temperature for α' formation is linearly dependent on molybdenum content. Dominant stabilization effects become operative above 9 pct Mo.

Acknowledgments

The authors wish to express their appreciation of the sponsorship of this project by the Flight Research Laboratory, Wright-Patterson Air Force Base, Dayton, Ohio, and for their permission to publish this paper.

Some of the introductory work on this project was carried out under the supervision of J. P. Sheehan. The metallographic preparation and photography was done by C. A. Johnson.

References

[1] M. Hansen, E. L. Kamen, H. D. Kessler, D. J. McPherson: *Trans.* AIME (1951) **191**, p. 881; JOURNAL OF METALS (October 1951).

[2] H. Bumm and V. Dellinger: *Ztsch. Metallkunde* (1937) **29**, p. 29.

[3] A. R. Troiano and F. T. McGuire: *Trans.* A.S.M. (1943), **31**, p. 340.

[4] A. B. Greninger and A. R. Troiano: *Trans.* A.S.M. (1940), **28**, p. 537.

[5] *Metals Handbook*, pp. 265 (1948). Cleveland A.S.M.

Technical Note

Extent of Strain of Primary Glide Planes in Extended Single Crystalline Alpha Brass

by R. Maddin

IN studying the relation between the orientation of new grains and that of the deformed matrix of axially extended and recrystallized single crystals of face-centered cubic metals, a two-stage rotation process[1] is generally used where the first rotation is made in order to account for an "adjustment of orientation to the environment of strain".[2] It has been argued that in spite of the difference of orientation, which may amount to as much as 12° (in α brass), between the octahedral plane as observed in the parent lattice and in the recrystallized grain, it is believed to be a common plane in the sense that it constituted the nucleus in the parent strained crystal from which the new grain grew.[3]

A possible source of the deviation in orientations of a common pole in the new grain and that of the deformed single crystal matrix from which it has grown may be found in the distribution of strain resulting from the plastic deformation. It might be expected in view of the incongruent nature of shear[4] that the perfection of the octahedral plane along which glide has occurred is disrupted and that this disruption constitutes the strain from which nuclei of new grains can grow during recrystallization. Evidence for the existence of strain along glide planes was first detected by Taylor[5] in 1927 and substantiated by Collins and Mathewson[6] in 1940. In their investigations, however, the deformed single crystalline specimens (aluminum) were cut mechanically along the glide planes followed by mechanical polishing. X-ray exposures (glancing angle) of only 8 min with filtered radiation were used. It was later shown[7] that this type of surface preparation did not remove with all certainty the mechanically disturbed surface. It was felt that a re-investigation of this phenomenon using more refined techniques might reveal a more correct extent of the strain resulting from the deformation which might correlate the deviation of the common pole of the recrystallized grain with the acting slip plane of the matrix crystal.

In accordance with these thoughts, a single crystal of α brass (70/30 nominal composition) $\frac{1}{2}$ in. in diam x 5 in. long, tapered as in previous experiments,[7] was extended and carefully documented with respect to elongation and shear. Disks about $\frac{1}{8}$ in. thick parallel to the primary slip planes were cut from the specimen by means of an etch cutter.[8] These disks represented volumes of the specimen which had been extended 0, 5, 10, 15, and 20 pct. Copper K_α monochromatic radiation was obtained by reflecting 35,000 v copper radiation from the cleavage face of a pentaerythritol crystal. The monochromatic radiation was collimated and led on to the disk set at the proper θ angle for reflection from the primary (111) planes. The monochromatic beam was aligned in a plane containing the active slip direction. Following a 10 hr exposure at the theoretical Bragg angle, the disk was reset at $\theta + 1°$, $\theta - 1°$, $\theta + 2°$, $\theta - 2°$, etc., until no Bragg reflection was obtained. The disk was then rotated 90° about its polar axis, and the same X-ray procedure was used. The results are shown in Table I.

Table I. Extent of Strain in Disks Investigated

Elongation Pct	Stress Axis Rotation Degrees	Shear Abgleitung	Variation in θ Angle	
			Parallel to Slip Direction, Degrees	Perpendicular to Slip Direction, Degrees
0	0	0	2	2
5	1.3	0.088	6	7
10	2.6	0.240	11	8
15	4.0	0.311	13	13
20	5.6	0.407	25	20

It may be seen from the results in Table I that the plastic deformation (20 pct elongation) produces fragments of the glide plane which are rotated or tilted as much as 25° from the normal position on a purely block slip model. In addition to the large variation in θ angle in the slip direction, there is a variation in θ as much as 20° in the direction at right angles to the direction of slip, i.e., $\langle 110 \rangle$.

In view of the results shown, it may now be argued that the strain distribution finds its origin in the incongruent nature of the slip process.[4] The use of the two-stage rotation process seems valid in attempting to explain the relation between the orientation of recrystallized grains and the matrix from which they have grown.

Acknowledgment

This work was sponsored by the ONR under Contract Number N6 onr 234-21 ONR 031-383. The author would like to thank N. K. Chen for reading and correcting the manuscript.

References

[1] R. Maddin, C. H. Mathewson, and W. R. Hibbard, Jr.: The Origin of Annealing Twins. *Trans.* AIME (1949) **185**, p. 655; JOURNAL OF METALS (September 1949).

[2] J. A. Collins and C. H. Mathewson: Plastic Deformation and Recrystallization of Aluminum Single Crystals. *Trans.* AIME (1940) **137**, p. 150.

[3] N. K. Chen and C. H. Mathewson: Recrystallization of Aluminum Single Crystals After Plastic Extension. Unpublished.

[4] C. H. Mathewson: Structural Premises of Strain Hardening and Recrystallization. *Trans.* A.S.M. (1944) **33**.

[5] C. H. Mathewson: Critical Shear Stress and Incongruent Shear in Plastic Deformation. *Trans.* Conn. Acad. of Arts and Science, (1951) **38**, p. 213.

[6] G. I. Taylor: Resistance to Shear in Metal Crystals, Cohesion and Related Problems. Faraday Soc. (1927) 121.

[7] R. Maddin and W. R. Hibbard, Jr.: Some Observations in the Structure of Alpha Brass After Cutting and Polishing. *Trans.* AIME (1949) **185**, p. 700; JOURNAL OF METALS (October 1949).

[8] R. Maddin and W. R. Asher: Apparatus for Cutting Metals Strain-Free. *Review of Scientific Instruments* (1950) **21**, p. 881.

R. MADDIN, Member AIME, is Assistant Professor of Metallurgy, Johns Hopkins University, Baltimore, Md.

TN 103E. Manuscript, Nov. 23, 1951.

Solubility of Carbon and Oxygen in Molybdenum

by W. E. Few and G. K. Manning

IT has been known for some time that both intergranular carbide and intergranular oxide phases cause brittleness in molybdenum. Parke and Ham[1] indicated that 0.0025 pct O present in molybdenum after solidification from the melt was sufficient to induce intergranular brittleness during forging. However, material containing 0.06 pct C could still be forged. However, adding this amount of carbon to insure deoxidation causes the formation of carbides on freezing. These carbides are precipitated at grain boundaries, and Rengstorff and Fischer[2] have shown they have an unfavorable effect on the room-temperature ductility of molybdenum. Taker[3] in 1928 proposed that the solubility of carbon was a constant value of 0.30 pct from room temperature up to 1800°C. In 1935, Sykes, Van Horn, and Tucker[4] obtained X-ray data suggesting that the solid solubility of carbon in molybdenum was between 0.07 and 0.09 pct at temperatures from 1500° to 2100°C. The α-solubility line for carbon was included in the Mo-C diagram given in the Metals Handbook[5] as a tentative line based on the data of Sykes, Van Horn, and Tucker.

In order to determine the partial phase diagrams for these systems, it was necessary to construct a high-temperature furnace suitable for heat treating molybdenum at temperatures up to 4000°F. A molybdenum resistance furnace was built for this purpose in which samples could be heat treated in a purified atmosphere and quenched from any desired temperature.[6]

Experimental Work

Solubility of Carbon: Arc-cast molybdenum supplied by the Climax Molybdenum Co. and 18-gage molybdenum wire samples produced by powder metallurgy at the Fansteel Metallurgical Co. were used in determining the α-solubility line for the Mo-C system. The cast molybdenum contained 0.032 pct C initially. Two lots of 18-gage wire were used, one containing 0.011 pct C and the other 0.005 pct C initially. All material contained a carbide phase as received. Fig. 1 illustrates the carbides found in the untreated material.

Heat treatment in a purified hydrogen atmosphere was found to reduce the carbon content in the as-cast molybdenum. Purified argon also decarburized molybdenum samples at temperatures above 3500°F; however, the carbon content remained constant during heat treatment in purified argon at lower temperatures. The argon was purified by passing it over titanium at 750°C and then through a magnesium perchlorate drying tower. The hydrogen was purified by passing it through a commercial hydrogen deoxidizer, followed by a drying tower.

Table I. Results of Heat Treatments on Both Cast and Powder Metallurgy Molybdenum

All specimens quenched after the indicated time at temperature.

Temperature, °F	Cast or Wire Specimen	Heat Treatment	Carbon, Pct (±0.003)	Metallographic Observations
4000	C	Argon atmos., 1 hr	0.005	Single phased
4000	C	Argon atmos., ½ hr	0.006	Single phased
4000	C	Argon atmos., ¼ hr	0.015	Single phased
4000	C	Argon atmos., ½ hr	0.018	Single phased
4000	C	Argon atmos., ¼ hr	0.022	Contained excess carbide
4000	C	Argon atmos., ¼ hr	0.023	Contained excess carbide
3500	W	Argon atmos., 1 2/3 hr	0.010	Single phased
3500	C	Argon atmos., ½ hr	0.009	Single phased
3500	W	Argon atmos., ½ hr	0.010	Single phased
3500	W	Argon atmos., 2 hr	0.011	Single phased
3500	W	Argon atmos., 5 hr	0.011	Single phased
3500	W	Argon atmos., 5 hr	0.012	Single phased
3500	C	Argon atmos., 1 hr	0.013	Contained excess carbide
3500	C	Argon atmos., 3 hr	0.018	Contained excess carbide
3000	W	10-cm press. H_2, ½ hr	0.004	Single phased
3000	W	10-cm press. H_2, 1 hr	0.005	Single phased
3000	C	Argon atmos., 5 hr	0.005	Single phased
3000	W	Argon atmos., 1 hr	0.009	Contained excess carbide
3000	W	Argon atmos., 5 hr	0.010	Contained excess carbide

Specimens having different initial carbon contents were heat treated in argon at 3500°F for periods ranging from 5 min to 5 hr and were analyzed for carbon. Samples of the same final carbon content had the same microstructures regardless of time at temperature. Furthermore, a gradient between center and surface in the amount of undissolved carbide particles present was never observed. It was concluded that at these low carbon levels, and at the high temperatures involved, diffusion proceeds so rapidly that the specimen is always substantially homogeneous in carbon content, in spite of the gradual loss in carbon.

Based on the above findings, the following procedure was used to determine the carbon-solubility limit at 3000°, 3500°, and 4000°F. At each of these temperatures, a number of samples were heat treated, as shown in Table I, and rapidly cooled to room temperature. Since the samples lost carbon in proportion to the length of time heated, a series of samples were obtained of varying carbon contents. By use of a rapid cooling rate, the phases present at the high temperature were retained at room temperature.

All samples were examined microscopically. Those found to contain either no excess carbide phase or only a very small amount were then analyzed for carbon. The samples actually analyzed for carbon

W. E. FEW, Junior Member AIME, and G. K. MANNING, Member AIME, are associated with Battelle Memorial Institute, Columbus, Ohio.

Discussion on this paper, TP 3257E, may be sent, 2 copies, to AIME by Dec. 1, 1952. Manuscript, Oct. 11, 1951. Philadelphia Meeting, October 1952.

The study was part of a program underway at Battelle Memorial Institute titled "A Metallurgical Study of Molybdenum" with funds appropriated by the Office of Naval Research under Contract No. N9-onr-82100, Task Order No. N9-onr-82101.

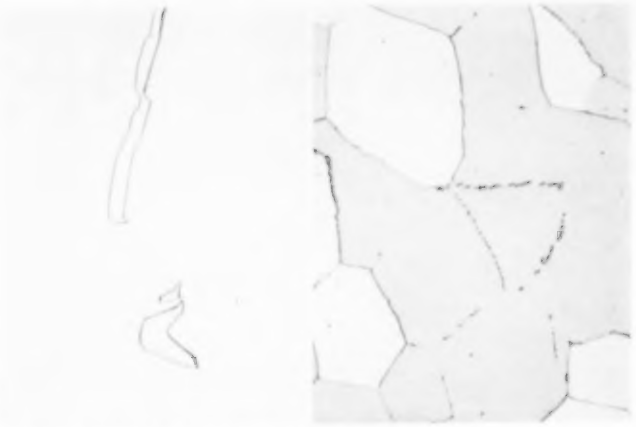

Fig. 1 (left)—Typical carbide particles observed in both as cast and powder metallurgy molybdenum when received. X1000.

Area reduced approximately 50 pct for reproduction.
a (left)—Cast molybdenum.
b (right)—Powder metallurgy molybdenum.

Fig. 2 (below)—Solubility limit of carbon in the Mo-C system.

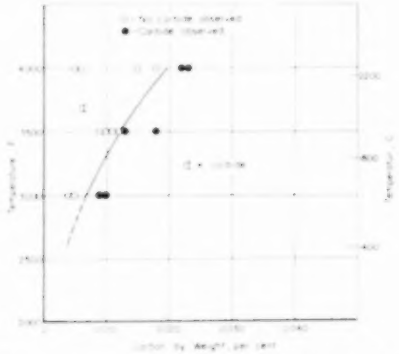

were those which had carbon contents very close to the solubility limit. Consequently, the solubility line must lie between the compositions of the highest carbon sample which did not show an excess carbide phase and the lowest carbon sample which did. Fig. 2 is a plot of the α-solubility line as determined from the data presented in Table I. Fig. 3, a and b, shows representative micrographs of samples used to establish the solubility line. When no excess carbide was visible as in Fig. 3b, the total carbon, as reported by chemical analysis, was assumed to be in solid solution.

Solubility of Oxygen. During early work to establish the α-solubility line for the Mo-O system, it became apparent that the volatilization of molybdenum oxide presented a serious experimental difficulty. It has been established that the molybdenum oxide, MoO_3, exhibits an appreciable vapor pressure above about 1500°F.[5] There is also reason to believe, as the result of work at the Climax Molybdenum Co., that the oxide inclusions observed metallographically in molybdenum are MoO_2.

During the present work, it was found, when wires were heated to 2000°F in the presence of several microns of oxygen pressure, that a dark brown oxide formed on the surface. This coating disappeared if the oxygen pressure was lowered slightly. However, the cross-section of the wire decreased as the wire was held in an atmosphere of low pressure oxygen, and a blue-black precipitate formed in the colder portions of the furnace. Since MoO_3 is white, this suggests that, at temperatures above 2000°F, some lower oxide of molybdenum has an appreciable vapor pressure. However, it could be that MoO_3 is the only volatile oxide and that the blue-black precipitate observed in the colder portion of the furnace forms by disproportionation of MoO_3. Because there is some doubt, the term molybdenum oxide is employed in subsequent pages without attempting to specify the chemical formula.

Several methods for measuring the solubility of oxygen in molybdenum were tried. An attempt was

a—Molybdenum sample containing 0.015 pct C, quenched from 1500°F. Solubility limit has been exceeded.

b—Molybdenum sample containing 0.010 pct C, quenched from 1500°F. All carbon is in solid solution.

Fig. 3—Representative micrographs of molybdenum samples studied in establishing the solubility limit of carbon in molybdenum. X1500. Area reduced approximately 50 pct for reproduction.

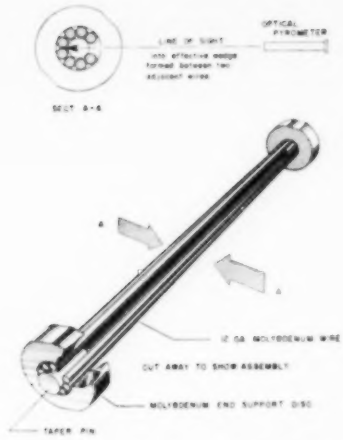

Fig. 4 (left)—Specimen assembly for heating molybdenum wires in low pressure oxygen.

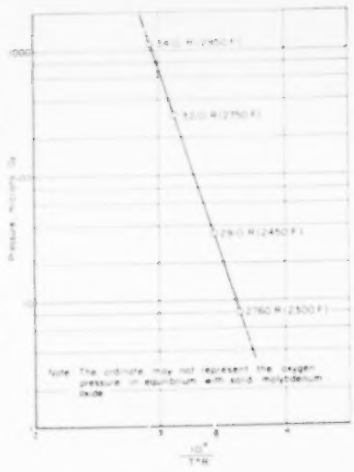

Fig. 5 (right)—Pressure necessary to produce a solid oxide on the surface of the wire.

made to use a flowing atmosphere of pure oxygen at a controlled low pressure, such that a thin layer of molybdenum oxide was maintained on the wire surface. It was planned to remove the surface oxide film, either chemically or mechanically, and to then analyze the wire for oxygen. The procedure proved unsuccessful because it was found that oxide was formed not only at the wire surface but also below the wire surface. The reason for the internal oxide formation under these conditions is not clear, but it may have been caused by temperature fluctuations. When an oxide film was formed on the wire surface, the emissivity increased and the temperature dropped several hundred degrees Fahrenheit. The temperature drop was compensated for by increasing the current flow in the wire. However, as the temperature was raised, there was a tendency to exceed the desired temperature, volatilize the oxide film, and then repeat the entire cycle in trying to establish the desired conditions. Such temperature cycling may have been the cause of the internal oxide formation.

Next, an attempt was made to use a closed system in which the furnace was initially charged with a low pressure of oxygen and then sealed off completely. It was thought that an oxide film might form on the wire surface which would persist for sufficient time to establish equilibrium across the wire but eventually would volatilize. Furthermore, it was hoped that the internal oxides would disappear at the same time the surface film disappeared. The treatment would be stopped at the time the surface film disappeared. Analysis of the wire would indicate the dissolved oxygen in equilibrium with the solid oxide. However, the procedure was not successful because at temperatures above about

Table II. Results of Heat Treating Molybdenum in an Atmosphere of Low Pressure Oxygen

Type of Molybdenum	Temperature of Heat Treatment	Time at Temperature, Hr	Atmosphere During Heat Treatment	Metallographic Examination	Oxygen, Pct by Weight
Climax 26	None		As cast	Excess oxide	0.0074*
Climax 59	None		As cast	Excess oxide	0.0030*
Fansteel wire	None		As drawn	Single phased	0.0017†
Fansteel wire	1800°F	3	O_2	Excess oxide	
Fansteel wire	1800°F	5	O_2	Excess oxide	
Fansteel wire	2000°F	1	O_2	Single phased	0.0040†
Fansteel wire	2260°F	1	O_2	Excess oxide	0.0061†
Fansteel wire	2300°F	3	O_2	Excess oxide	0.0056†
Fansteel wire	2450°F	1/2	O_2‡	Single phased	0.0048†
Fansteel wire	2450°F	2	O_2‡	Single phased	0.0042†
Fansteel wire	2500°F	1/2	O_2	Excess oxide	0.0128†
Fansteel wire	2500°F	1/2	O_2	Excess oxide	0.0134†
Fansteel wire	2500°F	1	O_2	Excess oxide	0.0071†
Fansteel wire	2500°F	3	O_2	Excess oxide	0.0242†
Fansteel wire	2500°F	5	O_2	Excess oxide	0.0228†
Fansteel wire	2750°F	1/2	O_2‡	Single phased	0.0049†
Fansteel wire	2750°F	2	O_2‡	Single phased	0.0040†
Fansteel wire	2950°F	1/2	O_2‡	Single phased	0.0055
Fansteel wire	2950°F	2	O_2‡	Excess oxide	0.0087
Climax 59	3000°F	5	Purified argon	Single phased	0.0040

* Accuracy of analysis = ±0.0005 pct.
† Accuracy of analysis = ±0.0002 pct, or 10 pct of reported values, whichever is greater.
‡ About 90 pct of the oxygen pressure required to maintain an oxide film on the wire surface.

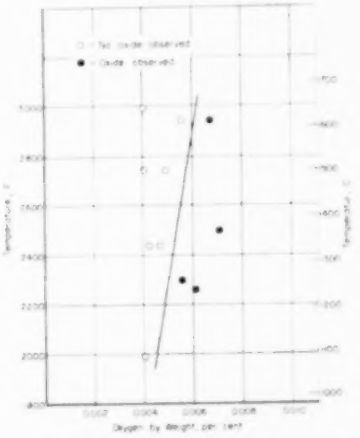

Fig. 6—Solid solubility of oxygen in molybdenum.

a—Cast molybdenum. X1500. b—Powder metallurgy molybdenum. X1000.

Area reduced approximately 50 pct for reproduction.

Fig. 7—Typical oxide particles observed in cast and powder metallurgy molybdenum

2500° F, the oxide film persisted only for a short time—so short a time that there was no assurance that there was not an oxygen-concentration gradient within the wire.

Finally, a modification of the first procedure (in which a flowing atmosphere of oxygen was maintained) was used. The molybdenum wires were heated to the desired temperature and the oxygen pressure slowly raised until an oxide film formed. This pressure was recorded. The oxide film was then removed by evacuating the system and raising the temperature of the wire if necessary. A new cycle was started. The wire was reheated to the desired temperature and the oxygen pressure raised to about 90 pct of the pressure at which an oxide film had formed. After the desired period of time, the wire was rapidly cooled to room temperature. It was then examined metallographically to determine whether or not internal oxide particles had formed. Those samples exhibiting no oxide, or containing only a small amount of oxide, were analyzed for oxygen. This procedure was found to be satisfactory and was used in obtaining the following data.

Eight 12-gage wires connected in parallel were heated by passing an alternating current through the cage. Fig. 4 shows the details of the cage. Temperatures were determined by sighting an optical pyrometer through the gap in the cage onto the inside cage wall. It had previously been determined that the inside surface of the cage represented black-body conditions.

The furnace was first evacuated to about 2 microns and the wire cage raised to the desired temperature. While still pumping on the furnace, a controlled leak of pure oxygen was allowed to enter the furnace through two needle valves connected in series. As the oxygen pressure was increased, a point was reached at which oxide formed on the wire surfaces. This point could be detected by a decrease in the black-body temperature of the wire and a decrease in the emissivity difference between the inside and outside of the cage.

The oxygen pressure required to maintain a solid oxide film on the wire surface was determined for the temperature range 2300° to 2950° F. Fig. 5 is a plot of the oxygen pressure just sufficient to produce a solid oxide on the wire surface vs. temperature. It should be pointed out that this curve does not represent the oxygen pressure in equilibrium with solid molybdenum oxide; rather, it represents the oxygen pressure (as read in the cold portion of the furnace) at which the rate of oxide formation balances the rate of oxide vaporization.* At temperatures above 2950° F, the wire reduced in cross-section so rapidly that experiments could not be performed satisfactorily.

The heat-treating conditions and resulting oxygen determinations (by vacuum fusion) of the samples treated in the above manner are given in Table II. The a-solubility line, as determined from the data in Table II, is presented in Fig. 6. The line in Fig. 6 represents a three-phase equilibrium between gaseous oxygen, molybdenum oxide, and oxygen dissolved in metallic molybdenum. There is no certainty, however, that the oxygen pressures recorded in Fig. 5 are the true equilibrium pressures. With a few exceptions, only samples found to be single phased or showing quite small amounts of oxide, as determined by the microscope, were analyzed for oxygen. Fig. 7 shows micrographs of samples containing an excess oxide phase.

References

(1) R. M. Parke and J. L. Ham: The Melting of Molybdenum in the Vacuum Arc. *Trans.* AIME (1947) **171**, p. 416; METALS TECHNOLOGY (September 1946).

(2) G. W. P. Rengstorff and R. B. Fischer: Cast Molybdenum of High Purity. JOURNAL OF METALS (February 1952); *Trans.* AIME, p. 157.

(3) T. Takei: On the Equilibrium Diagram of the Molybdenum-Carbon System. *Sci. Rpts.*, Tohoku Imp. Univ. (1928) **17**, p. 939.

(4) W. P. Sykes, K. R. Van Horn, and C. M. Tucker: A Study of the Molybdenum-Carbon System. *Trans.* AIME (1935) **117**, pp. 173-189.

(5) Mo-C Phase Diagram. *Metals Handbook* (1948) Cleveland, A.S.M.

(6) W. E. Few and G. K. Manning: A 4000° Furnace. *Metal Progress* (1951) **59**, No. 3, p. 364.

(7) M. W. Mallett: Purification of Argon. *Industrial and Engineering Chemistry* (October 1950) **42**, p. 2095.

(8) K. K. Kelly: Contributions to the Data on Theoretical Metallurgy. Free Energies of Vaporization and Vapor Pressures of Inorganic Substances. U. S. Bur. Mines, *Bull.* 383 (1935).

* There is a temptation to use the data given in Fig. 5 as a basis for calculating the ΔF of formation of the oxide phase (indicated "oxidation Mark"). If the oxygen pressures recorded are equal to the dissociation pressure of the oxide, then the free energy of the reaction may be calculated from:

$$\Delta F^\circ = RT \ln P_{O_2}$$

The data may yield quite acceptable values for the ΔF° of the reaction when used in this way. However, it may be that the data do not represent the true dissociation pressures of the oxide and, therefore, will not yield acceptable ΔF° values for the following reasons: 1—The system was proceeding at a time, but certainly finite, rate when the observations were made. 2—An oxide vapor phase formed at the wire surface. The vapor pressure of the oxide is not known, but it may have been sufficient to appreciably lower the oxygen pressure at the wire surface beyond that observed in the cold portion of the furnace.

Influence of Carbon On The Lattice Parameter of Molybdenum

by Rudolph Speiser, J. W. Spretnak, W. E. Few, and R. M. Parke

At very low concentrations, carbon dissolves interstitially in molybdenum resulting in a linear expansion of lattice parameter with increase of carbon in solid solution. Geometrical consideration of the relative size of carbon atom to size of interstice approximately predicts the observed volume expansion.

THE element carbon, occurring in molybdenum, either as an unavoidable impurity, or purposely added, markedly affects the mechanical properties of molybdenum. Several investigators[1-3] have noted the occurrence of molybdenum carbide at the grain boundaries of cast molybdenum, and Fischer and Rengstorff[4] have shown that this intergranular constituent can induce intergranular brittleness.

The appreciable change, with temperature, of the solid solubility of carbon in molybdenum, found by Few and Manning,[5] suggests other important effects upon mechanical properties. Finally the relative atom diameters of carbon and molybdenum (the ratio of atom diameters is 0.59) are indicative, by analogy with iron (ratio of carbon atom diameter to iron atom diameter is 0.65), of a possible interstitial solid solution. If carbon dissolves interstitially in molybdenum, anelastic effects and age-hardening effects, similar to those observed in other body-centered cubic metals, could be expected. However, from the work of Sykes, Van Horn, and Tucker,[6] it might be inferred that carbon forms only a substitutional solid solution with molybdenum. These considerations made it desirable to study the effect of carbon on the lattice parameter of molybdenum in greater detail than heretofore.

All heat treating was done in a high temperature furnace[7] built specifically for heat treatment of molybdenum. The temperatures and times of heat treatment were determined from the α solubility limit for the Mo-C system.[5] These heat treatments were carried out in argon which was purified with respect to N_2 and H_2O.[8] Purification of the argon was accomplished by passing the argon over hot (750° C) titanium and then through a magnesium perchlorate drying tower. As many as six samples were run concurrently and quenched at different times without interrupting the furnace cycle. Both the purity of the furnace atmosphere and ability to quench samples from any temperature up to 4000° F were of prime importance in the successful heat treatment of samples for the lattice parameter investigation.

R. SPEISER and J. W. SPRETNAK, Member AIME, are Associate Professors, Dept. of Metallurgy, Ohio State University, Columbus, Ohio; W. E. FEW, Junior Member AIME, and R. M. PARKE, Member AIME, are associated with Battelle Memorial Institute, Columbus.

Discussion on this paper, TP 3240E, may be sent, 2 copies, to AIME by April 1, 1952. Manuscript, Sept. 25, 1951; revised, Dec. 6, 1951. New York Meeting, February 1952.

This work was done under contract between the Office of Naval Research and Battelle Memorial Institute, and under subcontract between the Ohio State University Research Foundation and Battelle Memorial Institute.

Carbon Analysis

The Leco Combustion apparatus was used for carbon analysis. This apparatus is capable of an accuracy of ± 0.003 pct for a 1 g sample in the range below 0.10 pct. However, it is felt the degree of accuracy is somewhat better than this limit in view of the consistency evident by cross checking a number of determinations. The Battelle Analytical Laboratory consistently reported check results to within ± 0.001 pct C.

X-ray Measurements

The molybdenum wire specimens (20 mils) were carefully filed down to about 12 mils and then etched with nitric acid to 8 mils. Carbon analyses were made on specimens before reduction in size; however, since there was no evidence of surface carburization, it is probable that the carbon was uniformly distributed throughout the sample. The resultant specimens were strain free and small enough to minimize the error in the lattice parameter determinations due to X-ray absorption.

Diffraction patterns were obtained with a Debye-Scherrer powder camera 114.59 mm in diam utilizing the Straumanis type asymmetrical film mounting. Nickel-filtered copper $K\alpha$ radiation and zirconium-filtered molybdenum $K\alpha$ radiation were used. Line positions on the film were measured with a traveling microscope equipped with a vernier scale permitting measurement to 0.001 cm. The average of five readings was used to determine the position of each line.

The lattice parameter for each specimen was determined from the data by the extrapolation method of Bradley and Jay,[9] i.e., the intercept at 90° of the straight line obtained by plotting the apparent lat-

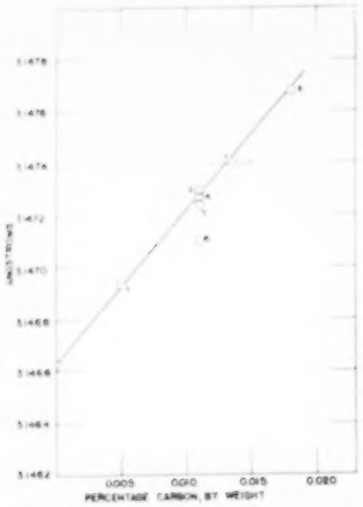

Fig. 1—Lattice parameter measurements of molybdenum with varying carbon content

Numbers refer to sample numbers, data for which are given in Table I.

tice parameter for a given Bragg reflection angle θ vs $\cos^2\theta$. Only back reflections were used in this plot.

Results of Parameter Measurements

The results of the measurements of lattice parameters of molybdenum samples with varying carbon contents are presented in Table I and are plotted in Fig. 1. The parameter for pure molybdenum is that given by Lee and Chang.[7] The 0.0135 pct C specimen was furnished by Climax Molybdenum Co. The carbon content was reported as 0.012 to 0.015 pct. All parameters reported here are in Angstrom units.

Table I. Lattice Parameters of Molybdenum Carbon Alloys

Sample No.	Type Material	Heat Treatment	C, Pct	Lattice Parameter, A
0*		None	0.00	3.14664
1	Wrought wire	Held 3000°F for ¼ hr, quenched (in water-cooled steel plate)	0.005	3.14694
2	Wrought wire	Held 3500°F for ¼ hr, quenched	0.011	3.14729
3	Climax rod	Held 4000°F for ¼ hr, quenched	0.018	3.14768
4	Wrought wire	Held 3000°F for ¼ hr, quenched	0.011	3.14726
5	Wrought wire	Held 3800°F for ¼ hr, quenched. Re-heated to 3000°F for ¼ hr, quenched	0.011	3.14722†
6	Wrought wire	Held 3800°F for ¼ hr, furnace cooled to 2000°F, held ¼ hr, quenched	0.011	3.14710†
7	Wrought wire	Sample, Climax Molybdenum Co., as-received	0.012-0.015	3.14740

* Data of Lee and Chang.[7]

† Not used in fitting data to equation of a straight line because of heat treatment.

Referring to Fig. 1, it is evident that a good linear positive relationship (with the exception of point No. 6) exists between the lattice parameter of molybdenum and the carbon content in solid solution. Thus, in the range of concentration studied in this research, carbon expands the lattice parameter of molybdenum, contrary to the previous report of Sykes et al.,[5] who claimed a contraction of the parameter with increasing carbon content. The present data extrapolate very well to the value of 3.14664A for pure molybdenum given by Lee and Chang.[7]

The least squares line of best fit is $a = 0.05705$ (wt pct C) + 3.14665. The correlation coefficient is $r = 0.996$, indicating a high degree of correlation. The standard deviation of the correlation coefficient is 0.00326, meaning that the current estimate of this statistic lies in the range of the true correlation coefficient ± 0.00978. The standard error of estimate of the lattice parameter (δ_{eq}) is 0.000029, giving a total expected error of ± 0.00009.

The lattice parameter for specimen No. 6 lies considerably below the straight line drawn through the other points in Fig. 1. This is undoubtedly due to the fact that, although the specimen contains 0.011 pct C, all the carbon is not in solution. Carbon, whether at the grain boundary or precipitated as the carbide, would not contribute to the lattice parameter expansion of molybdenum since the size of the lattice parameter would only depend upon the amount of carbon in solid solution. The anomalous behavior of specimen No. 6 is due to the heat treatment it received, see Table I.

The data in Table I and Fig. 1 yield definite information on the nature of the solid solution formed by carbon in molybdenum. The ratio of the radius of the carbon atom to the radius of the molybdenum atom is 0.59. Therefore, if the solid solution were of the substitutional type, carbon would contract the lattice of molybdenum. In the interstitial type, carbon would expand the parameter. Since the current data show that carbon does indeed expand the lattice, the conclusion must be drawn that carbon forms an interstitial solid solution in molybdenum. This conclusion is in agreement with Hagg's rule[8] concerning the effect of atomic size ratios on solid solution formation.

It is interesting to calculate what the expansion of the molybdenum lattice parameter would be on the basis of Vegard's law[9] due to the interstitial solid solution of carbon. The interstitial octahedral holes in a body-centered cubic crystal structure are not symmetrical. The dimension of the hole in the direction between the two atoms in the ($\frac{1}{2}$ $\frac{1}{2}$ $\frac{1}{2}$) positions in two adjacent unit cells is $(1 - \sqrt{3}/2) \times a = 0.42$A ($a = 3.147$A for molybdenum), whereas the dimension of the hole in the plane bisecting this line is $(\sqrt{2} - \sqrt{3}/2) \times a = 1.72$A. The diameter of a carbon atom with a coordination number of 6 is ~ 1.60A. A carbon atom placed in this distorted octahedral hole will cause a linear contraction of the lattice parameter a of $(1.72 - 1.60) \times \cos 45° = 0.08$A and an expansion of $1.60 - 0.42 = 1.18$A. But these dimensional changes can take place in any of three directions, hence the net isotropic expansion will be:

$$\frac{1.18 - 0.08}{3} = 0.37\text{A}$$

Now a 0.005 pct by weight solution of carbon in

molybdenum is a ratio of carbon : molybdenum :: 1 : 2500. One carbon atom is shared between two unit cells, therefore, the average increase in the lattice parameter of molybdenum due to the solution of 0.005 pct by weight of carbon is:

$$\frac{4}{2500} \times 0.37 = 0.0006\text{A}$$

The observed increase in lattice parameter is ~ 0.0003A, which is in good agreement with the prediction considering that it is probable that there is a contraction of the carbon atom upon dissolving interstitially in the molybdenum lattice.

Conclusions

At very low concentrations, carbon dissolves interstitially in the molybdenum lattice resulting in a linear increase in the lattice parameter with an increase of carbon in solid solution.

References

[1] R. B. Fischer and J. H. Jackson: The Ductility of Cast Molybdenum. *Trans.* AIME (1950) **188**, pp. 1149-1153; JOURNAL OF METALS (September 1950).

[2] R. M. Parke and J. L. Ham: The Melting of Molybdenum in the Vacuum Arc. *Trans.* AIME (1947) **171**, pp. 416-427; METALS TECHNOLOGY (September 1946).

[3] C. A. Zapffe, F. K. Landgraf, and C. O. Worden: Fractographic Study of Cast Molybdenum. *Trans.* AIME (1949) **180**, pp. 616-636; METALS TECHNOLOGY (August 1948).

[4] R. B. Fischer and G. W. P. Rengstorff: Cast Molybdenum of High Purity. JOURNAL OF METALS (February 1952), *Trans.* AIME, p. 157.

[5] W. E. Few and G. K. Manning: The Solid Solubility of Carbon and Oxygen in Molybdenum. This issue, p 271.

[6] W. P. Sykes, K. R. Van Horn, and C. M. Tucker: A Study of the Molybdenum-Carbon System. *Trans.* AIME (1935) **117**, pp. 173-189.

[7] W. E. Few and G. K. Manning: A 4000° Furnace. *Metal Progress* (1951) **59**, No. 3, p. 364.

[8] M. W. Mallett: Purification of Argon. *Industrial and Engineering Chemistry* (October 1950) **42**, pp. 2095.

[9] A. J. Bradley and A. H. Jay: A Method for Deducing Accurate Values of the Lattice Spacing from X-ray Powder Photograph Taken by the Debye-Scherrer Method. *Proc.* Physical Soc. (London) (1932) **44**, pp. 563-579.

[10] E. E. Lee and S. S. and Y. L. Chang: The Accurate Evaluation of Lattice Spacings From Back Reflection Photographs. *Proc.* Physical Soc. (London) (1941) **53**, pp. 517-528.

[11] G. Hagg: Gesetzmassigkeiten im Kristallbau bei Hydriden, Boriden, Carbiden und Nitriden der Ubergangselemente. *Ztsch. Physik Chem.* (B) (1931) **12**, pp. 33-56.

[12] L. Vegard: The Constitution of Mixed Crystals and the Space Occupied by Atoms. *Ztsch. Physik* (1921) **5**, pp. 17-26.

Technical Note

Relation Between the Volume of Martensite And The Number of Martensitic Plates per Unit Volume

by E. S. Machlin

RECENTLY, there has been much activity in the field of nucleation of martensitic transformations.[1-3] One of the problems in this field is the calculation of the rate of nucleation (number of plates nucleated per unit untransformed volume per unit time) in terms of observable parameters. Two such observable parameters are the fraction of the length of a straight line which corresponds to the portion of the total length of the line that lies in the martensitic phase and the number of plates intersected by this straight line per unit length of line. Because of the necessity of a valid answer to this problem, the following investigation was undertaken.

Although this problem has been treated in the past, a derivation of the relation between the volume and linear fractions of martensite will be described to illustrate the method used in the succeeding analyses.

It is assumed that the martensitic plates are in the form of a right circular cylinder having a small height relative to the radius of the base. The volume fraction of martensite is then:

$$f_v = \sum_i \sum_j N_{ij} h_i A_j \qquad [1]$$

where f_v is the volume fraction of martensite, and N_{ij} is the number of plates per unit total volume having the area A_j and the height h_i.

The linear fraction of martensite is obtained as follows. For the plates having the particular area A_j and height h_i, the fraction $\sin\theta\, d\theta$* will have their cylinder axes between the angles θ and $\theta + d\theta$ to the straight line along which the linear fraction of mar-

E. S. MACHLIN, Member AIME, is Assistant Professor of Metallurgy, Columbia University, New York.

TN 106E. Manuscript, Dec. 19, 1951.

* It is assumed in this step that the orientation of the martensitic plates in space is random. Then the fraction of the axes lying between θ and $\theta + d\theta$ is $\frac{2 \times 2\pi R \sin\theta \times R d\theta}{4\pi R^2} = \sin\theta\, d\theta$.

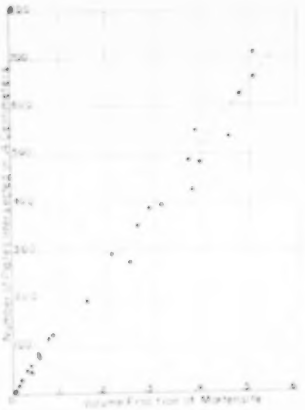

Fig. 1—Relation between number of martensite plates per unit length of linear traverse and volume fraction

tensite is observed. The contribution of these particular plates to the linear fraction intersected by the straight line is:

$$\int_0^{\pi} f_1 \, d\theta = \sin\theta \, d\theta \, N_{v_1} A_1 \cos\theta \frac{h_1}{\cos\theta} \qquad [2]$$

In eq 2 the term $\sin\theta \, d\theta \, N_{v_1} A_1 \cos\theta$ is the number of plates which intersect the straight line per unit length of line, and $h_1/\cos\theta$ is the length of line intersected per plate. Further, $\sin\theta \, d\theta \, N_{v_1}$ is the number of plates per unit volume having area A_1 and height h_1 arranged with their axes at the angle θ to the line. Also, $A_1 \cos\theta$ represents the "collision" cross-section of these plates. In other words, all plates having the collision cross-section $A_1 \cos\theta$ which also have their centers of symmetry within the cylinder of volume $A_1 \cos\theta$ will intersect the axis of this cylinder.

The total linear fraction intersected by the straight line is then

$$f_1 = \sum_{\theta} \int_0^{\pi} f_1 \, d\theta = \sum_{\theta} \sum_{\theta} N_{v_1} A_1 h_1 \int_0^{\pi} \sin\theta \, d\theta$$
$$= \sum_{\theta} \sum_{\theta} N_{v_1} A_1 h_1 = f_1 \qquad [3]$$

The basis of lineal analysis as applied to martensitic plates is thus established.

The number of plates intersected per unit length of line is by the above reasoning:

$$N_1 = \sum_{\theta} \sum_{\theta} \int_0^{\pi} \sin\theta \, d\theta N_{v_1} A_1 \cos\theta \qquad [4]$$
$$= \tfrac{1}{2} \sum_{\theta} \sum_{\theta} N_{v_1} A_1 \qquad [5]$$

If h_1 is a constant, then a simple relation between the number of plates intersected per unit length of line and the volume fraction exists. Eq 1 becomes in this case:

$$f_1 = h \sum_{\theta} N_{v_1} A_1 \qquad [6]$$

[1] The volume of the plates already formed is neglected in this treatment but can easily be accounted for by substituting $C_1 \left(\frac{V_v}{2}\right)^{2/3}$ for A_1, where C_1 is π for a sphere and 2 for a cube.

But in this case:

$$N_1 = \tfrac{1}{2} \sum_{\theta} N_{v_1} A_1 \qquad [7]$$

Hence:

$$N_1 = (\tfrac{1}{2} h) f_1 \qquad [8]$$

Just this simple relation, eq 8, was found by Molinder[4] in his investigation of the martensitic transformation in chromium steels. His data are reproduced in Fig. 1. The value of the thickness h calculated from the slope is 1.5×10^{-4} cm. This value is of the order of magnitude of the thickness observed from micrographs of the transformation in this alloy.

Using this result, the desired relation between the volume fraction and the number of nuclei activated can be obtained. It is assumed that the plates subdivide the austenite into subvolumes such that the area of the next plates to form are proportional to the two-thirds power of the volume in which the plates form. Hence:

$$f_1 = h \sum_{\theta} N_{v_1} A_1 = h \sum_{\theta} \frac{2}{V_v} C_1 \left(\frac{V_v}{2}\right)^{2/3}$$

$$f_1 = \frac{C_1 h}{V_v^{1/3}} \frac{(2^{1/3})^n - 1}{2^{1/3} - 1} \qquad [9]$$

and $$N_1 = \sum_{\theta} N_{v_1} = \sum_{\theta} \frac{2}{V_v} \frac{2^n - 1}{V_v} \qquad [10]$$

where V_v is the average volume of an austenite grain, and C_1 is the parameter of order of 5 for spherical shape and 1 for cubic shape of the subvolume of austenite.

For M larger than 4, eliminating M in eqs 9 and 10 yields:

$$f_1 = 4C_1 h \left[N_1^{1/3} - \frac{1}{V_v^{1/3}} \right] \qquad [11]$$

A more accurate relation takes into account the volume of the plates already formed and is:

$$f_1 = 4C_1 h \left[N_1^{1/3} - 1/V_v^{1/3} \right] = \frac{C_1 h}{0.6} \left[N_1^{1/3} - \frac{1}{V_v^{1/3}} \right] \qquad [12]$$

Summarizing, it appears that the assumption of a constant thickness for martensitic plates is consistent with the data. Using this assumption a relation can be obtained between the volume fraction of martensite and the number of martensitic plates per unit volume (the number of nuclei activated per unit volume). The basis of the application of lineal analysis for measuring the volume fraction of martensitic plates is also re-established.

References

[1] G. V. Kurdjumow and O. P. Maksimova: Kinetics of Austenite to Martensite Transformation at Low Temperatures. *Doklady Akademii Nauk SSSR* (1948) **61**, No. 1, pp. 83-86.

[2] S. C. Das Gupta and B. S. Lement: Isothermal Formation of Martensite at Subzero Temperatures in a High Chromium Steel. *Trans.* AIME (1951) **191**, p. 727; JOURNAL OF METALS (September 1951).

[3] E. S. Machlin and M. Cohen: The Isothermal Mode of the Martensitic Transformation. To be published in *Trans.* AIME, JOURNAL OF METALS, 1952.

[4] A. G. Molinder: Stabilization and Conditioning in Two Low-Alloyed Chromium Steels. M. S. Thesis, M.I.T., 1949.

Preferred Orientation of Arc-Cast Molybdenum Sheet

by M. Semchyshen and G. A. Timmons

The predominant orientation in both straight-rolled and cross-rolled molybdenum is the {100} [110] texture. Upon complete recrystallization, this same texture predominates, but there is less spread about the ideal orientation. A secondary orientation about the [111] direction as the axis develops in cross-rolled sheet. Compression-rolled sheet exhibits random orientation in the plane of the sheet. Some mechanical properties were measured at varying angles to the rolling direction to determine the effect of preferred orientation on anisotropy in molybdenum sheet which had been straight, cross, or compression rolled.

THE development of the arc-cast process has made available large ingots of molybdenum from which it is possible to roll sheet of considerable size. It is anticipated that such sheet will be further fabricated by spinning, drawing, stamping, or forming. Anisotropy of physical properties caused by the preferred orientation developed in the sheet during rolling may be expected to affect the behavior of the metal when subjected to these fabricating operations. To produce a sheet which will be most amenable to the fabrication of a given shape by a particular operation, consideration should be given to the directions and magnitudes of plastic deformations produced in the operation. When possible, the rolling schedule should be controlled to develop a texture which favors the required deformation.

The existence of preferred orientations in rolled molybdenum sheet has been reported by Jeffries,[1] Konobejewsky,[2] Fujiwara,[3] Goss,[4] and Ransley and Rooksby.[5] None of these investigators obtained sufficient X-ray data to permit the construction of pole figures; instead, they based their conclusions upon Debye-Scherrer patterns of a limited number of positions. Ransley and Rooksby devoted some attention to transcrystalline cleavage at 45° to the rolling direction, indicating that it is appreciable in polycrystalline material only when the crystals are in the ideally preferred condition, and that this condition is only approached if the metal has been rolled successively in two perpendicular directions. In a recent paper, Custers and Riemersma[6] introduced the first pole figures to describe the textures of straight-rolled and cross-rolled molybdenum sheet.

To increase the knowledge concerning the generation and effects of preferred orientations in molybdenum sheet, an investigation was undertaken to determine the effects of variations in rolling schedule and annealing treatments on preferred orientation, and to correlate preferred orientations with some mechanical properties. The orientations of straight-rolled, cross-rolled, and compression-rolled sheet have been determined by X-ray analysis, both as-rolled and after recrystallization. Pole figures have been constructed to describe the textures produced by these various rolling procedures.

Texture of Cast Molybdenum Ingots

In the arc-cast process, molybdenum powder is pressed into a vertical column which is sintered to increase its strength as it proceeds downward into a water-cooled mold, where the metal is melted in an alternating-current arc established between the end of the formed powder electrode and the metal bath at the top of the growing ingot.

Since the solid-liquid interface moves continuously upward in the mold, the crystal axes are not normal to the cold surface of the mold but have the curvature shown in Fig. 1a. X-ray analysis reveals that the cube axis is the fiber axis and that it is normal to the cold surface of the mold; that is, the [100] direction is parallel to the longitudinal axis of the ingot. This substantiates recent work by

M. SEMCHYSHEN and G. A. TIMMONS, Members AIME, are associated with the Research Laboratory, Climax Molybdenum Co. of Michigan, Detroit.

Discussion on this paper, TP 3254E, may be sent, 2 copies, to AIME by May 1, 1952. Manuscript, Sept. 19, 1951. New York Meeting, February 1952.

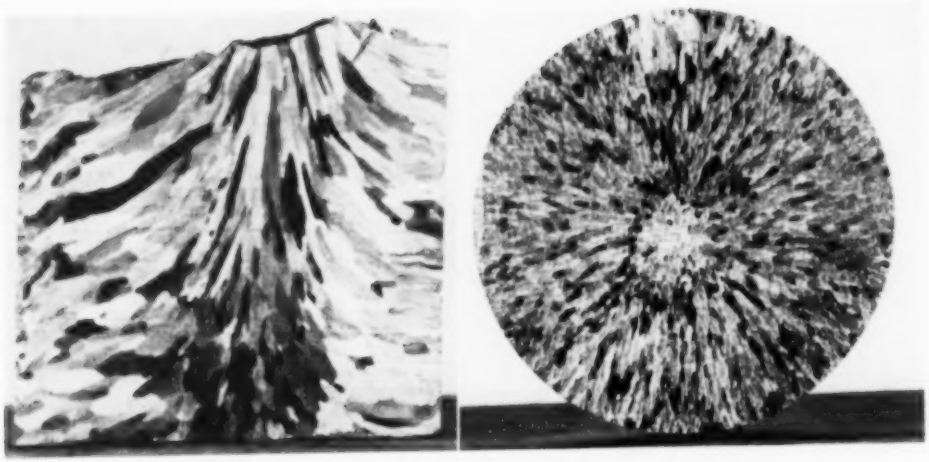

Fig. 1—Longitudinal and cross sections of a 3 in. arc cast molybdenum ingot.

Fischer and Jackson.[3] Thus, the arc-cast molybdenum ingot exhibits a preferred orientation similar to that of other body-centered cubic metals when solidified in metal molds.

Experimental Procedure

Preparation of Sheet: The two ingots from which the sheets for this investigation were produced, were melted and cast by the vacuum-arc process.[4] The ingots contained less than 0.2 pct impurities, which included carbon contents of 0.03 and 0.05 pct, respectively.

The ingots were hammer forged to sheet bars $^1/_4$ in. thick at forging temperatures in the range 2400° to 1900° F. X-ray diffraction patterns of the $^1/_4$ in. sheet bars detected no preferred orientation, indicating that the forging operation had destroyed the casting texture. The forged bar was rolled to strip 0.075 to 0.087 in. thick after heating to 2150° F.

* The terms straight, cross, and compression rolling commonly have the following interpretation and are so employed in this report:

1—Straight rolling: All rolling conducted parallel to the original longitudinal axis of the ingot.

2—Cross rolling: Rolling in two perpendicular directions, i.e., alternate rolling parallel to the longitudinal axis of the ingot and at right angles to the axis; sufficient passes are made in one direction to reduce the sheet thickness about 25 pct before changing the rolling direction.

3—Compression rolling: During the rolling operation, the sheet is rotated 10° to 20° between each successive pass. A reference direction is arbitrarily selected for compression-rolled sheet and all computations of the specimens is based upon this direction.

Three separate procedures were followed to cold reduce the strip to thinner gages. In each procedure most of the sheet was retained at a thickness of 0.010 in., but some small sections were reduced to the minimum thicknesses that could be obtained with the laboratory rolling mill available for these experiments. These minimum thicknesses ranged from 0.0065 to 0.0055 in., corresponding to total reductions of the strip equivalent to 88.5 to 94 pct. The three procedures are described as follows:

1—Straight rolling* at room temperature without intermediate annealing: Reduction for pole figure sample, 93.3 pct; reduction for mechanical test sample, 88.5 pct.

2—Cross rolling at room temperature without intermediate annealing: Reduction for pole figure sample, 90 pct; reduction for mechanical test sample, 85 pct.

3—Compression rolling; owing to the peculiar nature of this procedure, the sheet developed a greater width than in the other two rolling schedules, therefore the metal was heated to 500° F between each pass until a thickness of 0.036 in. was obtained to reduce its hardness and thus facilitate reduction in the small two-high rolling mill. From 0.036 in. to the final thicknesses of 0.010 in. and 0.0055 in., the sheet was rolled at room temperature in a four-high mill which was capable of rolling the wider sheet

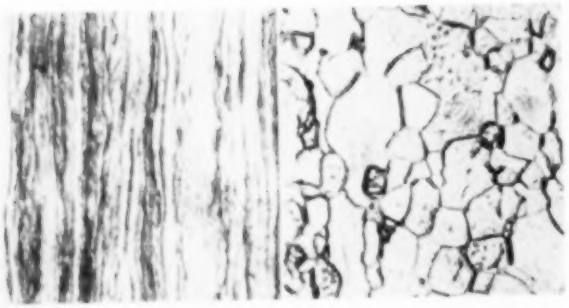

Fig. 2—Molybdenum sheet 0.0065 in. thick reduced 93.3 pct by cold rolling. Etched in 0.65 pct NaOH + 2.33 pct $K_3Fe(CN)_6$. X1000.

Area reduced approximately 50 pct for reproduction.
a (left)—As-rolled.
b (right)—Annealed 15 min at 2100° F.

Fig. 3—{100} pole figure for straight rolled molybdenum sheet reduced 93 pct by cold rolling. As-rolled.

□ {110} as rolling direction, {100} as rolling plane
◇ {110} as rolling direction, {113} as rolling plane
{110} as rolling direction, {117} as rolling plane
{112} as rolling direction, {111} as rolling plane

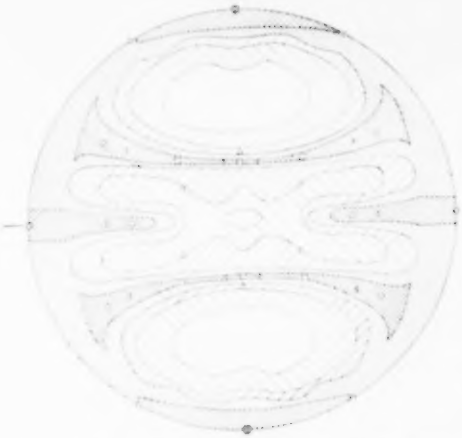

Fig. 4—{110} pole figure for straight rolled molybdenum sheet reduced 93 pct by cold rolling. As-rolled.

□ {110} as rolling direction, {100} as rolling plane
◇ {110} as rolling direction, {113} as rolling plane
{110} as rolling direction, {117} as rolling plane
{112} as rolling direction, {111} as rolling plane

without heating. No intermediate annealing was used at any stage of this procedure. Reduction for pole figure sample, 88.5 pct; reduction for bend test sample, 83.5 pct.

Samples from each sheet were annealed in a vacuum furnace at 2400°F for 15 min to accomplish complete recrystallization, and additional samples were annealed at 2800°F in the same furnace to determine whether any change in preferred orientation resulted from excessive grain growth. Microstructures of the straight-rolled sheet are shown in Fig. 2 before and after annealing at 2400°F.

X-ray Technique: Specimens for pole figure determinations were prepared from the samples which had received the greatest amounts of cold rolling, in order to obtain diffraction patterns representative of the maximum degree of preferred orientation for each rolling schedule. Prior to X-ray exposure, all specimens were etched in hot 90 pct KOH + 10 pct $NaNO_3$ to remove oxide films and to reduce the thickness to 0.005 in.

Unfiltered molybdenum radiation was used for all diffraction patterns. The X-ray beam was collimated through a pinhole system. The specimen was mounted in a goniometer which permitted accurate measurement of the angle of rotation about the vertical axis of the specimen without removing the specimen from its mounting during the entire series of exposures. The starting position was selected so that the X-ray beam was perpendicular to the rolling plane and the rolling direction of the sheet specimen was vertical. A series of transmission patterns was obtained from 0° to 85° in 5° intervals, by rotating the specimen clockwise about the vertical axis. A second series of photograms was made after the specimen had been rotated 90° in its own plane and then rotated clockwise in 5° intervals about the new vertical axis. A few additional photograms were made when the specimen was rotated counterclockwise while held in both of the positions described above. These photograms confirmed the existence of

Table I. Pole Figure Data

Figure	Type of Rolling and Annealing Treatments	Planes Represented
3, 4, 5.	Straight-rolled, as-rolled	{100}, {110}, {112}
6, 7.	Straight-rolled, annealed at 2400°F, completely recrystallized	{100}, {110}
8, 9.	Cross-rolled, as-rolled	{100}, {110}
10, 11.	Cross-rolled, annealed at 2400°F, completely recrystallized	{100}, {110}
12	Compression-rolled, as-rolled	{110}

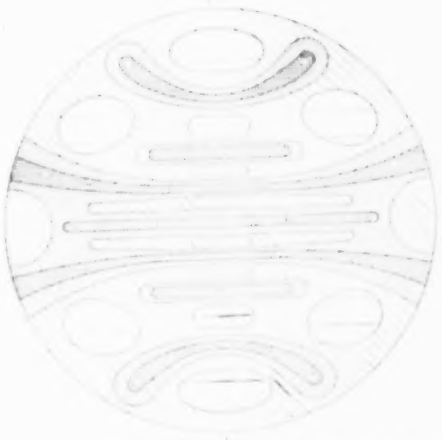

Fig. 5—{112} pole figure for straight rolled molybdenum sheet reduced 93 pct by cold rolling. As-rolled.

□ {110} as rolling direction, {100} as rolling plane
{110} as rolling direction, {112} as rolling plane

Fig. 6—{100} pole figure for straight rolled molybdenum sheet reduced 93 pct by cold rolling. Annealed at 2400°F.

□	{110} as rolling direction.	{100} as rolling plane.
◇	{110} as rolling direction.	{113} as rolling plane.
	{110} as rolling direction.	{112} as rolling plane.
	{112} as rolling direction.	{111} as rolling plane.

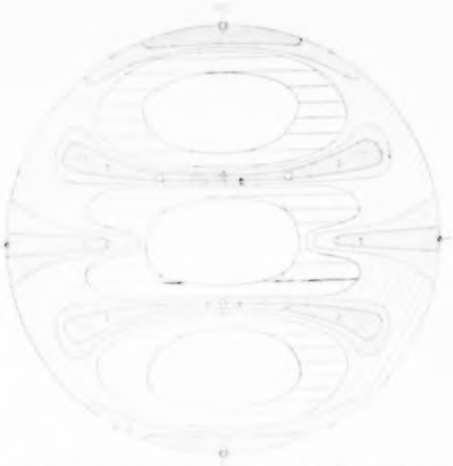

Fig. 7—{110} pole figure for straight rolled molybdenum sheet reduced 93 pct by cold rolling. Annealed at 2400°F.

□	{110} as rolling direction.	{100} as rolling plane.
◇	{110} as rolling direction.	{113} as rolling plane.
	{110} as rolling direction.	{112} as rolling plane.
	{112} as rolling direction.	{111} as rolling plane.

Fig. 8—{100} pole figure for cross rolled molybdenum sheet reduced 90 pct by cold rolling. As rolled.

□	{110} as rolling direction.	{100} as rolling plane.
	{112} as rolling direction.	{111} as rolling plane.
	{110} as rolling direction.	{111} as rolling plane.

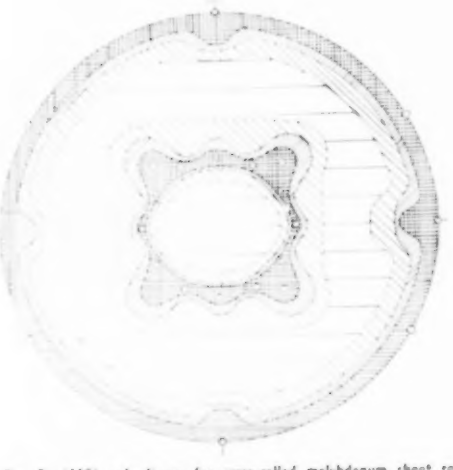

Fig. 9—{110} pole figure for cross rolled molybdenum sheet reduced 90 pct by cold rolling. As rolled.

□	{110} as rolling direction.	{100} as rolling plane.
	{112} as rolling direction.	{111} as rolling plane.
	{110} as rolling direction.	{111} as rolling plane.

a plane of symmetry perpendicular to the rolling plane and containing the rolling direction.

At the high angles, part of the pattern was a reflection pattern. In rotating up to 85°, the most useful portion of the pattern in the range 60° to 85° was not transmitted but was reflected. This permitted more accurate evaluation of the central portion of the pole figure.

The intensities of the Debye rings for the (200), (110), and (112) planes were estimated by eye and graded into five classes: none, weak, medium, strong, and very strong. The exposure time was varied in such a way that the maximum intensities of the films would be the same for the various angles of rotation of the specimen.

The annealing treatment coarsened the grains so much that it became necessary to use an integrating device to obtain reflections from a sufficient number of grains to eliminate spotty Debye rings.

Pole Figures

Pole figures were plotted according to the methods which have been described by Barrett[7] and Decker,[8] and in which the orientations are represented as the

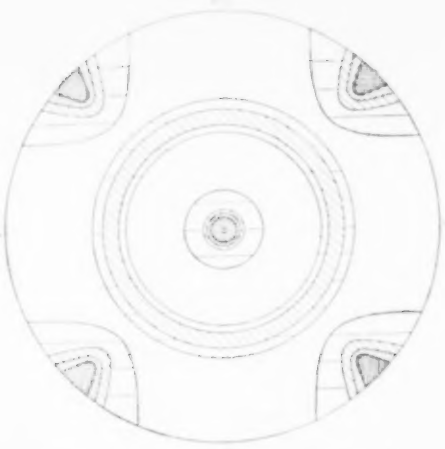

Fig. 10—{100} pole figure for cross-rolled molybdenum sheet reduced 90 pct by cold rolling. Recrystallized at 2400°F.
□ {110} as rolling direction, {100} as rolling plane.

Fig. 11—{110} pole figure for cross-rolled molybdenum sheet reduced 90 pct by cold rolling. Recrystallized at 2400°F.
□ {110} as rolling direction, {100} as rolling plane.

stereographic projection of the poles of a family of crystallographic planes. They are reproduced in Figs. 3 to 12 in the order given in Table I. The plane of the sheet is parallel to the plane of stereographic projection in all the figures. The rolling direction is vertical and the transverse direction is horizontal. The conclusions drawn from these data are consistent with the pole figures from all planes represented.

Straight-Rolled, As-Rolled (Figs. 3 to 5): The principal orientation is the {100} parallel to the rolling plane with the [110] direction lying along the direction of rolling. The {100} [110] texture is the mean orientation and there is a spread about the rolling direction (as an axis), extending as much as 40° each way; while the spread around the transverse direction is only 7° each way.

It has been reported that molybdenum has only one slip plane which is operable at room temperature. One investigator[7] has reported that this plane is the (112) plane, but another investigator[8] recently reported that it is the (110) plane; therefore the pole figure for the (112) plane, for straight-rolled sheet as-rolled, is also included in this investigation. This pole figure is shown in Fig. 5.

Straight-Rolled, Recrystallized (Figs. 6 and 7): Upon complete recrystallization, the scatter from the mean orientation has decreased somewhat, now being about 28° around the rolling direction as an axis and about 5° around the transverse direction, each way from the ideal orientation. In other words, recrystallization has brought about a closer approach to the ideal orientation.

Cross-Rolled, As-Rolled (Figs. 8 and 9): Here again the {100} [110] texture predominates. Cross rolling has brought about a greater spread about the transverse direction and a greater concentration of grains with the (110) plane parallel to the second rolling direction. Although the pole figure for the {110} planes suggests a rotational symmetry about the [001] direction perpendicular to the rolling plane, it is apparent from the pole figure for the

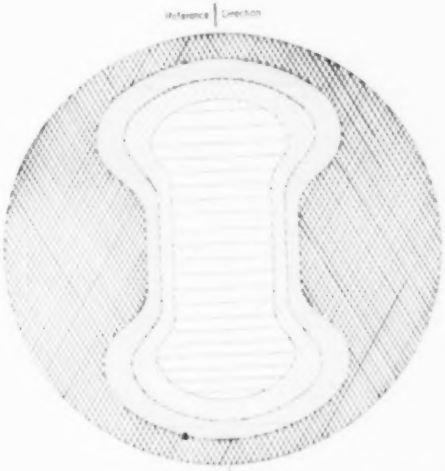

Fig. 12—{110} pole figure for hot compression rolled molybdenum sheet reduced 88.5 pct by hot rolling.

{100} planes that the spread about the mean orientation {100} [110] is limited to about 8° in both directions and that complete symmetry is about the [111] direction perpendicular to the rolling plane. Thus, the region of heavy intensity at the circumference of the {110} pole figure is the result of rotational symmetry about the [111] direction as an axis when the [111] direction is perpendicular to the rolling plane. The results of this phase of the investigation are in agreement with the findings of Custers and Riemersma.[9]

Cross-Rolled, Recrystallized at 2400°F (Figs. 10 and 11): After full recrystallization, the predomi-

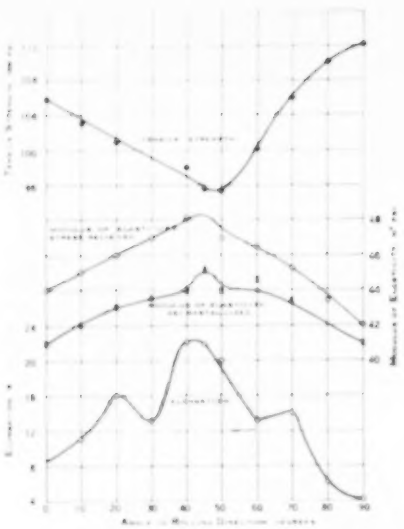

Fig. 15—Tensile properties of straight rolled sheet. As rolled.

nant texture is still [100] [110], and the spread from the mean orientation is only 5° in either direction. There has been a marked diminution in the number of grains contributing to the [111] rotational texture. This leads to the conclusion that the [100] [110] texture is the more stable.

Compression Rolled (Fig. 12). It is apparent from the pole figures presented for straight-rolled and for cross-rolled molybdenum that varying degrees of anisotropy can be expected. In an attempt to produce

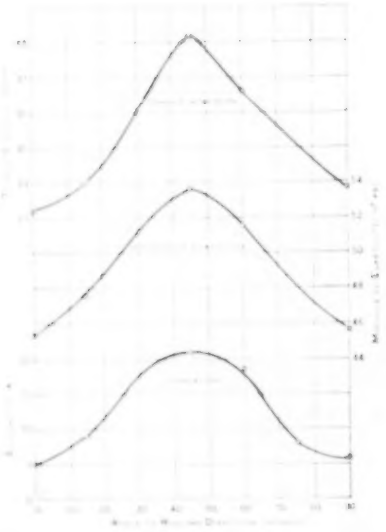

Fig. 16—Tensile properties vs. direction in cross rolled, stress relieved molybdenum sheet.

isotropic molybdenum sheet, compression rolling was investigated. The pole figure is typical of random orientation (cf. Decker); therefore, it is concluded that compression rolling of molybdenum sheet develops a random orientation. Although the pole figures indicate random orientation in the plane of the sheet—that is, different directions in the sheet are equivalent—complete randomness in all directions was not necessarily obtained; a fiber texture may exist along the compression axis.

Diffraction photograms for completely recrystallized (annealed 15 min at 2400 F) compression-rolled sheet were identical to those of the sheet as-rolled. It was concluded, therefore, that a recrystallization anneal had no effect upon the texture of compression-rolled sheet.

Effect of Higher Annealing Temperatures. In addition to the samples discussed above, other samples representative of each type of rolling were annealed at 2800 F. X-ray patterns for these samples showed that the same orientation existed after annealing at 2800 F as after annealing at 2400 F. Thus it is concluded that the preferred orientation present at complete recrystallization remains substantially unchanged after subjecting the sheet to annealing temperatures 400° to 800° F above the recrystallization temperature where excessive grain growth occurs.

Mechanical Properties

The preferred orientation developed during the rolling of molybdenum sheet gives rise to anisotropy of mechanical properties. The degree of anisotropy has been demonstrated by tensile tests and bend tests performed on straight-rolled, cross-rolled, and compression-rolled sheet.

In order to be consistent in the mechanical property tests, sheet 0.010 in. thick was selected for the tension and the bend tests. Although it is recognized that the orientations in the 0.010 in. sheet may not be identical with the 0.0055 to 0.0065 in. sheet, there is only a small difference in the percentage of cold reduction. Therefore, it has been assumed that the preferred orientation revealed by the X-ray diffraction patterns in the thinnest gage sheets are prevalent and operative in the tension and bend test samples.

Tensile Tests. The tensile properties of straight-rolled and cross-rolled sheets were determined on samples cut at various angles to the rolling direction. All samples were given a 15-min anneal at 1800 F to relieve the residual stresses brought about by rolling and by preparation of the specimens prior to tensile testing. Metallographic examination provided evidence that 1800 F for 15-min would produce not more than 20 pct recrystallization in any of the sheets studied in this investigation. Additional samples of the straight-rolled sheet were annealed at 2400 F for 15-min to effect complete recrystallization; these samples were used for modulus determinations only.

The tensile test specimens were machined to gage sections ½ in. wide x 1 in. in length. The modulus of elasticity was determined in an apparatus in which the sample was stressed by means of a dead-weight load, and the strain was measured by means of two SR-4 strain gages fastened on opposite faces of the specimen. The fixed end of the specimen holder was a universal ball-and-socket joint, to minimize eccentric loading. It was found that for

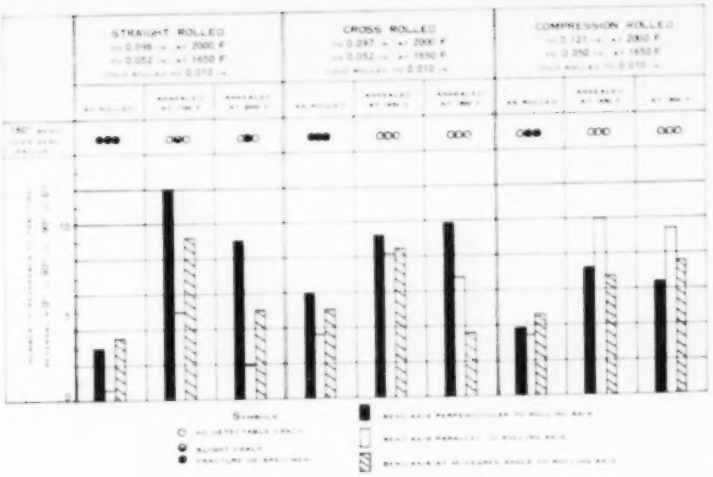

Fig. 15—Bend properties of molybdenum sheet.

completely recrystallized specimens a stress of approximately 9000 psi could be applied without causing permanent set; therefore, it was at this stress that the modulus was determined for all samples.

In order to determine the tensile strength and elongation values, the same specimens were loaded in a hydraulic tensile machine at the rates of 20 pct per hr in the elastic range and 60 pct per hr in the plastic range. The values for tensile strength are based on the original cross-sections of the specimens.

The tensile strength, elongation, and modulus of elasticity of straight-rolled, stress-relieved sheet are plotted against rolling direction in Fig. 13. The modulus of elasticity of the completely recrystallized samples is also included. In Fig. 14 are presented tensile properties vs. rolling direction for cross-rolled sheet.

In the straight-rolled sheet the modulus of elasticity for the recrystallized samples is consistently lower than for the stress-relieved samples at all angles to the direction of rolling by a factor of approximately 10 pct. In the determination of the modulus, a zero strain reading was obtained after tensile stressing of the specimen. This established the fact that no plastic deformation had occurred, even in the recrystallized samples which had the lowest yield strength. Therefore the reduction in moduli may be attributed to the annealing treatment which influenced such factors as hardness, grain size, and deviation from ideal preferred orientation—all of which have been shown[7] to affect the modulus value. It was not unexpected that the modulus curves for straight-rolled and for cross-rolled sheet did not coincide, since the pole figures had shown an appreciable difference in the preferred orientations of the straight and cross-rolled materials.

The elongation and tensile strength curves of Figs. 13 and 14 are a further indication of the anisotropy of rolled molybdenum sheet. Opinsky and Smoluchowski,[7] making a theoretical analysis of the dependence of slip in a body-centered cubic lattice on orientation for the case of simple tension, have shown the relationship between the resolved shear stress on the slip plane in the slip direction and the crystallographic orientation of the axis, for the (112) slip plane in the [111] direction. At crystallographic angles of 19°, 45°, and 71° there is equal maximum resolved shear stress on four plane-direction combinations, but only on two plane-direction combinations at any other angles. It is tempting to speculate that the maxima shown in the elongation curve of Fig. 13 at 20°, 45°, and 70° are related to an increased probability for slip at these angles, since molybdenum has been reported to slip on a (112) plane in the [111] direction. The higher resolved shear stress at 45° in comparison to the resolved shear stresses at 19° and 71° may account for the maximum elongation at 45° for both straight and cross-rolled sheet.

Druyvesteyn[8] has reported the elastic constants for a molybdenum crystal, basing his computation upon the modulus of elasticity and modulus of rigidity of cross-rolled, polycrystalline molybdenum sheet. The corrections made by Druyvesteyn for the departure from ideal orientation involved only scatter from the ideal {100} [110] texture. The present pole figure work indicates that in cross-rolled molybdenum sheet there are too many variations from the ideal orientation to permit the use of such modulus data as indicative of the elastic constant for a single crystal of molybdenum.

For cross-rolled sheet, the variation of the modulus of elasticity with the angle between the final rolling direction and the direction of tension stress is shown in Fig. 14. The minimum modulus is obtained in the rolling direction and the maximum at 45° to the rolling direction. The agreement between these values and those reported by Druyvesteyn is shown in Table II.

Table II. Minimum and Maximum Modulus of Elasticity Values

Angle, Degree	Modulus of Elasticity, Dyne per Sq Cm	
	Druyvesteyn	Present Investigation
0	2.94×10^{12}	3.1×10^{12}
45	3.61×10^{12}	3.7×10^{12}

Bend Tests. Three types of bend tests at room temperature were used for all specimens in this phase of the program: 1—90° reversal test, 2—180° bend test over 0.08 in. radius, and 3—180° bend test over zero radius (flattening test). Specimens ½ in. wide x 2 in. long were used for all bend tests.

The 90° reversal test was conducted on apparatus similar to the Jenkins bend tester. The specimen was clamped in a vise, the jaws of which were rounded to a radius of 0.08 in., and was bent over the rounded jaws from the upright position through 90°, back to the upright position, then to the —90° position, and finally to the original upright position. The complete cycle is defined as one reversal. The number of reversals to the first appearance of fracture was recorded.

In the 180° test over 0.08 in. radius, the specimen was bent over the end of a plate 0.160 in. thick, the end of which had been ground to a half cylinder. All the specimens were bent 180° over the 0.08 in. radius without fracture, therefore the more severe, flattening test was performed. The 0.08 in. radius plate was removed and the specimen was flattened on itself, that is, over a "zero" radius. This flattening test is more severe than a "crimp" test, where the specimen is flattened over a radius represented by half the thickness of the sheet.

The specimens were tested in three directions with reference to the final rolling direction: parallel, perpendicular, and at 45°. The results of the bend tests are presented in Fig. 15.

The straight-rolled molybdenum sheet exhibited the highest degree of anisotropy of the sheets in the group studied.

The stress-relieved sheet developed the highest bend ductility in the direction of rolling (axis of bend perpendicular to the direction of rolling). The number of reversals for samples of the straight-rolled sheet in the direction of rolling was greater than for any other samples in the group. For the straight-rolled sheet, intermediate bend ductility was developed at 45° to the rolling direction and the minimum ductility at 90° to the direction of rolling (bend axis parallel to the rolling direction). The same relationships occurred in the recrystallized specimens, but the number of reversals was appreciably lower for each direction.

The stress-relieved, cross-rolled sheet developed the most uniform bend ductility of any of the samples studied. These samples, which were annealed at 1650°F for 1 hr, contained no detectable recrystallized grains when examined under the microscope. Annealing at 1800°F caused approximately 20 pct recrystallization; there was a measurable increase in bend ductility for the rolling direction but a marked decrease in ductility transverse to the direction of rolling and at 45°.

The compression-rolled sheet was the most consistently isotropic sheet of the group, as evidenced by the uniformity of bend ductility for three angles, 0°, 45°, and 90° to an arbitrarily selected direction, when the sheet was tested as-rolled, stress-relieved, and partially recrystallized.

Conclusions

1—Arc-cast molybdenum exhibits a casting texture in which the [100] direction is parallel to the longitudinal axis of the ingot.

2—Preferred orientations are developed in cold-reduced molybdenum sheet during the rolling process. When the sheet is straight rolled only, the predominant orientation is [100] [110] with a considerable spread about the rolling direction. Upon recrystallization the basic texture remains the same, but the spread about the rolling direction is somewhat decreased.

3—In cross-rolled, cold-reduced molybdenum sheet the predominant texture is again the [100] [110]; however, the spread about either rolling direction is small. A secondary orientation develops which may be described as rotational symmetry about the [111] direction as an axis when this direction is perpendicular to the rolling plane. Upon recrystallization of the cross-rolled sheet, the [100] [110] orientation continues to predominate, and the secondary orientation about the [111] direction is markedly decreased.

4—Cold-reduced, compression-rolled sheet develops a random orientation as-rolled, and this orientation remains unchanged after the sheet has been annealed at temperatures appreciably above the recrystallization temperature.

5—Annealing temperatures as high as 800°F above the recrystallization temperature (approximately 2000°F is sufficiently high to effect complete recrystallization in most cold-rolled molybdenum sheet) produced excessive grain growth, but did not produce any change in the recrystallization texture.

6—Both straight-rolled and cross-rolled molybdenum sheet exhibit anisotropy of mechanical properties. For both types of rolling the modulus of elasticity and the elongation as determined in the simple tension test attain maximum values when the sheet is stressed at an angle of 45° to the rolling direction. In the bend test, straight-rolled sheet exhibits the greatest anisotropy, regardless of heat treatment; cross-rolled sheet approaches isotropic behavior when stress relieved, but anisotropic behavior as-rolled and when partially recrystallized; compression-rolled sheet exhibits the most nearly isotropic behavior as-rolled, as-stress relieved, and when partially recrystallized.

References

(1) Zay Jeffries: *Trans.* AIME (1924) **70**, p. 303.

(2) S. T. Konobejewsky: *Ztsch. Physik* (1926) **39**, p. 415.

(3) Takeo Fujiwara: World Eng. Congress, Tokyo. Paper No. 371 (1929).

(4) N. P. Goss: *Trans.* A.S.M. (1930) **17**, p. 241.

(5) C. E. Ransley and H. P. Rooksby: *Journal* Inst. Metals (1933) **62**, p. 205.

(6) J. F. H. Custers and J. C. Riemersma: *Physica* (1946) **12**, p. 135.

(7) R. M. Parke and J. L. Ham: *Trans.* AIME (1947) **171**, p. 416; METALS TECHNOLOGY (September 1946).

(8) C. S. Barrett: *Structure of Metals*, p. 158 (1943) New York, McGraw-Hill Book Co.

(9) B. F. Decker: *Proc.* A.S.T.M. (1943) **43**, p. 785.

(10) L. C. Tsien and Y. S. Chow: *Proc.* Royal Soc. (1937) **163A**, p. 19.

(11) D. J. Mack: *Trans.* AIME (1946) **166**, p. 68; METALS TECHNOLOGY (December 1945).

(12) A. Opinsky and R. Smoluchowski: A Symposium on the Plastic Deformation of Crystalline Solids. Mellon Institute, Pittsburgh (May 19-20, 1950) p. 216. Published under the joint sponsorship of Carnegie Institute of Technology and the Department of the Navy, Office of Naval Research.

(13) M. J. Druyvesteyn: *Physica* (1941) **8**, p. 439.

(14) R. B. Fischer and J. H. Jackson: *Trans.* AIME (1950) **188**, p. 1149; JOURNAL OF METALS (September 1950).

(15) N. K. Chen and R. Maddin: *Trans.* AIME (1951) **199**, p. 937; JOURNAL OF METALS (October 1951).

Properties of Magnesium-Thorium And Magnesium-Thorium-Cerium Alloys

by T. E. Leontis

ONLY a limited amount of information has been published on the effect of thorium as an alloying ingredient in magnesium. McDonald[1] showed that the addition of thorium in amounts up to 3 pct increases significantly both the ductility and the strength of rolled magnesium sheet. A recent publication by Sauerwald[2] indicates that thorium contributes strength and creep resistance at elevated temperatures to magnesium in both the cast and wrought states. The observations of Sauerwald are confirmed in this paper, which presents the results of a systematic study of the effects of compositional variation on the tensile properties, creep resistance, conductivity, density, and metallography of Mg-Th alloys containing up to 50 pct Th both in the sand-cast and in the extruded states. The effect of the addition of cerium to Mg-Th alloys is also reported.

Experimental Methods

The alloys studied in this investigation were prepared in small laboratory melts according to the melting practice described by Nelson[3] as the crucible method. Electrolytic magnesium was used as the starting material to which the thorium* was introduced in metallic form. It was observed that the behavior of thorium in molten magnesium with respect to reaction with protective fluxes is similar to that of rare-earth metals. In order to obtain the highest possible alloying efficiency, it is necessary to use non-MgCl$_2$ fluxes and to apply all the precautions described by Marande[4] for melting, alloying, and casting magnesium-rare-earth alloys. Under these conditions it is possible to obtain an alloying efficiency in the range of 85 to 95 pct. The Mg-Th-Ce alloys were made with cerium of the highest purity available, not with the commercial product "misch-metal" which contains approximately 50 pct Ce. The total rare-earth content of this material was 97.1 pct, of which 0.3 pct was rare-earth metals other than cerium; the major impurities comprising the balance were iron and magnesium. The thorium and cerium contents of each alloy were determined chemically.

Test bars 6½ in. long with a 2½ in. long reduced section of ½ in. diam were cast in sand molds using a four-bar pattern. In most cases, a 3 in. diam extrusion billet 10 in. long was cast in a steel mold from the same melt used for making the sand-cast test bars. For the higher thorium alloys, it was necessary to remelt the foundry scrap from the test bars in order to make the extrusion billets. The billets were scalped to a diameter of 2 15/16 in. and the ends faced to a length of 9¼ in. as limited by the size of the extrusion container. The alloys were extruded into ½ in. diam rod on a 500-ton direct-extrusion press. The details of the extrusion process are as follows:

Billet preheat	925°F (2 to 16 hr)
Container temperature	900°F
Die temperature	900°F
Extrusion speed	10 ft per min
Reduction ratio	36:1
Percent reduction	97.3

Alloys containing up to 10.2 pct Th were preheated at 925°F for 2 hr; all alloys with higher thorium contents were preheated for 16 hr. In order to establish the effect of extrusion temperature, billets of

T. E. LEONTIS, Member AIME, is associated with the Metallurgical Laboratories, Magnesium Dept., Dow Chemical Co., Midland, Mich.

Discussion on this paper, TP 3249E, may be sent, 2 copies, to AIME by May 1, 1952. Manuscript, Aug. 3, 1951. New York Meeting, February 1952.

The work reported in this paper was performed under the sponsorship of the Office of Naval Research.

* Most of the thorium used for this work was furnished by the Atomic Energy Commission.

Fig. 1—Tensile properties of sand cast Mg-Th alloys, T6 condition

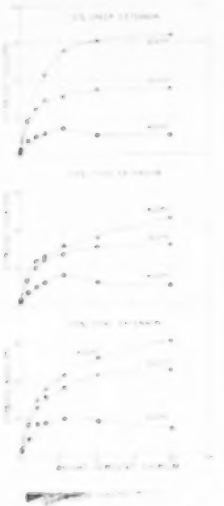

Fig. 2—Creep limits of sand cast Mg-Th alloys, T6 condition

each of the four alloys containing 1 to 6 pct Th were extruded also at 650°F using the same reduction and speed. Preheating of the billets for these tests was performed at 700°F for 1 to 2 hr.

Metallographic determination of the solidus temperatures of the various alloys are summarized as follows:

Alloy Composition, Pct		Solidus Temperature, °F
Th	Ce	
0.97		1170
2.1		1156
3.2		1141
5.8		1107
10.2 to 49.9		1062
2.0	3.11	1077
6.0	3.19	1065
10.1	3.22	1063

The solidus temperatures were determined on as-cast specimens. Heat treatment of the specimens for 24 hr at 1050°F prior to the solidus determinations raises the solidus temperature of the 2.1 and 3.2 pct Th alloys by 4° and 13°F, respectively, but has no effect on any of the other alloys. The results indicate that a eutectic between magnesium and a Mg-Th compound exists at the magnesium end of the constitution diagram. Furthermore, the solid solubility limit of thorium in magnesium lies between 5.8 and 10.2 pct.

On the basis of these results all sand-cast Mg-Th alloys were heat treated at 1050°F for 24 hr, whereas the Mg-Th-Ce alloys were heat treated at the same temperature for 16 hr. The heat-treating time on the latter alloys was reduced in order to minimize the degree of internal oxidation and alloy depletion at the surface that is observed in these alloys. It is of interest to note that neither binary Mg-Th nor binary Mg-Ce alloys exhibit internal oxidation when heat treated under the above conditions, provided a concentration of about 1 pct SO_2 is maintained in the furnace atmosphere. The internal oxidation in Mg-Th-Ce alloys cannot be suppressed even by decreasing the heat-treating temperature to 1000°F. Both Mg-Th and Mg-Th-Ce alloys in the extruded state were heat treated at 1050°F for 4 hr; the working of the extrusion process greatly facilitates the solution and coalescence of the intermetallic compound so that the shorter heat-treating time is adequate. All bars were cooled from the heat-treating temperature on an iron top bench under a fan blast. Test bars were aged at 400°F for 16 hr either subsequent to heat treatment or on the as-fabricated material. Throughout the paper the following designations are used to indicate the various tempers:

T5 = Direct age at 400°F (16 hr)
T4 = Solution heat treated at 1050°F
T6 = T4 + age at 400°F (16 hr)

The methods of tension and creep testing have been discussed in detail in previous publications.[6,7] Tension and creep testing of sand-cast Mg-Th alloys were performed on cast test bars without machining the surface. In order to eliminate the oxidized zone on the surface of Mg-Th-Ce test bars, these were machined to a diameter of $\frac{3}{8}$ in. for tension tests and to a diameter of 0.450 in. for creep tests. Thus, a gage length of 1.5 in. was used on the latter tension tests instead of the conventional 2 in. gage length used with the $\frac{1}{2}$ in. diam bar. Tension tests on the $\frac{1}{2}$ in. diam extruded alloys were performed on $6\frac{1}{2}$ in. long specimens with a reduced section of

Table I. Tensile Properties of Sand Cast Mg-Th Alloys in the As Cast and the Solution Heat Treated Conditions at Room Temperature

Th, Pct	Grain Size, In.	As Cast			T4 Condition		
		E, Pct	TYS	TS	E, Pct	TYS	TS
0	100 pct commercial	6.0	2.9	12.6	5.8	2.8	12.3
0.97	80-100 pct commercial	6.5	3.6	14.0	7.0	3.1	14.4
2.1	80-100 pct commercial	4.0	4.2	12.7	7.5	3.6	16.4
3.2	80-100 pct commercial	2.8	4.7	12.6	7.5	4.3	17.4
5.8	0.008-0.10						
	100-80 pct commercial	2.0	4.2	11.1	3.0	4.7	17.9
10.2	0.04-0.09		12.4	13.0	2.0	12.5	18.9
19.9	0.03-0.04					13.6	18.8
49.9	0.03-0.04						

E, pct = percent elongation in 2 in.
TYS = Tensile yield strength in 1000 psi
TS = Tensile strength in 1000 psi

Table II. Creep Limits of Sand-Cast Mg - 49.9 Th Alloy

Test Temperature, °F	100 Hr Creep Limits, 1000 psi		
	0.1 Pct Creep Extension	0.2 Pct Total Extension	0.5 Pct Total Extension
500	7.8	7.8	
600	2.2	2.7	4.0

Table III. Comparison of Creep Limits of Mg - 5.8 Pct Th in the As Cast and in the T6 Conditions

Test Temperature, °F	100 Hr Creep Limits, 1000 psi					
	As Cast			T6 Condition		
	0.1 Pct Creep Extension	0.2 Pct Total Extension	0.5 Pct Total Extension	0.1 Pct Creep Extension	0.2 Pct Total Extension	0.5 Pct Total Extension
400	10.8	7.1	9.4	14.0	8.0	10.7
500	6.5	3.9	7.4	7.7	6.7	9.0
600	1.9	2.5	3.1	3.5	4.0	4.9

$^{3}/_{8}$ in. diam and a gage length of 1.5 in. Extruded creep specimens having a reduced section of 0.450 in. were used. Compression tests on the extruded alloys were performed on specimens $1^{1}/_{2}$ in. long using the full $^{1}/_{2}$ in. diam of the extruded rod except in the Mg-Th-Ce alloys where enough metal was machined from the cylindrical surface of the heat-treated specimens to remove the oxidized layer. Yield strengths were determined by the offset method from autographic stress-strain curves at 0.2 pct deviation from the modulus line. Each result is the average of two tests.

Space does not permit the presentation of the complete creep curve for each test. Instead, the creep characteristics of each alloy are defined by the three creep limits given below:

1—Creep limit based on 0.1 pct creep extension in 100 hr
2—Creep limit based on 0.2 pct total extension in 100 hr
3—Creep limit based on 0.5 pct total extension in 100 hr

Derivation of these creep limits from log extension vs. log stress plots of the original data has been described previously.[7] No significance is attached to the creep rates obtained during the 100 hr test, because in many cases the tests are still in primary creep at the end of the test and in some cases even third-stage creep may occur during the test.

Discussion of Results

Mechanical Properties of Sand-Cast Alloys: Addition of thorium increases the strength of magnesium in the sand-cast state at room and elevated temperatures but decreases markedly the ductility as measured by the elongation in the tension test. Fig. 1. The brittleness of the Mg + 49.9 pct Th composition prevented the execution of tensile tests at temperatures below 600°F. Even at 600°F, this alloy broke at a stress of 15,000 psi without yielding. These alloys are amenable to heat treatment; comparison of the data in Table I with those in Fig. 1 shows that increases in strength ranging from 2000 to 4000 psi are realized by aging subsequent to solution heat treatment. The grain size values in Table I show that thorium exerts only a mild grain-refining action on magnesium. However, the grain size of Mg-Th alloys may be reduced markedly by the addition of zirconium, as demonstrated by Sauerwald.[8] Heat treatment at 1050°F has no effect on the grain size. Although the strength properties of Mg-Th alloys

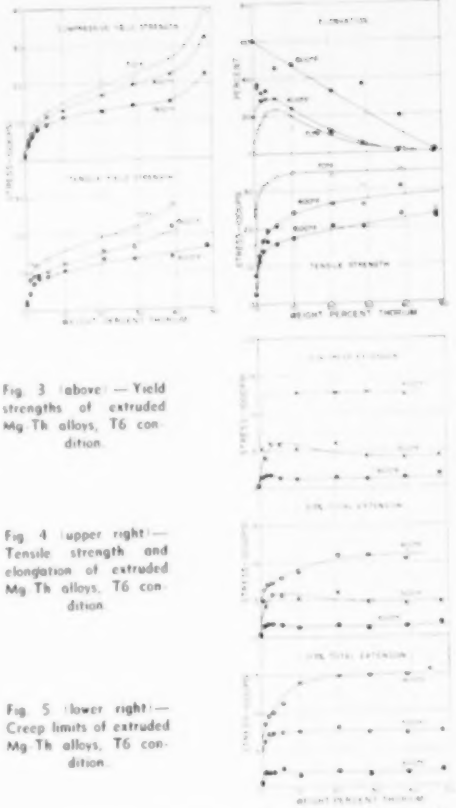

Fig. 3 (above) — Yield strengths of extruded Mg-Th alloys, T6 condition.

Fig. 4 (upper right) — Tensile strength and elongation of extruded Mg-Th alloys, T6 condition.

Fig. 5 (lower right) — Creep limits of extruded Mg-Th alloys, T6 condition.

Table IV. Tensile Properties of Sand-Cast Mg-Th-Ce Alloys

Room Temperature

Th, Pct	Ce, Pct	Grain size, in.	As-Cast E, Pct	As-Cast TYS	As-Cast TS	T5 Condition E, Pct	T5 Condition TYS	T5 Condition TS	T4 Condition E, Pct	T4 Condition TYS	T4 Condition TS	T6 Condition E, Pct	T6 Condition TYS	T6 Condition TS
3.0	3.11	0.08-0.09		12.9	14.1		14.6	15.8	0.5	12.1	15.6		15.2	18.6
6.0	3.19	0.06-0.07		15.2	16.4			17.4	0.5	14.2	17.4		16.6	20.6
10.1	3.22	0.04-0.05		17.5	17.8			19.0	0.5	15.0	18.2		17.5	20.4
*	3.0	0.02-0.03	1	9	15				4	10	18	2	13	20

T6 Condition

		200°F			400°F			500°F			600°F		
3.0	3.11	1.2	13.4	17.0	1.5	12.0	19.1	3.2	11.2	18.8	9.5	7.6	15.4
6.0	3.19	1.5	16.5	20.9	1.5	14.7	20.1	3.0	14.1	21.6	6.5	11.0	19.2
10.1	3.22	1.0	15.6	21.2	1.5	15.8	21.0	1.8	14.2	21.4	4.0	10.9	19.4
*	3.0	8	12	20	12	11	19	15	10	17	40	8	11

T5 Condition

		100°F			600°F		
3.0	3.11	2.2	11.4	17.2	11.2	7.6	15.0
6.0	3.19	1.3	14.2	18.7	4.6	10.1	17.4
10.1	3.22	0.7	15.4	18.8	7.6	11.8	18.2

E, Pct = Percent elongation in 1.5 in.
* Data from ref. 6.

Fig. 6—Electrical conductivity of Mg-Th alloys at 95°F

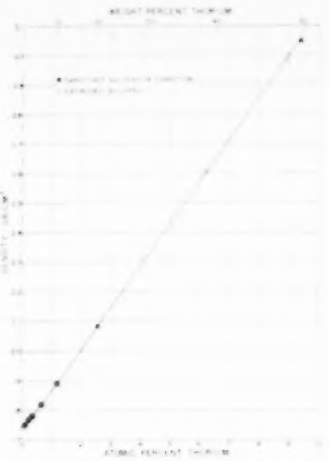

Fig. 7—Density of Mg-Th alloys at 25°C (77°F)

are not exceptionally high, these alloys exhibit remarkable temperature resistance as illustrated by the relatively small loss in strength between room temperature and 600°F. Mg-Th alloys are similar to magnesium-rare-earth alloys in this behavior. The level of strength properties of Mg-Th alloys, however, is considerably lower than that observed in magnesium alloys containing such rare-earth metals as didymium, Ce-free mischmetal, and mischmetal of equivalent alloy content.[7]

The curves in Fig. 2 show that Mg-Th alloys exhibit high resistance to creep at elevated temperatures. The creep limits determined on Mg + 49.9 pct Th at 500° and 600°F (Table II) follow the trends of the curves established by the lower thorium contents. The decrease in creep limits at 600°F with increasing thorium content beyond 5.8 pct is believed to be associated with the smaller grain size of the higher thorium contents. The creep resistance of Mg-Th alloys at 500° and 600°F is the highest observed to date in any magnesium alloy.

Creep tests have been performed on Mg + 5.8 pct Th also in the as-cast condition. Comparison of these results with the creep characteristics in the T6 condition (Table III) shows that the heat treatment effected a distinct improvement in the creep resistance of this alloy at all temperatures.

Addition of 3 pct Ce to alloys containing 3.6 and 10 pct Th increases significantly the yield strength of these alloys at temperatures up to 400°F but has no effect on the tensile strength, Table IV. The increase in strength is accompanied by a marked de-

Table V. Creep Limits of Sand-Cast Mg-Th-Ce Alloys

		100 Hr Creep Limits, 1000 psi								
		500°F						600°F		
Th, Pct	Ce, Pct	0.1 Pct Creep Extension	0.2 Pct Total Extension	0.5 Pct Total Extension	0.1 Pct Creep Extension	0.2 Pct Total Extension	0.5 Pct Total Extension	0.1 Pct Creep Extension	0.2 Pct Total Extension	0.5 Pct Total Extension
T6 Condition										
3.6	3.11	15.6	8.0	12.6	8.3	5.9	7.5	2.5	2.5	2.8
6.0	3.19	14.6	8.4	14.0	6.2	5.9	6.8	2.1	2.5	3.2
10.3	3.22	12.3	10.6	13.2	6.4	5.9	6.6	1.7	2.0	2.9
5.8*	0.0	9.2	7.8	10.2	4.9	4.9	5.6	2.3	2.3	3.0
T5 Condition										
3.6	3.11	12.9	8.6	12.1				2.0	2.4	3.1
6.0	3.19	12.2	9.0	13.3				1.6	2.3	2.7
10.3	3.22	11.6	8.0	14.0				2.0	2.3	3.1

* Data from ref. 8

Table VI. Tensile and Compressive Properties of Extruded Mg-Th Alloys in the As-Extruded and the Solution Heat Treated Conditions at Room Temperature. Alloys Extruded at 900°F

			As-Extruded				T4 Condition			
Th, Pct	Grain Size (0.001 In.) As-Extruded	T4 and T6 Conditions	E, Pct	TYS	CYS	TS	E, Pct	TYS	CYS	TS
0	5-40	70-150	2.8	16.4	4.1	24.0	2.3	5.8	4.8	14.4
0.97	1-5	5-10	23.5	12.7	9.5	29.4	13.7	9.1	5.6	26.0
2.1	0.5-1	5-15	29.0	13.8	10.7	27.6	24.0	9.3	7.3	25.5
3.2	1	4-8	31.5	13.4	13.2	27.0	28.0	8.9	8.5	25.0
5.8	0.5-1	2-7	30.0	12.5	13.0	27.4	28.6	9.0	9.5	26.7
10.2	0.5	1-2	22.5	14.0	14.5	29.2	23.0	12.0	12.7	28.7
20.3	0.5	0.5-0.8	13.6	19.7	19.8	30.6	15.6	16.1	17.0	28.9
29.8	0.5	0.5	7.8	21.7	21.3	31.0	8.6	18.2	17.8	27.5
38.9	0.5	0.5	1.8	23.9	26.2	34.1	3.3	23.0	22.3	31.1
48.3	0.5	0.5			33.4	30.0			33.8	27.4

E, Pct = Percent Elongation in 1.5 in.
CYS = Compressive yield strength in 1000 psi

crease in elongation. Even at 600°F, where no benefit in strength is realized from the addition of cerium, the ductility is impaired. Comparison with the properties of Mg + 3 pct Ce alloy shows that all the Mg-Th-Ce alloys have higher strength properties. However, the Mg-Th-Ce alloys are still not equivalent to the best magnesium-rare-earth alloys.[7]

The data in Table V show that some improvement in creep limits at 400°F based on total extension is realized from the addition of cerium to Mg-Th alloys. This is a direct result of the higher static properties of these alloys. At 500° and 600°F, however, the Mg-Th-Ce alloys have somewhat lower creep limits than the Mg-Th alloys of corresponding thorium content. It is of interest to note that the creep resistance of Mg + 3 pct Ce at 400° and 500°F is increased by the addition of thorium, whereas at 600°F there is little, if any, effect.

Mechanical Properties of Extruded Alloys: The extruded Mg-Th alloys show the same high degree of temperature resistance that has been noted for the cast alloys, Figs. 3 and 4. The strength properties of these alloys at 300° and 500°F do not differ much from those at 400°F; they have been omitted from Figs. 3 and 4 in order to avoid crowding. Comparison of the properties in the T6 condition with those

Table VII. Tensile and Compressive Properties of Mg-Th Alloys Extruded at 650°F

		Room Temperature								T5 Condition											
		As-Extruded				T5 Condition				400°F				500°F				600°F			
Th, Pct	Grain Size, 0.001 In.	E, Pct	TYS	CYS	TS	E, Pct	TYS	CYS	TS	E, Pct	TYS	CYS	TS	E, Pct	TYS	CYS	TS	E, Pct	TYS	CYS	TS
0.97	1.5-2.0	30.6	13.8	16.8	30.0	30.6	17.0	16.2	30.2	50.6	10.6	11.6	13.6	35.6	9.8	9.8	13.2	54.0	7.8	7.1	11.0
2.1	1.0-1.5	32.7	17.8	18.4	30.0	30.0	19.5	20.0	32.0	44.6	13.4	13.0	15.7	39.6	11.4	11.2	14.6	80.0	7.2	5.2	10.0
3.2	0.5	20.6	21.8	29.5	32.0	29.4	21.1	25.6	33.0	41.0	14.5	14.8	16.8	39.0	12.2	11.7	15.1	94.0	6.2	5.6	9.5
5.8	0.5	29.4	22.2	21.7	31.2	27.3	23.2	27.1	34.1	38.7	16.7	16.3	18.4	36.0	13.8	13.6	16.0	117.5	6.3	6.5	9.4

E, Pct = Percent elongation in 1.5 in.

Table VIII. Creep Limits of Mg-Th Alloys Extruded at 650°F and Tested in the T5 Condition

	100 Hr Creep Limit, 1000 psi								
	400°F			500°F			600°F		
Th, Pct	0.1 Pct Creep Extension	0.2 Pct Total Extension	0.5 Pct Total Extension	0.1 Pct Creep Extension	0.2 Pct Total Extension	0.5 Pct Total Extension	0.1 Pct Creep Extension	0.2 Pct Total Extension	0.5 Pct Total Extension
0.97	11.5	11.6	11.6	1.0	1.3	2.2			
2.1	12.8	10.6	12.0	1.0	1.4	1.7			
3.2	10.5	10.0	11.0	1.0	1.1	1.4	<1.0	<1.0	<1.0
5.8	10.1	8.5	13.0	0.9	1.0	1.4	<1.0	<1.0	<1.0

Table IX. Tensile and Compressive Properties of Extruded Mg-Th-Ce Alloys

			Room Temperature											
			As-Extruded				T4 Condition				T6 Condition			
Th, Pct	Ce, Pct	Grain Size, 0.001 In. As-Extruded	T4 and T6 Condition	E, Pct	TYS	CYS	TS	E, Pct	TYS	CYS	TS	E, Pct	TYS	CYS	TS
3.11	3.00	0.4-0.5	0.5-1.0	15.3	17.2	16.4	29.8	17.3	14.6	14.2	28.0	14.0	15.6	15.1	31.2
5.65	3.21	0.3-0.4	0.4-1.0	14.0	16.6	18.4	29.3	16.0	15.5	15.2	27.6	13.4	17.6	16.6	32.6
9.48	3.07	0.3-0.4	0.3-1.0	10.8	21.8	24.2	31.4	15.8	18.9	20.0	28.3	13.3	20.6	21.4	33.1
*—	3.0	0.5-1.0	1-3	11	21	15	33	13	18	11	30	8	24	14	35

		T6 Condition									
		300°F			400°F			500°F			600°F		
Th, Pct	Ce, Pct	E, Pct	TYS	TS	E, Pct	TYS	TS	E, Pct	TYS	TS	E, Pct	TYS	TS
3.11	3.00	22.0	13.4	24.1	21.6	12.0	22.6	25.3	10.8	22.0	49.0	8.2	15.0
5.65	3.21	12.6	15.2	25.6	17.6	14.9	25.0	21.6	13.1	24.0	30.6	9.8	16.2
9.48	3.07	8.0	17.2	25.1	17.0	16.2	25.4	14.6	14.7	23.0	26.4	10.4	14.6
*—	3.0	22	15	29	17	14	20	26	11	17	28	7	11

E, Pct = Percent elongation in 1.5 in.
* Data from ref. 9.

Table X. Creep Limits of Extruded Mg-Th-Ce Alloys. T6 Condition

		100 Hr Creep Limits, 1000 psi								
		400°F			500°F			600°F		
Th, Pct	Ce, Pct	0.1 Pct Creep Extension	0.2 Pct Total Extension	0.5 Pct Total Extension	0.1 Pct Creep Extension	0.2 Pct Total Extension	0.5 Pct Total Extension	0.1 Pct Creep Extension	0.2 Pct Total Extension	0.5 Pct Total Extension
3.11	3.00	11.6	8.7	12.0	4.6	4.6	5.6	1.3	1.4	1.9
5.65	3.21	10.5	9.0	12.0	4.3	4.5	6.2	1.0	1.1	1.3
9.48	3.07	11.0	9.8	12.0	2.9	3.0	4.2	0.92	0.95	1.3
*—	3.0	8.7	8.2	9.3	2.1	2.3	3.1	0.72	0.90	1.1

* Data from ref. 9.

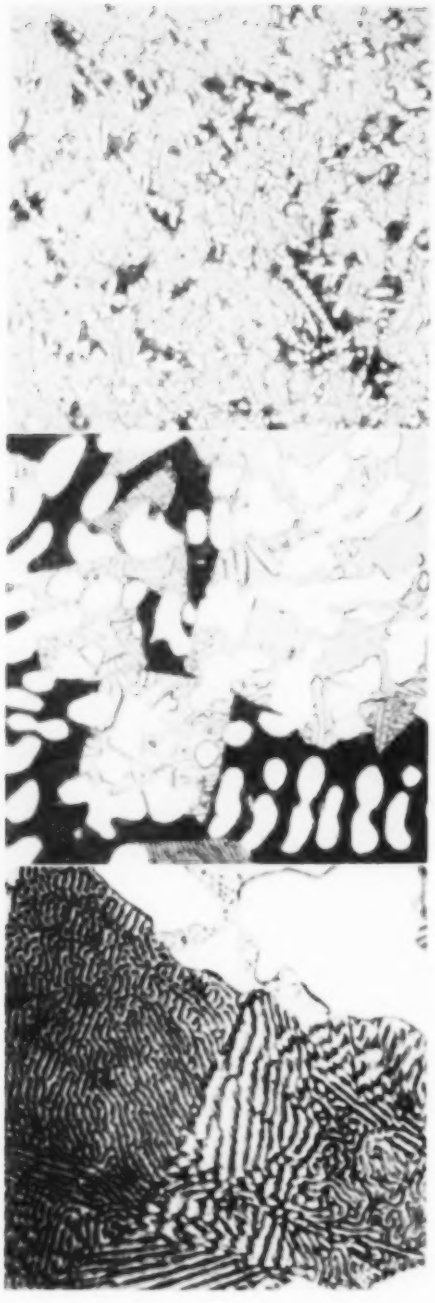

Fig. 8—Sand cast Mg 4.9 pct Th alloy, as cast condition. Glycol etchant.

a (top)—General structure. X100.
b (center)—Structure of coarse eutectic. X500.
c (bottom)—Structure of fine eutectic. X1000.

in the as-extruded and in the T4 condition (Table VI) shows that the extruded alloys exhibit a somewhat higher degree of age-hardening than the cast alloys. Extruded Mg-Th alloys show two additional outstanding characteristics: 1—high ductility particularly in the range of 1 to 10 pct Th; and 2—equivalence in tensile and compressive yield strengths in alloys containing more than 2 pct Th. Actually, the ductility remains high even in alloys containing as much as 20 pct Th.

The creep limits of extruded Mg-Th alloys, Fig. 5, increase much more sharply with the addition of the first few percent thorium than the corresponding cast alloys. However, at higher thorium contents the extruded alloys do not develop as high creep resistance as the cast alloys. It is remarkable that increases in thorium content beyond 3 to 6 pct up to 50 pct produce no further increase in creep strength. The creep limit based on 0.1 pct creep extension at 400°F could not be established accurately on alloys containing less than 10 pct Th, because these compositions suffer exceedingly high deformations upon application of the load. However, the values of these creep limits all lie above 10,000 to 12,000 psi; hence the curve established by 10 to 40 pct Th alloys at 12,500 psi has been extended at the same level down to 1 pct Th.

Considerably higher strengths at temperatures up to 500°F can be attained in Mg-Th alloys by extruding at 650°F instead of 900°F, Table VII. These low temperature extrusions were tested at all temperatures in the T5 condition in order to determine the effect of temperature on material having the highest possible strength at room temperature. The creep data on the low temperature extrusions (Table VIII) show that these materials exhibit somewhat higher creep resistance at 400°F but markedly lower creep resistance at 500° and 600°F than the high temperature extrusion tested in the T6 condition. These observations corroborate the findings on extruded magnesium-rare-earth alloys,[7] that is, the highest creep resistance at elevated temperatures is obtained by extruding at a relatively high temperature and testing in the solution heat-treated and aged condition.

The addition of 3 pct Ce increases the strength and decreases the ductility of Mg + 3, 6, and 10 pct Th at temperatures up to 500°F, Table IX; at 600°F, however, no significant advantage is realized from the addition of cerium. The properties of Mg + 3 pct Ce alloy from ref. 9 are included in Table IX for comparison. The increase in static properties resulting from the addition of cerium leads to higher creep limits at 400°F based on total extension. At 500° and 600°F a definite impairment in creep resistance results from the addition of cerium. All the Mg-Th-Ce alloys have higher creep resistance than the corresponding Mg-Ce alloy over the entire temperature range investigated.

By way of comparison of extruded Mg-Th alloys with extruded magnesium-rare-earth alloys,[7] the outstanding feature of the Mg-Th alloys is their significantly higher creep resistance at 500° and 600°F. As far as static strength is concerned, there is no question that magnesium alloys containing mischmetal, didymium, cerium-free mischmetal, and, even, cerium are superior to Mg-Th alloys. The level of creep resistance of some of the extruded magnesium-rare-earth alloys at 500° and 600°F is raised to that of extruded Mg-Th alloys by the addition of manganese (ref. 9).

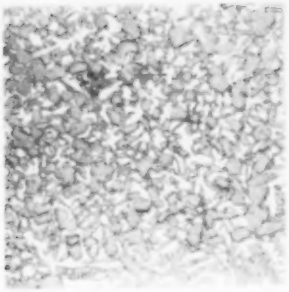

Fig. 9 — Sand-cast Mg-9.9 pct Th alloy, T6 condition. Glycol etchant. X100

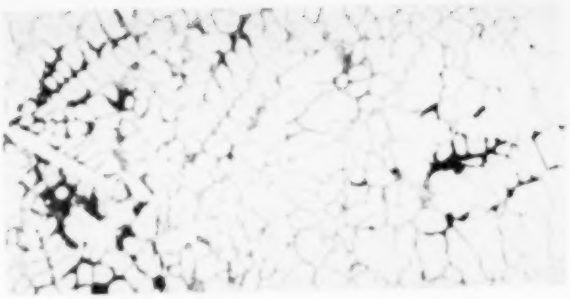

a—Mg-9.9 pct Th. b—Mg-10.2 pct Th.

Fig. 10—Sand-cast Mg-Th alloy, as-cast. Glycol etchant. X100

Fig. 11—Sand-cast Mg-Th alloys, T6 condition. Glycol etchant.

a—Mg-9.9 pct Th. X100. c—Mg-10.2 pct Th. X100.

b—Same as a. Shows two compounds. X250. d—Same as c. Shows only one compound. X250.

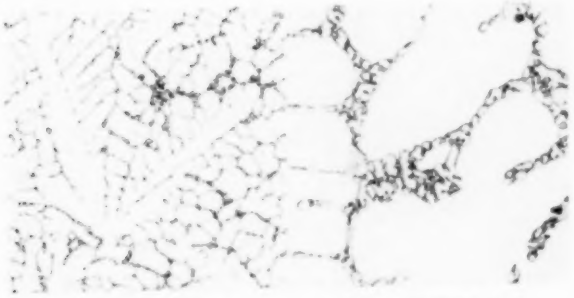

a—Dendritic structure. X100. b—Structure of eutectic. X500.

Fig. 12—Sand-cast Mg-10.1 pct Th-3.22 pct Ce, as-cast condition. Glycol etchant.

Fig. 13—Sand-cast Mg-10.1 pct Th-3.22 pct Ce, T6 condition. Glycol etchant. X100

Electrical Conductivity. Electrical conductivity was measured on a Kelvin bridge in a constant temperature room held at 95 F. In the composition range where most of the thorium is present as an intermetallic compound, the electrical conductivity decreases linearly with increasing volume percent thorium (Fig. 6). The decrease, however, is much more rapid in the solid-solution region. The composition of the transition agrees well with the solid-solubility limit predicted from the solidus measurements. The linearity of the relation between conductivity and volume percent thorium after aging at 700 F over the entire composition range from 0 to 50 pct Th indicates that the solubility of thorium in magnesium even at that temperature must be very low and that aging at 700 F causes complete precipitation of thorium. The deviation of the curves from linearity after aging at lower temperatures simply indicates incomplete precipitation.

Density. The density of each alloy was determined by weighing carefully machined specimens on an analytical balance under two conditions: 1—in air, and 2—in perchlorethylene. Thorium markedly increases the density of magnesium, Fig. 7. In the region of solid solubility there is a slight negative deviation from Vegard's law, but in the two-phase region the density increases linearly with increasing atomic percent thorium. Undoubtedly, the deviation from Vegard's law would be greater, had the densities been determined in the solution heat-treated condition.

Metallography. The metallographic structure of Mg-Th alloys presents some interesting characteristics. The as-cast structure of sand-cast Mg + 49.9 pct Th contains a large amount of free intermetallic compound, the particle shape of which gives the impression that this might be the primary phase, Fig. 8a. In addition there are present also two distinct eutectics: 1—a relatively coarse eutectic, the compound constituent of which is continuous in many areas with the large compound particles, Fig. 8b, and 2—an exceedingly fine eutectic which can be resolved only at high magnifications, Fig. 8c. There are also present dendrites of magnesium solid-solution phase. This raises some question as to whether the large compound particles are the primary phase, even though their idiomorphic shape seems to indicate that they were the first to freeze. This may arise entirely from divorcement of a eutectic. Heat treatment of this composition at 1050 F (24 hr) coalesces the compound in both eutectics, but the compound in the fine eutectic forms irregularly shaped particles which are a distinctly different phase, Fig. 9. Increasing the heat-treating time at 1050 F to 96 hr or increasing the heat-treating temperature fails to eliminate either one of these two intermetallic compounds. In the absence of any information on the constitutional diagram of the Mg-Th system, it is difficult to analyze these observations intelligently. X-ray diffraction studies of this composition confirm the presence of two compounds both of which appear to have a large unit cell containing many atoms.

Sand-cast test bars of alloys containing 30 and 40 pct Th were not available, but specimens from chill-cast 2 in. diam billets of these compositions were found to show essentially the same characteristics as described above, except that they contained proportionately smaller amounts of intermetallic phases. The structures of sand-cast alloys containing 10.2 and 19.9 pct Th (Fig. 10) both show a network of compound, which results from divorcement of the eutectic, and a fine eutectic having the same structure as that shown in Fig. 8c. The black areas in Fig. 10 are the fine eutectic. The free compound as well as that in the eutectic areas is completely coalesced in both alloys by heat treating at 1050 F for 24 hr (Figs. 11a and c) and in the Mg + 10.2 pct Th alloy the compound is no longer the continuous phase. There is still a trace of a second compound in Mg + 19.9 pct Th (Fig. 11b) but the 10.2 pct Th alloy contains only one compound (Fig. 11d). These observations have been confirmed by X-ray diffraction. Alloys of lower thorium content are structurally similar to Mg + 10.2 pct Th, except that the amount of compound decreases with decreasing thorium content. However, there is present a small amount of second phase even in the 0.97 pct Th alloy. In general, Mg-Th alloys show no visible precipitate upon aging at 400 F.

Addition of cerium to Mg-Th alloys introduces a Mg-Ce compound in the structure. This compound appears to form a relatively coarse ternary eutectic with magnesium solid solution and the Mg-Th compound (Fig. 12b). The dendritic pattern of the as-cast state is evident in Fig. 12a. The predominance of the Mg-Ce compound is shown more clearly in the structure of the T6 condition shown in Fig. 13. The structures of the other Mg-Th-Ce alloys studied are similar to that illustrated here except that in the alloy containing 3 pct Ce the eutectic is largely divorced in the as-cast condition.

The extruded alloys exhibit no unusual characteristics. Essentially, the structures consist of stringers of intermetallic compound in the magnesium solid-solution matrix, similar to those of magnesium-rare-earth alloys illustrated in ref. 9.

Summary

1—The properties of sand-cast and extruded Mg-Th alloys containing up to 50 wt pct Th have been determined.

2—Thorium increases the strength properties of magnesium over a wide temperature range. These alloys exhibit marked temperature resistance.

3—The most outstanding characteristic of Mg-Th alloys is their high creep resistance at 500 and 600 F. At these temperatures, the creep resistance of Mg-Th alloys is the highest observed in any magnesium alloy to date.

4—One detracting feature of sand-cast Mg-Th alloys is their relatively coarse grain size. The grain size can be effectively reduced by the addition of zirconium with an attendant increase in strength and ductility. These effects will be discussed in a subsequent paper.

References

1 J. C. McDonald: *Trans.* AIME (1941) **143**, p. 179.

2 J. C. McDonald: U. S. Patent 2,371,531 (Mar. 13, 1945).

3 F. Sauerwald: *Ztsch. anorg. allgem. Chem.* (1949) **258**, p. 296.

4 C. E. Nelson: *Trans.* AIME (1944) **159**, p. 392.

5 R. F. Marande: *Materials and Methods* (1946) **23**, p. 418.

6 T. E. Leontis and J. P. Murphy: *Trans.* AIME (1946) **166**, p. 293; METALS TECHNOLOGY (April 1946).

7 A. A. Moore and J. C. McDonald: *Proc.* A.S.T.M. (1946) **46**, p. 970.

8 T. E. Leontis: *Trans.* AIME (1949) **185**, p. 968; JOURNAL OF METALS (December 1949).

9 T. E. Leontis: *Trans.* AIME (1951) **191**, p. 987; JOURNAL OF METALS (November 1951).

Plastic Deformation of Magnesium Single Crystals

by E. C. Burke

and

W. R. Hibbard, Jr.

Plastic deformation in magnesium single crystals was studied by tensile tests at room temperature utilizing an improved preparation and testing technique. Consistent critical resolved shear stress values for basal slip were obtained. The advent of pyramidal slip at room temperature was rationalized upon the basis of grip constraints. A bend-twinning hypothesis was advanced as an explanation of mechanical twinning which occurs as a complex stress-relief mechanism.

INVESTIGATIONS of the plastic deformation of magnesium have been limited to the determination of the fundamental kinetics which may be summarized as follows: 1—Twinning on the {102}.[1] 2—Slip on the (001) plane in the [100] direction at room temperature.[2] 3—Slip on the {101} or {102} plane in the [100] direction above 225°C.[3] 4—Critical resolved shear stresses for basal slip in tension at room temperature of 83 g per sq mm with a variation from 57 to 127 g per sq mm.[3]

Bakarian[4] studied the compression of thin wafers of magnesium single crystals and classified the components of the deformation mechanisms as follows: 1—The Basal field: (001) at an angle of less than 20° to the compression surface. Fracture along {101} or slip on (001) followed by {101} fracture. 2—The prism field: (001) at an angle greater than 60° to the compression surface. Twinning on the {102} generally occurring during the early stages of loading, basal slip in the areas of original orientation and (001) slip within twins. 3—The central field: (001) at angles greater than 20° but less than 60° to the compression surface. Slip on the (001). 4—The critical resolved shearing stress for {101} slip above 225°C was 400 g per sq mm.

Observations of mechanical twins in hexagonal close-packed metals have been summarized by numerous investigators[5] emphasizing a lateral or rotational atomic adjustment, in addition to the pure twinning shear, and the importance of reorienting the basal plane to a position more favorable for continued slip, rather than the resulting small dimensional changes. Criterion for the operative twinning planes has not been clearly established. Schmid and Boas[5] surmised that an energy condition related to the atom movements is the determining factor. Miller[6] observed that twinning stresses in zinc crystals decreased as the amount of prior deformation increased.

Preparation of Specimens

Magnesium single crystals ½ in. in diam x 8 in. long were grown from the melt under an argon atmosphere in a gradient furnace similar to that described by Jillson.[7] Magnesium containing 0.018

E. C. BURKE, Student Associate AIME, formerly Graduate Student, Yale University, is now with the Magnesium Dept., The Dow Chemical Co., Midland, Mich., and W. R. HIBBARD, JR., Member AIME, formerly Associate Professor of Metallurgy, Yale University, is now with the Research Laboratory, General Electric Co., Schenectady.

Discussion on this paper, TP 3250E, may be sent, 2 copies, to AIME by May 1, 1952. Manuscript, Aug. 30, 1951; revised, Jan. 7, 1952. New York Meeting, February 1952.

This paper represents part of a thesis by E. C. Burke submitted in partial fulfillment of requirements for the degree of Doctor of Philosophy to the Faculty of the Graduate School of Yale University, May 1951.

Fig. 1—Orientation of crystals used for critical resolved shear stress determinations.

pct Si was not suitable due to the nucleating effects of Mg$_2$Si, which settled to the bottom of the mold and inoculated a burst of crystals during the initial solidification of the metal.

Magnesium of the following analysis was successfully solidified into 43 single crystals (a 98 pct yield), three at a time. The composition in weight percent was: Al, 0.003 pct; Ca, < 0.01; Cu, 0.002; Fe, < 0.001; Mn, 0.008; Ni, < 0.001; Pb, < 0.002; Si, < 0.01; Sn, < 0.001; and Zn, < 0.01.

The single crystals were oriented by the back-reflection Laue method described by Greninger.[7] The Laue spots showed that the crystals were free from any lineage imperfections detectable by this X-ray technique.

Bakarian's technique of preparing gage lengths of tensile specimens by etching was improved by eliminating the intermittent rubbing with emery paper and by using electroplaters' scotch tape to cover the grip ends instead of picein. Lubricating grease was applied periodically to the edge of the tape adjacent to the gage to produce even fillets. Because strain gages reinforce the specimen and retard the slip process slightly, it was necessary to etch an additional "step" in the center of the gage section where they were attached. This was accomplished by allowing 25 pct HCl to drop from a burette on a strip of cloth $^3/_4$ in. wide, in contact with the middle of the 3 in. gage section of the specimen, which was revolved slowly by an electric motor. The localized action produced an extra step $^3/_4$ in. wide and approximately 0.005 to 0.010 in. smaller in diameter than the remainder of the gage section.

No eccentricity resulting from etching could be detected in the gage section, approximately 0.4 in. diam. However, the small tip section, $^1/_8$ in. diam, often etched preferentially to a ribbon, although no significant crystallographic dependence was apparent.

The diameters of the specimens were measured optically with a traveling microscope (accuracy, 0.0001 in.) within 0.001 in. for each $^1/_4$ in. station along elements of the bar, 90° apart.

The tensile loading equipment described by Miller[8] was used with a balanced 6/1 lever arm, loaded by a flow of sand between 222 to 225 g per min.

The strain measurements were determined by SR-4 A-8 strain gages connected to a Dynalog strain time recorder with a polar chart rotating at 1/12 rpm. The accuracy of the instrument is 5 microin. of strain and by careful interpolations 2.5 microin. of strain may be estimated.

The strain gages were mounted on the surface of the crystal at a position of minimum surface dis-

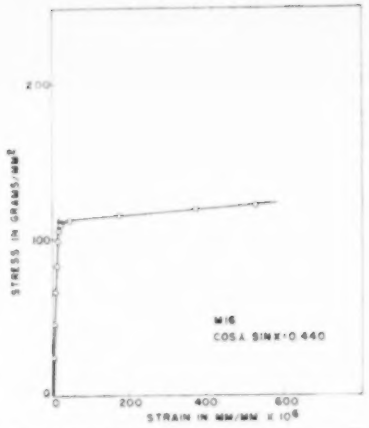

Fig. 2—Stress strain curve for M16 where χ = 58.

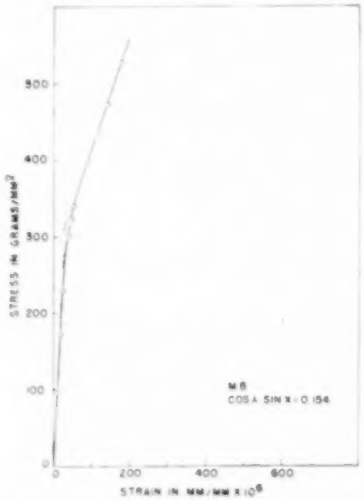

Fig. 3—Stress strain curve for M8 where χ = 9.

Table I. Summary of Tensile Data

Crystal No.			sin χ cos λ		Yield Stress, G per Sq Mm	S_c Critical Resolved Shear Stress, G per Sq Mm
M8	9	9	0.154	2.92	207	47.3
M17	10.5	11	0.181	0.30	245	44.8
M19	13	13	0.230	0.43	190	46.0
M9	17	18	0.277	0.17	170	47.0
M20	17	18	0.275	0.27	145	40.5
M15	27	27	0.400	0.07	118	47.4
M14	24	28	0.434	0.11	100	43.4
M27	30	32	0.469	0.34	106	49.7
M23	30	32	0.452	0.147	100	45.2
M10	30	30.5	0.440	1.32	110	48.5
M12	71	72	0.292	0.14	150	43.8
M24	72	74	0.261	0.36	190	49.5
M18	75	78	0.190	0.36	210	40.0
M30	80	80	0.122	0.25	340	42.3
M21 (101)	70	74	0.168			
M21 (001)	0	14	0.001			

* Average of four X-ray determinations.
† Standard error of mean = ±0.7%.

tortion, which corresponded to the minor axis of the predicted (001) glide ellipse as determined from X-ray data.

Grips were fitted with hard drawn piano wires, 0.0241 in. diam and 6 in. long, aligned concentrically with the axis of the grips and seated in small hemispheres of steel.

Results and Discussion

Outline of Data Presentation. Stress-strain curves were obtained in tension under room temperature conditions, 22° ± 2°C, with a loading rate of 18 g per sq mm per min. Metallographic examination of the gage section of each specimen was correlated with the X-ray orientation. The operative slip planes were determined from observed traces by stereographic methods and the salient features of the microscopic examination were documented by micrographs. The orientations of the crystals used are presented in Fig. 1.

A crystal was stretched just beyond its yield point, unloaded, allowed to remain at room temperature for 24 hr and reloaded, and after one week had elapsed following the second loading, loaded a third time. The temperature was 22° ± 2°C throughout the entire period. These tests showed that no appreciable recovery occurred under the conditions involved and in this respect magnesium is similar to aluminum.[7] It was concluded that the effect of recovery need not be considered in extrapolating the yield point.

Critical Resolved Shear Stress Determinations. Figs. 2 and 3 are typical stress-strain curves for the range of crystals presented in Fig. 1. If true axiality is accompanied by a sharp knee in a stress-strain curve, it is evident that the eccentricity of loading was quite small in these tests. The intersection of the dashed lines on the figures represents the yield stress[7] used for the calculation of the critical resolved shear stress. The complete results of the tensile testing data are summarized in Table I.

The yield stress of the crystals plotted against the orientation function, $\cos \lambda \cdot \sin \chi$, defines a parabolic curve symmetrical about an axis at 45°, Fig. 4, and strongly substantiates the critical resolved shear stress law.[7]

Comparison of Fig. 4 with the results of Schmid[3] and Bakarian[4] disclosed marked differences in the yield stress values. The Schmid data exhibit considerable scatter from the theoretical parabola, Fig. 5, with a reported critical shear stress of 82.9 g per sq mm. This value is apparently the mathematical average of 22 tests with individual values ranging from 57 to 127 g per sq mm. Bakarian's tensile results, 55 and 87.7 g per sq mm, averaged 77.8 g per sq mm, which is in fair agreement with Schmid's value of 82.9 g per sq mm. The present critical resolved shear stress was found to be 46 g per sq mm ± 0.75, which is approximately one half of the previously reported value.

Schmid, using dividers, found that the parabolic plot for the unresolved yield stress for magnesium crystals varied by a factor of four according to their orientation, as shown in Fig. 5. The present data in Fig. 4 is a considerably flatter parabola with values which vary only by a factor of three, when the maximum yield strengths are considered at an orientation function of 0.15 for both sets of data. The gross extension determinations by dividers are equivalent to significant strains beyond the true yield stress, i.e., actually an offset yield strength.

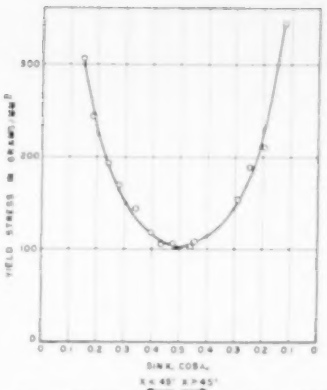

Fig. 4—Orientation dependence of the yield stress of magnesium crystals from the present data.

However, by virtue of the low strain hardening present in oblique basal plane orientations, the determined yield values would be only slightly higher than the true yield stress. On the other hand, acute orientations of the basal plane exhibit marked strain hardening; consequently, for these orientations the first detectable extension by the dividers method would be in considerable plus error, since the stress increase is much larger for the equivalent amount of offset than for oblique orientations. Comparison of Figs. 4 and 5 offers satisfying evidence for this rationalization, since the Schmid parabola corresponds to shear stress values of 127 g per sq mm at acute angles of the basal plane, while oblique orientations gave critical shear stress values from 57 to 85 g per sq mm.

Shear strengthening curves were calculated for the crystals using the usual formulas for small extensions. While the stress-strain curves show a pronounced difference in the rate of strain hardening, Fig. 6 demonstrates that orientation dependent

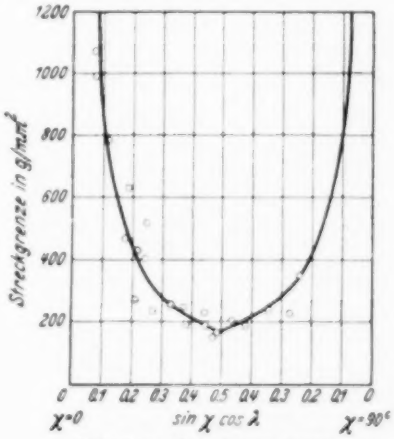

Abb. 81a. Magnesium (168).

Fig. 5—Orientation dependence of the yield stress of magnesium crystals (Schmid). Streckgrenze means yield point.

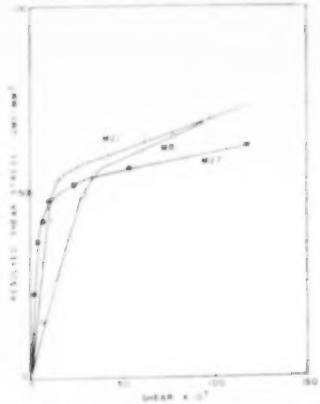

Fig. 6—Shear strengthening curves for different orientations including pyramidal slip

stress-strain curves may be represented reasonably by a single resolved curve. Thus, a shear strengthening curve may be considered a fundamental material characteristic which is independent of orientation within the errors of these tests.

Careful studies of the slip lines in magnesium disclosed that the spacing for shear values, 1×10^{-4}, was orientation dependent. Although the strain hardening rate was high when the basal plane was almost parallel to the axis, slip has occurred on rather widely separated areas, Fig. 7. Fig. 8 was taken on a crystal in which the basal plane was almost perpendicular to the axis and exhibiting a lower strain hardening rate. The slip is now present in closely spaced narrow packets of nonresolvable lines. Thus, the results are not in agreement with the hypothesis of Andrade[6] on the relationship of strain hardening to slip line spacing. Furthermore, it introduces serious doubts as to whether a metal has a single characteristic frequency, since the line spacing is orientation dependent for magnesium. Similar results were reported by Rosi[7] for aluminum at small extensions.

On the basis of dislocation theory, however, a greater number of slip lines would be expected with the slip plane perpendicular to the stress axis, since then a larger number of potential slip planes intersect the surface, where Frank-Read sources act most effectively.

The summary of tensile results, Table I, contains a column of values, ds/de, which are the slopes of the plastic regions of the stress-strain curves and represent the rate of strain hardening. No apparent correlation between the rate of strain hardening and orientation of these specimens exists, although qualitatively the strain hardening appears to increase as the (001) becomes either parallel or perpendicular to the axis.

Pyramidal Slip: The stress-strain relationship shown in Fig. 9 is for crystal M21 in which the (001) and [100] made an angle of 6° and 14° respectively with the axis. However, the critical resolved shear stress calculated for basal slip in this specimen was 31.2 g per sq mm, a value significantly lower than had been obtained in all the previous results.

The analysis of the operative slip system in M21 is presented in Fig. 10 which is a stereogram drawn with the specimen axis at the center of the projection, the primitive circle represents the polished surface of the crystal, and the point of observation corresponds to the position on this circle labeled "Reference Mark."

From this point of observation, the minor axis of the (001) glide ellipse should appear after a clockwise rotation of 30° about the specimen axis. However, repeated trials disclosed that the minor axis of the operative slip system was found after a clockwise rotation of 90°. At this position the slip lines became straight and uniformly spaced, at 10° to the specimen axis, Fig. 11. The entire projection was rotated stereographically until the [001] was at the center and pole of the trace was found to correspond to a {101} pole.

The specimen was not amenable to sufficient amount of deformation to determine the slip direction by X-rays. Since the slip direction invariably lies in the line of closest atomic packing and the {101} planes contain only one line of close-packed atoms, it is assumed that the close-packed direction must also operate in pyramidal slip.

Examination of the standard projection will disclose that {101} and (001) intersect along a line which is one of close atomic packing. In the present case, the slip direction was the same for both the (001) and {101} slip planes and was used to calculate the critical resolved shear stress for pyramidal slip as follows: basal slip, 31.2 g per sq mm; pyra-

Fig. 7—Randomly spaced slip lines in M13 at a position corresponding to the minor axis of the glide ellipse. Axis vertical. X500. Shear is 1.17×10^{-4}.

Fig. 8—Closely spaced packets of nonresolvable slip lines M30 at a position corresponding to the minor axis of the glide ellipse. Axis vertical. X500. Shear is 1.1×10^{-4}.

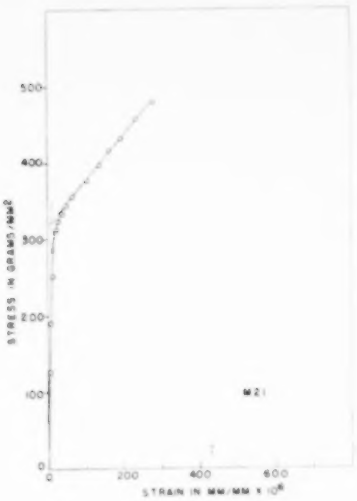

Fig. 9 (above)—Stress-strain curve for M21 which contained pyramidal slip.

Fig. 10 (right)—Stereogram of the operative slip system in crystal M21.

rather frequently. However, it may occur only under special stress conditions which will be described below.

Fig. 6 shows that the shear hardening characteristics for pyramidal slip in crystal M21 are essentially the same as for crystals which undergo basal slip. Bakarian has surmised that pyramidal and basal slip had similar strain hardening characteristics because of the close agreement between his work and Schmid's results on the orientation region where pyramidal slip was independent of prior basal slip. However, this investigation has shown that pyramidal slip may occur without prior basal slip and established that the rate of strain hardening in both systems is essentially the same.

Although the present investigation is the first to report two slip systems for magnesium in tension at room temperature, pyramidal slip has been mentioned previously. Schmid and Siebel[7] found that alternating stress fatigue tests on magnesium crystals frequently produced {101} traces as the surface of fracture. Bakarian reported that compression wafers of magnesium critically oriented for {101} twinning usually cleaved along the {101} plane. Schiebold and Siebel[8] found very fine {101} twins

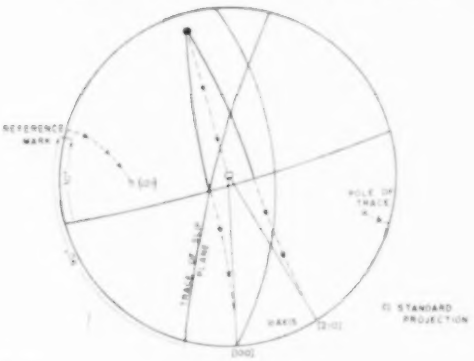

midal slip, 52.2 g per sq mm. Thus, the critical resolved shear stress on the pyramidal plane was about 10 pct greater than that acting on the basal plane in accordance with the resolved shear stress law, but considerably lower than the 400 g per sq mm value reported by Bakarian.[1] This small difference suggests that pyramidal slip might operate

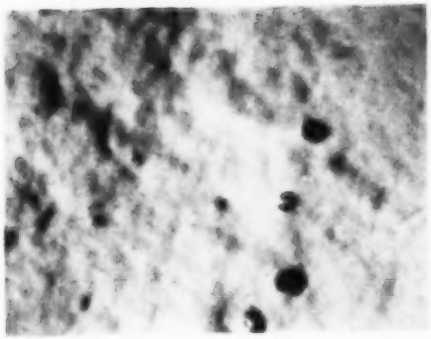

Fig. 11—Pyramidal slip at a position corresponding to the minor axis of the glide ellipse in M21. Axis vertical. X250.

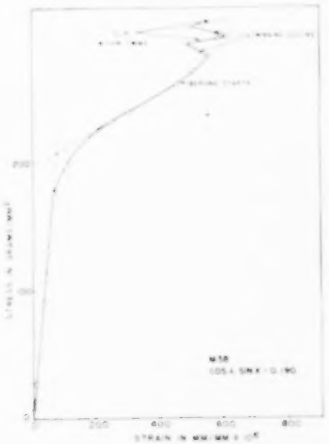

Fig. 12—Stress-strain curve for M38 where $\lambda_1 = 78$, $\lambda_2 = 79$.

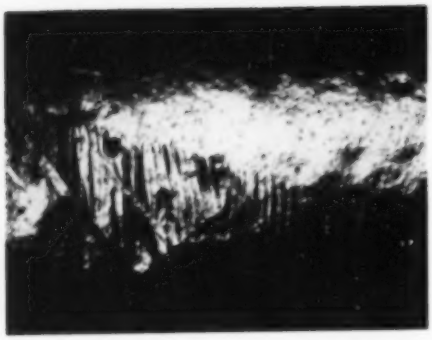

Fig. 13—Bend plane in M38 with twins confined to one side of bend plane. X20

in several instances but were not positive of their identification. On the other hand, {191} slip had been established above 222° C,[7] where the change in slip system is attributed to a preferential directionality of atomic vibration acting in conjunction with the potential energy of spacing. The general conclusion was made that the changing planes of slip indicated that strength rate variations with temperature were a function of the different slip systems. Although Andrade[7] found that body-centered cubic metals change their plane of slip at temperatures determined by the ratio of the test temperature to the melting point, irrespective of the resolved shear stress on the planes, the change in the slip plane in magnesium appears to be dependent upon shear stress considerations in conjunction with the grip constraints on the basal plane.

When the basal plane subtends an angle of 6° with the axis of the specimen as in M21, the gage length necessary for unconstrained movement of this plane would be 3.7 in. However, because the crystals had a standard gage length of 3 in. throughout these tests, the basal plane was longer than the free gage length. Consequently, the ends of the basal plane along its major axis were actually constrained by the grips and prevented from slipping. It should be noted that the angle between the [100] and the major axis of the basal plane is 14°, the calculated length of the [100] is 1.5 in. Thus, the important feature of this specimen is that although

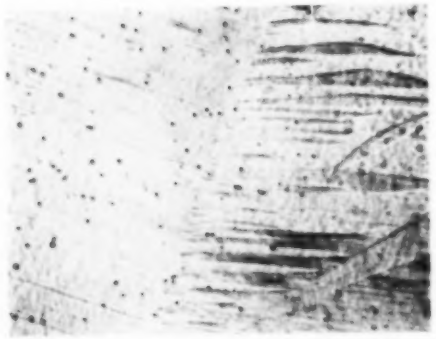

Fig. 14—Same area as Fig. 13 showing twins stopping abruptly at bend plane. Axis vertical. X100

the (001) is held by the grips, the [100] direction is free of grip constraints. On the other hand, {101} plane containing this [100] direction and forming an angle of 10° with the stress axis requires a gage length of only 2.2 in. in order to operate free of the grips. Thus, the {101} and [100] are the next densest atomic plane and direction in magnesium which were free to operate as a slip system at room temperature in this specimen.

These results furnish additional considerations for the plastic flow of polycrystalline metal. If grips may produce a new slip system in the simple extension of a single crystal, internal constraints such as grain boundaries in polycrystalline material may also activate additional slip planes not observed under simple testing conditions. The lattice adjustments from imposed stresses are a factor of fundamental importance to metal plasticity. The technique explained above for gripping specific crystallographic planes may become an important metallurgical research tool for evaluating plastic flow under the influence of experimentally controlled constraints, thus furnishing the necessary information to allow the synthesis of flow of polycrystalline material from the known operative slip systems and single crystal data.

Twinning and Bending. The stress-strain curve, Fig. 12, for specimen M38 exhibits a macroscopically heterogeneous flowing process in contrast to that for simple basal translation. Metallographic examination of the specimen disclosed that numerous twins were present in areas adjacent to and immediately beneath the mounted strain gage. The jagged sawtooth path of the curve is readily explainable on the basis of the dimensional changes accompanying twinning. However, a wire gage might produce similar readings if the mounting cement were separating from the specimen because of the surface rumpling due to twinning. Consequently, while there is little doubt that twinning produced the discontinuities, caution must be exercised in accepting the measured strain values as absolute quantities. It is believed that the stress values in the present test at which twinning occurred must be considered simply as an indication that the basal slip process occurs with greater ease than the mechanical twinning regardless of orientation. When the basal plane is approximately perpendicular to the axis, it has a smaller component of shear stress than the twinning planes which form an angle of approximately 45° with the axis, yet basal slip occurred first. The stress-strain curve for magnesium in Fig. 12 is for a constant loading rate and shows the effect of twinning on the strain values. If the data in Fig. 12 are transposed to show the effect of twinning on the stress values by assuming a rational strain hardening rate, a curve results with the same general characteristics as previously published for cadmium[8] during twinning.

Metallographic examination of M38 disclosed that twinning occurred only at grip intersections or immediately adjacent to the cemented wire gage. Since a complex stress distribution exists in the grip regions as a result of a flexural moment arising from the grips resisting the rotation of the slip plane, it is evident that bending or some other type of lattice accommodation must exist in conformity with the stress requirements.

Evidence of such compensatory adjustment is presented in Fig. 13. It will be noted that twins from

two operative {102} planes end abruptly at a bend plane on the compression side. In this specimen the twins apparently did not transgress this bend plane. At higher magnification, Fig. 14, the twins may be observed more readily with the (001) slip lines being sharply bent at the bend plane with many of the traces continuing undeflected through the twins. From the relative angles which the basal slip lines make with the stress axis, it is apparent that the lattice reorientation within the bend region has lagged behind the lattice rotation due to slip across the boundary. Consequently, the region adjacent to the bend plane must be subjected to complex stresses which are distinctly heterogeneous and may be most conveniently characterized as bending, since one side is in tension while the other side presents evidence of compression. These micrographs suggest that magnesium may deform plastically by flexural glide (Biegegleitung)."

Detailed study of the twinning along this plane disclosed that the twins decreased in size and number as the amount of bending decreased. Furthermore, the twinning decreased as the distance from the bend plane increased, an indication that the magnitude of lattice bending and its resulting stresses must be a factor in mechanical twin formation. Fig. 15 emphasizes the pronounced tendency of the basal plane to bend sharply after initial basal slip. Basal slip occurred first since the same slip lines appear on each side of the bend plane. The twins in this region decrease in number and size as compared to those in Fig. 14.

Based on the details of the strain process for specimen M38 discussed above, the irregular progress of the stress-strain curve in Fig. 12 can now be rationalized into its component parts as follows:

1—Elastic strain followed by basal slip in the conventional manner up to the point marked "Bending starts" in Fig. 12. 2—At this point, there is an increase in the rate of strain hardening indicative of the bending strains which were produced to relieve the constraints of flexural gliding. The rate of strain hardening during bending is twice that for simple basal shear, which is a measure of the higher strain complexity of the former. 3—The bending produces compression stresses of suitable magnitude to cause twinning near the bend plane. These twins cause a structural reorientation which produces a lengthening of the crystal along the stress axis and thus a decrease in the stress followed by a corresponding decrease in strain indicated in Fig. 12 by the portion of the curve labeled "Twinning occurs." 4—Basal slip now can occur within the reoriented twin causing an increase in the tensile strain but a lower strain hardening rate in the area of the curve in Fig. 12 labeled "Slip within twins." 5—When the strain reaches its former level prior to twinning extrapolated to the present stress level, bending again occurs, followed by twinning, slip within the twins, in a cyclic manner, raising and lowering the strain for a constant loading rate.

Crystal M12 with the basal plane at an angle of 72° to the stress axis exhibited a behavior similar to M38, the constraints again forming a bend plane with twins in its immediate vicinity, Fig. 16. In this sample the twins were observed to cross the bend plane slightly, nevertheless, they were preferentially formed in the area of the bend region in which rotation due to slip has lagged behind that on the other side of the bend plane. Within several of the twins, slip on the reoriented basal plane was clearly visible. The twinning in this sample was also confined to two {102} planes. The amount and size of the twins decreased with the extent of bending and strongly substantiated the observations on M38. Similar bending and associated twinning was found in M30. These experimental observations seem to establish that twinning in magnesium is directly related to a bending phenomenon.

From purely geometrical considerations the length-change relationships in the twinning of magnesium favor twinning in tension when the basal plane is perpendicular to the axis. However, depending upon the orientation of the specimen, certain {102} planes could produce extension in the direction of the axis even when the basal plane was parallel to the axis. This work has demonstrated that the geometrical requirements alone are not solely a criterion for twinning, since the orientation in which twinning occurred is restricted to regions in which the basal plane forms an angle of 72° or more with the stress axis.

Identification of Bend Plane The orientation of the bend plane was determined by the same method as described in a previous section for the determination of pyramidal slip with the line of sight for the observation perpendicular to the axis of the crystal. Repeated trials utilizing the procedure established

Fig. 15—Bend plane in M38 with small twins confined to one side and which do not intersect the bend plane. Axis vertical. X100.

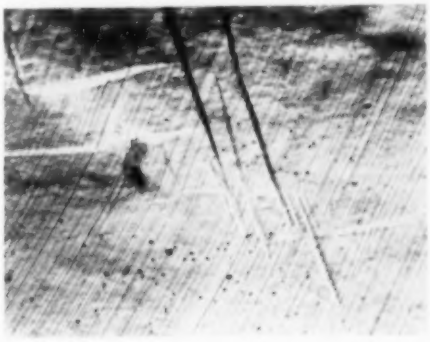

Fig. 16—Bend plane in M12 with small twins crossing the bend plane and basal slip within twins. Axis horizontal. X100.

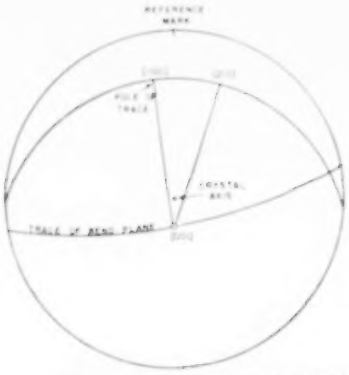

Fig. 17—Determination of orientation of the bend plane as a second order prism, {110}.

that the active slip direction, [100], was the pole of the bend plane, Fig. 17. Consequently, the bend plane is a second-order prism, {110}, which is perpendicular to the basal plane and intersects the basal plane at 90° to the slip direction. Numerous other investigations have described fragmentation due to slip as a rotation about an axis in the slip plane at right angles to the slip direction.[7,8,9]

The bend plane in magnesium crystals terminated in two distinct ways, either ending in very fine twins, or completing the customary elliptical trace. In the stereogram, Fig. 17, the traces of the bend plane and the basal slip ellipses on the specimen surface should have opposite senses, i.e., they would be tangent to one another at their major axes. In Fig. 18 it will be seen that this is precisely the existing condition. In contrast to deformation bands, which have appreciable width, the bend plane is extremely well delineated with no marked evidence of a displacement of basal slip lines in this area. Immediately beyond the termination of the bend the basal slip lines appeared normal in all respects, indicating that no additional mechanism is necessary to compensate for the bending moment.

Jillson[10] performed compression experiments on basal cleaved tablets of zinc and noted that bending occurred frequently about a [210] axis, rarely about a [100]. Since [210] directions are the intersection of second-order prisms, {110}, with the basal plane, it is apparent that the bend plane is the same crystallographic plane in both metals. It was also observed that twinning was invariably accompanied by traces of a plane termed an "accommodation plane."[10] Similar striations have been seen frequently by various investigators.[7,8,9]

Discussion of Relationship Between Twinning and Bending: Previous attempts have been made to establish a criterion for determining the cause of mechanical twinning. Gough[11] states that for zinc, twinning may occur on those pairs of planes which do not include slip direction. Andrade[12] found that the operative planes in hexagonal close-packed structures were those which intersected the slip plane at 60° to the slip direction. Bakarian[7] restated the rule for magnesium as follows: "The operative pair of planes are those for which the intersection with the slip plane makes an angle as near 90° with the projection of the compression axis on the basal plane as is geometrically possible."

It has been demonstrated in the present work that {001} bending is intimately associated with twinning, probably the amount of bending being critical. Mathewson[13] stated that: "Twinning is supposed to occur by progressive slip together with a slight secondary adjustment along neighboring planes of the form {102}. There does not appear to be any plane that would permit twinning without distortion in hexagonal close-packed metals." The slight secondary adjustment may be seen in a {110} projection of the atomic arrangement in which alternate layers of atoms must be periodically raised and lowered to complete a perfectly twinned structure. In other words, the twinning shear in hexagonal close-packed metals requires an additional displacement of atoms at right angles to the apparent direction of twinning. Barrett[1] stated: "In magnesium, there is a slight overall bending, of course, that is caused by the homogeneous twinning shear which is superimposed on the local atomic movements." This additional adjustment or slight bending may be satisfied by the operation of the {110} bend plane discovered in this investigation.

Bending connotes a neutral axis with tension and compression stresses on either side of the axis. Consequently, the amount of atomic displacement occurring during bending would vary not only in amount but also in sign with respect to the neutral axis. Therefore, the atomic displacements accompanying basal flexure about a [210] direction furnish the movements conducive to twinning. The series of micrographs disclosing that twinning ceases at the bend plane demonstrates that bending is a vital and necessary part of twinning.

Observations on hexagonal close-packed metals furnish many examples which would generally conform to this bend-twinning hypothesis. For instance, it has been established by Bakarian that magnesium, regardless of orientation, twins readily when suddenly twisted or bent. Miller[9] found that twinning in zinc occurred with a decreasing stress value (stress resolved on the operative {102} plane in the twinning shear direction) as the amount of prior basal deformation increased. If, in the latter case, the prior slip is considered to produce small bending regions which must necessarily be present due to grip constraints as the basal plane rotates toward

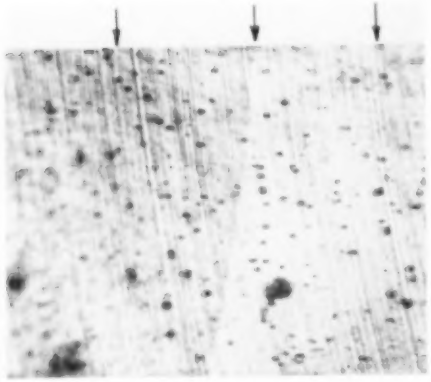

Fig. 18—Bend plane and basal slip lines are tangent at the major axis of each trace. Axis horizontal. X100

the axis and about the pole of the slip plane, then, as the intensity of bending increases, twins would be produced to relieve the stress. Hence, continued slip would introduce additional bending, thus decreasing the externally applied stresses required for twinning. Miller's results suggest that such conditions may exist, since the twinning stress decreases in spite of the prior basal slip and concomitant strain hardening.

The former geometrical requirements hypothesized for twinning[1,2,3] are believed to be a result of the manner of testing or geometry of the specimen rather than a fundamental criterion of twinning. Because the bend plane is that {110} which intersects the basal plane at 90° to the slip direction, the operative twinning planes would simply reflect the position of the bend plane. As the manner of testing and the geometry of the specimen may change the constraint effects during deformation, i.e., kinking in compression, it is concluded that in magnesium twinning results primarily as a complex stress relief mechanism arising from the bending accommodation of the basal plane to external grip constraints without the necessity for a critical resolved stress.

Summary of Results

1—A thermal gradient furnace was constructed and calibrated for the production of single crystals of magnesium. A technique of providing an argon protective atmosphere prevented contamination and assured single crystals with every run.

2—It has been demonstrated that Mg_2Si is an exceedingly strong nucleation agent and must be present in amounts less than 0.01 pct in order to permit the growth of single crystals.

3—A technique for the preparation of tensile specimens was used which eliminated all mechanical cutting, producing a specimen with a reduced gage length having a surface finish equal to a metallographic polish. Etching techniques were developed for producing a localized step in the gage section, which compensated for the support action of the wire gage on the slip process.

4—The mechanism of plastic deformation in tension at room temperature was studied on crystals over a complete range of orientations. The modes of deformation were classified as follows:

a—Basal plane within 6° of the axis: {101} slip operated until the flexural moment of the grips caused twinning on the compression side of the specimen, whereupon slip upon the reoriented basal plane of the twin became operative.

b—Basal plane > 6° but < 72° to the axis: Basal slip was the sole operating deformation mechanism. No evidence of the participation of auxiliary planes was observed.

c—Basal plane > 72° to the axis: Sequence of deformation in this region was that basal slip was operative initially, then rotation of the basal plane and grip constraints caused the formation of a bend plane, whereupon {102} twinning occurred in the localized region of the bend plane with slip on the reoriented basal plane of the twin as well as flexure of the basal plane in the matrix.

5—A critical resolved shear stress value of 46 g per sq mm ± 0.75 for basal slip in magnesium furnished additional evidence in support of the critical resolved shear stress law.

6—Strain hardening rates for basal slip vary with orientation, generally becoming greater as the (001) plane becomes either parallel or perpendicular to the axis and approaches a minimum as the (001) subtends an angle of 45° with the axis.

7—No evidence of recovery was found in magnesium crystals which had been held at 22°C for one week after extensions of 1.7×10^{-3} in.

8—Slip line spacings for basal slip appear to be orientation dependent for small amounts of shear and indicate that there is no single characteristic slip line spacing in magnesium.

9—Pyramidal slip, {101}, was found at room temperature when the basal plane was nearly parallel to the axis, the critical resolved shearing stress for this slip system being 52 g per sq mm. The advent of this new slip system at room temperature was rationalized upon the basis of grip constraints on the basal plane.

10—Pyramidal slip produces essentially the same strain hardening characteristics as the basal slip process.

11—Orientations of the basal plane at an angle greater than 72° to the axis exhibited a marked tendency for the (001) plane to bend sharply about a bend plane determined to be a second-order prism {110}, which intersects the basal plane at 90° to the slip direction.

12—Twinning on the {102} planes was associated with the {110} bend plane suggesting that twinning results primarily as a stress relief mechanism arising from the bending accommodation of the basal plane to external grip constraints, rather than from a critical resolved shearing stress for twinning.

References

[1] C. H. Mathewson and A. J. Phillips: *Trans.* AIME (1928) **53**, p. 445.
[2] E. Schmid and G. Wasserman: Handb. d. Tech. Mech. (1931) **411**, p. 319.
[3] E. Schmid: *Ztsch. Electrochemie* (1931) **37**, p. 447.
[4] P. W. Bakarian and C. H. Mathewson: *Trans.* AIME (1943) **152**, p. 226.
[5] W. Boas and E. Schmid: *Kristallplastizität*. (1935).
[6] C. H. Mathewson: *Trans.* AIME (1928) **72**, p. 7.
[7] C. S. Barrett: Seminar on Cold Working of Metals (1948) A.S.M. Cleveland.
[8] R. F. Miller: *Trans.* AIME (1934) **111**, p. 135.
[9] D. C. Jillson: *Trans.* AIME (1950) **188**, p. 1005, Journal of Metals (August 1950).
[10] A. B. Greninger: *Trans.* AIME (1936) **122**, p. 74.
[11] E. N. daC Andrade and R. Roscoe: *Proc.* Phys. Soc. (1937) **49**, p. 152.
[12] F. Rosi and C. H. Mathewson: *Trans.* AIME (1950) **188**, p. 1159; Journal of Metals (September 1950).
[13] E. N. daC Andrade and P. J. Hutchings: *Proc.* Royal Soc. (1935) **148A**, p. 120.
[14] E. Schmid and G. Siebel: *Metallwirtsch.* (1934) **13**, p. 453.
[15] E. Schiebold and G. Siebel: *Ztsch. Physik* (1931) **69**, p. 458.
[16] E. N. daC Andrade and Y. S. Chow: *Proc.* Royal Soc. (1937) **163A**, p. 19.
[17] W. Boas and E. Schmid: *Ztsch. Physik* (1929) **54**, p. 16.
[18] H. Mark, M. Polanyi, and E. Schmid: *Ztsch. Physik* (1922) **12**, p. 58.
[19] G. I. Taylor: *Trans.* Faraday Soc. (1928) **24**, p. 121.
[20] C. H. Mathewson: *Trans.* A.S.M. (1944) **32**, p. 38.
[21] N. K. Chen: D. Eng. Thesis, Yale University (1950).
[22] D. C. Jillson: *Trans.* AIME (1950) **188**, p. 1129; Journal of Metals (September 1950).
[23] O. E. Romig: *Trans.* AIME Proc. I.M.D. (1927) p. 90.
[24] M. J. Buerger: *Ztsch. Kristallog.* (1934) **89**, p. 195.
[25] H. J. Gough: *Proc.* A.S.T.M. (1933) **33**, Part II, p. 3.
[26] R. F. Miller: *Trans.* AIME (1936) **122**, p. 176.

Zirconium-Chromium Phase Diagram

by E. T. Hayes, A. H. Roberson, and M. H. Davies

ZIRCONIUM has been produced on a pilot-plant scale for only a few years, but the potential uses have led a large number of research establishments to engage in a thorough study of the metal and its alloys. The work described in this paper is part of a cooperative project between the Bureau of Mines and the Air Materiel Command. The Zr-Cr system was one of the first investigated because of the possibilities of improving the properties at elevated temperatures, the chemical corrosion resistance, and the mechanical properties of zirconium in a manner similar to the enhancement of the properties of titanium by additions of chromium. There is no published work on the Zr-Cr system but from the similarity of the metals involved it was expected that it would be similar to the Zr-Fe[1] and Ti-Cr[2] systems.

The materials used in this investigation were prepared in the Bureau of Mines laboratory at Albany, Ore. Zirconium was produced by magnesium reduction of zirconium tetrachloride, and a typical analysis is as follows: Fe, 0.06 pct; O, 0.08; N, 0.01; C, 0.02; and other impurities such as Al, Pb, Ni, Ti, and Si less than 0.01 pct each.

High purity chromium was prepared by treating crushed electrolytic chromium in a stream of dried and purified hydrogen.[3] The resulting powder contained about 0.01 pct O and about 0.1 pct total metallic impurities.

All alloys were prepared by arc-melting 50 g briquetted compacts of the desired composition in a Kroll-type[4] arc furnace using an inert atmosphere. The furnace was evacuated twice and backfilled with helium, which was gettered by melting a center zirconium button immediately before the alloys were melted. Alloys were remelted at least once to insure greater uniformity of composition and subsequently were annealed in vacuum at 1250°C for 48 hr. Fairly homogeneous alloys were obtained by this means, a slight loss of chromium from the surface by evaporation during the high temperature homogenization was noted. All alloys were analyzed for chromium and gave results in good agreement with the nominal composition. Spot checks on tungsten and nitrogen showed pick-up of these elements to be negligible. Over 70 alloys were prepared for use in this investigation; only the critical ones are shown in Table I.

Alloys containing up to 10 pct Cr were amenable to hot working at 850°C and a number of these were sheath rolled to 1/16 in. thickness. Specimens were cut from the sheet for use as metallographic samples.

For the thermal analysis a differential couple was used in conjunction with an X-Y recorder, the temperature of the specimen and the difference in temperature between it and the standard nickel body were recorded simultaneously. Heating and cooling rates of 5°C per min were used. The sensitivity of the instrument was such that a difference in temperature between the specimen and standard equivalent to 0.1 mv produced a deflection of 1 in. on the recording chart. The chromel-alumel thermocouples were checked against a Bureau of Standards calibrated thermocouple.

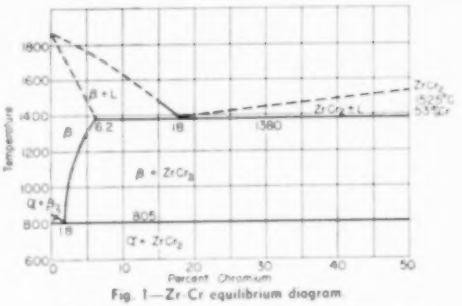

Fig. 1—Zr-Cr equilibrium diagram.

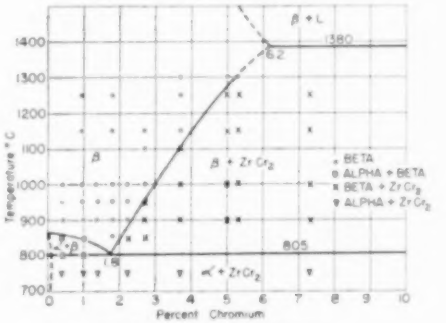

Fig. 2—α field of Zr-Cr diagram.

Melting-point determinations were made in a high vacuum induction furnace using an optical pyrometer. The pyrometer, calibrated against nickel, copper, and zirconium (iodide process) under near black body conditions, was focused on the base of a hole drilled in cylindrical samples.

A North American Philips Geiger counter X-ray spectrometer was used for all diffraction studies. This instrument, in addition to supplying precise intensity measurements of planar reflections, has an added advantage in that metallographic specimens mounted in bakelite can be used directly, and this

Table I. Analyses of Zr-Cr Alloys

Alloy No.	Cr, Wt Pct	Alloy No.	Cr, Wt Pct	Alloy No.	Cr, Wt Pct
WA 1452	0.18	WA 2962	4.6	WA 2857	24.6
1453	0.28	2959	5.0	3047	25.1
1454	0.43	3090	5.3	2958	30.2
3037	0.94	3038	5.9	2942	35.4
2078	1.35	3091	7.3	3056	39.8
3088	1.8	3092	9.2	3057	45.3
3034	1.9	3037	9.8	3065	48.8
2077	2.2	2855	15.0	3066	53.2
3035	2.7	2963	18.0	3067	55.1
3089	3.7	2961	19.8	3081	59.6

E. T. HAYES and A. H. ROBERSON are Physical Metallurgists, and M. H. DAVIES is British E.C.A. Fellow, U. S. Bureau of Mines, Albany, Ore.

Discussion on this paper, TP 3252E, may be sent, 2 copies, to AIME by May 1, 1952. Manuscript, Sept. 17, 1951, revised, Jan. 7, 1952. New York Meeting, February 1952.

Papers by authors of the U. S. Bureau of Mines staff are not subject to copyright.

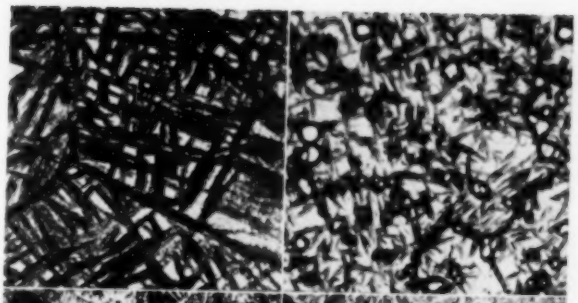

Fig. 3—100 pct acicular α (transformed β). 0.94 pct Cr alloy quenched from 1150°C. X250. Etchant, Villella's reagent.

Fig. 4—Acicular α (transformed β) plus $ZrCr_2$. 5.0 pct Cr alloy quenched from 1125°C. X500. Etchant, Villella's reagent.

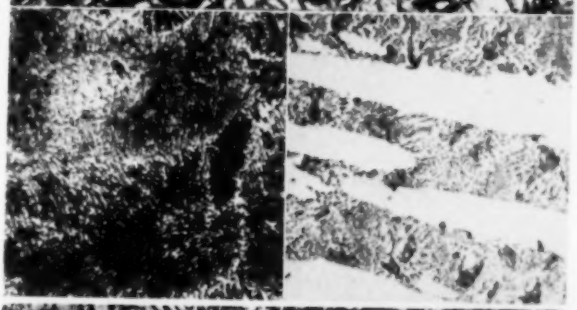

Fig. 5—100 pct eutectoid. 1.8 pct Cr alloy slow-cooled from 1200°C. X500. Etchant, Villella's reagent.

Fig. 6—α plus eutectoid. 0.94 pct Cr alloy slow-cooled from 1200°C. X500. Etchant, Villella's reagent.

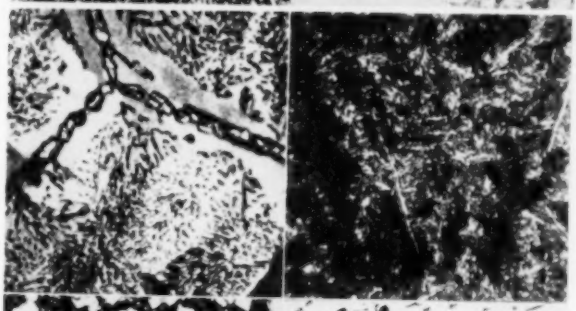

Fig. 7—Eutectoid plus compound. 2.7 pct Cr alloy slow-cooled from 1200°C. X500. Etchant, Villella's reagent.

Fig. 8—100 pct eutectic. 1.8 pct Cr alloy as-cast. X500. Etchant, Villella's reagent.

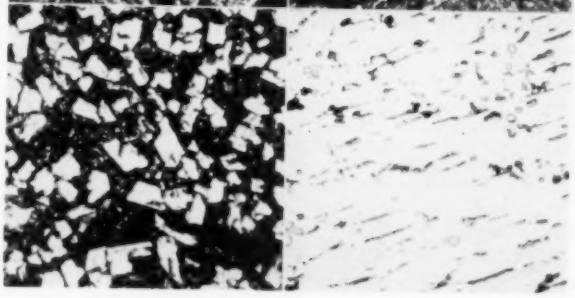

Fig. 9—Eutectic plus $ZrCr_2$ as-cast. X500. Etchant, Villella's reagent.

Fig. 10—100 pct $ZrCr_2$. 53 pct Cr alloy as-cast. X500. Etchant, Villella's reagent.

technique was used for the low chromium alloys. The higher chromium alloys were brittle and thus easily crushed to a fineness of −200 mesh. Use of the powdered material gives more reliable values for the relative intensities of lines in the diffraction spectrum and this became important in determining the complete structure of the intermediate-phase $ZrCr_2$.

Heat treatment of all alloys was carried out in vacuum furnaces capable of heating the specimens to 1200° or 1450°C. Furnaces were constructed in such a manner that specimens could be quenched directly into cold vacuum oil without breaking the vacuum seal.

Constitution Diagram

The diagram as determined in this investigation is presented in Fig. 1. The solubility of chromium in α zirconium was not determined precisely and was assumed to be negligibly small. The endeavor to determine the solubility at various temperatures by metallographic techniques was made increasingly difficult by the small amount of Zr-Fe eutectoid always present which tended to obscure any effects of small chromium additions. Examination of the

Table II. Thermal Arrests of Zr Cr Alloys

Cr, Pct	Thermal Arrest, °C	
	Heating	Cooling
0.94	818	808
1.35	818	803
2.2	807	801
5.0	814	803
9.2	821	809

diffraction patterns of alloys containing 0.16, 0.28, and 0.43 pct Cr quenched from 800°C showed no shift in the pattern at the highest angles observed (140° to 150°) and thus indicated only a very small solubility of chromium in α zirconium.

Delineation of the β field depended entirely on metallographic examination, since the β could not be retained by quenching; thus X-ray methods to determine the limit of solubility of chromium in β zirconium were inapplicable. To determine the solubility of chromium in β zirconium, a series of alloys of varying chromium contents was quenched and slow cooled from several temperature levels above the eutectoid temperature. All alloys, after hot working, were homogenized 168 hr at 1000°C under helium. Specimens were then reheated 2 to 16 hr and quenched or slow cooled. The minimum quenching temperature which gave structures consisting of 100 pct transformed β served to place the phase boundary. A detail of the β field is shown in Fig. 2. The maximum solubility of chromium in β zirconium was determined to be about 6.2 pct at the eutectic temperature. Fig. 3 illustrates the typical structure of the β field, while Fig. 4 shows the structure of an alloy quenched from just outside that field.

The β phase decomposes eutectoidally, and the slowly cooled 1.8 pct Cr alloy, Fig. 5, consists entirely of α plus $ZrCr_2$ eutectoid. A typical microstructure of furnace-cooled hypoeutectoid alloys is shown in Fig. 6, the structure consisting of primary α grains in a matrix of eutectoid. Fig. 7 shows a slowly cooled 2.7 pct Cr hypereutectoid alloy, the structure consisting of $ZrCr_2$ plus eutectoid.

Thermal analysis results for unalloyed zirconium and for very low chromium alloys indicated a transformation range of as much as 100°C, and this probably is attributable to the small amount of impurities, more particularly the oxygen, in Kroll zirconium.[5] Hence the upper limit of the α + β field has been placed by extrapolation from the eutectoid point to the accepted value for the α to β transformation in the pure metal. Thermal analysis was used to establish the eutectoid temperature and representative values are shown in Table II. On the basis of the cooling curves the eutectoid temperature was placed at 805° ± 5°C.

Examination of the as-cast structures served to place the eutectic composition at about 18 pct Cr. Fig. 8 shows the microstructure of the 18.0 pct alloy.

Use of the optical pyrometer to determine arrests in induction heated samples gave an average value of 1380°C for the eutectic temperature, based on seven specimens containing 15 to 45 pct Cr. Liquidus temperatures of 1425° and 1466°C were found on the 25.1 and 35.4 pct Cr alloys.

Specimens containing more than 1.8 pct Cr, when annealed at 1250°C, showed increasing amounts of a second phase with increasing chromium content.

The amount of this bright etching second phase (identified as the compound $ZrCr_2$) increased in alloys of increasing chromium content up to 53 pct Cr, where it occupied the entire field. Fig. 9 shows the microstructure of the 30 pct as-cast alloy. The field is composed of about 30 pct $ZrCr_2$ in a matrix of eutectic. In Fig. 10 the entire field is occupied by a bright etching compound marked by fine cracks, which were probably produced by cooling stresses or during the mechanical polishing.

Hardness measurements showed increases corresponding to the amount of $ZrCr_2$ present. The hardness of the compound approximated 900 VHN. A little difficulty was encountered in measurement due to the extreme friability of the compound with its resultant distortion of the indentation.

The melting point of the single-phase 53 pct alloy was found to be about 1525°C.

Analysis of the X-ray diffraction patterns of the compound indicated a face-centered cubic lattice. The compound occurs at a composition satisfied by the formula $ZrCr_2$ and is therefore probably structurally analogous to the compound $TiCr_2$ reported by Duwez, which has a face-centered cubic lattice of the Cu_2Mg type.

Structure factor calculations based on the Cu_2Mg structure and applied to $ZrCr_2$ showed close agreement between calculated and observed values of the relative intensities of the lines in the diffraction pattern of the compound. The lattice parameter was determined to be 7.21A.

Summary

An investigation of the equilibrium system of binary alloys of zirconium and chromium in the composition range 0 to 50 pct Cr was undertaken, but this range was slightly extended to include the intermetallic compound $ZrCr_2$ found to exist at 53 wt pct Cr. The main features of the diagram to be noted are:

1—Negligible solubility of chromium in α zirconium.

2—The eutectoid decomposition of β zirconium at 805°C and 1.8 pct Cr.

3—The maximum solubility of chromium in β zirconium at the eutectic temperature of about 6.2 pct Cr.

4—The eutectic reaction occurring at 1380°C and 18 pct Cr.

5—The existence of an intermetallic compound $ZrCr_2$ (53 wt pct Cr), melting at 1525°C. The compound has a face-centered cubic Cu_2Mg type structure, a_o = 7.21A.

Acknowledgments

The authors wish to express their appreciation to the Air Materiel Command, Wright-Patterson Air Force Base, who sponsored the work described in this paper, and who granted permission for its publication. Acknowledgment is made to the following coworkers who made substantial contributions to this study: W. L. O'Brien and R. S. Kemper, metallography; O. G. Paasche, X-ray; R. L. Carpenter, thermal analysis; J. R. Havill, melting point determinations; and V. V. Donaldson, alloy preparation.

References

[1] E. T. Hayes, A. H. Roberson, and W. L. O'Brien: *Trans.* A.S.M. (1951) **43**, p. 888.

[2] P. Duwez: A.S.M. preprint No. 3 (1951).

[3] W. J. Kroll, W. F. Hergert, and L. A. Yerkes: *Journal* Electrochem. Soc. (1950) **97**, (8), p. 258.

[4] A. D. McQuillan: *Journal* Inst. Metals (London) (1950-1951) **78**, p. 249.

[5] W. Kroll: *Trans.* Electrochem. Soc. (1941) **78**, pp. 35-47.

On the Mechanism of Precipitation In Copper-Beryllium Alloys

by A. H. Geisler, J. H. Mallery, and F. E. Steigert

The existing data on precipitation in Cu-Be alloys have been reconciled with some new data to present a more complete and rational analysis of the atomic rearrangements involved in the process. Two different coherent precipitates were proposed. Each is responsible for a type of diffuse X-ray diffraction effect.

THE nature of the atomic rearrangement involved in the precipitation of the compound γ-Cu-Be from supersaturated solid solutions of the copper-base alloys has been the subject of two extensive investigations.[1,2] The precipitate in this alloy system has a rather simple structure; at equilibrium it has a body-centered cubic unit cell with copper atoms on the corner sites and beryllium atoms on the center site. While a simple mechanism would be expected to obtain for the precipitation process, those which have been proposed do not adequately explain all of the reported data. The purpose of the present report is to rationalize some of the previous observations and to contribute new data on the subject obtained by the usual techniques of structure analyses. The Cu-Be system of alloys represents one of the most extensively investigated precipitation systems, so a detailed review of the pertinent literature on structure is in order.

Striations: Since one of the important features of the mechanism—the habit plane—is determined by microscopic examination, microstructural features that have been observed should be considered at this time in order to assess their role in the precipitation process in Cu-Be alloys. One of the most prominent features appears as regularly oriented markings or stripings (ripples or striations) across the crystals on a suitably polished and etched sample of the aged alloy. These have been observed and interpreted by many workers. Masing and Dahl[3] observed striations in both the α and β phases of a 2.5 pct Be alloy, and attributed them to the beginning of the precipitation of very fine γ crystals along favored planes of the α matrix and to the local decomposition of the β crystals into α plus γ. These markings were apparent in both the α and β phases of the micrographs given by Smith[4] for a 2.75 pct Be alloy, while Moore[5] detected them in the α matrix phase using polarized light. Desch[1] attributed the markings to fine precipitate particles lined up on a family of matrix planes like Masing and Dahl had done, and he identified the planes as those of the {111} family, the slip planes of the matrix. The striations were presumably the structure which Northcott[6] referred to as "martensitic." He found that this structure was present in samples that had been aged under widely different conditions with hardness values ranging from 160 to 400 VHN. Later Guinier and Jacquet[7] also found striations in both the α matrix and secondary β phase. Their analyses showed that the striations were along {110} planes of the matrix phase, apparently in contradiction of the results of Desch. They found that the striations were developed during aging on the surface of a specimen that had been polished prior to aging.[8] On this basis they concluded that the striations represented mechanical deformation by slip along {110} planes of the matrix resulting from precipitation stresses.[7,8] Similar but fainter striations were observed in the same manner on an Al-Cu alloy sample, in which the change in volume was much less than for Cu-Be alloys and

A. H. GEISLER, Member AIME, and J. H. MALLERY are associated with General Electric Research Laboratory, The Knolls, Schenectady, and F. E. STEIGERT is at the University of Indiana, Bloomington.

Discussion on this paper, TP 3259E, may be sent, 2 copies, to AIME by May 1, 1952. Manuscript, Sept. 17, 1951. New York Meeting, February 1952.

Fig. 1—Stereographic projection of {100} poles of cubic precipitate in cubic matrix with the orientation relationship $(001)_\gamma$ // $(001)_M$ and $[100]_\gamma$ // $[1\bar{1}0]_M$.

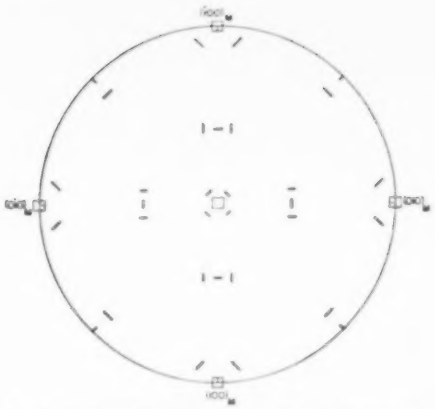

Fig. 2—Stereographic projection showing locations of {100} poles observed by Guy, Barrett, and Mehl[12] for Cu-Be precipitate in a 1.8 pct Be alloy crystal that had been aged 142 hr at 500°C.

thus less deformation would be expected. Evidence for crystal distortion and fragmentation as a consequence of precipitation and of a type similar to that for cold working has been reported by Barrett.[9] Gayler[7] concluded that in Cu-Be alloys the striations were due to the development of strains in the lattice accompanying the formation of the new phase similar to the interpretation of Guinier and Jacquet; however, in the Al-Cu alloys the striations were due to accelerated precipitation in strained areas of the matrix crystals as suggested by Masing and Desch for Cu-Be alloys. Harker and Murphy[10] have pointed out the similarity of the striations found for Cu-Be alloys with those for ordering Cu-Au alloys, and concluded that they were evidence for "order-hardening." Miyatani[11] has more recently confirmed the results of Guinier and Jacquet that the striations were traces of {110} planes, and he concludes that: "the precipitate forms on layers parallel to the {110} planes of the matrix." All of the observations can be reconciled if it is assumed that two types of striations may appear in Cu-Be alloys: 1—those due to the accelerated precipitation of fine particles along [111] slip bands that had been formed in the matrix by quenching stresses, etc., prior to aging, and 2—those due to mechanical straining of the matrix by slip on {110} planes as the result of precipitation stresses. These two types have been distinguished for ordering Co-Pt alloys.[13] They appear on a relatively gross scale when precipitate particles are submicroscopic. Thus, the conclusion of Miyatani is misleading; the habit plane of the precipitate is characteristic of a third type of geometric configuration—the Widmanstätten figure—which requires separate consideration.

Recrystallization Reaction: The second prominent feature that has been observed in the microstructure of Cu-Be alloys appeared as lamellar nodules of matrix plus equilibrium precipitate located at grain boundaries of the parent grains. These formed and grew as aging progressed.[1,12] The reaction has all the characteristics of a recrystallization process and thus has been referred to as such in a recent report where the data are reviewed in detail.[9] It will suffice to state here that this is a supplementary reaction and that studies of the mechanism of precipitation should be concerned only with the formation of precipitate particles that are uniformly distributed within the parent crystals. While the phenomena of striations and recrystallization play a part in the precipitation process, they are not considered to be features directly inherent in the crystallographic mechanism of the formation of the phase.

Widmanstätten Relations: Although the crystallographic orientation relationship is known, the habit plane of the γ precipitate has not yet been determined. Guy[12] has presented a micrograph that exhibited plate-like particles of the precipitate, but all the traces were not sufficiently well developed to permit a determination of the habit plane. In regard to crystallographic orientation relationship, Guinier and Jacquet[7] considered that the [001] axis of the

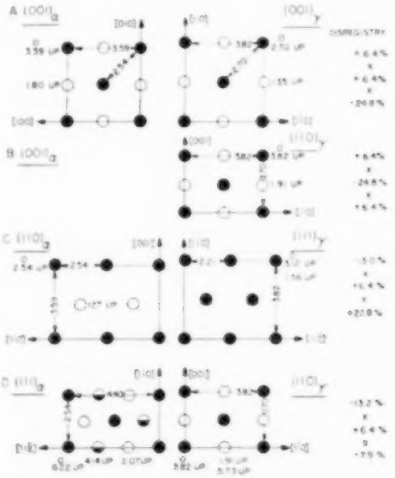

Fig. 3—Atom positions on various low index planes for the matrix (left) and equilibrium precipitate γ (center) and the disregistry from matching (right).

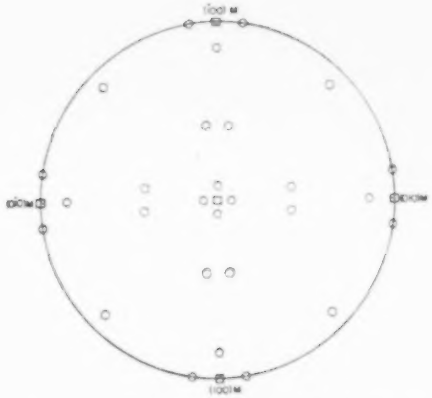

Fig. 4—Stereographic projection of {100} poles of cubic precipitate in cubic matrix with the orientation relationship $(111)_\gamma // (110)_\alpha$ and $[\bar{1}10]_\gamma // [001]_\alpha$.

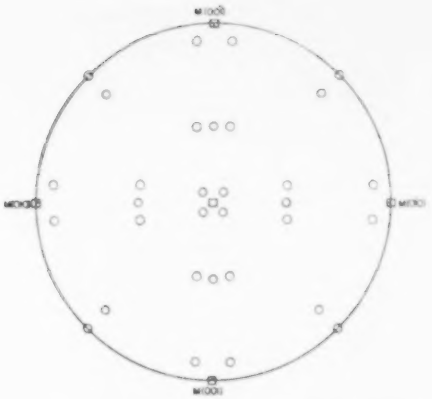

Fig. 5—Stereographic projection of {100} poles of cubic precipitate in cubic matrix with the orientation relationship $(\bar{1}10)_\gamma // (111)_\alpha$ and $[001]_\gamma // [\bar{1}10]_\alpha$.

body-centered cubic precipitate, γ, coincided with the [001] axis of the face-centered cubic matrix, α, and [100], with [110], as in Fig. 1, but they stated that this orientation is only approximate. Guy and coworkers[7,17] precisely determined the orientation as shown by Fig. 2. The relationship was considered to be irrational with a tilt of 8° of $[001]_\gamma$ from $[001]_\alpha$ and a spread of ±2° of $[100]_\gamma$ from $[110]_\alpha$.

Diffuse Diffraction Effects: Guinier[1,2] and Guy[7] and their coworkers have analyzed the diffuse streaks which appear in X-ray patterns for aged single crystals. The results of both investigations agreed in that an indeterminate periodicity existed in the lattice structure normal to {100} matrix planes. Guinier attributed this to a segregation of beryllium atoms to form new, small platelets dispersed parallel to cube planes in the solid solution with the same atomic spacings in the plane, but having a composition different from the mean which results in a contraction of the spacing of the (100) plane. Both groups of workers proposed a mechanism for the formation of γ which involved a contraction of α normal to the (100) plane; however, such a mechanism assumed that the habit plane was (100) and did not take into consideration the apparently "irrational" nature of the orientation relationship. In addition to two-dimensional diffraction effects, Elistratov et al.[18] have observed one-dimensional diffraction effects for a Cu-2 pct Be alloy similar to those which were first reported for Al-Ag and Al-Mg-Si alloys.[19] Their technique involved coarse-grained polycrystalline samples with diffraction from crystals of unknown orientations, so that at first they were not able to identify the crystallographic directions associated with either the one-dimensional or two-dimensional aggregate. Later[20] they used the single-crystal technique described by Geisler and Hill[19] and found that the one-dimensional diffraction was along <100> directions and the two-dimensional diffraction on {100} planes. The latter agreed with results of Guinier and Guy.

Lattice Distortion and Transition Structure: A prominent feature that has been observed in X-ray patterns of Cu-Be alloys has been the extreme broadening and diffuseness of matrix lines which develop during precipitation.[1,2,4] On aging at 300°C the lines at high angles in the back-reflection portion of the pattern become so broad and diffuse that they were not detected.[4] The broadening on aging at 350°C could be due to change in concentration of the matrix alone, but that observed on aging at 150° to 250°C was considered in part to be due to stresses accompanying the formation of the γ particles.[4] In regard to strains in the precipitate which might be indicative of a coherent precipitate, Dahl and coworkers[6] found that at the lower aging temperatures the γ crystals precipitated in a form which gave indistinct X-ray lines. They stated that it is possible that γ precipitated out in a strained condition, which could cause a widening of the lines, although probably the indistinctness of the lines was largely due to the fine particle size of the precipitate. While Guinier and Jacquet concluded that no transition structure was formed during the aging of Cu-Be alloys, it is apparent that the previously described platelets which caused the diffuse diffraction effects qualify as a coherent transition structure sometimes referred to as an epitaxy of the γ precipitate. Guy, Barrett, and Mehl[7] were unable to detect a transition lattice and concluded on the basis of powder patterns that no structure other than the equilibrium precipitate grows large enough to afford three-dimensional diffraction.

On the basis of the previous work on the mechanism of precipitation in Cu-Be alloys there are at least three features which need further study: 1—rationalization of the orientation relationship, 2—determination of the habit plane for γ, and 3—further searching for the coherent transition structure.

Experimental Technique

The X-ray diffraction studies were conducted on two single-crystal samples that had been prepared by Guy.[5] Their composition was 1.73 pct Be, and they had been thinned to 0.005 in., heat treated in vacuum for 1½ hr at 800°C, and quenched directly to the aging temperature. Since 100 hr aging at 300°C was required to develop diffraction spots from three-dimensional precipitate in Laue patterns,[4] aging times of 1, 3, and 18 hr were chosen in order

Fig. 6—Microstructure of 2 pct Be alloy that had been slowly cooled from 850° C. Potassium dichromate etch. X250

to assure that they represented early stages of precipitation. According to the electrical resistance measurements for the single crystal aged at 300° C (Fig. 12 of ref. 3), these time periods corresponded to approximately 10, 25, and 50 pct respectively of the total decrease that was due to precipitation.

The samples which were used for microscopic examination were of commercial Be-Cu strip of 0.060 in. thickness with a nominal 2 pct Be composition.

Orientation Relationship

In order to explain the orientation relationship that had been determined by Guy[3] in Fig. 2, the atomic arrangement on various low index planes of the matrix (α) and equilibrium precipitate (γ) were compared. Four possible combinations are shown in Fig. 3. The interatomic distances are given in Angstrom units, while the column at the right lists the required changes of the matrix spacing or strain in percent in the three orthogonal directions. Relationship *A* or its equivalent *B* is that proposed by previous workers as an approximation. Relation C involves only slightly more total strain; however, the locations of cube poles for this relationship, shown in Fig. 4, are distinctly different from those observed, Fig. 2. On the other hand, relationship *D*, Fig. 3, requires somewhat less total strain for, while a contraction of 13.2 pct replaces an expansion of 6.4 pct in the conjugate plane, a contraction of only 7.9 pct replaces the 24.8 pct contraction normal to the conjugate plane for relationship *A*. Although a choice between *A* and *D* would be difficult to make on the basis of disregistry alone, the distribution of {100}$_\gamma$ poles predicted by *D* and shown in Fig. 5 is rather promising. Comparison with the observed, Fig. 2, shows excellent agreement. For the rational relationship of Fig. 5 some {100}$_\gamma$ poles occur at an angle of 9°44′ from the {100}$_\alpha$ poles of the matrix crystal. The difference between this and the observed angle of about 8° is probably within the experimental error. The observed spread of ±2° could be due to strain, resulting either from mechanically or thermally applied stress or from the spontaneous stresses of precipitation described earlier.

Fig. 7—Stereographic projection of {111} poles causing precipitate traces in three grains shown in Fig. 6 and sketched in lower right quadrant.

Habit Plane of the Equilibrium Precipitate

In order to determine the habit plane of the precipitate, attempts were made to grow a well-developed Widmanstätten pattern by a variety of treatments. Microscopically resolvable precipitates were present after aging for 100 hr at 600° and after slowly cooling (50° C per hr) from above the solvus temperature. The latter treatment provided the best structure for analysis. Fairly well-developed plates of precipitate appeared as shown by Fig. 6. While some of these were along twin boundaries and might represent localized precipitation as at grain boundaries, others appeared throughout the grains and twins. The three largest crystals in the bottom half of the micrograph were separated by straight boundaries which proved to be twin boundaries. These grains are labelled *A*, *B*, and *C* in the sketch at the lower right of Fig. 7. Twin boundaries and the directions of the three or four traces for particles remote from twin boundaries are also shown in the sketch. Some of the traces for the plate-like precipitate particles were parallel to twin boundaries in each part of the twin, suggesting at once that the habit plane was the same as the twin plane, i.e., {111}. This proved to be the case when an analysis by stereographic projection was made of the precipitate and twin boundary traces, Fig. 7. Starting with crystal *A* stereographic planes, which must contain the poles of the crystal planes that cause the traces, were plotted normal to the traces. Next an orientation was found in which a {111} pole fell on each of the four stereographic planes. Finally, the orientation of the correct twins of *A* was found to put {111} poles on the data for crystals *B* and *C*. In this way ten traces were correlated with {111} planes. Only two traces were absent. It may be concluded that the habit plane of plate-like particles of the equilibrium precipitate is the {111} family.

With the two new facts concerning the equilibrium precipitate in Cu-Be alloys its mechanism of formation can be postulated. It would be expected that the precipitate structure would evolve by movement of atoms in the (111) plane of the matrix in such a manner as to assume the (110) stacking of the precipitate, since (111)$_\alpha$ is the habit plane and (111)$_\gamma$ is parallel to (110)$_\alpha$. Such a mechanism is

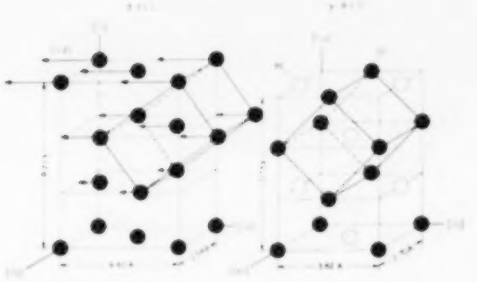

Fig. 8—A mechanism of forming the equilibrium precipitate γ (right) from the matrix (left) employing the $(111)_\gamma // (110)_\alpha$ relationship and $(111)_\gamma$ habit plane.

illustrated by Fig. 8. To form γ the atoms in α would move in the $[11\bar{2}]$ direction an amount which varies from 0 to 2.20A for every 6th layer. A contraction of 13.2 pct in the atomic spacing in the $[11\bar{2}]_\gamma$ direction, an expansion of 6.4 pct in the $[\bar{1}10]_\gamma$ direction and a contraction of 7.9 pct in the $[111]_\gamma$ direction are also required to form the γ cell. An orthorhombic transition structure coherent on $(111)_\gamma$ would be predicted from this mechanism rather than the tetragonal one mentioned by Guy.

Intermediate Structure—γ'

When oscillating crystal patterns were made for the single-crystal sample that had been aged 18 hr at 300°C, several three-dimensional diffraction spots were observed which could not be attributed to the equilibrium precipitate, γ. As shown in Fig. 9, one reflection with its β component was moderately intense. This reflection appeared in the approximate location for what would be a (110) matrix reflection ($d = 2.54$), if this were not a forbidden reflection of the face-centered cubic lattice. Among the numerous patterns that were made with 15° oscillation, [001] or [110] axis of oscillation and copper or cobalt radiation, the interplanar spacings corresponding to five definite non-matrix reflections were as follows: ~2.78A, 2.54A, 1.97A, 1.86A, and 1.56A. These were used to identify the intermediate structure which was designated γ'.

Although five different types of reflections hardly seem enough to determine a new crystal structure, the interplanar spacings in combination with the positions of the spots on the film as determined by orientation relationship were sufficient to dismiss some of the postulated intermediate structures. For example, the reflections could not be explained by a transition structure coherent on the (100), plane and formed by a simple contraction along the [001] direction as proposed by Guinier and Guy. Likewise a simple readjustment of the $(111)_\gamma$ spacing to form a rhombohedral cell coherent on the (111) matrix plane would satisfy only three of the observed reflections, although various combinations of parameters were investigated. Next, possible cells that could result from shifting of the (111) matrix layers were tried. These included the previously mentioned orthorhombic cell; however, no choice of the intermediate c parameter corresponding to (111) matrix layer spacing would satisfy more than half of the observed reflections.

The most fruitful attempt to determine the intermediate structure γ' was made by assuming that a prior structure was formed coherent on the (100) plane as suggested by the analyses of diffuse diffraction effects by Guinier and Guy. A prior structure, later designated γ'' (see Fig. 17), would have a monoclinic cell with $(100)_{\gamma''}$ coherent on (001) of the matrix and would be sheared over to the extent where $(\bar{1}10)_{\gamma''}$ is parallel to $(\bar{1}\bar{1}1)$ matrix. These conditions specify discrete lattice parameters. The intermediate structure could then form by loss of coherency on (001), and further shear to produce a tetragonal cell without changing the orientation of the $(\bar{1}10)_{\gamma'}$ plane or the atomic spacing along $[\bar{1}10]$ of the matrix. The latter condition was imposed because the one interplanar spacing for γ' was the same as that for the (110) planes of the matrix. The described conditions demand that the γ' structure be face-centered tetragonal with $a = 3.95$A and $c = 2.54$A. The cell could also be described as body-centered tetragonal with $a = 2.79$A and $c = 2.54$A for convenience in relating it to the equilibrium precipitate γ. The observed data are satisfied by the proposed structure for γ' as shown by a comparison in Table I where the columns labeled Y refer to the vertical coordinate of the reflection on the films. All the observed reflections agree with calculated Y coordinates and d values, although a number of expected reflections were not observed. Intensity values were rated relative to each other rather than relative to matrix reflections which would all be strong on the scale used. Actually some of the γ' reflections were very weak which probably explains the failure to observe others of them.

The intermediate structure γ' is not coherent to the (111) matrix plane; however, examination showed that it could be considered coherent on the (112) type matrix plane. In Fig. 10, the α-matrix structure is drawn at the left with the $(\bar{1}12)$ plane as base while at the right the γ' structure is drawn with (120) as base. The atomic spacing on the base planes

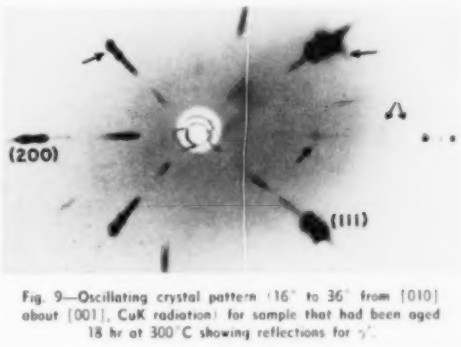

Fig. 9—Oscillating crystal pattern (16° to 36° from [010] about [001], CuK radiation) for sample that had been aged 18 hr at 300°C showing reflections for γ'.

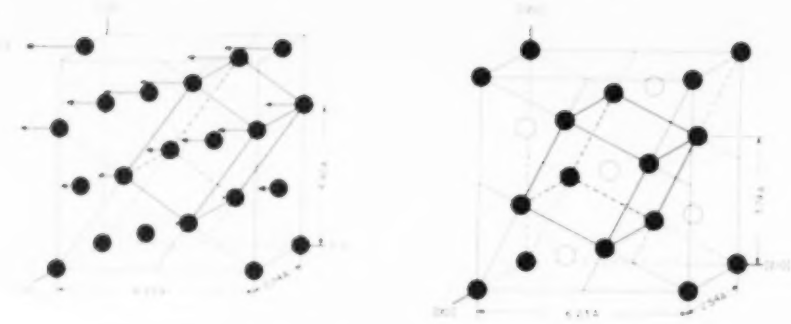

Fig. 10—A mechanism of forming the coherent precipitate γ' (right) from the matrix (left).

is the same within experimental error thus satisfying the requirement for coherency. A proposed mechanism for the formation of γ' from α is illustrated by the diagram at the left in Fig. 10. Atoms on the (112)$_\alpha$ plane shift in a [111] direction to take up sites at the heads of the arrows and at the same time the (112) plane spacing contracts 15 pct. The resulting orientation of $(112)_\alpha$ parallel to $(120)_{\gamma'}$ differs by only 1.2° from $(111)_\alpha$ parallel to $(110)_{\gamma'}$. Such a small difference would not be detected in the usual analyses of orientation relationships; however, this mechanism would predict a (112)$_\alpha$ habit plane with a maximum number of traces in the Widmanstätten pattern and a geometry of diffuse diffraction effects different from the (111)$_\alpha$ habit plane.

Early Diffuse Diffraction Effects

Analyses of the diffuse scattering from aged Cu-Be crystals by the most suitable technique yet developed revealed that the diffuseness was not only in $\langle 100 \rangle_\alpha$ directions, but in other directions also. The technique involved making a series of Laue patterns for slightly different orientations of the matrix crystal and analyzing the diffuse CuK$_\alpha$ and K$_\beta$ spots. Portions of typical Laue patterns for the same sample that had been used for the determination of the γ' structure by the oscillating crystal method are shown by Fig. 11. While some of the particles apparently were large enough to afford three-dimensional diffraction when the oscillating crystal method was used, most of the particles were small and produced intense two-dimensional diffraction. Analyses showed that thin platelets of precipitate were present parallel to $\{100\}_\alpha$ and $\{112\}_\alpha$ planes of the matrix in this sample which had been aged 18 hr at 300°C. Most of the diffuse effects corresponded to the rod-like elements that are plotted in the reciprocal lattice projection shown by Fig. 12. Arrow heads indicate the rising end of the rods, and the Z-coordinate indicates the approximate location of the group of rods, whether it be near the zero layer or first layer level of the matrix reciprocal lattice. The configuration near the (111)$_\alpha$ matrix was rather complex and consequently only rods that could be clearly defined are shown in Fig. 12. The spots for the sample that had been aged 1 hr were too diffuse to permit rigorous analysis. Consequently the sample was aged for an additional hour, after which the structure was the same

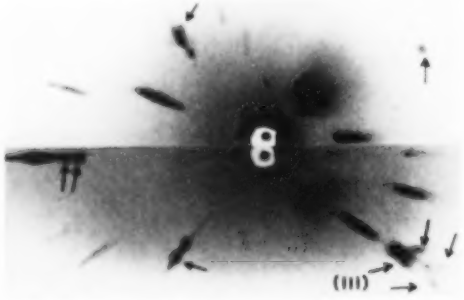

Fig. 11—Laue patterns for crystal that had been aged 18 hr at 300°C showing CuK$_\alpha$ and K$_\beta$ spots for platelets. [001] vertical with beam 36° from [010] for upper pattern and 26° from [010] for lower pattern.

Table I. Reflections for the Intermediate Structure—γ' Body-Centered Tetragonal, c_0 = 2.79, c_1 = 2.54 Rotation about [110], —CuK$_\alpha$ Radiation

	Observed			Calculated		
hkl	d, Å	Y, cm	Intensity	d, Å	Y, cm	Intensity
(100)	2.78	0.00	M	2.79	0.00 0.48 1.00 2.38	M
(001)	2.54	0.00 1.50	M S	2.54	0.00 1.59 3.02	M S
(110)	1.97	0.00 1.50 2.52 4.10	M	1.97	0.00 1.19 2.52 4.12 4.56	S
(101)*	1.88	* *	W	1.88	0.23 0.40 1.94 2.85 3.24	S
(111)	1.56	1.50 2.52 3.92	M	1.56	0.40 1.50 1.99 2.52 3.08 3.82 4.12	W

* Not expected to occur when rotation is about $\langle 110 \rangle_{\gamma'}$. Calculated values for rotation about $\langle 100 \rangle_{\gamma'}$. Observed only on Laue patterns as diffuse streaks through the equator near the $\langle 200 \rangle_{\gamma'}$ reflection.

S means strong, M, medium, W, weak.

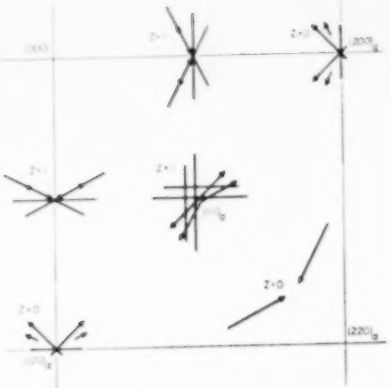

Fig. 12—Reciprocal lattice projection of diffuse rods (CuK_α radiation) that were observed in series of Laue patterns for crystal aged 18 hr at 300°C.

Fig. 13—Reciprocal lattice projections of diffuse rods (CuK_α radiation) that were observed in series of Laue patterns for crystal aged 2 to 3 hr at 300°C.

as that of the sample which had been aged 3 hr. Results for the 2 and 3-hr aging are consolidated in Fig. 13 which shows only <100> rods. Possibly there were other rods also near the (111) matrix reflection.

The identity of the {100} and {112} platelets can be established by comparing the observed diffraction effects with those predicted for the three precipitate structures γ'', γ', and γ. The reciprocal lattice projections in Figs. 14, 15, and 16 are for thin platelets of these three structures parallel to their respective habit planes, {100}, {112}, and {111} of the matrix. Platelets of the equilibrium structure, γ, could not be causing the observed effects since Fig. 16 predicts rods along <111> directions of the matrix and none were observed. On the other hand, the observed effects very well agree with some of those predicted for γ'' and γ'. Rods parallel to $[010]_\gamma$ and $[100]_\gamma$ which pass through the $(100)_\gamma$, $(111)_\gamma$, and $(200)_\gamma$ nodes in Figs. 12 and 13 are precisely those predicted for γ'' in Fig. 14 and thus can be attributed to diffuse $\{100\}_{\gamma''}$ or $\{110\}_{\gamma''}$ reflections. The inclined rods in Fig. 12 agree with those for γ' in Fig. 15 that would be predicted to occur at the Z-coordinates given in Fig. 12.* While all of the observed rods that have been plotted in Figs. 12 and 13 can be reconciled with those predicted, failure to detect some of the predicted can be attributed to: 1—the investigated volume of reciprocal space did not include the entire volume which was included in determining the predicted rods; 2—projected rods directed approximately towards (000) might be observed only on one film in the series and thus insufficient data would be obtained to determine their direction; 3—some of the observed diffraction effects near (111), were too confusing to be rationalized, possibly because of the several rods here with projections directed approximately towards (000); and 4—rods through matrix points and directed precisely towards (000) would diffract on Laue spots with the exception of small angle diffraction near (000). The data are sufficient to conclude that thin platelets of γ'' are formed parallel to {100} planes during aging of 2 to 18 hr at 300°C and platelets of γ' on {112} planes are also present after aging 18 hr.

* Since the reciprocal lattice drawings represent projections, the third or vertical coordinate of points for the precipitate in Figs. 14 to 16 must be ascertained before comparing the predicted rods with the observed rods in Figs. 12 and 13 at the designated Z-coordinates. This can be done visually by locating the three associated precipitate points which fall on a pair of perpendicular lines that are parallel to the $(010)_\alpha$ and $(100)_\alpha$ directions. The Z-coordinate which is perpendicular to the plane of projection is the third coordinate associated with the group of three points but not shown in the projection by the particular point in question. On this basis it can be seen that of the points which project near $(101)_\gamma$—that is midway between (000) and $(200)_\gamma$—only the three $(100)_\gamma$ reflections which have equivalent points below $(111)_\alpha$ in Fig. 15 are expected near Z = 1 as observed in Fig. 12. The other two $(100)_\gamma$ points are near Z = 0 while the four $(111)_\gamma$ points are near Z = 2.

Discussion of Results

The dimensions and relative orientations of the unit cells of the three precipitates which form during the aging of Cu-Be alloys are shown by way of summary in Fig. 17. The γ'' structure is coherent on {100} matrix planes, and it produces the one and two-dimensional diffraction effects that have been observed by accelerated growth respectively along <100> matrix directions and across {100} matrix planes. Although three-dimensional diffraction effects were not observed for γ'', the assumed structure better explains the observed diffuse rods than would a tetragonal structure formed by a simple dilation of the {100} matrix plane stacking as proposed by Guy and Guinier. A sheared structure rather than their coherent, tetragonal one is required to explain the doubled <100> rods near (111), in Fig. 12.

The second precipitate, γ', which coexists with γ'' in samples aged at 300°C grows to a size capable of three-dimensional diffraction. It is coherent on {112} matrix planes; it grows as plates on this family of planes when the thickness is small and causes diffuse diffraction effects that are rod-like and along <112> directions of matrix reciprocal lattice. The orientation relationship of the γ' structure is the same as that proposed by Neerfeld and Mathieu[7] for ferrite formed by transformation in Fe-Ni alloys.

The equilibrium precipitate γ forms a Widmanstätten figure of plates on the four (111) matrix planes which is visible when the particles are grown to a microscopically resolvable size at high temperatures. While in Fig. 6 some of the particles are along twin boundaries, Masing and Dahl[8] have published a micrograph for a slowly cooled 1.46 pct Be alloy which shows a maximum of four well-developed

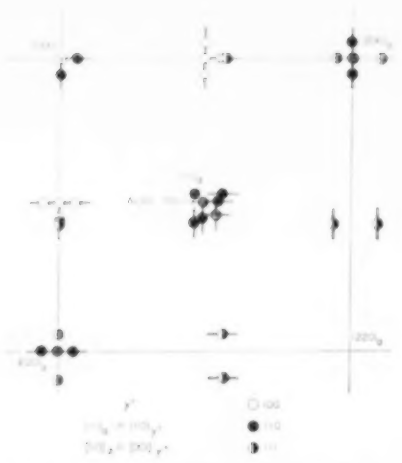

Fig. 14—Reciprocal lattice projection of rods that would be expected for thin platelets of the γ'' precipitate on {100} planes of the matrix.

Fig. 15—Reciprocal lattice projection of rods that would be expected for thin platelets of the γ' precipitate on {112} planes of the matrix.

known annihilated by twin boundaries (see lower grain in their Fig. 21). This confirms the results reported here. At the lower aging temperatures the γ which is detected in powder patterns is presumably that in the lamellar nodules which contain recrystallized matrix and which form mainly at boundaries of the original grains. In regard to crystallographic orientation relationships, the inadequate approximation proposed by Guy and Guinier for γ is replaced by a more rational one when the {311} habit is recognized and the {110}$_\gamma$ conjugate plane is considered. The rational orientation relationship of (111)$_\gamma$ parallel to (110)$_\alpha$ describes the data which had been determined by Guy. It also is supported by the observations which were reported by Dahl and coworkers.[6] In their X-ray diffraction

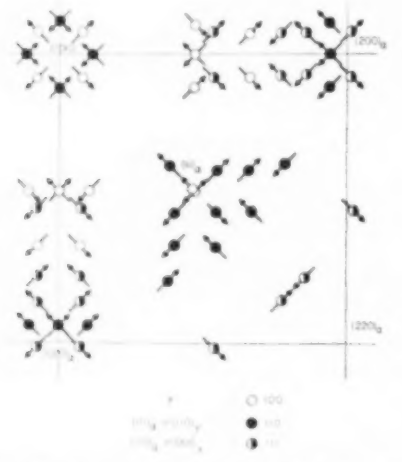

Fig. 16—Reciprocal lattice projection of rods that would be expected for thin platelets of the γ precipitate on {111} planes of the matrix.

-studies on aged cold-drawn wire they found that the precipitate had a fiber texture mainly with a ⟨110⟩$_\gamma$ direction in the direction of drawing whereas the texture of the matrix was the usual wire texture with a ⟨111⟩$_\alpha$ direction in the drawing direction. Thus, the precipitate must have formed with a (110)$_\gamma$ plane parallel to a (111)$_\alpha$ plane of the matrix.† The relationship for the body-centered cubic lattice γ is identical with that proposed by Nishiyama[7] for the formation of ferrite in an Fe-Ni alloy. The crystallographic structures involved in forming both γ' and γ from the matrix are very similar or identical to those involved in the formation of ferrite from austenite in iron-base alloys. On this basis possibly the relation proposed by Neerfeld and Mathieu and that by Nishiyama both might obtain for different forms of the ferrite. Although the small difference in orientation of 1° 2′ makes a choice between the two relationships difficult on the basis of three-dimensional diffraction as recently pointed out by Nishiyama and Doi,[8] studies of two-dimensional diffraction effects provide a clear distinction as to whether (111) or (112) is the conjugate plane in the matrix.† A re-examination of the case of Fe-Ni might well profit by the results reported here for Cu-Be.

The overall mechanism of precipitation in Cu-Be alloys should be considered at this time. It is not possible to decide whether the three precipitates form consecutively by transformation of one into the other followed by further growth or whether they are independently nucleated and grow competitively at rates that depend upon temperature and degree of supersaturation. Perhaps all that can be said is that with increasing time they appear in the order γ'', γ', then γ. In this order the specific

† Subsequent to the writing of the manuscript recent work by Gruhl and Wassermann[9] has come to the attention of the authors. These investigators also obtained the same result for the conjugate planes of γ. From aging studies on coarse-grained polycrystalline samples, they reported evidence for a transition structure which they interpreted as a body-centered tetragonal lattice coherent on {100}$_\alpha$ planes. The transition structure was considered to be merely ordered α, since the new reflections were at locations for superlattice lines for the matrix, however, the matrix reflections in their patterns were so diffuse that it would be difficult to unambiguously identify the structure.

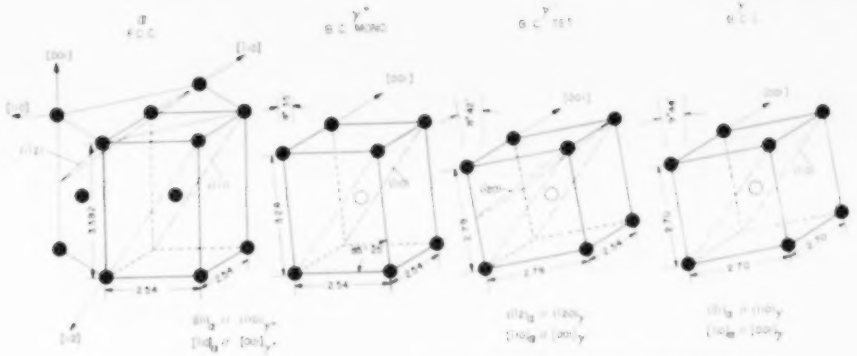

Fig. 17—Unit cells and their relative orientations for structures involved in precipitation in Cu-Be alloys.

volume based on unit cell dimensions continuously decreases from that of the matrix to that of the equilibrium precipitate, as shown by the data in Table II. The largest decrease occurs in the interval $\alpha \rightarrow \gamma''$ which could be interpreted that γ'' has almost the full complement of small Be atoms characteristic of γ. The smaller difference between γ'' and γ' and between γ' and γ may be attributed to coherency strains alone. All three precipitates form at general areas within the matrix crystals, since they were detected in single crystal studied and thus any one is not characteristic of a special site; however, the formation of any of the three is probably accelerated at sites of low activation energy such as grain boundaries, twin boundaries, or slip bands. Since the habit planes are different for the three structures, it might be concluded that they form independently rather than by the sequence $\gamma'' \rightarrow \gamma' \rightarrow \gamma$. On the other hand, the habit planes contain a direction in common, the [110], and it is conceivable that a particle might grow as γ'' along the (001)$_\alpha$ plane to a limiting size, then grow further as γ' along the (112)$_\alpha$ plane, and finally grow to microscopically resolvable sizes as γ along the (111) plane. As yet there is no evidence for the presence of γ as extremely thin plates, so growth of γ' on (112) could be rather extensive before the growth as γ on (111) commences.

The nature of the strains which must arise in the partially impoverished matrix as the precipitates form warrants more consideration. Matrix strains are believed to be the source of age hardening. Coherency of the precipitate with the parent matrix requires that the adjoining impoverished matrix be also strained. Such strains have been identified in systems such as Cu-Ni-Co where the amount of precipitate is similar to that of impoverished matrix.[7] For Cu-Be alloys it is found that rather sharp reflections for the impoverished matrix appeared adjacent to parent matrix reflections in the oscillating crystal patterns of the sample that had been aged 18 hr at 300°C. It was possible to calculate reflections for various strained structures expected for the various precipitates that would equally explain the collective set of matrix spots. Such strained matrix structures included a tetragonal cell for {100} coherency (γ''), an orthorhombic cell for {112} coherency (γ'), and a rhombohedral cell for {111} coherency (γ). The calculated interplanar spacings for all of the strained cells agreed with the observed within the limit of accuracy of the measurements so that a choice was not possible; however, they all involved strains of $^3/_4$ to 1 pct, while isotropic depletion of the matrix produces a $^1/_2$ pct change in lattice parameter of the cubic cell. Such strains would be expected to require plastic deformation of the matrix and on this basis the striations are explained. Guinier suggested that the {110} planes rather than the normal {111} slip planes are those chosen for the deformation because the {110} planes are normal to the proposed {100} habit plane of the precipitate. This is in conformance with the idea that the maximum stresses occur normal to the precipitate plates. It also applies to all three precipitates presented here, for as indicated earlier the (110) plane is normal mutually to all three habit planes, (001), (112), and (111). While the 8° tilt of [001] from [001], reported by Guy can be reconciled by the more appropriate choice of conjugate planes, i.e., (110) parallel to (111)$_\gamma$, the ±2° tilt about [110], can be attributed to asterism due to deformation of the matrix manifested by the striations. When the matrix deforms on {110} planes, blocks of the matrix apparently are misaligned about a [110] direction in the (110) plane of slip. Thus, the γ precipitate particles which are precisely oriented relative to the immediate matrix cover a small spread in orientation relative to the undeformed matrix. This would suggest that one of the coherent forms of the precipitate preceded γ if the deformation is characteristic of the coherent forms of the precipitate only.

Summary and Conclusions

1—The existing data on precipitation in Cu-Be alloys have been reconciled with some new data to present a more complete and rational analysis of the crystallographic mechanism.

Table II. Volume Changes Accompanying Precipitation in Cu-Be

Phase	Average Volume per Atom, A³
Matrix — α	11.59
↓	10.46
↓	9.91
↓	9.84
Impoverished α	11.80

2—Three different precipitates which appeared with increasing time of aging of the 1.7 pct Be alloy at 300 C were identified.

3—The first precipitate, γ'', has a body-centered monoclinic unit cell with $a = b = 2.54$A, $c = 3.24$A, and $\beta = 85.25°$. It is coherent on {100} matrix planes and produces one and two-dimensional diffraction effects by anisotropic growth respectively along <100> directions and {100} planes in the course of its development.

4—The second precipitate, γ', has a body-centered tetragonal unit cell with $a = b = 2.79$A and $c = 2.54$. It is coherent on {112} matrix planes and produces two-dimensional diffractions effects by plate-like growth on {112} matrix planes. Its orientation relationship is (112)$_\gamma$ // (120)$_{\gamma'}$ and [110]$_\gamma$//[001]$_{\gamma'}$.

5—The third precipitate is the equilibrium phase γ which has the orientation relationship (111)$_\gamma$ // (110)$_{\gamma'}$ and [110]$_\gamma$ // [001]$_{\gamma'}$. It forms as plate-like particles on {111}$_\gamma$ habit planes when precipitation is conducted at high temperatures. At lower aging temperatures γ is one of the products of the nodular recrystallization reaction that occurs predominantly at grain boundaries.

6—A choice between the possibility of independent nucleation of γ'', γ', and γ and the consecutive reaction $\gamma'' \rightarrow \gamma' \rightarrow \gamma$ cannot clearly be made yet.

7—The habit planes of the three precipitates contain a [110]$_\gamma$ direction in common which might permit a reaction based on consecutive formation. Similarly the three habit planes are all perpendicular to {110}$_\gamma$ planes on which striations or ripples are observed in the microstructure. Coherency stresses in the impoverished matrix lead to plastic deformation of the matrix on these planes normal to the plate-like precipitate particles. The deformation results in a spread of ±2° in the orientation of the γ precipitate about [110]$_\gamma$ directions.

References

[1] A. Guinier and P. Jacquet: On the Age Hardening of Copper-Beryllium Alloys. *Compt. Rend.* (1943) **217**, pp. 22-24.

[2] A. Guinier and P. Jacquet: Study of the Hardening of the Copper-Beryllium Alloys. *Revue Metall.* (1944) **41**, pp. 1-16.

[3] A. G. Guy, C. S. Barrett, and R. F. Mehl: Mechanism of Precipitation in Alloys of Beryllium in Copper. *Trans.* AIME (1948) **175**, pp. 216-238; METALS TECHNOLOGY (February 1948).

[4] G. Masing and O. Dahl: Changes in the Microstructure of Beryllium-Copper Alloys Due to Age Hardening. *Beryllium*. Siemens-Konzern, translated by R. Rimbach and A. J. Michel, Chem. Cat. Co. (1932) pp. 180-187.

[5] J. K. Smith: Copper-Beryllium Bronzes. *Trans.* AIME (1932) **99**, pp. 65-76.

[6] K. H. Moore: Precipitation Hardening and Secondary Structure. *Physical Review* (1934) **45**, p. 296.

[7] C. H. Desch: *The Chemistry of Solids*. (1934) p. 146. Ithaca, N. Y.: Cornell Univ. Press.

[8] L. Northcott: Veining and Sub-boundary Structures in Metals. *Journal* Inst. Metals (1936) **59**, pp. 225-252.

[9] A. Guinier and P. Jacquet: Striated Structure of Age-hardened Alloys. *Nature* (1945) **155**, p. 695.

[10] C. S. Barrett: A New Microscopy and Its Potentialities. *Trans.* AIME (1945) **161**, p. 54.

[11] M. L. Gayler: Striated Structure of Age-hardened Alloys. *Nature* (1945) **156**, p. 333.

[12] D. Harker and M. J. Murphy: A Study of Age Hardening Using The Electron Microscope and Formvar Replicas. *Trans.* AIME (1945) **161**, pp. 75-89.

[13] S. Miyatani: Precipitation in Single Crystals of Beryllium-Copper Alloy. *Journal* Phys. Soc. Japan (1949) **4**, p. 181. See *Chem. Ab.* (1950) **44**, 4744h; JOURNAL OF METALS (May 1951) p. 382.

[14] J. B. Newkirk, A. H. Geisler, D. L. Martin, and R. Smoluchowski: Ordering Reaction in Cobalt-platinum Alloys. *Trans.* AIME (1950) **188**, pp. 1249-1260; JOURNAL OF METALS (October 1950).

[15] H. Bumm: On the Precipitation Process in Copper-Beryllium Alloys. *Ztsch. Metallkunde* (1937) **29**, pp. 30-32.

[16] A. H. Geisler: Precipitation from Solid Solutions of Metals. *Phase Transformations in Solids*. pp. 387-544 (1951) New York: John Wiley & Sons.

[17] A. G. Guy: Oscillating Crystal X-ray Method Applied to Orientation Relationships. *General Electric Review* (Aug. 1946) **49**, pp. 28-32.

[18] A. M. Elistratov, S. D. Finkelshtein, and A. I. Pashilov: Anomalous Diffraction Effects in X-ray Patterns of Aged Polycrystalline Alloys. *Doklady Akad. Nauk. S.S.S.R.* (1949) **68**, pp. 1017-1020.

[19] A. H. Geisler and J. K. Hill: Analyses and Interpretations of X-ray Diffraction Effects in Patterns of Aged Alloys. *Acta Cryst.* (1948) **1**, pp. 238-252.

[20] A. M. Elistratov: Diffraction Effects in X-ray Patterns of Single Crystals of Copper-Beryllium Alloy. *Doklady Akad. Nauk. S.S.S.R.* (1949) **69**, pp. 337-340.

[21] O. Dahl, E. Holm, and G. Masing: X-ray Investigation of the Age-Hardening Process in Beryllium-Copper Alloys. *Beryllium*. Siemens-Konzern, translated by R. Rimbach and A. J. Michel, Chem. Cat. Co., (1932) pp. 188-240.

[22] H. Tanimura and G. Wassermann: On the System Beryllium-Copper. *Ztsch. Metallkunde* (1933) **25**, pp. 179-181.

[23] K. Kawamura: Mechanism of Age Hardening in Copper-Beryllium Alloys. *Sci. Repts.* Tohoku Imp. Univ. 1st series, K. Honda Ann. Vol. (1936) pp. 702-714.

[24] F. W. Jones and P. Leech: Precipitation in Copper-Beryllium Alloys. *Journal* Inst. Metals (1941) **67**, pp. 9-24.

[25] H. Neerfeld and K. Mathieu: The Mechanism of the γ/α Transformation of Iron. *Arch Eisenh.* (1949) **20**, pp. 69-73.

[26] G. Masing and O. Dahl: The Structure of Beryllium-Copper Alloys. *Beryllium*. Siemens-Konzern, translated by R. Rimbach and A. J. Michel, Chem. Cat. Co. (1932) p. 114.

[27] Z. Nishiyama: X-ray Investigation of the Mechanism of the Transformation from Face-Centered to Body-Centered Cubic Lattice. *Sci. Rep.*, Tohoku Imp. Univ. (1934) **23**, pp. 637-643.

[28] Z. Nishiyama and M. Doi: Lattice Relationship of Gamma-Alpha Transformation Caused by Stress in Iron Alloys. *Mem. Inst. Sci. and Ind. Res.* (1951) **8**, pp. 86-96.

[29] W. Gruhl and G. Wassermann: On the Course of Precipitation in Copper-Beryllium Alloys. *Metall.* (1951) **5**, pp. 93-98, 141-145.

Correction

In the February 1952 issue: TP 3214E. *Diffraction Patterns and Crystal Structure of* Si_3N_4 *and* Ge_3N_4, by W. C. Leslie, K. G. Carroll, and R. M. Fisher. P. 205, the subcaption for Fig. 1 should read: 1 pct nital etch. X2000. Area reduced approximately 50 pct for reproduction.

AIME OFFICERS
President—
Vice Presidents—
President Elect and Treasurer—
AIME STAFF
Secretary—
Ass't Secretaries—

aime NEWS

High Pressure Blowers, Alloy Conservation, Pelletizing, Refractories, Coal and Coke Research Are Topics on Iron and Steel Conference Agenda

The 35th Conference of the Blast Furnace, Coke Oven and Raw Materials Committee and National Open Hearth Steel Committee will be held at the William Penn Hotel, Pittsburgh, Mar. 31 to Apr. 2, 1952. Iron and steel authorities will meet informally and in technical session to discuss mutual problems in operation and management of plants, maintenance, metallurgy, refractories, coal and coke, fuels, beneficiation, raw materials, and production.

The registration fee will be $5.00 for AIME members and $7.00 for nonmembers at either conference. All registrants will receive a copy of the Proceedings when compiled. The annual Fellowship Dinner will be held Tuesday evening, April 1.

The complete Conference program will appear in the April issue of JOURNAL OF METALS.

Preliminary Program of National Open Hearth Conference

SUNDAY, MARCH 30

3:00 pm to 9:00 pm
Registration

MONDAY, MARCH 31

8:00 am to 5:00 pm
Registration

9:30 am
General Session:
Announcements and Reports; McKune Award Paper.

10:30 am
Increasing Open Hearth Production:
Checker Maintenance to Increase Flame Intensity; Oxygen for Flame Enrichment and Decarburization; Methods of Decreasing Charging Time.

11:00 am
Acid Open Hearth Round Table Discussion and Luncheon

2:00 pm
Operating Metallurgy:
Conservation of Alloys, Manganese, Aluminum, Use of Boron, Exothermic Alloys; Effect of Various Elements on Hot Workability; Steel Bath Temperature Measurement; Significance of Furnace Block.

2:00 pm
Refractories and Masonry:
Plastic and Castable Refractories; Basic, High Alumina, and Silica Brick Combinations in Furnace Ends; Rammed Hearths; Scheduling Furnace Repairs to Increase Availability; Hot Metal Mixer Linings.

TUESDAY, APRIL 1

9:00 am to 5:00 pm
Registration

9:30 am
Fuels and Combustion:
Fuel Burners; Future Sulphur Content of Fuel Oils; Instrumentation; High Pressure Natural Gas for Atomizing Oil; Designing a Furnace to Use Natural Gas; Uptake Dimensions.

9:30 am
Cold Metal Session and Basic Foundry Practice:
Slag Control with Burnt Lime; Economics of Use of Oxygen; Effect on Production of High Pig Iron; Bath Pyrometry in Basic Steel Foundries; New Method of Charging.

2:00 pm
Training Open Hearth Personnel:
Visual Aids as a Tool for Training; Training Program. Effects of Foreign Ores as Open Hearth Charge Ore on Production Rates.

6:30 pm
Reception

7:00 pm
Annual Fellowship Dinner

WEDNESDAY, APRIL 2

8:00 am to 4:00 pm
Registration

9:30 am
Plant Trip
All day visit to Irvin Works, Carrie Blast Furnaces, Homestead Works, U. S. Steel Co.

Preliminary Program of Blast Furnace, Coke Oven, and Raw Materials Conference

SUNDAY, MARCH 30

1:00 pm to 9:00 pm
Registration

MONDAY, MARCH 31

8:00 am to 5:00 pm
Registration

9:30 am
Blast Furnace Operating Session:
Results of 35 Psi Turbo Blower; Controlled Differential Pressure; Conditioned Blast; Multiple Correlation of Variables.

2:00 pm
Beneficiation Session:
Krupp-Renn Process; Pilot Pelletizing Plant; Heat Hardening of Taconite Pellets; Self-Fluxing Sinters.

TUESDAY, APRIL 1

9:00 am to 5:00 pm
Registration

9:30 am
Blast Furnace Session:
Operation of an Experimental Furnace; Manganese Distribution Between Slag and Metal; Controlled Charging of Coke; Fire Clay and High Alumina Refractory Linings.

12:30 pm
Luncheon and Annual Business Meeting:
All registrants to Blast Furnace, Coke Oven, and Raw Materials Conference are invited to attend this luncheon and business meeting.

2:00 pm
Coal and Coke Session:
Coal and Coke Research, Tromp Heavy Media Washing Process; Overall Efficiency of Coal Washing; Free Expansion Coke Ovens; High Volatile Coal for Coke.

2:00 pm
Blast Furnace General Session:
Greenawalt Sinter; A Practical Application of Ore Sizing; Operation With and Without Coke from Low Volatile Coals; Physical Conditions in Combustion and Smelting Zones.

6:30 pm
Reception

7:00 pm
Annual Fellowship Dinner

WEDNESDAY, APRIL 2

9:00 am to 4:00 pm
Registration

9:30 am
Plant Trip
All day visit to Irvin Works, Carrie Blast Furnaces, Homestead Works, U. S. Steel Co.

New England Regional Conference Program Set

IMD Group to Meet in Boston, April 25, 26

The Sixth Annual New England Regional Conference of the Institute of Metals Div., AIME, will be held at the Hotel Kenmore in Boston, April 25 to 26, 1952. Features of the conference include a plant trip on Friday morning, April 25, and a technical session in the afternoon. At the banquet in the evening, Fred L. Whipple will speak on *Interplanetary Travel*. A Symposium on Metal Failures will be held Saturday morning, April 26, and the conference will close with a luncheon, and the Regional Conference business meeting. The Conference Committee members are Albert I. Blank, Chase Brass & Copper Co., Chairman; James H. Moore, National Research Corp., Vice-Chairman; Winston H. Sharp, Pratt & Whitney Aircraft, Secretary; Leo P. Tarasov, Norton Co., Treasurer; John A. Swift, Swift Industrial Chemical Co., Past Chairman; Michael B. Bever, Massachusetts Institute of Technology, Chairman Technical Program Committee; George S. Downing, General Electric Co.; Bruce S. Old, Arthur D. Little, Inc.; Lloyd E. Raymond, Singer Mfg. Co.; William L. Stearns, Bridgeport Brass Co.; Maur J. Weldon, Henry G. Thompson & Son Co.; and Franklin H. Wilson, American Brass Co.

Requests for advance registration forms should be sent to Winston H. Sharp, Pratt & Whitney Aircraft, East Hartford 8, Conn. Requests for hotel reservations should be sent to Hotel Kenmore, Boston, Mass., and special consideration will be given those mentioning the Regional Conference.

FRIDAY, APRIL 25

9:00 am—Main Lobby
Conference Registration

9:45 am
Plant Visit

2:00 pm—Embassy Room
Technical Session

Developments in the Theory of Metal Cutting: M. C. Shaw, Massachusetts Institute of Technology, Cambridge. With motion pictures.
Vacuum Metallurgy: J. H. Moore, National Research Corp., Cambridge.
Problems in the Use of Copper and its Alloys in the Electrical Industry: W. A. Reich, Works Laboratory, General Electric Co., Schenectady.
Continuous Casting of Steel: T. Y. Wilson, Allegheny Ludlum Steel Corp.

5:30 pm—Silver Room
Cocktail Hour

6:30 pm—Embassy Room
Banquet

Interplanetary Travel: Fred L. Whipple, Dept. of Astronomy, Harvard University, Boston.

SATURDAY, APRIL 26

9:30 am—Embassy Room
Symposium on Metal Failures

Mechanism of Failure in Metals: E. Orowan, Massachusetts Institute of Technology, Cambridge.
Design Aspects of Metal Failures: C. Lipson, Consultant.
Fatigue Considerations in Aircraft Engine Development: M. H. Young, Materials Laboratory, Wright Aeronautical Corp.

12:30 pm—Green Room
Luncheon

Luncheon will be followed by the Regional Conference business meeting. All IMD members are invited to attend.

Engineering Foundation Reports Project Progress

In the annual report to the Engineering Foundation Board, Technical Director Frank T. Sisco presented a summary of current projects. The following projects sponsored by AIME were reported:

Alloys of Iron Research—This project is expected to be completed in 1953, when the last monographs will be published. The manuscript for *The Alloys of Iron and Nickel—Steels and Cast Irons*, is finished and should be published shortly. The draft for *The Alloys of Iron and Aluminum* has been completed and the volume should be ready for publication by the middle of 1952.

Diffusion in Steel—This is a long-range study of diffusion kinetics in steel. Self-diffusion rates have been determined for ferromagnetic iron between 707° and 768°C. The rates between 707° and 745°C were about those expected from an extrapolation of the data obtained previously on paramagnetic alpha iron at higher temperatures, but they were anomalously low between 745° and 768°C. Apparently the anomaly is connected with the magnetic change at the curve temperature, 768°C. Further studies will be made. Data also have been obtained on the effect of titanium on the self-diffusion rates of alpha and gamma iron, and the diffusion rate of titanium in these allotropic forms of iron has been determined. This project is supported by the AEC and Office of Air Research and Development.

Mechanical Properties of Alloyed Ferrites at Low Temperatures—The first phase of the project has been completed.

Experimental work on high purity alloys of iron and aluminum, iron and silicon, and iron, aluminum, and silicon, has been terminated. From the test data obtained, yield strength, flow stress, fracture stress, strain hardening, energy to fracture, tensile transition temperature, total strain, and necking strain properties can be calculated.

IMD Fall Meeting Paper Deadline

Apr. 15, 1952 is the deadline for all Institute of Metals Div. papers to be presented at the fall meeting, Oct. 20 to 22, at the Hotel Adelphia, Philadelphia.

Staff Appointments Made

At the meeting of the Executive and Finance Committees, H. Newell Appleton, as head of the newly organized Institute Activities Dept., was made an Assistant Secretary of the Institute instead of Assistant to the Secretary, his former title. John V. Beall was appointed as Manager of Publications of the Institute to succeed Thomas E. Lloyd whose resignation was effective February 1. Mr. Beall will continue as Editor of MINING ENGINEERING.

Bessemer Steelmen Meet

An off-the-record meeting of the AIME Bessemer Steel Committee was held Jan. 16, 1952 at the Duquesne Club, Pittsburgh. Bessemer operators and metallurgists discussed many problems concerning this phase of steelmaking. The subjects on the agenda were: Mixers, Blowing Equipment, Vessel Charging Equipment, Iron Quality, Vessel Linings and Bottoms, Converter Design, Blowing, Steel Ladles, Deoxidation, Pouring Practice, Soaking Pit and Rolling Mill Practice, Yield, Applications of Bessemer Steel, Fume Control, Turbo Hearth, Recent Developments in European Practice, Aluminum Nitride Content of Bessemer Steel. In the absence of A. B. Wilder, J. W. Schroeder, also of National Tube Div., U. S. Steel Co., acted as chairman of the meeting.

Award President's Banner

The winner of the President's Banner for the largest number of new applications for membership in its last quarter of 1951, in proportion to its membership, is the Southwestern New Mexico Section. The Banner was presented by President Peirce at the Welcoming Luncheon on February 18. The second highest percentage was attained by the Southwest Texas Section; third by Carlsbad Potash; and fourth by the newly formed Mexico Section.

Student Conclave Planned

On January 25, at a meeting of the Executive Committee of the St. Louis Section the following is one of the items voted:

Voted a revolving fund of $1000, from the gift of 1951 Annual Meeting of Guarantors refunds, to finance an annual student's conclave of our five student affiliates. The first is scheduled for mid-April to be held here. On alternate years thereafter a conclave will be held at each school in turn. It is believed the fund will finance three affairs and that it will become a permanent fixture thereafter. L. P. Davidson was appointed Chairman of the Committee to organize the meeting which, after organization, will be conducted entirely by the students themselves.

Bessemer steelmen who attended the Pittsburgh meeting. First Row: A. C. Von Philp, Wheeling Steel Corp.; G. McMorran, U. S. Steel Co.; R. E. Edwards, Jones & Laughlin Steel Corp.; L. T. Sanchez, J. W. Schroeder, W. G. McDonough, National Tube Div., U. S. Steel Co.; G. M. Yocom, Wheeling Steel Corp.; H. C. Dunkle, Republic Steel Corp. Second Row: R. C. Johnston, Republic Steel Corp.; J. A. Glasgow, D. W. Heidgerd, Jones & Laughlin Steel Corp.; C. E. Williams, W. H. Mayo, U. S. Steel Co.; K. Gordon, S. J. Dougherty, Weirton Steel Co.; J. M. Kirkpatrick, Youngstown Sheet & Tube Co. Third Row: E. R. Holstein, U. S. Steel Co.; R. E. Woodbury, Republic Steel Corp.; G. G. Blean, Jones & Laughlin Steel Corp.; A. C. Flanders, R. J. Walter, Wheeling Steel Corp.; J. J. Veselich, Weirton Steel Co.; E. P. Best, A. M. Byers Co.; M. G. Morrison, Youngstown Sheet & Tube Co.; E. B. Story, A. M. Byers Co.

AIME dues are payable January 1 of each year. Copies of the journals are sent regularly for the first three months of the new year pending receipt of dues. If dues are not received at AIME headquarters by the middle of March, or when the wrappers for the April issues are run off, the member's stencil is removed from the circulation list, and there will be delay in receipt of the April issue. When dues are finally paid, back issues will be supplied to the extent only that copies are available. Duplicate bills should be mailed early in March to those in arrears, and prompt payment at that time, or before, is urgently requested. Resignations, to be accepted as from a member in good standing, must be received before March 31.

Northwest Conference Program Chairmen Named

Program chairmen for the Pacific Northwest Joint Conference have been announced as follows: R. G. Vercoe, Industrial Minerals Div.; A. Y. Bethune, Extractive Metallurgy Div.; Ray Ward, Physical Metallurgy Div.; J. P. Spielman, Mineral Industry Education Div.; and J. Johnson, Iron & Steel Div. H. P. Sherman is in charge of the hotel and meetings; R. O. Oscarson, finance; and W. S. Peterson, publicity.

A luncheon on Saturday, May 10, will feature a talk on northwest gas and the banquet speaker on Saturday evening will be J. F. Bell, president of the Portland Gas & Coke Co. He will present a nontechnical talk on *Quartz and Mica Mining in Brazil* with color photography illustrations. The Spokane Chapter of the WAIME is planning a program for the ladies attending.

Chicago Section Meets

At the February 6 meeting of the Chicago Section, AIME, Harry W. McQuaid, consulting metallurgical engineer, spoke on the comparison of electric furnace and open hearth economics. Mr. McQuaid gave an analysis of the effect of markets and degree of integration on the melting requirements, and economics of small semi-integrated steel producing units in remote areas. He compared the operating costs and investments required for hot metal and cold pig iron open hearth plants, and a modern electric furnace melt shop. He also discussed the availability of raw materials with some emphasis on the direct reduction of iron ore by the use of low cost hydrogen and concluded on the probable future position of electric arc furnaces.

Student Chapter Approved

Recognition of a Student Chapter of AIME at the Wisconsin Institute of Technology at Platteville, Wis., was approved at the meeting of the Executive and Finance Committees on January 9. The following are officers of the new chapter: Carl R. Christiansen, Faculty Sponsor; George L. Sullivan, Counselor; and James Webster, Secretary, Student Chapter.

Minerals and Metals Advisory Board Organized

A new Minerals and Metals Advisory Board has been organized under the National Academy of Sciences-National Research Council. This Board will serve as a research advisory group to the Dept. of Defense and to civilian governmental agencies responsible for research and development in mineral technology and metallurgy for the defense effort.

Dr. Francis C. Frary, recently retired director of research and now technical advisor of the Aluminum Co. of America, will head the new Board as chairman. Dr. Zay Jeffries, retired vice-president of the General Electric Co., and Dr. Robert F. Mehl, director, Metals Research Laboratory, Carnegie Institute of Technology, will serve as vice-chairmen of the Board.

The new Board will continue advisory service to the Research and Development Board and will have the added responsibility of advising civilian defense agencies through the Director of the Bureau of Mines.

The Board's interests are expected to cover advisory services in the appraisal of technical problems involved in the production and use of metallic and nonmetallic minerals.

"The 1952 Metals Branch cloth-bound annual Transactions volume containing the papers appearing in the JOURNAL OF METALS Transactions section during 1952 will carry the Volume number 194. Volumes are released early in the year following the date they carry."

Coming Events

Mar. 1-7. ASTM, spring meeting and committee week, Hotel Statler, Cleveland.

Mar. 10-11. National Electrical Mfrs. Assn., spring meeting, Chicago.

Mar. 10-14. National Assn. of Corrosion Engineers, annual convention, Galveston.

Mar. 17. AIME, Chicago Section, National Open Hearth Steel Committee, Del Prado Hotel, Chicago.

Mar. 19-20. American Institute of Chemical Engineers, Atlanta Biltmore Hotel, Atlanta.

Mar. 17-21. ASTE, annual meeting, Chicago.

Mar. 18-19. Steel Founders' Society of America, annual meeting, Chicago.

Mar. 19. AIME, Western Section, National Open Hearth Steel Committee, Rodger Young Auditorium, Los Angeles.

Mar. 20. AIME, Philadelphia Engineering Bldg., University of Pennsylvania, Philadelphia.

Mar. 22-Apr. 6. Chicago International Trade Fair, Navy Pier, Chicago.

Mar. 24-26. ASME, spring meeting, Seattle.

Mar. 31-Apr. 2. AIME, annual conference, Blast Furnace, Coke Oven, Raw Materials Committee and Open Hearth Steel Committee, William Penn Hotel, Pittsburgh.

Apr. 1. Society for Applied Spectroscopy, Society Vacuum Training Center, 63 Park Row, New York.

Apr. 7-9. American Society of Lubrication Engineers, annual meeting, Statler Hotel, Cleveland.

Apr. 9. AIME, Chicago section, Chicago Bar Assn., Chicago.

Apr. 9-11. Society of Plastics Industry, reinforced plastics div., Chicago.

Apr. 17. AIME, Philadelphia, Engineering Bldg., University of Pennsylvania, Philadelphia.

Apr. 21. AIME, Chicago Section, National Open Hearth Steel Committee, Phil Smidt & Sons, Whiting, Ind.

Apr. 21-23. SAE, national aeronautical meeting, New York.

Apr. 22. Assn. of Consulting Chemists & Chemical Engineers, Inc., general symposium, Hotel Belmont Plaza, New York.

Apr. 25-26. AIME, New England Regional Conference, Kenmore Hotel, Boston.

Apr. 26-May 11. Liege International Fair, Liege, Belgium.

Apr. 29-30. Metal Powder Assn., annual meeting and exhibit, Drake Hotel, Chicago.

May 1-7. American Foundrymen's Society, International Foundry Congress and Show, Convention Hall, Atlantic City, N. J.

May 6-9. Scientific Apparatus Makers' Assn., annual meeting, Edgewater Beach Hotel, Chicago.

May 22-24. American Society for Quality Control, annual convention, Onondaga County War Memorial, Syracuse, N. Y.

June 16-20. Industrial Finishing Exposition, International Amphitheatre, Chicago.

June 23-27. ASTM, 50th anniversary meeting, Hotel Statler, New York.

July 1-Sept. 30. Centennial of Engineering, Chicago.

Sept. 10-12. Porcelain Enamel Institute, annual shop practice forum, University of Illinois, Urbana, Ill.

Sept. 11-13. American Institute of Chemical Engineers, Palmer House, Chicago.

Sept. 22-25. American Mining Congress, Metal and Nonmetallic Mining Convention and Exposition, public auditorium, Denver.

Oct. 3. AIME, Southern Ohio Section, National Open Hearth Steel Committee, Deshler-Wallick Hotel, Columbus, Ohio.

Oct. 10. AIME, Eastern Section, National Open Hearth Steel Committee, Warwick Hotel, Philadelphia.

Oct. 22-24. Porcelain Enamel Institute, Greenbrier Hotel, White Sulphur Springs, W. Va.

Oct. 28. Assn. of Consulting Chemists & Chemical Engineers, Inc., annual symposium, Hotel Belmont Plaza, New York.

Personals

Francis C. Frary has been named chairman of the newly formed Minerals and Metals Advisory Board. **Zay Jeffries**, retired vice-president of General Electric Co. and **Robert F. Mehl**, director of the Metals Research Laboratory, Carnegie Institute of Technology will serve as vice-chairmen of the Board.

Wesley Hyatt is now project engineer for Kaiser Engineers, Inc., Oakland.

George W. Jernstedt has been appointed manager of engineering for the special products development div. of Westinghouse Electric Corp., Pittsburgh.

Paul Zinner, regional director of Region V, Minneapolis, Bureau of Mines, has been appointed chief of the Minerals Div., Washington, D. C. **Paul T. Allsman** will succeed Mr. Zinner.

Thomas J. Moore, Jr. has been named general manager of the Brainard Steel Div., Sharon Steel, Warren, Ohio.

Ray W. Guard is a research associate with the General Electric Research Laboratory, Schenectady.

William Joseph Fretague has joined the metallurgical div., Oak Ridge National Laboratory.

Donald G. Ashe is now concentrator metallurgist, Cananea Consolidated Copper Co., Cananea, Sonora, Mex.

Richard A. Matuszeski has accepted a position as supervisor in the metallurgical dept. of the National Lead Co., Cincinnati. He had been senior engineer in the tungsten and chemical div. of Sylvania Electric Products, Inc., Towanda, Pa.

C. D. King has been appointed vice-president and chairman, engineering committees, U. S. Steel Co., Pittsburgh.

C. D. KING

Donald E. Hohenhaus is now detail engineer for the Boeing Airplane Co., Seattle, Wash.

John S. Murray, Jr. has accepted a position as metallurgist with the Aluminum Co. of America, New Kensington, Pa.

Russell Charles Nelson is now a chemist for the Oak Ridge National Laboratory, Union Carbide & Carbon Co., Oak Ridge.

J. C. Foster has been appointed assistant chief engineer, Bethlehem Steel Co., succeeding **A. J. Fisher** who recently was made general manager of Bethlehem's Johnstown plant.

Alan R. Pels has joined the Bridgeport Brass Co., Bridgeport, as a research metallurgist.

John W. Tomlinson is a research worker at the Imperial College of Science and Technology, London.

Paul Dick is now with the Frankford Arsenal, Philadelphia, as a research metallurgist.

ARTHUR W. THORNTON

Arthur W. Thornton has been appointed assistant general superintendent at National Works of U. S. Steel's National Tube Div., Pittsburgh. He had been division superintendent in charge of pipe production, finishing, and shipping.

J. M. Kimbrough, Jr. has been promoted to assistant district manager for the Republic Steel Corp. He had been in the Chicago office and now will be located in Detroit.

P. F. Dolan, assistant general manager of Bethlehem Steel Co.'s Sparrows Point plant, has retired. Prior to his last position he had been superintendent of the blast furnace div. **L. F. Coffin** succeeds Mr. Dolan.

Sunao Tokunaga was appointed manager of the new Tokyo Research Laboratories of Kamioka Mining & Smelting Co., Tokyo.

W. J. HARRIS, JR.

W. J. Harris, Jr. has resigned from the Naval Research Laboratory to take the post of executive secretary to the Minerals and Metals Advisory Board, National Academy of Sciences. Mr. Harris is Chairman of the Institute of Metals Div. Membership Committee, AIME, for 1952. He also had the chairmanship for 1951.

C. L. Austin, executive vice-president of Jones & Laughlin Steel Corp., has been elected president. Mr. Austin succeeds **Admiral Ben Moreell** who will remain as chairman of the board.

J. E. Hovis has been named general manager for the Bloom Engineering Co., Inc. and **H. J. Howe** has been appointed secretary.

John G. Leschen has been appointed liaison representative in the field of metallurgy at the General Electric Research Laboratory, Schenectady.

S. T. Jazwinski has resigned as senior staff engineer, metallurgical dept., Ford Motor Co., Detroit. He has been appointed chief metallurgist of the Central Iron & Steel Co., Harrisburg, Pa., and their subsidiaries, Phoenix Iron & Steel Co. and Chester Iron Co.

H. A. Steane has accepted an appointment to the staff of Mount Morgan Ltd., Queensland, Australia.

Wilbur L. Mudge, metallurgist, Atomic Power Div., Westinghouse Electric Co. is now in Pittsburgh. He had been located at Bloomfield, N. J.

Drury I. Connor has been appointed Washington representative for the Bohn Aluminum & Brass Corp., Detroit.

I. L. Barker has been appointed superintendent of smelting and refining, Cerro de Pasco Corp., La Oroya, Peru. He has been with the corporation since 1934.

BEN H. ALEXANDER

Ben H. Alexander has been promoted to engineering manager at the Boston electronics div., Sylvania Electric Products, Inc. He had been section head at the metallurgical laboratory, Bayside, N. Y.

H. W. Franz is now associated with the Kaiser Aluminum & Chemical Corp., alloys div., Newark, Ohio.

Jerome M. Jenkins has accepted a position in the research dept. of the Bethlehem Steel Co., Bethlehem, Pa.

Robert N. Millar has joined the British General Electric Co., Ltd., Sydney, Australia, as chief mechanical engineer.

John J. B. Rutherford, metallurgist, tubular products div., Babcock & Wilcox Co., has been appointed a member of the Interim Advisory Committee on Alloy Steels of the American Petroleum Institute.

Thomas Turner, vice-president in charge of industrial relations, Westinghouse Electric Corp., has been reassigned vice-president in charge of the motor and control div., Buffalo. **T. I. Phillips** succeeds Mr. Turner as staff vice-president in charge of manufacturing. **Robert D. Blasier** and **John E. Payne** were elected vice-presidents.

Fritz V. Lenel, professor of metallurgy at Rensselaer Polytechnic Institute, is now engaged in two fields of research for the Dept. of the Navy. Dr. Lenel is a past Chairman of the Institute of Metals Div. Powder Metal Committee, AIME.

Frederick R. Jeffrey is now manager of the ore dept. of International Minerals & Metals Corp. and also treasurer and assistant to the president of the National Zinc Co., Inc.

D. F. Kidd is the newly elected president of the Canadian Institute of Mining and Metallurgy.

Starr Thayer, consultant of Houston, and **Earl A. Gulbransen**, advisory engineer to Westinghouse Research Laboratories, East Pittsburgh, have been designated to receive the 1952 annual Frank Newman Speller and Willis Rodney Whitney Awards from the National Assn. of Corrosion Engineers.

Lowell T. Smith has been appointed assistant metallurgical engineer of the metal dept., research and development div., Olin Industries, Inc., East Alton, Ill.

G. L. Ratcliffe was elected vice-president of National Lead Co., New York. He has been member of the board of directors since 1948.

W. B. Porter has been reelected president of the Hegeler Zinc Co., Danville, Ill. **E. K. Minear** was also reelected as vice-president; **M. E. Thompson**, secretary-treasurer; **C. E. Smutz**, comptroller and assistant treasurer; and **C. H. Buckingham**, assistant secretary. The following were elected as directors of the company: **H. C. Crays, George V. Dole, Walter T. Gunn, Woods H. Martin, James B. F. Melville**, and **W. B. Porter**.

Gordon R. Ball, vice-president, general manager and a director of the Bank of Montreal, has been elected a director of the International Nickel Co. of Canada, Ltd.

G. O. Curme, Jr., has been named a director of Union Carbide & Carbon Corp. to succeed the late **James A. Rafferty**. Dr. Curme, as vice-president, is in charge of all research activities for the corporation.

Ramanatha Krishnaswamy is presently assistant professor of metallurgy in the College of Mining and Metallurgy, Benares Hindu University, Banaras, India.

Edmund C. Burke is research metallurgist with the Dow Chemical Co., Midland, Mich.

James R. Thompson has retired from the position of manager of the metallurgical dept., American Steel & Wire Co. He joined the company in 1901 in Cleveland.

Harry H. Yeager is now general superintendent of plant operations for Harbison-Walker Refractories Co. He has been associated with the firm in the operating dept. since 1905 and until recently served as general district superintendent, Pittsburgh.

Charles A. Scharschu has been made chief metallurgist and assistant technical director, Allegheny Ludlum Steel Corp., Brackenridge, Pa. He had been director of research.

Elmer A. Jones has become assistant general manager of the Southeast Missouri Div., St. Joseph Lead Co. He had been assistant general mine superintendent.

Guinn E. Metzger is teaching at the School of Mines of the University of Alaska. He is assistant professor of metallurgy.

K. V. Aiyer, Bombay, India, has joined the Associated Cement Co. as metallurgist.

Milton G. Amdur is now metallurgical engineer for the Colonial Smelting & Refining Co., Inc., Columbia, Pa.

Frank P. Barton, assistant manager, metallic products div., the Eagle Picher Co., has been transferred from Cincinnati to East Chicago, Ind.

R. C. Amero has joined the Gulf Research & Development Co., Harmarville, Pa., as chemical engineer.

C. W. Hawn is now employed by the St. Joseph Lead Co., Southeast Missouri Div., Bonne Terre, Mo.

Erik V. Enevik, Uddeholm Co. of America, Inc., has been transferred to Los Angeles. He had been located in the New York office.

Alton K. Guard has become project engineer for the Morrison-Knudsen Co., Inc., working on the Monsanto Chemical Co. construction operation at Soda Springs, Idaho.

John W. Gilmore is research engineer for North American Aviation, Inc., Downey, Calif.

Bently H. McLeod has resigned as chief metallurgist from the Magnet Cove Barium Corp., Malvern, Ark. He is now in the consulting engineering dept. of the Dorr Co., Stamford, Conn.

Obituaries

Daniel Eppelsheimer, Jr. (Member 1928) has died. Mr. Eppelsheimer was born at Philadelphia on Aug. 5, 1876. He graduated from the University of Pennsylvania in 1897, receiving the degree of B.S. in electrical engineering. After graduation he joined the American Bridge Co. In 1905 he was chief engineer for the Montreal Rolling Mill Co. Later he became managing director for the Toronto & Belleville Rolling Mill Co. For approximately two years he was employed by the Indiana Steel Co. as assistant chief engineer. He later joined the American Rolling Mill Co., Middletown, Ohio. He was promoted to special engineer, and then chief engineer, consulting engineer, and vice-president and consulting engineer, respectively.

H. Comer Wolf (Member 1936) died on Oct. 28, 1951. Born at Indianapolis, Dec. 20, 1888, he attended West Point and graduated in 1909. From 1909 to 1919 he was an Army instructor, signal, construction and design and also did private engineering consulting. For several years he did consulting and supervisory work on oil shale plants and lands. In 1932 Mr. Wolf was engaged in design, construction and operation of rock asphalt mines and plants in Missouri and Kentucky.

He worked on design and plant lay-out of iron mines and a process for treating Pyrite. He was a member of various technical societies.

Benjamin F. Tillson (Member 1905) retired head of the mining dept. and assistant superintendent of the N. J. Zinc Co. died suddenly on Dec. 4, 1951. Born in Norwich, N. Y., April 11, 1884, Mr. Tillson received his bachelor of philosophy degree from Yale University in 1905. Two years later he received his mining engineering degree from Columbia University. He joined the N. J. Zinc Co. following graduation from Columbia, and remained with the firm until his retirement in 1950. During the first world war he represented the AIME as a technical consultant on the technical advisory committee of the Office of Civilian Defense for the New York area. He served as chairman of the advisory board of the National Safety Council and of the U. S. Bureau of Mines. During the thirties Mr. Tillson was named as special consultant to the association of contractors for the Lincoln and Queens midtown tunnels in New York. After his retirement from the N. J. Zinc Co. he served as a private consulting engineer.

Donald G. Lauck (Member 1947), district manager, E. J. Lavino & Co., died during May 1951. Born in Philadelphia, he received a B.A. degree from Pennsylvania State College, and an M.A. degree from the University of Pittsburgh in 1944. Mr. Lauck had been associated with E. J. Lavino & Co. for many years working in various departments. He was in the mineral dept. for approximately two years and then joined the refractories div. In 1945 he was made district manager of sales and engineering, located in Pittsburgh.

Kenneth Moodie (Member 1937) died on Sept. 12, 1951. Mr. Moodie was born in Canada and attended the McGill University in Montreal. He graduated in 1895 with a B.A.Sc. Following graduation he joined the Western Electric Co., Chicago as a draftsman, later becoming mechanical engineer and assistant chief draftsman, plant engineer, and chief inspector of the power apparatus dept., respectively. Several years later Mr. Moodie was made assistant superintendent, locomotive shops for the Canadian Pacific Railway Co., Montreal. In 1914 he became associated with the Rosedale Coal & Clay Products Co., Ltd. as chief engineer and superintendent. He joined Burns & Co., Calgary, Alta. in 1924, as mechanical superintendent. He was engaged as combustion engineer for the Dept. of Public Works, British Columbia, for several years. At the time of his death he was residing in Victoria, B. C.

Norman F. Robertson (Member 1928), president John Robertson Co., Inc., died in August 1951. Born in Brooklyn on Apr. 5, 1899, he attended Stevens Institute of Technology, Hoboken, N. J. In 1921 he was a machinist and draftsman for John Robertson Co., Brooklyn. Later, Mr. Robertson was made secretary of the firm and then became president.

NECROLOGY

Date Elected	Name	Date of Death
1919	H. P. Banks	Unknown
1902	H. A. Barker	Unknown
1936	J. J. Clifford	Mar. 15, 1951
1916	Alvin M. Cummings	Jan. 6, 1952
1928	J. Eppeisheimer, Jr.	1950
1907	B. G. Kluge	*Unknown
1950	Fred H. Loftus	1951
1939	T. F. Maddick	Nov. 8, 1951
1908	John M. Moubray	Oct. 4, 1951
1902	Robert W. Pringle	Unknown
1949	Ernest F. Pullen	Unknown
1942	P. W. Ravey	Sept. 20, 1950
1930	William B. Rose	Nov. 19, 1951
1927	Ernest Arthur Satchell	Unknown
1921	Sibyl Walker Smith	Dec. 7, 1951
1919	Raleigh P. Trimble	Jan. 9, 1951
1940	Donald K. Weaver	Unknown
1936	H. Comer Wolf	Oct. 28, 1951
1927	Theodor Zuschlag	Jan. 14, 1952

Proposed for Membership
— Metals Branch AIME —

Total AIME membership on Dec. 31, 1951 was 17,482; in addition 2229 Student Associates were enrolled.

ADMISSIONS COMMITTEE

Thomas G. Moore, Chairman, Carroll A. Gaither, Vice-Chairman; George B. Cortese, F. W. Hinrichs, Albert J. Phillips, Lloyd C. Gibson, R. D. Mollison, John T. Sherman. Alternates: A. C. Bruhker, H. W. Hitzrot, Plato Malozemoff, Ivan Given, T. D. Jones, and W. A. Clark, Jr.

The Institute desires to extend its privileges to every person to whom it can be of service, but does not desire as members persons who are unqualified. Institute members are urged to review this list as soon as possible and immediately to inform the Secretary's office if names of people are found who are known to be unqualified for AIME membership.

In the following list CJS means change of status, R, reinstatement, M, Member; J, Junior Member; A, Associate Member; S, Student Associate.

Alabama
Birmingham—Alderson, George E. (M); (R, M)

Arizona
Phoenix—Mitchell, Owen L. (M); (R, C.S.—S-M)

California
Compton—Rogers, Richard E. (A)
Edwards—Hess, James Gordon, Jr. (J); (R, C.S.—S-J)
Oakland—Meyers, Charles L., Jr. (J); (C.S.—S-J)
Palo Alto—Parkman, Ralph (A); (C.S.—S-A)

Colorado
Denver—Allen, Louis B. (M)

Idaho
Kellogg—Kroll, Alvin F. (M); Prindle, Fred L. (M)

Illinois
Champaign—Nevitt, Michael V. (S); (C.S.—J-S)
Chicago—Briske, Hubert W. (M); (C.S.—J-M); Gross, Arthur J. (J); Laffin, Judson M. (J); Robinson, Alfred W. (M); Wells, Lloyd L., Jr. (M); (C.S.—J-M)
Homewood—Russell, John V. (M); (C.S.—J-M)
Park Ridge—Von Luhrte, Carl E. (M)
Peoria—Langston, Merritt E. (J); (C.S.—S-J)
Rockford—Simonovich, Richard R. (J); (C.S.—S-J)

Indiana
Bloomington—Griffin, Samuel E. (J); (C.S.—S-J)
Gary—Irani, Keki K. (J); (C.S.—S-J); Pearson, Oscar (M); (R.C.S.—J-M); Skwarlo, John J. (J); (R.C.S.—S-J)
Indianapolis—Benbow, James M. (J); (C.S.—S-J); Morris, Robert J. (J); (C.S.—S-J)
Munster—Kyle, Fred Robert (J)

Massachusetts
Arlington—Buffum, Donald C. (M); (C.S.—J-M)

Michigan
Ann Arbor—Bush, Spencer H. (M); (R.C.S.—S-M); Kiessel, William R. (J); (C.S.—S-J)
Detroit—Naslasius, John B. (J); (C.S.—S-J)
Garden City—Dietrick, Donald J. (J)
Grosse Pointe—Macauley, John B. (M)
Ishpeming—Bar, Thomas E. (J); (C.S.—S-J)
Rembold, H. Walter (M); (R.C.S.—J-M)

Minnesota
Minneapolis—Schulz, Norman F. (A)

Missouri
Brentwood—Moon, Albert H. (J); (C.S.—S-J)
Joplin—Spooner, Philip V. (M)

Nebraska
Omaha—Skow, Ray C. (M); (R.C.S.—S-M)

Nevada
Henderson—Lottridge, Richard W. (M); (R, C.S.—A-M)

New Jersey
Bloomfield—Kindquist, Eric B. T. (M); (C.S.—J-M)
Fanwood—Colton, Robert A. (M); (C.S.—J-M)
Keyport—Sherban, Daniel V. (M)
Metuchen—Roe, William R. (J); (C.S.—S-J)
Woodbridge—Mosher, Merrill A. (M)

New Mexico
Carlsbad—Lair, Woodrow W. (M)
Hurley—Hubbard, Thomas J. (M)

New York
Bellport—Klamut, Carl Joseph (J); (C.S.—S-J)
Brooklyn—Archer, Robert (J); (R.C.S.—S-J); Glass, Clarence (A)
Buffalo—Griffith, Owen M. (A)
Flushing—Queally, Justin M. (J); (C.S.—S-J)
Raiklen, Hyman I. (M); (R.C.S.—S-M)
Jamaica—McCormick, Walter R., Jr. (M); (R, C.S.—J-M)
New York—Greenwood, John G. (M); (R, M)
Schenectady—Keeler, James H. (M); (C.S.—S-M)
Syracuse—Weller, Daniel L. (J); (C.S.—S-J)

Ohio
Cleveland—Mueller, John W. (M); (C.S.—J-M); Newman, David P. (J); (R.C.S.—S-J)
Columbus—Eichen, Erwin (J); (C.S.—S-J); Lowrie, Harold W., Jr. (M); Sanders, David A. (J); (C.S.—S-J)
Salem—Sabol, Frank P. (M)
Terrace Park—Maupin, Addison (M)
Tiltonsville—Mancuso, Nicholas (J); (C.S.—S-J)

Pennsylvania
Drexel Hill—Hecht, Oswald H. (M)
Latrobe—Moersch, Christian F., Jr. (A); Rogers, James H. (A); Shupe, Kay M. (J); (R.C.S.—S-J)
Midland—Kondratenko, Walter (A); (C.S.—S-A)
New Kensington—Kiessling, Maxwell D. (J); (C.S.—S-J); Smith, Charles O. (A); (C.S.—S-A); Towner, Raymond J. (J)
Philadelphia—Campion, John (J); Damiano, Victor V. (J); (C.S.—S-J)
Pittsburgh—Chirigos, John (J); (R.C.S.—S-J); Gurland, Joseph (J); (R.C.S.—S-J); Hayden, Thomas A. (M); Langenburg, Frederick C. (J); (C.S.—S-J); Mead, Harry W. (J); (R.C.S.—J-P.A.-J); Roelofs, Robert F. (M); Shenkwiler, Francis P. (M); Thompson, William C. (A)
Wheatland—Levy, Reuben W. (M)

Utah
Salt Lake City—Fassell, W. Martin, Jr. (M); (R.C.S.—S-M); Westhaver, Loren J. (M)

Africa
Sierra Leone, Freetown—Stobart, John A. (A)

Australia
New South Wales—Trengove, John R. (J); (C.S.—S-J)

Canada
British Columbia, Trail—Bainbridge, Robert (M); Robertson, Allan G. (M)
Ontario—Eller, Garnet G. (J); (C.S.—S-J); Ross, Alvin H. (M); Shany, Robert C. (J); (C.S.—S-J)
Ontario, Brockville—Cooper, James D. (J); (C.S.—S-J)
Ontario, Welland—Makepeace, Charles E. (A)
Montreal—Campbell, James G. (M); MacEwan, James U. (M)

Chile
Santiago—Kral, Charles A. (M); (R.C.S.—J-M)

India
Bombay—Aiyer, Krishna V. (M); (C.S.—J-M); Jasdanwalla, F. A. (J)

Japan
Tokyo—Chiyoda-ku-Shimatoura, Tetsuo (M); Mori, Sadao (M)

Open Hearth . . . .
Blast Furnace . . .
Coke Oven . . . . . .
Raw Materials . . .

CONFERENCE

Pittsburgh, March 31 to April 2

★ ★

Your company should be among those advertising in the April issue of JOURNAL OF METALS—official publication and only publication representing the Blast Furnace, Coke Oven, Raw Materials and Open Hearth Conferences.

Write or wire for space reservations now. Plates must be in New York by March 5.

★ ★

JOURNAL OF METALS
29 West 39th Street New York 18, N. Y.

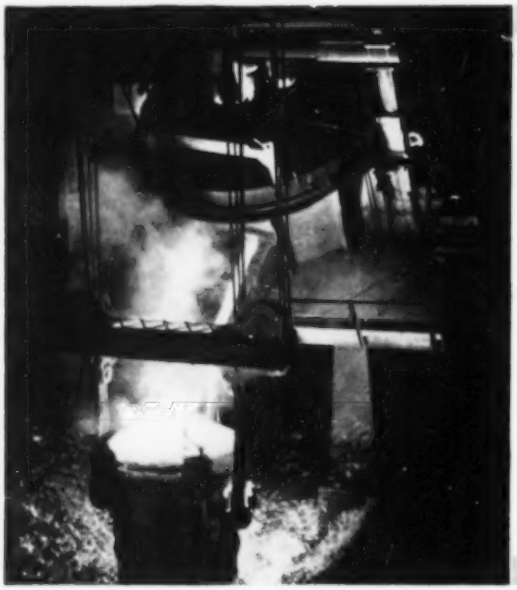

Heroult

ELECTRIC MELTING FURNACE

. . . as ever, the dependable furnace for the production of high-grade stainless, alloy and rimming steels.

Removable roof of new design now available for the larger furnaces.

AMERICAN BRIDGE DIVISION
UNITED STATES STEEL COMPANY
General Offices: 525 William Penn Place, Pittsburgh, Pa.
Contracting Offices in New York, Philadelphia, Chicago, San Francisco and other principal cities

USS **AMERICAN BRIDGE**
UNITED STATES STEEL

This Continuous Process demanded CERTAIN PERFORMANCE

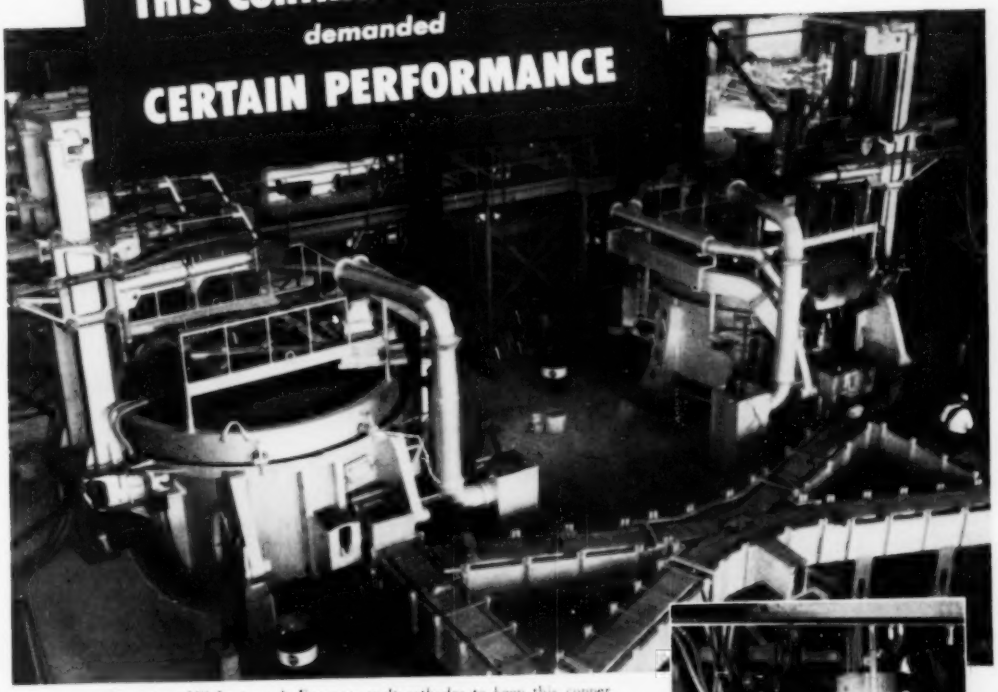

Two size "M" Lectromelt Furnaces melt cathodes to keep this copper refinery in continuous operation. A third, not shown, melts anode scrap.

So for the melting part of this electrolytic copper refinery operation, the logical choice was Lectromelt*. Because from the electrical brain that guides its operation to the massive shell of the furnace itself, Lectromelt is built to be a production tool. It will give you long, trouble-free service and correspondingly low-cost operation (we sell mighty few replacement parts!).

For smelting or melting, refining or reducing—Lectromelt engineers will help you design your process and tailor-make the installation to your needs. Write for your copy of "Moore Rapid Lectromelt Furnaces for Smelting and Refining Operations." Pittsburgh Lectromelt Corporation, 326 32nd Street, Pittsburgh 30, Pa.

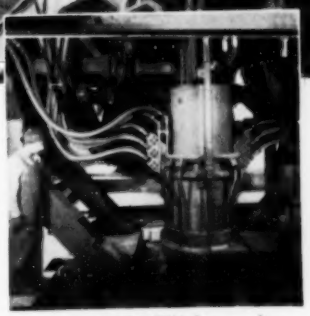

A typical 1500-KVA Lectromelt smelter at charging floor level. Three electrodes in line.

Manufactured in . . . CANADA: Lectromelt Furnaces of Canada, Ltd., Toronto 2 . . . ENGLAND: Birlec, Ltd., Birmingham . . . AUSTRALIA: Birlec, Ltd., Sydney . . . FRANCE: Stein et Roubaix, Paris . . . BELGIUM: S. A. Belge Stein et Roubaix, Bressoux-Liege . . . SPAIN: General Electrica Espanola, Bilbao . . . ITALY: Forni Stein, Genoa.

MOORE RAPID

WHEN YOU MELT... *Lectromelt*

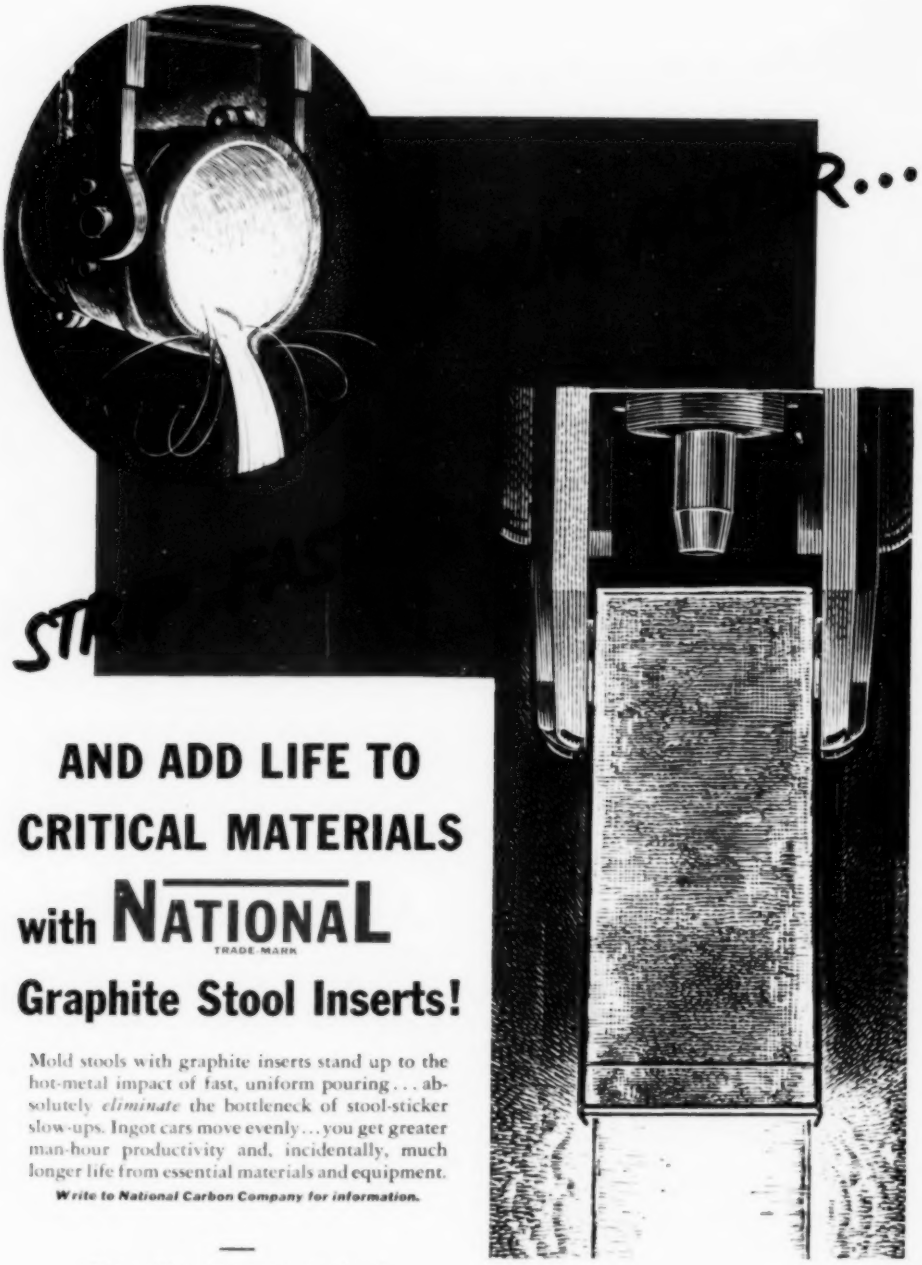

AND ADD LIFE TO CRITICAL MATERIALS with NATIONAL TRADE-MARK Graphite Stool Inserts!

Mold stools with graphite inserts stand up to the hot-metal impact of fast, uniform pouring . . . absolutely *eliminate* the bottleneck of stool-sticker slow-ups. Ingot cars move evenly . . . you get greater man-hour productivity and, incidentally, much longer life from essential materials and equipment.

Write to National Carbon Company for information.

The term "National" is a registered trade-mark of Union Carbide and Carbon Corporation

NATIONAL CARBON COMPANY
A Division of Union Carbide and Carbon Corporation
30 East 42nd Street, New York 17, N. Y.
District Sales Offices: Atlanta, Chicago, Dallas, Kansas City, New York, Pittsburgh, San Francisco
In Canada: National Carbon Limited, Montreal, Toronto, Winnipeg